HYDROMETALLURGICAL BENEFICIATION OF ILMENITE

by

Amanda Qinisile Vilakazi

A dissertation submitted to meet the requirements for the degree of

Master of Science

In the faculty of Natural and Agricultural Sciences

Department of Chemistry
University of the Free State
Bloemfontein

Supervisor: Prof. W. Purcell
Co-supervisor: Dr. M. Nete

July 2017

DECLARATION BY CANDIDATE

I hereby declare that this dissertation submitted for Master's degree in Chemistry at the University of the Free State is my own original work and has not been previously submitter to another university or faculty. I further declare that all sources cited and quoted are acknowledged by a list of comprehensive references.

Signature ……..… **Date**……

Amanda Qinisile Vilakazi

ACKNOWLEDGEMENT

I hereby wish to express my gratitude to a number of people who made this research a success.

Prof. W. Purcell (Supervisor): for his guidance, persistence and patience throughout the research project. Your expertise is highly acknowledged. Thank you for giving me the opportunity to further my academic career.

Dr M. Nete (Co-supervisor): No words can express my gratitude towards your role in the success of this thesis. Thank you for your countless guidance, support and motivation, not to mention your assistance in reviewing each and every chapter with excellence.

The analytical chemistry group (L. Ntoi, S. Xaba, D. Nhlapo, H. Mnculwane, G. Malefo, A. Ngcephe, D. Mona, Dr T. Chiweshe and Dr S. Kumar) and P. Nkoe, thank you for your assistance and for providing a fun and productive environment.

I also wish to thank my mother **M.M. Vilakazi** and my uncle K.P. Vilakazi; you made the last months of my studies a success with your patience and Love. To the family at large, thank you for your support; "*Ngiyabonga Binda, Mphephethe*"

Amanda Qinisile Vilakazi

TABLE OF CONTENTS

Table of Contents

Table of Contents

Table of Contents

LIST OF FIGURES

List of Figures

List of Figures

LIST OF TABLES

List of Tables

List of Tables

List of Tables

LIST OF ABBREVIATIONS

Analytical equipment

BSE	Backscattered electron images
EBSD	Electron Backscatter Diffraction
CHNS micro analyser	Carbon, hydrogen, nitrogen, sulphur micro- analyser
ICP-OES	Inductive coupled plasma-optical emission spectroscopy
IR	Infrared
SEM-EDS	Scanning electron microscopy-Energy dispersive spectroscopy
XRF	X-ray fluorescence
XRD	X-ray diffraction
UV-Vis	Ultra violet- visible spectroscopy

Ligands and solvents

acacH	Acetylacetone
MIBK	Methyl isobutyl ketone
TOPO	Trioctylphosphine oxide
NaTPB	Sodium tetraphenyl borate
NaPT	2-Mercaptopyridine N-oxide Sodium salt
phen	phenantroline

Miscellaneous terms

EIEs	Easily ionisable elements
MxOy	Metal oxide

Statistical terms

RSD	Relative standard deviation
LOD	Limit of detection
LOQ	Limit of quantification
R^2	Linear regression coefficient
S_m	Standard deviation of the slope
S_b	Standard deviation of y-intercept
S	Standard deviation
m	slope

SI units

^{o}C	Degree Celsius
M	Molar
ppm	Parts per million

KEY WORDS

Beneficiation

Dissolution

Hydrometallurgy

Ilmenite

Iron

Qualitative analysis

Quantitative analysis

Recovery

Separation

Titanium

1 Motivation of the study

1.1 Background of the study

Titanium, one of the early transition metals, is extensively used in the production of high strength, corrosion resistant and thermally stable metal alloys for the aerospace and armour industries. In spite of its abundance (ranked 9th of all the elements) it still has some of the highest production costs compared to other metals and these prevent the metal to fulfil its full potential in applications in the maritime and automotive industries. Old manufacturing technology, high demanding energy requirements and loss of material or metal are some of the production problems or issues associated with titanium metal production.[1,2] Titanium is mainly produced from minerals such as ilmenite (Fe,Mn,Mg)TiO_3 and rutile (TiO_2) while smaller quantities are produced from perovskite ($CaTiO_3$) and titanite or sphene ($CaTiSiO_5$).[3] Major deposits of ilmenite are located in South Africa, Australia, China, Norway, Canada, Madagascar, India and Vietman while rutile deposits are found in Sierra Leone, United States, India and South Africa.[4]

Ilmenite ($FeTiO_3$) is one of the most important containing titanium ores[5] and contains between 40 and 65 % titanium dioxide content and the remaining elements are either ferrous or ferric oxide and sometimes small quantities of vanadium, magnesium and/or manganese. It is commonly distributed in hard rock and placer deposits

1 Cui, C., Hu, B., Zhao, L. and Liu, S., Titanium alloy production technology, market prospects and industry development, *Journal of Material and Design*, 32, pp.1684-1691 (2011)

2 Ko, B. and Van Leeuwen, S., Characteristics and uses of titanium, Stainless Steel World, pp.1-4 (2008)

3 Force, E.R., Geology of Titanium-Mineral Deposits, Issue 259, Geological Society of America, pp.3-6 (1991)

4 Bedinger, G.M., Titanium Mineral Commodity Summaries 2016, U.S. Geological Survey, pp.176-177 (2016)

5 Force, E.R., Titanium content and titanium partitioning in rocks, *Geology and Resources of Titanium,* pp.A2-A3 (1976)

(**Figure 1.1**) while heavy mineral sands (placer deposits) are major sources of ilmenite.[6] Currently ilmenite accounts for 92 % of the global titanium mineral production. Rutile (TiO_2) has a titanium dioxide content of 93 - 96 %, but it is not easily found in natural deposits.[4]

Figure 1.1: Massive ilmenite rock from St-Urban, Quebec, Canada (magmatic rock) and ilmenite sand from Melboume, Florida (placer deposit).[7]

Commercially, ilmenite is mainly beneficiated for its titanium content, while the iron is mostly regarded as waste. Ilmenite, which is naturally magnetic, is separated from non-magnetic minerals such as rutile and zircon using wet and dry magnetic separation techniques and further processed for the beneficiation of titanium and iron (see **Chapter 2, Figure 2.9**).[8] After the ilmenite separation from other gunge minerals, titanium and iron are separated through a smelting process using carbon reduction to produce titanium slag and molten iron (pig iron) in a blast furnace (**Equation 1.1**). Titanium slag which contains approximately 90 % TiO_2 and approximately 10 % of FeO is further beneficiated using the sulphate and chloride processes for the production of titanium dioxide and titanium metal.[9]

$$FeTiO_3 + C \longrightarrow TiO_{2(slag)} + Fe_{(metal)} + CO_{(gas)} \qquad \textbf{1.1}$$

6 Gosen, B.S., Fey, D.L. and Shah A.K., Deposit Model for Heavy-Mineral Sands in Coastal Environments, U.S. Geological Survey, pp.9-19 (2014)

7 Ilmenite, [Accessed 10-02-16]. Available from: geology/com/minerals/ilmenite.shtml

8 Filippou, D. and Hudon, G., Iron removal and recovery in the titanium dioxide industries, *Journal of the Minerals and Materials Society*, 61, pp.36-42 (2009)

9 Gázquez, M.J., Bolívar, J.P., Garcia-Tenorio, R. and Vaca, F., A review of the production cycle of titanium dioxide pigment, *Materials Sciences and Applications*, **5**, pp.441-458 (2014)

Titanium metal production consumes only a small percentage of the total titanium production per annum.[4] The most important properties that make titanium attractive to industrial applications include its low density and high tensile strength. This gave titanium containing alloys the highest strength-to weight ratio, a property important for metals in the steel industry. It is a very reactive metal, but can resist corrosion both in sea water (the only metal immune to micro-biological corrosion) and acids. As an alloyed metal, it can also resist corrosion better than copper-nickel alloys and has a low modulus elasticity which is half that of steel and nickel alloys. The most common titanium alloy is Ti 6Al - 4V (6 % aluminium, 4 % vanadium, 90 % titanium) and it is usually used in medical applications such as knee replacement implant. The metal is also used in the aerospace industry, architecture, chemical and automotive applications.[10,11] The molten iron which is produced during the smelting of the ilmenite is further processed for production of cast steel billets or steel powders and has limited applications due to its high carbon content (3.5 - 4.5 %).[12]

In 1913 titanium dioxide replaced lead as white pigment for the first time due to its high refractive index and currently this titanium product accounts for approximately 95 % of the titanium market. Titanium dioxide has the ability to absorb the destructive UV light and convert it into heat. It also has an improved chemical stability and brightness (whitest in powder form) compared to lead oxide and it is therefore widely used in the production of paper, plastic and paints.[10,11,13] TiO_2 is mainly manufactured using the sulphate and chloride processes (see **Chapter 2, Section 2.3.3**).[4,9] China is one of the biggest producers of TiO_2 with approximately 270 production facilities and these plants utilises mostly the sulphuric acid process (with chlorination production process at a smaller scale) and they beneficiate both titanium and iron present in the ilmenite.[12]

10 Fadeel, B.(ed), Handbook of Safety Assessment of Nanomaterials: From Toxicological Testing of Personalized Medicine, p.72 (2015)

11 Ti Facts, [Accessed 02-03-2016]. Available from: http://c.ymcdn.com/sites/www.titanium.org/resource/resmgr/Docs/TiFacts.pdf

12 Pig iron, [Accessed 15-08-2016]. Available from: http://metallics.org.uk/pigiron/

13 Leyers, C. and Peters, M.(ed), Titanium and Titanium Alloys: Fundamentals and Applications, pp.4,393-407 (2003)

1.2 Motivation of the study

Heavy mineral sands are widely distributed along the South African coastal regions and include minerals such as zircon, rutile, monazite and ilmenite which are very important for South Africa's economy. Worldwide, South Africa has the second largest deposit of ilmenite and the mineral is separated from the rest of the heavy mineral sands and used as main titanium source. The mining activities are concentrated along the eastern and western coast north of Cape Town (**Figure 1.2**) and include the Namakwa sand and Richards Bay mines.[14,15]

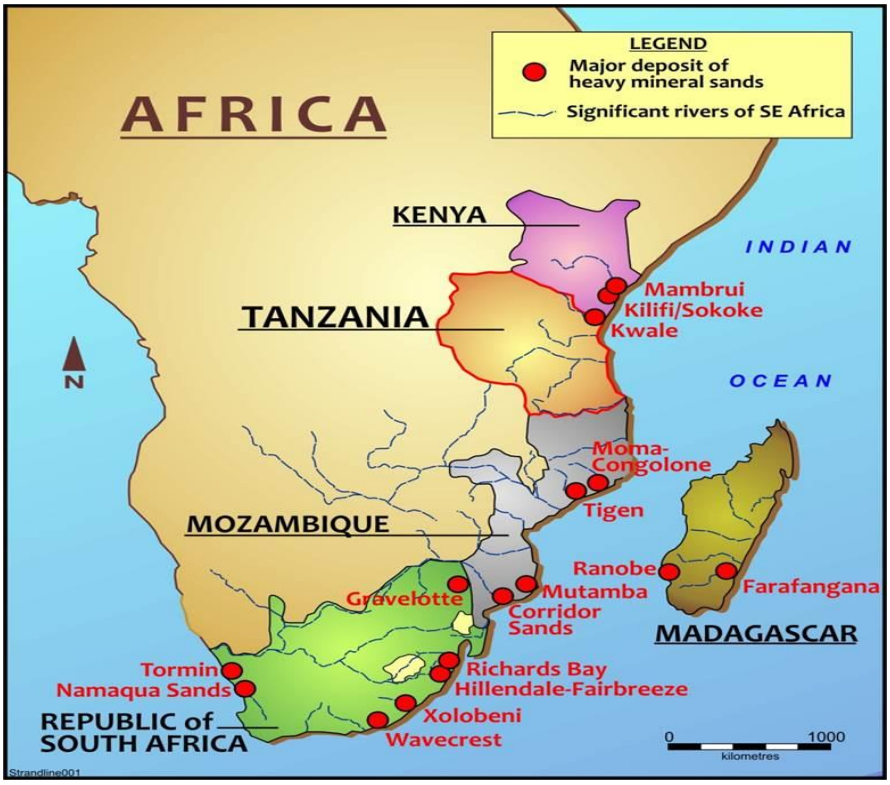

Figure 1.2: Major heavy mineral sand deposits in South Africa and other south eastern countries.[16]

14 Kotzé, H., Bessinger, D. and Beukes, J., Ilmenite smelting at Ticor SA, *South African, Pyrometallurgy*, pp.203-214 (2006)

15 Shaping South Africa through science, [Accessed 15-02-2016]. Available from: http://www.sabc.co.za/news/a/2adf4d804a311f9aa4e0efa53d9712f0/-Shaping-South-Africa-through-science-20151013

16 Tanzania Mineral Sands Project- Strandline Resources Limited, [Assessed 03-09-2016]. Available from: http://www.strandline.com.au/irm/content/tanzania-mineral-sands-project-100-strandline.aspx?RID=371&RedirectCount=1

Current research in titanium beneficiation is concentrated in finding alternative processes due to the increase in titanium demand and the high production cost associated with the current processes. Pyro metallurgical and electrochemical processes utilized for ilmenite beneficiation in South Africa are extremely energy demanding and therefore very expensive.[17] In production facilities in the country, the ilmenite is smelted at 1650 ºC through a reduction process to form two different products, namely a molten iron and a titanium slag (85 - 90 % TiO_2).[18,19] This molten iron is used in steel production while the partially beneficiated titanium slag is exported. Titanium dioxide pigment is produced at a smaller scale in the country and there is no production of titanium metal. South Africa clearly lacks a downstream industry for titanium and loses large amounts of foreign investment and capital due to its exports of this valuable commodity. The country earns approximately $ 0.20/kg when exporting, the partially beneficiated titanium metal slag and pays $ 30/kg to import it as pure titanium metal. Ilmenite beneficiation has become a priority for the South African government (AMI) projects to develop and sustain the economic grown in South Africa. The only titanium plant to produce any value-added titanium products running in South Africa is located in Pretoria and produces only titanium-powder. Both the Council for Science and Industry Research (CSIR) and Department of Science and Technology (DST) are currently involved in processes and initiatives such as the AMI to stimulate and develop the titanium metal.[15,19,20]

The potential to increase the titanium value chain and therefore economic value relies on a thorough understanding of the physical and chemical properties of this mineral as well as its final elements (Ti and Fe) and this requires the development of new skills through thorough and fundamental research. This study investigated the

17 Dworzanawski, M., The role of metallurgy in enhancing beneficiation in the South African mining industry, *The Journal of Southern African Institute of Mining and Metallurgy,* **113**(9), pp.667-683 (2013)

18 Zhang, W., Zhu, Z. and Cheng, C.Y., A literature review of titanium metallurgy processes, *Hydrometallurgy*, 108, pp.117-188 (2011)

19 Jordan, P., Evaluation of reductants used for ilmenite smelting based on CO_2 reactivity (Boudouard reaction) measurements, *The Journal of Southern African Institute of Mining and Metallurgy*,**111**(6), pp.385-392 (2011)

20 Campbell, K., SA moves to use titanium-ore platform to build new high-tech industry, [Accessed 03-08-16]. Available from: http://www.engineeringnews.co.za/article/sa-moves-to-use-titanium-ores-base-to-build-new-high-tech-industry-2013-08-30

potential of the hydrometallurgical processing of ilmenite. The study entails the investigation of the possible dissolution of ilmenite at relatively moderate temperatures using microwave dissolution and flux fusion. The difference in aqueous chemistry for titanium and iron will also be investigated to utilise those different in the possible separation of the two elements from the dissolved ilmenite.

1.3 Aim of the study

The main purpose of this study is centred at the development of cost and energy efficient analytical and separation techniques for the beneficiation (dissolution, separation and purification) of ilmenite and the objectives of the study included:

- Performing an in-depth literature study on analytical techniques for analysis of titanium in ilmenite.
- Development of analytical procedure to accurately quantity Fe and Ti in pure metals and ilmenite.
- Development of low energy demanding dissolution method for ilmenite using techniques such as fusion and microwave digestion.
- Investigation in the use of different inorganic/organic ligands for selective precipitation of Fe and Ti.
- Investigating the separation of Fe and Ti using ion exchange with different resins.
- Investigating the separation of Fe and Ti with solvent extraction using different chelating agents and different solvent system.
- Performing statistical evaluation of the analytical data and report the results as a thesis.

2 Introduction

2.1 Introduction

In 1791, William Gregory studied a black sand sample called menachanite (now known as ilmenite) which he obtained from the Manaccan (Menacan) valley in the south-west of England. The sand was magnetic and looked very similar to gunpowder. He also found that the black sand contained a mineral with the following composition: magnetite (46 %), silica (3.5 %), reddish brown calx (45 %) and after heating also reported a mass loss of 4.94 %.[21] He also discovered that the magnetic part was rich in iron-oxide. At that stage iron was already a well-known metal of ancient origin and had been mined from approximately 1200 B.C.[22] The reddish brown calx which he could not identify gave the following products in different chemical environments: (i) a yellow solution when dissolved in sulfuric acid (ii) the colour changed from reddish brown to purple when reduced with either zinc, iron or tin and (iii) a purple slag was formed when the calx was fused with charcoal. Gregory named the unknown element (reddish brown calx) manachite and reported his findings to a German Science Journal and the Royal Geology of Cornwall.[21,23]

In 1795, Martin Heinrich Klaproth[24] studied a sample specimen from Hungary and after separating the Hungarian red schorl from this sample, he discovered that the sample consisted in part iron and also an unknown metallic oxide. He isolated the reddish brown mineral and found that it contained a new metal oxide which he named titanium after the Titans in Greek mythology due to its apparent strength. He also identified the same element (titanium) in the mineral titanite (33 % TiO_2). Aware

21 Mellor, J.W.A., A Comprehensive Treatise on Inorganic and Theoretical Chemistry, 12, p.1 (1924)

22 Nicholls, D., The Chemistry of Iron, Cobalt and Nickel: Comprehensive Inorganic Chemistry, pp.979-986 (1973)

23 Ensley, J., Nature's Building Blocks: An A-Z guide to the Elements, pp.559-565 (2011)

24 Weeks, M.E., The discovery of the elements XI: Some elements isolated with the acid of potassium and sodium: Zirconium, Titanium, Cerium, and Thorium, *Journal of Chemical Education*, **9**(6), pp.1233,1234 (1932)

of Gregory studies in 1791, he also studied the mineral sample from Manaccan and found the following composition; iron oxide (51 %), titanium dioxide (42.25 %), silica (3.5 %) and manganese oxide (0.25 %). The two mineral samples (from Cornwall and Hungary) contained the same metal oxide (TiO_2) and this confirmed Gregory's initial discovery of the element titanium.[21,24]

Ilmenite and rutile are the only titanium minerals which are currently commercially mined for titanium production. Rutile (TiO_2) has a higher titanium content compared to ilmenite, but Ilmenite ($FeTiO_3$) is the more abundant ore. Ilmenite is mined from heavy mineral deposits and magmatic rock deposits and then upgraded (due to its high iron content) to titanium slag and synthetic rutile. The synthetic rutile and the titanium slag are used as feedstock production for titanium processing to produce titanium dioxide and titanium metal.[4,9]

Titanium dioxide has been produced since the early 1900s.[9] The initial challenges were the production of pure titanium metal due to its high affinity for oxygen, carbon and nitrogen. In 1946, the US Bureau of Mines produced pure titanium using the Kroll method which involves conversion of TiO_2 to $TiCl_4$ followed by the reduction of the titanium chloride to titanium metal using magnesium as reducing agent (see **Equation 2.1** and **2.2**).[25] The process was capable of producing 7 kg (15 lb) batches of quality titanium powder. The Kroll process was later replaced by the Hunter's method which involved the reduction of $TiCl_4$ with sodium (**Equation 2.3**) at a temperature above 75 ºC but proved more complex with the difficulty to remove the produced NaCl waste. The Kroll process on the other hand was relatively cheaper, allowed a wide operational temperature ranges (711 - 1120 ºC) and the $MgCl_2$ by-product was easily removed by vacuum distillation.[26]

$$2FeTiO_{3(s)} + 7Cl_{2(g)} + 6C_{(g)} \xrightarrow{900^\circ C} 2TiCl_{4(g)} + 2FeCl_{3(s)} + 6CO_{(g)} \qquad \textbf{2.1}$$

$$TiCl_{4(g)} + 2Mg_{(l)} \xrightarrow{711\text{–}1120^\circ C} 2MgCl_{2(g)} + Ti_{(s)} \qquad \textbf{2.2}$$

25 Froes, F.H.(ed), Titanium: Physical Metallurgy, Processing, and Applications, pp.1-7 (2015)

26 Shamsuddin, M., Physical Chemistry of Metallurgical Processes, pp.367,369,366 (2016)

$$TiCl_{4(g)} + 4Na_{(l)} \longrightarrow 4NaCl_{(l)} + Ti_{(s)} \quad \textbf{2.3}$$

2.2 Titanium distribution

Titanium is one of the widely distributed elements on the planet/earth. It has been detected in human bodies and occurs in blood, bones and tissues and it is estimated that we consume approximately 0.8 mg of titanium per day. Titanium oxide bands are also found in the spectra of M-type stars.[23] Estimate concentrations of titanium for different environments are presented in **Table 2.1**.

Table 2.1: Titanium concentrations in different environments[27]

Location	ppb by weight	ppb by atoms
Universe	3000	80
Sun	4000	100
Meteorite (Carbonaceous)	550000	230000
Crustal rocks	6600000	2900000
Sea water	1	0.13
stream	3	0.06

During the Apollo 11 mission in 1969, astronauts obtained a basaltic rock which contained pyroxene, ilmenite and plagioclase. In this rock, it was found that Ilmenite is the third most abundant lunar mineral which crystallised from the lunar magma at approximately 1200 ºC.[28,29] A lunar sample from specimen 10085 (**Figure 2.1**) was compared with samples from terrestrial ilmenite or similar compositions from the olivine-labradorite-clinopyroxene-magnetite-ilmenite basaltic flow from the Pliocene age which was discovered in Obom Ethiopia. Both minerals were found to be very

27 Titanium: geological information, [Accessed 15-04-16]. Available from: https://www.webelements.com/titanium/geology.html

28 Levinson, A.A. and Taylor, R.S., Moon Rocks and Minerals: Scientific Results of the Study of the Apollo 11 Rocks Lunar Sample with Preliminary Data and Apollo 12 Samples, p.65 (1971)

29 Raymond, K.N. and Wenk, H.R., Lunar ilmenite (Refinement of the crystal structure), *Contributions to Mineralogy and Petrology*, **30**(1), pp.135-136 (1971)

similar proving that ilmenite does indeed occur in the moon as indicated by the elemental analysis reported in (**Table 2.2**).[29]

Figure 2.1: A basaltic rock from Apollo 11 which contains ilmenite.[30]

Table 2.2: Analysis of lunar and terrestrial ilmenite with microprobe analysis[29]

Composition	Weight percent	
	Moon	**Earth**
TiO_2	52.6	47.6
$FeO_{(total)}$	45.3	48.0
MgO	1.23	1.38
MnO	0.33	0.42
Al_2O_3	0.05	0.2
SiO_2	< 0.01	< 0.02
Cr_2O_3	0.78	0.08
V_2O_3	0.00	0.70
Total	**100.29**	**98.40**

Basaltic rocks collected by the Apollo 11 and 17 missions (aged to be 3.7×10^9 years old) showed an average TiO_2 content of 12 % which was higher compared to that obtained from the basaltic rock samples collected by the Apollo 12 and 15 missions which yields TiO_2 (3.2 and 2.2 %) with an estimated age of 3.2×10^9 years. These

30 10085-Coarse grained basalt, [Accessed 16-04-2016]. Available from: http://www.virtualmicroscope.org/content/10085-coarse-grained-basalt

led scientists to believe that the titanium content of lunar basaltic rocks is controlled by the age of its formation. Ca,Al-rich chondrules received a lot of attention in the 1970s due to their unusual spinel, melilite and pyroxene content. Martin and Mason *et al* obtained 1.0 - 1.5 % TiO_2 content and through a microprobe analysis while Marvin *et al* and Fuchs *et al* concluded that the host rock for this titanium deposits was pyroxene.[31]

In crustal rocks ilmenite occurs in two types of deposits, namely magmatic hard rock and place deposits. The magmatic hard rock deposits (primary deposits) contain economic viable concentrations of titanium and is often associated with anorthosite type of rocks from the Proterozoic period. The principal ore minerals of these deposits include ilmenite ($FeTiO_3$), hemo-ilmenite (exsolution lamellae), titanomagnetite and alvuspinel (Fe_2TiO_4). These minerals contain titanium dioxide concentrations between 10 - 45 % and 34 - 45 % iron oxide.[3] These deposits usually occur discordant in the host rock and therefore vary in size and shapes (dyke-like, tabular and lenticular). The host rock concentration is usually alkaline in nature due to high CaO and MgO content resulting in alkaline ilmenite samples.[3,32,33] China is rich in alkaline ilmenite which is found in titanoferous magnetite deposits at Panzhihua in the Sichuam province. Picroilmenite (magnesium rich ilmenite) is found in kimberlites in South Africa and is usually associated with diamond host minerals and as such is commonly used as an indicator for the presence of diamonds.[34,35] The oxide-apatite gabbronorite rocks are also becoming an important source for titanium extraction since these titanium ore deposits contain less Cr and Mg impurities. There are currently three well known mining locations where magmatic ilmenite is produced and these locations are Lac Tio (Quebec, Canada), Damia (China) and Tellnes (Norway)

31 Mason, B., High-titanium lunar basalts: A possible source in the Allende meteorite, *Geochemical Journal*, 9, pp.1-5 (1975)

32 Charlier, B., Namur, O., Bolle, O., Latypov, R. and Duchesne, J., Fe-Ti-V-P ore deposits associated with Proterozoic massif type anorthosites and related rocks, *Earth-Science Reviews*, 141, pp.56-81 (2015)

33 Cardarelli, F., Material Handbook: A Concise Desktop References, 2nd edition, pp.65-66,278-279 (2008)

34 Kogel, J.E., Trivedi, N.C. and Barker, J.M.(ed), Industrial Minerals and Rocks: Commodities, Market, and Uses, 7th edition, pp.987-995 (2006)

35 Kennedy, B.A.(ed), Surface Mining, 2nd edition, pp.246-258 (1990)

which mines the hemo-ilmenite type of ores from anorthosite and norite rocks (**Figure 2.2**).[3,32]

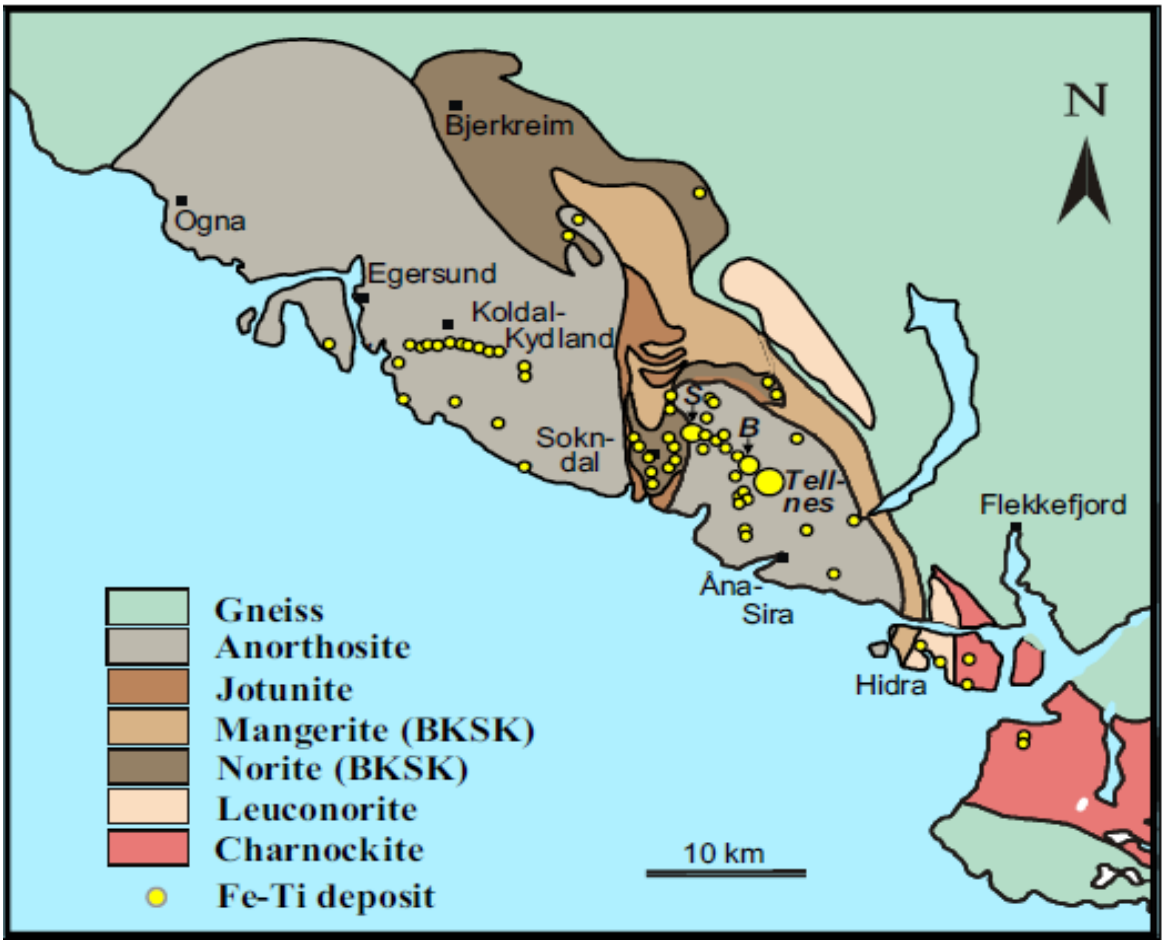

Figure 2.2: Tellnes deposits in Norway showing significant magmatic deposits Fe-Ti.[36]

Placer deposits (secondary deposits) are the most important titanium (Ti-Fe deposits) sources due to their global distribution. These deposits are mostly found as mineral sands which are naturally enriched by the gravity segregation of heavy minerals (density > 2.85 g/cm^3) and which are chemically resistant to weathering (**Table 2.3**). The composition of these minerals depends on the geological terrane as well as the impurities added during weathering.[3,35]

Table 2.3: Some common titanium containing heavy mineral sands and their specific gravity[6]

Minerals	Ideal composition	Specific gravity
Ilmenite	$FeTiO_3$	4.7
Zircon	$(Zr,Hf,U)SiO_4$	4.7
Rutile	TiO_2	4.2 - 4.3
Monazite	$(Ce,La,Y,Th)PO_4$	4.6 - 5.4
Garnet	$(Mg,Fe,Mn,Ca)Al_2OSi_3O_{12}$	3.1 - 4.3
Sillimanite	Al_2SiO_5	3.2
Corundum	Al_2O_5	4.0
Xenotime	YPO_4	4.4 - 5.1

Placer deposits are divided into beach sand dune and alluvial deposits. The ilmenite present in beach sand dune deposits usually contain high TiO_2 content (32 - 80 %) due to the leaching of iron during the weathering process and this forms leucoxene (modified ilmenite) with 70 - 80 % TiO_2. However, the weathering may also contribute significantly to an increase in impurities concentrations such as manganese and magnesium as well as radioactive minerals (such as monazite and zircon) which contain radionuclides such as uranium and thorium. Onshore winds may also blow the lighter grains inland and this can lead to an increase in both the titanium and impurities concentrations at the seaside point of the coastal dunes. These types of deposits are distributed along the Australian, South African, Mozambican, Madagascan, Indian and Vietnamese coastal regions. Alluvial placer deposits on the other hand are concentrated with titanium due to the weathering of garnet amphibolite and leucocratic garnet granulite. Economically explorable deposits from this source are rare and ilmenite in these deposits contains low titanium concentrations. The largest mining activity of this type of titanium deposit is the Gbangbama mine in Sierra Leone which mines intrusive anorthosite rutile deposits (TiO_2).[3,35]

36 Korneliussen, A., McEnroe, S.A. and Nilsson, L.P., An overview of titanium deposits in Norway, *Norges Geologiske Undersøkelse Bulletin,* 436, pp.27-38 (2000)

Titanium also occurs in different types of minerals (**Table 2.4**) mostly as oxides and silicate rocks.[3] Iron in these deposits can occur as oxides, hydroxides, carbonate and sulphate. Titanium oxide usually occurs as intergrowth clusters in the hematite (Fe_2O_3) and magnetite (Fe_2O_4) minerals. It also occurs in sphene, biotite, hornblende and in reduced concentrations in silicate minerals such askaersutitic amphibolite (10.3 % TiO_2) and melanitic andradite (17.1 % TiO_2).[3,23]

Table 2.4: Titanium containing minerals with estimated TiO_2 concentrations[6]

Mineral	Formula	TiO_2 percentage (%)
Rutile, Anatase, Brookite	TiO_2	95 - 100
Leucoxene	$FeTiO_3$	70 - 100
Altered ilmenite	$FeTiO_3$ - Fe_2TiO_9	53 - 70
Pseudorutile	$FeTiO_9$	60 - 65
Perovskite	$CaTiO_2$	58
Ilmenite	$FeTiO_3$	45 - 53
Titanite (Sphene)	$CaTiSiO_5$	40
Ulvospinel	$FeTiO_4$	36
Pseudobrookite	Fe_2TiO_5	33
Titanohematite	$(Fe,Ti)_2O_3$	0 - 34
Titanomagnetite	$(Fe,Ti)_2O_4$	0 - 30

2.3 Production, Market and Beneficiation

2.3.1 Production

The first industrial method developed for the extraction of titanium from its minerals was developed in 1916 by Farup and Jebsen.[36] Their method was adopted in 1917 by Titania A/S (in Norway) which mined the Storgangen deposit. In the same year (1916) titanium mining was initiated in the United States at Pablo Beach in Florida. This Florida mine which used ilmenite and rutile as stock material, became the

largest titanium mine during that period. Initially the titanium was mined to produce $TiCl_4$ which was used for bullets and smokescreen manufacturing. The Florida mines ceased their productions in 1928 leading to the exploration of new commercially viable deposits and by the 1940s a number of deposits were discovered. Amongst the newly discovered mines were the Tahawus deposit in New York, the eastern Quebec deposit and the Trail Ridge Sand deposits in Florida.[35] Commercial titanium production increased significantly during the 1950s due to its high demand in the aircraft industry which consumed approximately 70 % of the total titanium metal. [25,37] In that period titanium was produced from minerals deposits containing 30 % rutile (which decreased to < 1 % by 1981). Currently 92 % of titanium production is produced from ilmenite.[25] Several companies which include Remington Arms isolate the Ti from ilmenite using the sulphate process.[18] Many companies around the globe (see **Figure 2.3**) use the chloride beneficiation process instead of the old sulphate method for Ti production. The chloride route has several advantages which include easy waste disposal and low energy consuption.[15,18] However, the process also requires high grade TiO_2 feed stock such as titanium slag and rutile, which in turn calls for improved primary processes such as crushing and washing of the primary source.[38,39]

37 Global and China Titanium Dioxide Industry Report, 2015-2018, [Accessed 12-04-2016]. Available from: http://www.prnewswire.com/news-releases/global-and-china-titanium-dioxide-industry-report-2015-2018-300197732.html

38 Oil and Colour Chemists Association of Australia, Surface Coatings: Vol 1-Raw Materials and their Uses, p.305 (1983)

39 Wilson, A.D., Nicholson, J.W. and Presser, H.J.(ed), Surface Coatings-2, pp.183-184 (1988)

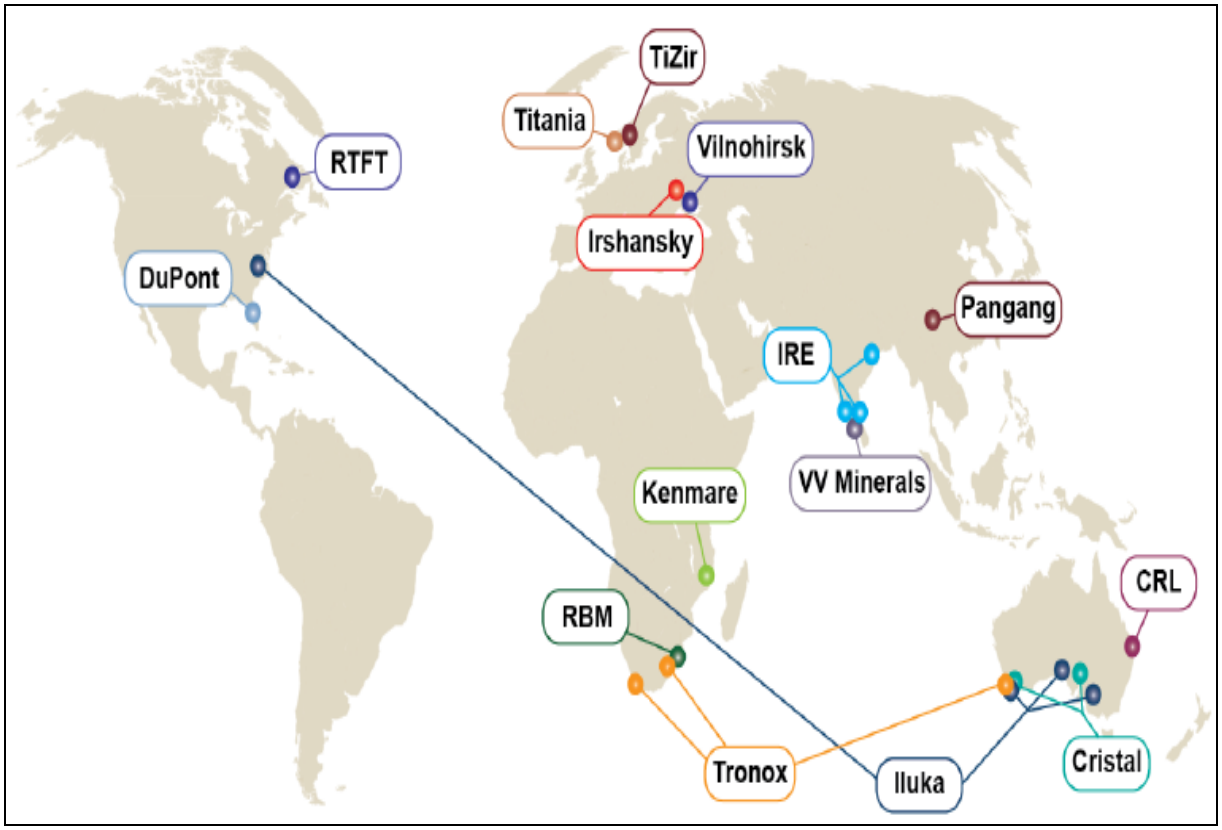

Figure 2.3: Major international suppliers of titanium.[40]

There are only a few campanies that produce titanium sponge in the world but interestingly the price for titanium sponge has managed to remain stable from 2010 and 2014 (**Figure 2.4**) due to improved titanium metal production process. China is the largest producer of titanium sponge and 110.000 metric tons was produced in 2014.[4]

40 McCoy, D., Feedstock pressure on titanium sponge market, [Accessed 14-04-2016]. Available from: http://c.ymcdn.com/sites/www.titanium.org/resource/resmgr/2010_2014_papers/McCoyDavidTiUSA2013SupplyTre.pdf

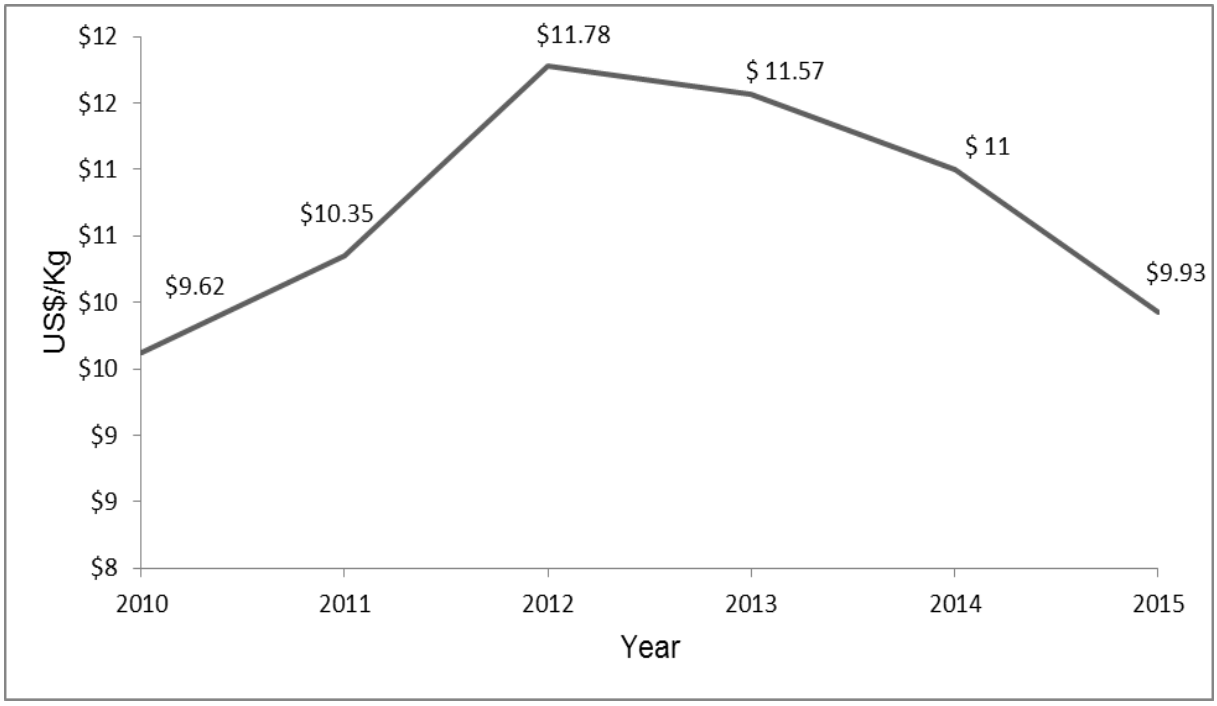

Figure 2.4: Titanium sponge metal price, yearend from 2010 to 2015.[4,42]

Currently a large percentage of titanium on the global market is extracted from heavy mineral sands, mainly due to convenient and cheaper processing of these primary sources compared to the mining and processing of mineral rocks. In most of these deposits, ilmenite is associated with high chromium content (Cr_2O_3) which makes the magnetic separation of ilmenite difficult as both Cr_2O_3 and $FeTiO_3$ have very similar magnetic susceptibility properties. Geologist have found another Ti containing mineral deposits such as the oxide-apatite gabbronorite and found that titanium in these deposits can be recovered simultaneously with vanadium and phosphorus since this type of deposits are low in Cr and Mg impurities. One of these deposits is found at the Fedorivka intrusion in Ukraine.[25,41]

The Tellnes mines (**Figure 2.2**) which took over from Titania A/S after it had ceased its production in 1965, produces 550.000 tons of ilmenite annually[36] while China, Australia and South Africa are currently the leading Ti producers (**Figure 2.5**) in the world. China has the largest ilmenite mine production capacity while Australia and South Africa produces ilmenite and rutile in significant quantities and have the world's

41 Gambogi, J. and Gerdemann, S.J., Titanium metal: extraction to application, [Accessed 19-04-2016]. Available from: http://www.osti.gov/scitech/servlets/purl/900531

largest natural reserves for both ores. In 2015, the estimated ilmenite and rutile production was 5,610 and 480 thousand metric tons respectively with the total world reserve estimated to be between 740,000 and 54,000 thousand metric tons.[4]

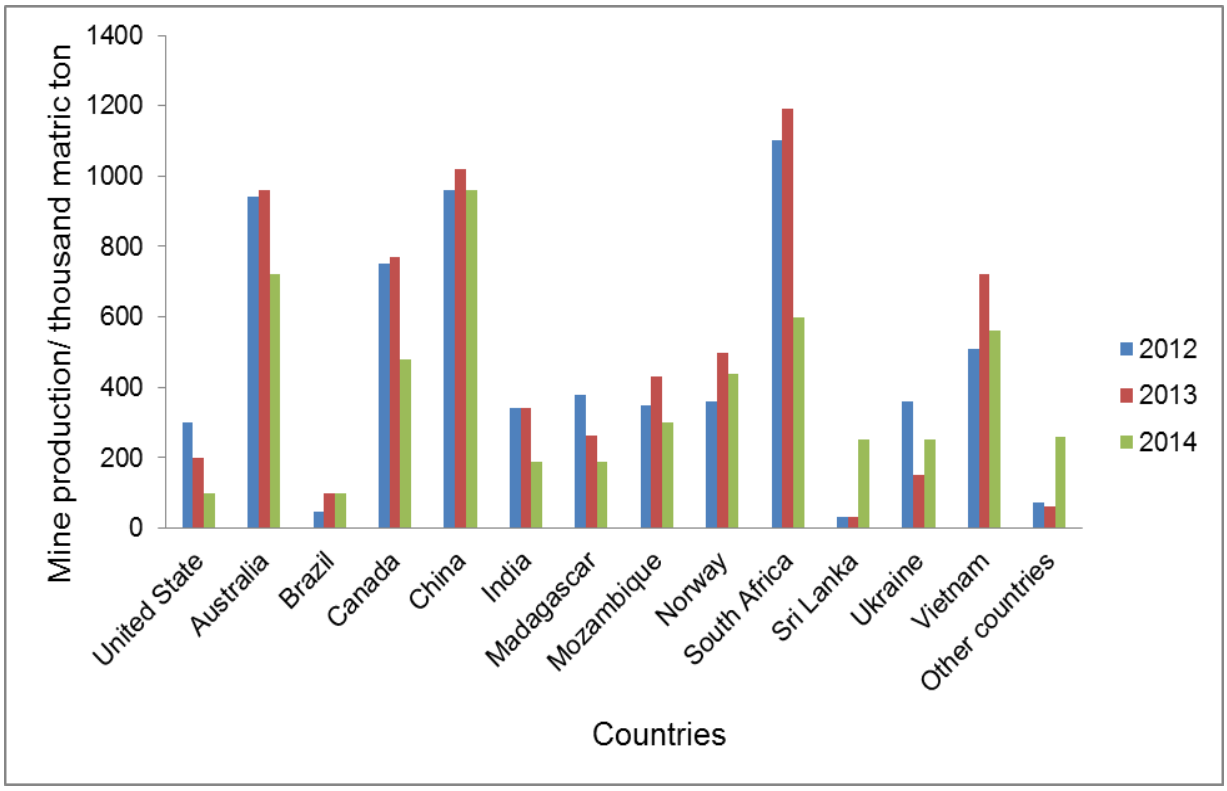

Figure 2.5: Mine production of ilmenite in different countries from 2012 to 2014.[4,42,43]

In China the titanium production from ilmenite only started in 1954 and currently titanium is mainly produced from ilmenite as mineral source. In addition to the local mining and production of titanium oxide, China also imports titanium from other countries such as Vietnam to meet its high demand for titanium to produce titanium dioxide and titanium sponge.[44,45] In this country the titanium ore resources are mostly distributed in the Sichuan, Shangdong, Hebei, Yunna and Hainan provinces and the ilmenite is usually mined together with monazite. Chinese titanium dioxide producers

42 Bedinger, G.M., Titanium Mineral Commodity Summaries 2015, U.S. Geological Survey, pp.170,173 (2015)

43 Bedinger, G.M., Titanium Mineral Commodity Summaries 2014, U.S. Geological Survey, p.173 (2014)

44 Titanium resources, reserves and production, [Assessed 02-15-2016]. Available from: http://metalpedia.asianmetal.com/metal/titanium/resources&production.shtml

use both the sulphate (large scale) and chloride processes.[45] A report by the USGS (2016) has indicated that a number of titanium dioxide plants in China with a production capacity of approximately 280,000 tons/year have been closed down due to environmental and overcapacity reasons.[4] China is also the largest consumer and importer of iron-ore as it beneficiates the iron from minerals such as hematite, magnetite and vanadium-titanium magnetite. In 2013, 12 % of the iron that was produced was obtained from ilmenite (Vanadium-titanium magnetite) with 64 % produced from magnetite. In 2014, China produced 1,510 million metric tons of iron from its mineral ore deposits which accounts for the largest iron production in the world.[46]

Currently Australia is the world's largest heavy mineral sands mining destiny and has the highest production and reserves for both ilmenite and rutile (**Figure 2.6**). Titanium mining in Australia started in 1934 and by 1956 the mining activities were extended to the western part of that country.[47] Illuka resources have been mining and processing the mineral sand deposit in Jacinth and Ambrosia since 2009. In 2011 the company discovered new deposits (Atacama) which contained up to 75 % of ilmenite and leucoxene (altered ilmenite). Bemax Resources limited started their first heavy mineral sands operation in the Murry Basin in 2005 and by 2006 Illuka resources took the initiative to reopen previously closed mines to mine and process the remaining heavy mineral sand deposits at these sites.[3]

45 Liu, H.C., Sung, W.P. and Yao, W.(ed), Computer, Intelligent Computing and Education Technology, volume 1, p.1134 (2014)

46 Lu, L.(ed), Iron ore: Mineralogy, Processing and Environmental Sustainability, pp.5-8 (2015)

47 Elsner, H., Assessment Manual: Heavy Minerals of Economic Importance, Bundesanstalt für. Geowissenschaften und Rohstoffe (BGR), pp.23-37 (2010)

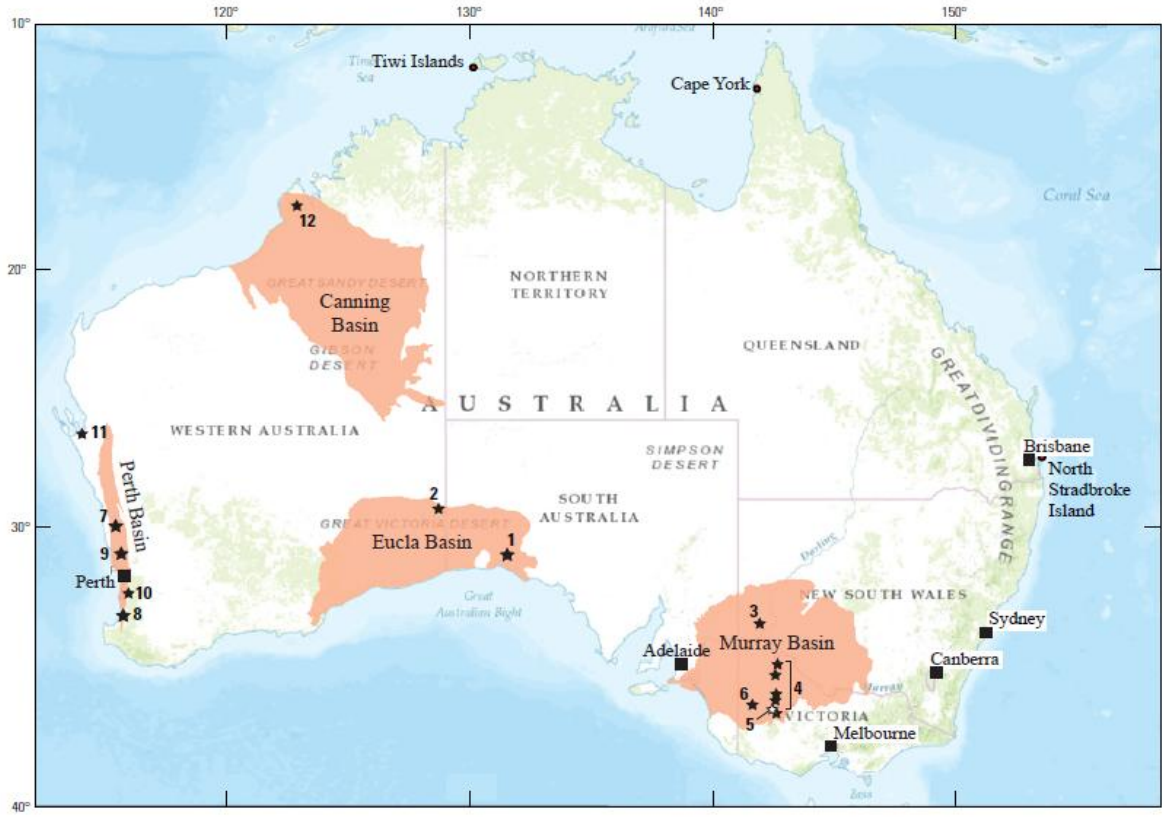

Figure 2.6: Australia with the main basins where titanium is mined.[3]

In South Africa titanium is produced from beach sand deposits. The major mines include Namakwa Sand, Richards Bay Minerals and Exxaro's Hillendale (see **Chapter 1, Figure 1.2**). The Richards Bay Minerals (RBM) operation (**Figure 2.7**) is situated in KwaZulu Natal. Since 1980 this company has been producing titanium slag (85 % titanium dioxide) as its primary product from ilmenite as source and 94 % titanium dioxide from rutile[48] using both the sulphate and chloride processing routes.[3] The pig iron which is produced during ilmenite beneficiation is used for the production of a low-manganese iron alloy. The plant has a capacity to produce about one million tons of slag and 550.000 tons of pig iron. A report from Rio Tinto (owners of RBM) indicated a decrease of 25 % in titanium dioxide slag production by 2015 due to lower demands for high grade feedstock.[49]

48 William, G.E. and Steenkamp J.D., Heavy mineral processing at Richards Bay Minerals, *South African Pyrometallurgy*, pp.181-187 (2006)

49 Rio Tinto: 2015 full year results, [Assessed-12-04-2016]. Available from: http://www.riotinto.com/documents/160211_Rio%20Tinto%202015%20full%20year%20results.pdf

Figure 2.7: Richards May Minerals (RBM) mining of heavy mineral sands.[50]

Namakwa Sand (operated by Tronox) is located in the Western Cape of South Africa and has been producing titanium slag (86.5 % TiO_2, 10 % FeO) since 1995 with annual capacity of 190.000 metric tons and has an estimated mine life of more than 20 years.[51,52] Recently (April 2016), a new mine (Fairbreeze mine) with an estimated mine lifespan of 15 years was opened by Tronox in KwaZulu Natal (**Figure 2.8**) to replace the KZN Hillendale production quota which was closed in 2014. Another important titanium producer is the Moma mine (**Chapter 1, Figure 1.2**) in Mozambique which started its operation in 2007. In 2013 the Moma mine produced 720,100 tons of ilmenite which has an estimate titanium mine life of more than 100 years.[53]

50 Supplier; Mineral-Loy, [Accessed 09-05-2016]. Available from: http://www.mineral-loy.co.za/suppliers/

51 Gous, M., An overview of Namakwa Sands ilmenite smelting operations, *The Journal of The South African Institute of Mining and Metallurgy*, 106, pp.189-190 (2006)

52 Positive Impact: Tronox Fairbreeze Mine in South Africa, Tronox, [Accessed 02-05-2016]. Available from: http://files.shareholder.com/downloads/TRX/0x0x785865/c54223d1-421f-4105-a4a7-27368fd78542/Fairbreeze%20Presentation%20-%20JF.pdf

53 Kenmare Resource plc Moma Titanium Minerals Mine, [Accessed 15-04-2016]. Available from; http://www.kenmareresources.com/~/media/Files/K/Kenmare-Resources-PLC/pdf/presentations/Moma%20Site%20310114.pdf

Figure 2.8: The Fairbreeze mine located in Mtunzini Kwa-Zulu Natal.[54]

2.3.2 Market

Titanium metal remains expensive relative to aluminium and steel (**Table 2.5**) resulting in relativel lower than expected global consumption of the titanium material. The high price of titanium is mainly due to its relatively high costs of mineral processing and extraction (**Table 2.6**).[25] The titamium market is also small and major buyers such as the military aircraft manufacturing industry prefer long term contract prices to avoid price flactuation and at the same this structure secure a profit for the suppliers.[55] Research done by the RAND Corporation indicate that the smaller markets are oftern exposed to instability due to supply and demand shocks as a result of smaller numbers of buyers and suppliers.[25,55]

Iron is a relatively cheap metal compared to titanium. Its market is dominated by magnetite, hematite, geothite and siderite as primary sources. Iron produced from

54 Proposed Exxarro mining at Mtunzini, [Accessed 30-08-2016]. Available from: http://www.mtunzini.co.za/exxaro.htm

55 Seong, S., Younossi, O. and Goldsmith, B.W., Titanium: Industry base, Price trends, and Technology initiatives, Rand Corporation, pp.29-32 (2009)

ilmenite processing is dominated by pig iron and steel production market due to its high carbon content (3.5 - 4.5 %). China has the largest pig iron production in the world and produced over 700 million metric tons in 2014. Worldwide both the production both pig iron and raw steel were estimated to be 110 million tons.[56]

Table 2.5: Comparison of titanium price with aluminium and steel[25]

Item	Contract prices, 2014 US$/lb		
	Steel	**Aluminum**	**Titanium**
Ore	0.02	0.10	0.22 (rutile)
Metal	0.10	1.10	5.44
Ingot	0.15	1.15	9.07
Sheet	0.30 - 0.60	1.00 - 5.00	50 - 150

Table 2.6: The cost of titanium containing material prior titanium metal production[25]

Precursor	2014, US$/lb	Cost of contained titanium,2014, US$/lb
[a]TiO_2	1.75	2.94
$TiCl_4$	1.00	4.00
Titanium sponge	5.44	5.44

[a] Metal grade

Ilmenite, rutile and titanium slag compete as feedstock resources for production of titanium dioxide and this product accounts for 95 % of titanium consumption in 2015. Ilmenites natural abundance makes it the cheap ore compared to rutile (**Table 2.7**).

56 Fanton, M.D., Iron and Steel Mineral Commodity Summaries 2016, U.S Geological Survey, pp.84-86 (2016)

Table 2.7: The price of different titanium dioxide manufactured from different sources[4]

TiO_2 precursors	Price (TiO_2) US$/Kg				
	2011	**2012**	**2013**	**2014**	**2015[e]**
Ilmenite (54 % TiO_2)*	0.195	0.300	0.265	0.155	0.110
Rutile (95 % TiO_2)*	1.350	2.200	1.250	0.950	0.840
Slag (80 - 95 % TiO_2)	0.463-0.489	0.694-0.839	0.538-0.777	0.720-0.762	0.742-0.755

[e] Estimates
*Minimum TiO_2 percentage

2.3.3 Beneficiation

2.3.3.1 Mining of ilmenite ore

The hard rock material which contains titanium is mined from the underground resources and uses blasting and the crushing of the rocks to expose/liberate the material from its surrounding.[41,57] On the other hand, the heavy mineral sands are mined on the surface using a dredge or dry method and the minerals which contain high concentration of titanium material are processed using conventional techniques such as froth flotation and gravity separation. The dry mining method entails the digging of the ore and its subsequent transportation using a pump or conveyor belts. This method is usually used for small scale mining as well as hard rock deposits and is used by QIT (Rio Tinto) in Canada for the mining of hard rock material and also by Namakwa Sands (Tronox) in South Africa for mining of the heavy mineral sands. The dredging method (relatively the cheaper method) uses a bucket wheel to draw underwater titanium ore to a floating wet mill. The titanium ore is then recovered from waste by a gravity separation process in a wet spiral concentrator.[58,59] Companies

57 Benjamin P., Mineral Sand Geology and Exploration, Iluka, 2011, [Accessed-06-07-2016] Available from; https://www.iluka.com/docs/company-presentations/mineral-sands-technical-presentation-sydney-3-may-2011

58 Titanium processing, [Accessed O6-07-2016]. Available from: https://global.britannica.com/technology/titanium-processing#ref623441

which uses this method of mining operations include Illuka Company in Australia and Kenma Resource in Mozambique which both mine the heavy mineral sands. Another method which is used (although uncommon) is the hydraulic mining technique which uses a high pressure water jet to split titanium minerals in unconsolidated placer deposits. The method is used by Fairbreeze mine which took over the KZN sands (previously ceased) activities in South Africa.[60,61]

Once the mineral sands have been mined, the titanium containing minerals are concentrated. There are different types of concentrators which vary with equipment's designs and capacity. A wet concentrator uses sizing and the gravity properties of heavy mineral sands while dry concentrator uses magnetic and electrostatic properties to concentrate the Ti containing ore.[58] Magnetic separation is commonly used to separate ilmenite from non-magnetic Ti containing minerals such as zircon and rutile **(Figure 2.9**). For ilmenite associated with high Cr_2O_3 content, the mineral is roasted at 730 - 800 ºC in a fluidised bed roaster to increase the magnetic susceptibility of Cr_2O_3 for the effective separation from the rest of the material. This step is necessary as both Cr_2O_3 and $FeTiO_3$ in its natural material have similar magnetic characteristics.[62]

59 Mineral Sands: An Overview of the Industry, [Accessed 02-05-2016]. Available from: https://www.iluka.com/docs/company-presentations/mineral-sands---an-overview-of-the-industry-by-greg-jones-manager-development-geology

60 Hydraulic mining, [Accessed 06-07-2016]. Available from: https://global.britannica.com/technology/hydraulic-mining

61 Mineral Sands Industry: Fact book, [Accessed 02-05-2016]. Available from: https://www.iluka.com/docs/default-source/industry-company-information/the-mineral-sands-industry-factbook-(feb-2014)

62 Tonder, W., South African Titanium: Techno-economic evaluation of alternatives to Kroll process, M.Eng. Thesis, Stellenbosch: Stellenbosch University, pp.22-24 (2010)

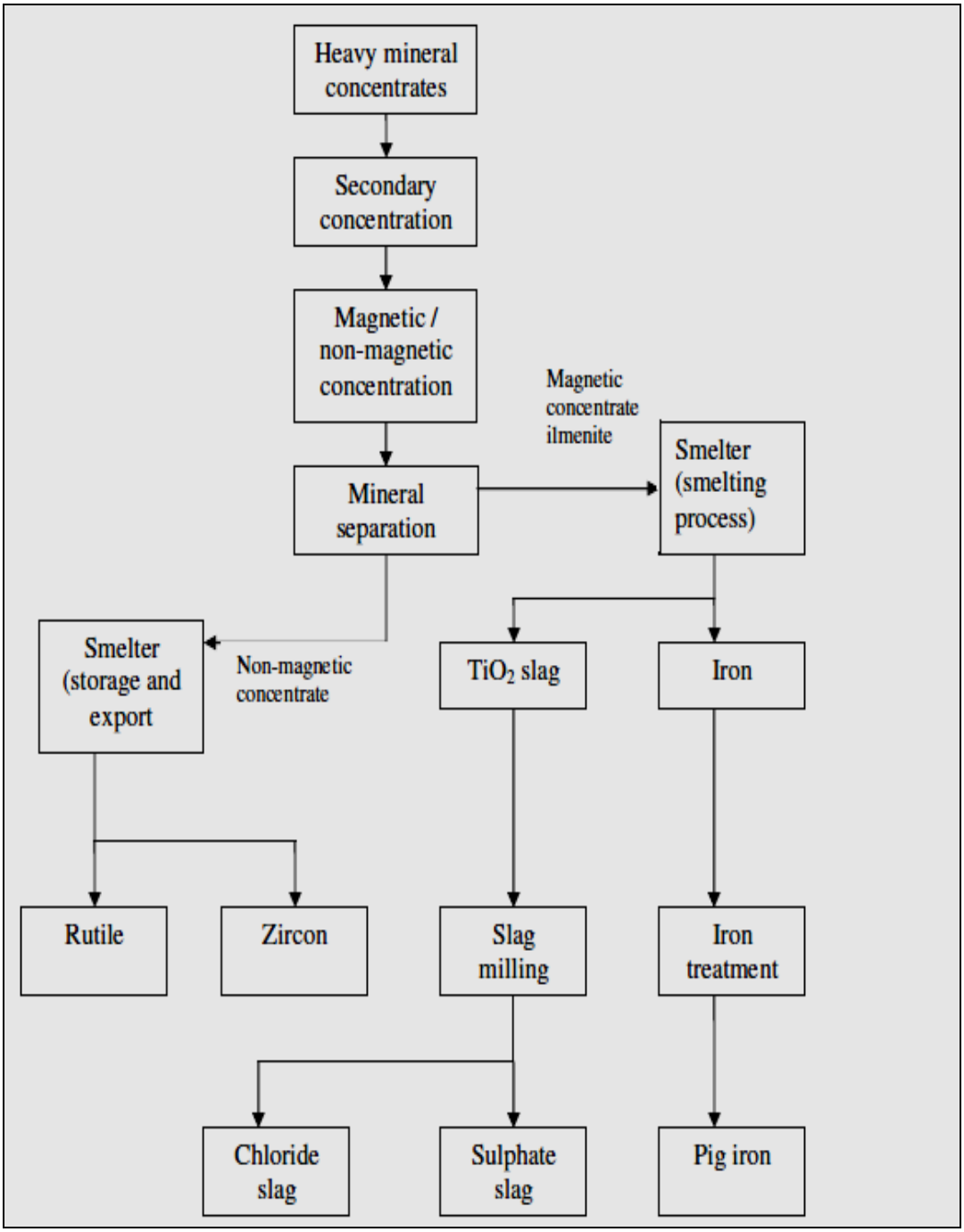

Figure 2.9: Separation of ilmenite from non-magnetic material and production of titanium slag using the smelting process.[63]

63 Motsie, R., An overview of South Africa's titanium mineral concentrate industry, Mineral Economics, pp.3-5 (2008)

2.3.3.2 Processing the ore

The processing of Ti minerals, like any other mineral processing process has to adhere to government environmental[64] and energy policies. These include environmentally friendly procedures, low waste production and cost effective processes. The existing processes such as the pyro/electro metallurgical processes often require the upgrading of ilmenite ore to synthetic rutile therefore increasing TiO_2 content in the product (**Figure 2.10**). Hydrometallurgical processes such as leaching, solvent extraction, ion exchange, and precipitation techniques can also be used for beneficiation of titanium ore. This process allows for the production of TiO_2 pigment without the upgrading of the ore to synthetic rutile.[9,18]

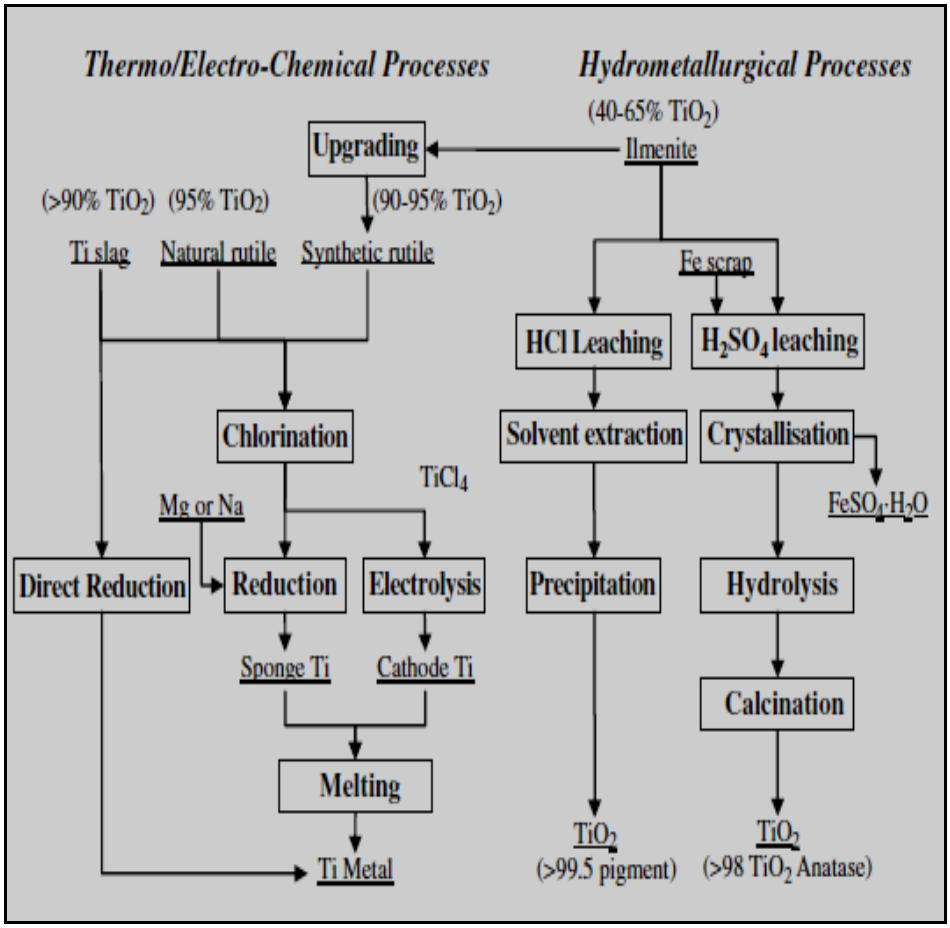

Figure 2.10: Beneficiation processes for the production of both Ti metal and TiO_2 using metallurgical processing.[18]

64 Manhique, A.J., Titanium recovery from low-grade titaniferrous minerals, PhD. Thesis, Pretoria: University of Pretoria, pp.8-14 (2012)

The two techniques used to upgrade the ilmenite ore is the smelting process which produces a titanium slag (85 - 90 % TiO_2) and the oxidation/reduction in solid state followed by acid leaching step which produces a product with 90 - 95 % TiO_2 content. The smelting process was invented in Canada to produce titanium slag (86 % TiO_2) which uses the sulphate process. In 1960s, E.L. Du Pont[65] developed the chloride process for the smelting process which is more environmentally friendly and this process was adopted by countries such as Canada, South Africa and Norway. In the smelting process, the iron content of ilmenite is removed as high purity pig iron (by-product) and produces a titanium slag (**Figure 2.9**) and requires very high temperatures (approximately 1650 ºC) to produce the titanium slag (synthetic rutile). For ilmenite rock deposits the titanium slag is often produced as a sulphate slag and cannot be used in chloride processing to produce titanium dioxide due to high impurity content which include the alkali earth oxides (CaO and MgO).[8] In South Africa, the smelting process is used by Richards Bay Minerals, Namakwa Sands and Exxaro KZN Sands. Although there are challenges such as intolerance to high impurities (especially in chloride slag), the process produces TiO_2 which contains more than 85 % titanium dioxide.

Rutile (TiO_2) is the preferred feedstock material for titanium processing. The synthetic rutile process is used to overcome the scarcity of rutile and to overcome the high price of rutile.[64] The oxidation/reduction method produces titanium dioxide with TiO_2 > 90 % while iron is recovered as fine oxide or the hydroxide.[8] The most common processing technique is the Becher process which was developed in 1961 by Robert Becher and was commercialised by the Illuka's predecessor company, RGC in 1969.[66] In the Becher process, iron is oxidised to Fe_2O_3 producing pseudo-brookite (Fe_2TiO_5) (**Equation 2.4**). The oxidised iron is then reduced to Fe metal at 1200 ºC by a carbothermic reaction in the presence of coal and sulphur (**Equation 2.5**). The solvated iron in solution is then precipitated using a 1 % NH_4Cl solution in the presence of oxygen at 80 ºC. The remaining iron is then leached to recover up to 90

65 Den Hoed, P. and Luckos, A., Oxidation and reduction of iron-titanium oxides in chemical looping combustion: A phase chemical description, *Oil & Gas Science and Technology- Review IFP Energies Nouvelles,* **66**(2), p.249 (2011)

66 Iluka's Synthetic Rutile Production, [Accessed 07-07-2016]. Available from: https://www.iluka.com/docs/mineral-sands-briefing-papers/iluka's-synthetic-rutile-production-june-2012

% TiO_2 with 0.5 M sulphuric acid.[18,67] Other methods which are used by different companies include the Murso, the Laporte, the Benelite and the Katoaka process. All this processes have been developed to upgrade ilmenite and they differ in their ore treatment and leaching procedure and have different advantages and disadvantages.[18] Iron in most of these processes is lost in the residue which is expensive to treat and is discarded as waste or scrap.[8]

$$4FeTiO_{3(s)} + O_{2(g)} \longrightarrow 2Fe_2TiO_{5(s)}) + 2TiO_{2(s)} \quad \textbf{2.4}$$

$$Fe_2TiO_{5(g)} + 3CO_{(g)} \longrightarrow 2Fe_{(s)} + TiO_{2(s)} + 3CO_{2(g)} \quad \textbf{2.5}$$

The two methods which are currently extensively used for the commercial production of titanium dioxide are the chloride and sulphate process. The chloride process (**Equation 2.6 and 2.7**) involves the conversion of titanium dioxide (impure rutile) with coke (C) in the presence of chlorine gas at a relatively high temperature (900 - 1000 ºC). This process is the more popular production method due to its lower cost and easy waste management.

$$2TiO_{2(s)} + 3C_{(l)} + 4Cl_{2(g)} \longrightarrow 2TiCl_{4(g)} + 2CO_{(g)} + CO_{2(g)} \quad \textbf{2.6}$$

$$TiCl_{4(l)} + O_{2(g)} \longrightarrow TiO_{2(s)} + 2Cl_{2(g)} \quad \textbf{2.7}$$

Iron in this process is recovered as chloride impurities. These impurities are usually neutralised with a diluted HCl solutions for disposal. The chloride process which uses ilmenite instead of titanium slag or synthetic rutile as starting material produces more waste. Some plants recover this iron chloride solution and uses it for wastewater treatment.[8]

In the sulphate process (**Equation 2.8 and 2.9**) ilmenite/ titanium slag is digested with concentrated sulphuric acid producing titanium oxygen sulphate ($TiOSO_4$) which is hydrolysed and heated (approximately 110 ºC) to produce TiO_2. If ilmenite is used

67 Noubactep, C., Metallic iron for environmental remediation: Learning from the Becher process, *Journal of Hazardous Materials*, 168, pp.1609-1612 (2009)

as feedstock, iron scrap is added to convert Fe^{3+} into Fe^{2+} and the iron is then recovered as $FeSO_4$. The rest of the iron is recovered as the hydroxide which is neutralised with diluted acid and disposed of.[8]

$$FeTiO_{3(s)} + 2H_2SO_{4(l)} \longrightarrow TiOSO_{4(l)} + FeSO_{4(s)} + 2H_2O_{(l)} \quad \textbf{2.8}$$

$$TiO_2{\cdot}nH_2O_{(l)} \longrightarrow TiO_{2(s)} + nH_2O_{(l)} \quad \textbf{2.9}$$

Titanium metal of 95 % purity was first obtained in 1887 by Lars Fredrik Nelson and Otto Patterson. In their process they used sodium to reduce the $TiCl_4$ in airtight steel cylinders and M.A Hunter modified this work and produced 99.9 % pure titanium metal.[23] In 1937 William Kroll altered Hunters method by using magnesium to reduce the titanium tetrachloride ($TiCl_4$) and currently the Kroll process is extensively used as an industrial method.[68] As previously described, the production of Ti metal involves the reaction of rutile or synthetic rutile with Cl_2 gas to produce $TiCl_4$. This intermediate is further purified in a vacuum distillation step. In the final step, the purified $TiCl_4$ is reduced with Mg or Na (C reduction producing titanium carbide) to produce pure Ti sponge which is conventional to the metal or used in Ti-alloy production. There are a number of processes which have been developed and showed good success in producing a pure titanium metal production (see **Table 2.8**)

68 Gerdemann, J.S., Titanium process technologies, *Advanced Materials and Processes*, **159**(7), p.41 (2001)

Table 2.8: Summary of the extraction processes and methods used to produce titanium metal[69,20]

Process	Method	Titanium product
FFC –Cambridge process, UK and USA	Electrolytic reduction of partially sintered TiO_2 electrode in molten $CaCl_2$	Powder blocks
CSIR, South Africa	H_2 reduction of $TiCl_4$	Sponge
OS processing, Japan	Calciothermic reduction of TiO_2	Titanium powder/sponge
CSIR Australia	-	Powder
QIT, Rio Tinto	Electrolytic reduction of Ti slag	Liquid
Amstrong/international Ti powder	Liquid Na reduction of $TiCl_4$ vapour	Powder

2.4 The mineral Ilmenite

Adolph Theodor Kupffer discovered Ilmenite (titanoferrite) in 1827 in the Ilmen Mountain, in Russia. The general chemical formula of ilmenite is $FeTiO_3$ with a typical chemical composition of (40 - 65 wt %) TiO_2 and (35 - 60 wt %) Fe_2O_3.[69] The basic properties of a pure ilmenite are presented in **Table 2.9**.

69 Nagesh, Ch.R.V.S., Ramachandran, C.S. and Subramanyam, R.B., Methods of titanium sponge production, *Transactions of the Indian Institute of Metals,* **61**(5), pp.314-348 (2008)

Table 2.9: Basic properties of pure ilmenite ($FeTiO_3$)[7]

Property	Value
Chemical classification	Oxide
Colour	Black
Streak	Black
Lustre	Metallic-submetallic
Mohs hardness	5.5 - 6
Specific gravity	4.7 - 4.8 g/cm^3
Crystal structure	Hexagonal
Cleavage	None
Twinning	{0001} simple, {10$\bar{1}$1} lamellar
Unit cell	a = b = 5.08854 (7) Å, c = 14.0924(3) Å, z = 6

The typical chemical formula of ilmenite in magmatic rocks is (Fe,Mn,Mg)TiO_3 due to the coexistence of this mineral with geikielite ($MgTiO_3$) and pyrophanite ($MnTiO_3$) in these rocks. In 1996 the FeO-Fe_2O_3-TiO_2 ternary system (**Figure 2.11**) developed by Buddington and Lindsley was adopted to describe minerals containing titanium and iron. This ternary system is important in the explanation of the magnetic properties of the ore during extraction, especially during magnetic separation. It is also used in the study of historical fluctuation in the earth's magnetic field rock.[70] Garbar *et al*[71] successfully used this system to describe the weathering behaviour of ilmenite. The ternary system shows the main titanium minerals from ilmenite to natural rutile and the iron content changes due to leucoxenization (weathering and leaching of the iron from the mineral) which only occurs above groundwater level. This leaching of iron oxide causes an increase in titanium dioxide percentage and reduces the ilmenite's magnetic susceptibility resulting in a stable TiO_2 (Rutile).[47]

70 Wilson, N.C. and Muscat, J., Structural and properties of ilmenite from first principles, *The American Physical Society,* pp.1-9 (2005)

71 Garnar, T.E., Geologic Classification and Evaluation of Heavy Mineral Deposits:12th Forum on the Geology of Industrial Mineral Deposits, Georgia Geological Survey Circular, Atlanta, 49, pp.25-35 (1978)

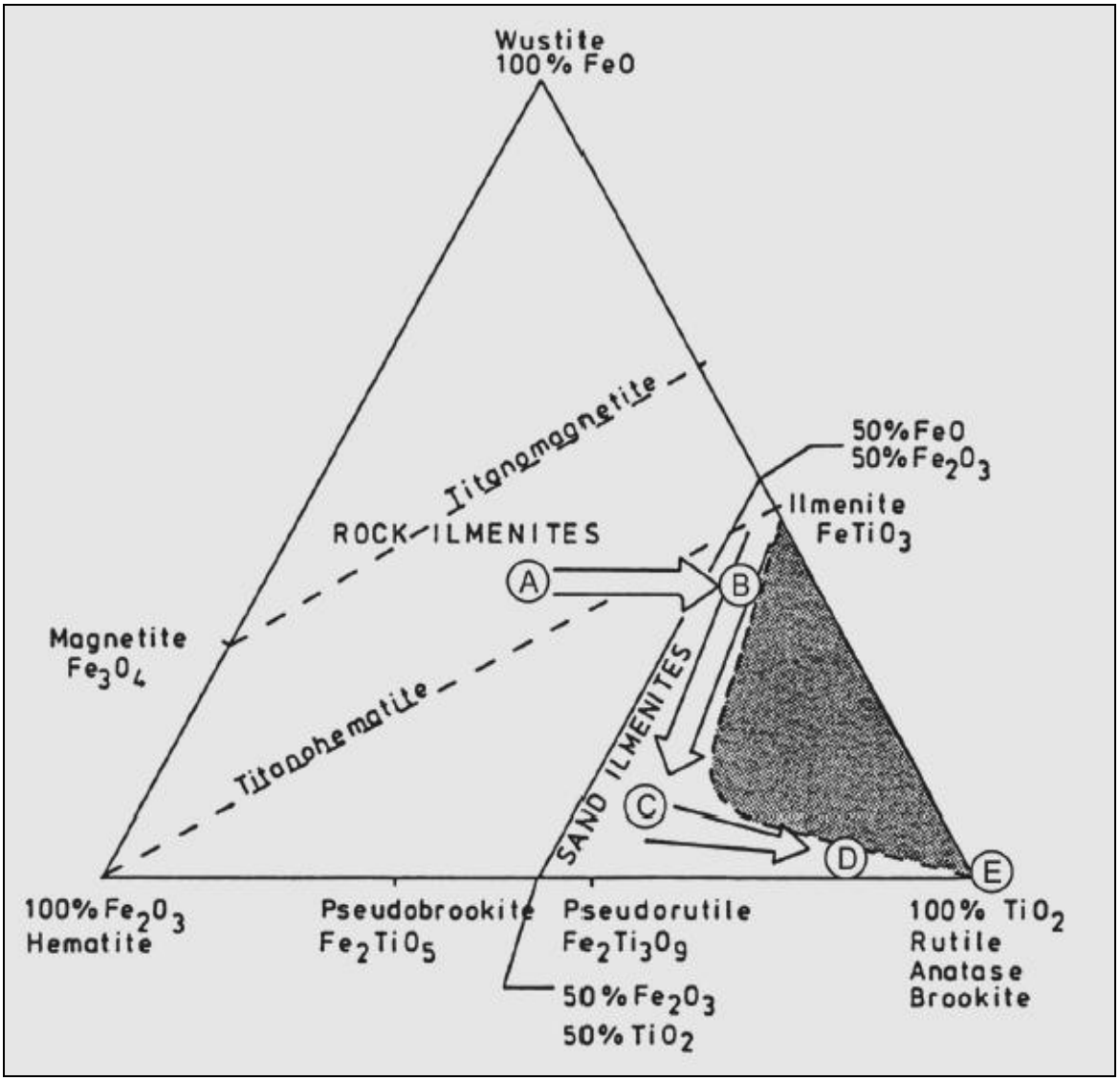

Figure 2.11: FeO-Fe_2O_3-TiO_2 ternary system (Garbar, 1978) with weathering sequence of ilmenite.[47]

Ilmenite is often mistaken for other iron containing minerals such hematite and magnetite due to its high magnetic susceptibility. Ilmenite has a hexagonal crystal structure (**Figure 2.12**) which is similar to corundum (Al_2O_3) and different from other iron minerals and displays lower magnetism compared to both hematite and magnetite. The crystal structure has alternating octahedral coordinated with iron and titanium layers.[34,64]

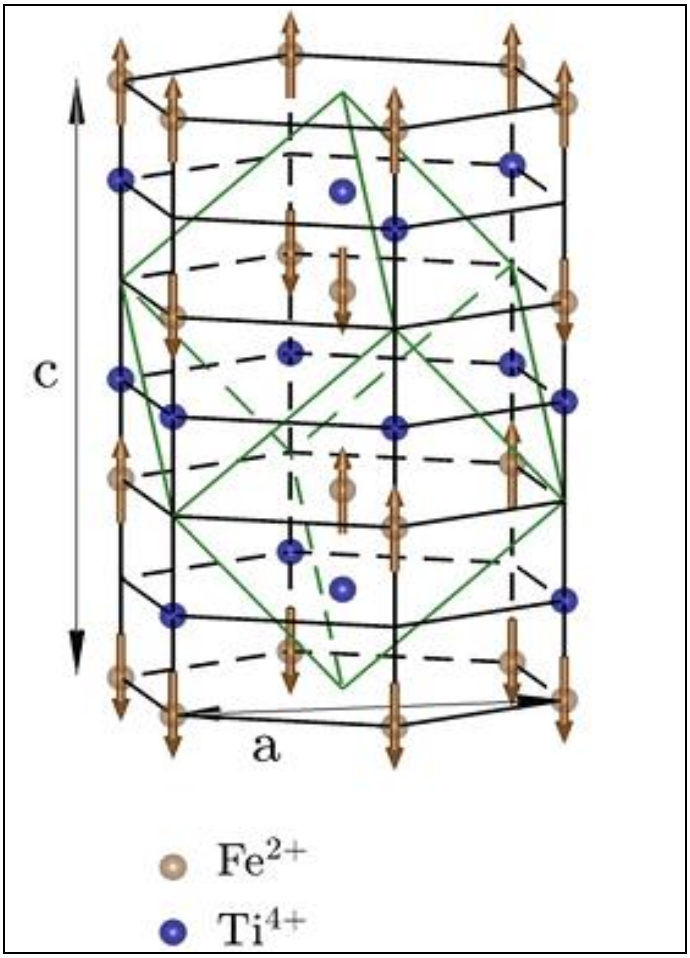

Figure 2.12: Crystal structure of ilmenite where the lattice parameter a = b = 5.038 Å and c = 13.772 Å.[72]

2.5 Titanium and Iron chemistry

Titanium and iron are early 3 d-block transitional elements and exist in a variety of oxidation states. Titanium has four valence electrons $3d^2 4s^2$. The most stable oxidation state is +4 followed by +3. In an oxidation state of +4 the titanium ion forms compounds which are similar in chemical properties to that of the group IV elements (Si, Ge, Sn, Pb). For example, the estimated ionic radii of Sn(IV) (0.71 Å) is very similar to that of Ti(IV) (0.68 Å). Moreover Sn(IV) has a octahedral covalent radii of 1.45 while that of Ti(IV) = 1.36. In an oxidation state of +3 titanium is paramagnetic

72 Brok, E., Sales, M. and Lefmann, K., Experimental evidence for lamellar magnetism in hemo-ilmenite by polarized neutron scattering, *Physical Review* B, **89**(5), 054430 (2014)

and its compounds are usually coloured.[73] Titanium reacts readily with carbon to form very stable TiC (carbides) and in this chemical state it difficult to reduce the metal in its pure form. At high temperatures (above 650 ºC) titanium can also react with nitrogen and sulphur to form TiN and TiS. At room temperature it is unreactive and is resistant to mineral acids attack by and aqueous alkali, but the metal dissolves in mineral acid mixture such as HCl or H_2SO_4 and HF.[73,75]

Iron occur in a number of different oxidation states, but the common and stable oxidation states are +2(d^6) and +3(d^5). It forms a number of complexes which are 6-coordinated and octahedral. Iron metal dissolves in diluted mineral acids such as HNO_3 and H_2SO_4. The metal can be produced by the reaction of iron oxide with carbon in a blast furnace.[73,75]

2.5.1 Physical and chemical properties of titanium and iron

Titanium and iron are the two most abundant transitional metals on earth with Ti being less abundant than iron. Both metals are good conductors of electricity (including heat), ductile and have high melting points (**Table 2.10**). Titanium is a silver grey metal with iron being silver white in its pure metallic state. Compared to titanium, iron has a low corrosion resistance and is oxidised to a red brown product in the presence of oxygen and water.[74,75] Pure iron (99.9 %, ferromagnetic) changes at a Curie point of 768 ºC and becomes paramagnetic while its magnetic properties decrease with an increase in impurity content, especially in minerals.[22]

73 Cotton, F.A. and Wilkinson, G., Advanced Inorganic Chemistry, 4th edition, p.751 (1980)

74 Anjali Acharya, A. and Gokhale V.A., Titanium: a new generation material for architectural applications, *Journal of Engineering Research and Applications*, **5**(2), pp.22-27 (2015)

75 Chambers, C. and Holliday, A.K., Modern Inorganic Chemistry, pp.369-372,391-400 (1975)

Table 2.10: Chemical and physical properties of Titanium and Iron[77,76]

Properties	Titanium	Iron
Natural state	Solid	Solid
Atomic number	22	26
Atomic mass	47.867	55.847
Atomic radius	0.145 nm	0.124 nm
Electron configuration	$[Ar]^3d^24s^2$	$[Ar]^3d^64s^2$
Oxidation state	+2, +3, +4	-1, 0, +1, +2, +3
Density, 20 °C	4.5 g/cm^3	7.9 g/cm^3
Melting point,	1950 K	1812 K
Boiling point,	3550 K	3160 K
Heat of fusion	3.38 kcal/mol	3.30 kcal/mol
Heat capacity	25.0 J/mol/K	25.1 J/mol/K
Thermal conductivity	21.9 W/m.K	25 W/m.K
Electrical resistivity	39 μΩcm	42 μΩcm
Young's modulus	120 GPa	211 GPa
Vickers micro-hardness	55 kg/mm^{-2}	66 kg/mm^{-2}

There are 23 different titanium isotopes and many of them are radioactive except ^{46}Ti, ^{47}Ti, ^{48}Ti, ^{49}Ti, and ^{50}Ti. ^{44}Ti (radioactive titanium) has been found to exist in the Cassiopeia Supernova and has a half-life ($t_{1/2}$) of 60 years. Iron has six radioactive isotopes with the most abundant and natural isotope being ^{56}Fe with 91.8 % natural abundance. Isotopic ^{57}Fe is used in nuclear magnetic resonance spectroscopy (NMR) analysis and Mossbauer spectroscopy due to its decay properties ($^{57}Co \rightarrow {}^{57}Fe$) giving off gamma rays of 14.4 keV.[77,78]

76 Oyama, S.T.(ed), The Chemistry of Transition Metal Carbides and Nitrides, pp.8-10,13 (1996)

77 Patnaik, P., Handbook of Inorganic Chemistry, pp.410-413,942-945 (2003)

78 Silver, J., Chemistry of Iron, pp.4-14 (1993)

2.5.2 Oxide compounds

Titanium forms stable oxides which include titanium oxide and titanium dioxides. Titanium dioxide (**Figure 2.13**) which is a common white pigment in titanium production has a high refractive index. It occurs naturally in minerals such as rutile, anatase and brookite.[77] It can also be produced with several chemical reactions which include a reaction of $TiCl_4$ with steam at 700 ºC (**Equation 2.10**). $TiCl_4$ can also be oxidised directly with oxygen to form titanium dioxide (see **Chapter 1, Equation 1.2**).

$$TiCl_4 + 2H_2O \longrightarrow TiO_2 + 4H_2 \qquad \textbf{2.10}$$

Iron oxide (**Figure 2.13**) occurs naturally in haematite (Fe_2O_3), magnetite (Fe_3O_4) and wustite (FeO) minerals. Fe_2O_3 can be prepared by the thermal decomposition of iron (II) sulphate at 480 ºC as indicated in **Equation 2.11**. The iron (II) formed dissolves in alkali solutions forming a ferrate (III) compound (**Equation 2.12)**. In the commercial industry Fe_2SO_3 is mixed with coke and limestone at 200 ºC in a blast furnace to produce a solid Fe_3O_4 product which can also undergo reduction to form FeO at the same temperature. In the presence of oxygen and water, iron forms hydrated iron (III) oxide (**Equation 2.13**). Iron (III) hydroxide ($Fe(OH)_2$) can be dehydrated to produce $Fe_2O_3 \cdot nH_2O_{(s)}$ which is red brown in colour.

$$2FeSO_4 \xrightarrow{\Delta} Fe_2O_3 + SO_2 + SO_3 \qquad \textbf{2.11}$$

$$Fe_2O_3 + 2OH^- \longrightarrow 2FeO_2^- + H_2O \qquad \textbf{2.12}$$

$$2Fe + 2H_2O + O_2 \longrightarrow 2Fe(OH)_2 \qquad \textbf{2.13}$$

Figure 2.13: Titanium dioxide powder and iron oxide powder producing dyes with different colours.[79,80]

2.5.3 Halide compounds

2.5.3.1 Titanium halides

Titanium reacts readily with halogens (Cl, F, Br, I) to produce the Ti^{4+}, Ti^{3+} and Ti^{2+} halides. The most important halide for this discussion is $TiCl_4$ which is commercially used to produce titanium metal from the Kroll process (**Equation 2.2**). $TiCl_4$ is a colourless liquid with a density of 1.73 g/cm^3 and a boiling temperature of 136.5 °C. It can react with water to form titanium(II) dioxide and HCl. $TiCl_3$ is a red violet compound with a density of 2.64 g/cm^3 and can be prepared from $TiCl_4$ by a reduction process in the presence of hydrogen gas at 600 ºC (**Equation 2.14**).[77] Titanium (IV) complexes are dominated by its halides chemistry as they are labile and form anionic adducts. $TiCl_4$ and $TiBr_4$ are usually used as starting materials during the preparation of six coordinated complexes of the type $TiX_4(L)_2$ (**Equation 2.15**, $TiCl_4(OPCl_3)_2$]). Common complexes of the Ti and Fe with their oxidation states are listed in **Table 2.12.** [84,81]

79 Get Chemistry Help: Iron oxide color, [Accessed 09-05-2016]. Available from : http://getchemistryhelp.blogspot.co.za/2013/05/iron-oxide-color.html

80 Titanium Dioxide, [Accessed 09-05-2016]. Available from: http://new-delhi.all.biz/titanium-dioxide-g285628#.VzA0soR97IU

81 Landis, V.J., Radiochemistry of Titanium, U.S. Atomic Energy Commission, pp.19-22 (1971)

$TiCl_{4(g)} + 1/2H_2 \longrightarrow TiCl_{3(g)} + HCl$ **2.14**

$TiCl_4 + 2POCl_3 \longrightarrow (TiCl_4(OPCl_3)_2$ **2.15**

2.5.3.2 Iron halides

Iron reacts with halogens to produce binary ferrous (II) and ferric (III) halides. FeX_2 halides (**Equation 2.16**) have a very high melting point, and are usually pale-coloured except for $FeCl_2$ which is yellow. Iron (III) halides (**Equation 2.17**) include $FeCl_3$ which is more stable compared to $FeBr_3$ and FeI_3 and easily decompose (reduced) back to $FeBr_2$ and FeI_2 and halogens.

$Fe + 2HX \longrightarrow FeX_2$ (X= F, Cl, Br) **2.16**

$2Fe + 3X_2 \longrightarrow 2FeX_3$ (X= F, Cl, Br) **2.17**

2.5.4 Coordination chemistry of iron and titanium

Iron complexes preferably form 6 coordinated octahedral complexes with neutral ligands. Iron(III) on the other hand forms 3 to 8 coordinated complexes which are usually octahedral, but tetrahedral and square pyramidal complexes have also been isolated. Both Fe(II) and Fe(III) form stable complexes with O and N donor ligands such as 2,2'-bipyradine, 1,10-phenanthroline, 8-hydroxyquinoline and acetyacetone. The stabilities of these complexes generally differ which is a function of the oxidation state of iron (**Table 2.11).**[82]

82 Nielsen, J.M. The Radiochemistry of Iron, U.S. Atomic Energy Commission, pp.8-14 (1960)

Table 2.11: The stability of some chelating compounds of Fe (II) and Fe(III)[82]

Chelating compounds	Iron oxidation state	Stability constant (log K)
Acetylacetone	Fe^{2+}	5.07
	Fe^{3+}	11.4
Oxalic acid	Fe^{2+}	4.7
	Fe^{3+}	9.4
8-hydroxiquinoline	Fe^{2+}	8.0
	Fe^{3+}	14.52
EDTA	Fe^{2+}	14.2
	Fe^{3+}	25.7
1,10-phenantroline	Fe^{2+}	4.96
	Fe^{3+}	-
2,2'- dipyridyl	Fe^{2+}	4.36
	Fe^{3+}	-

Fe(III) has a lower affinity for amine ligands compared to Fe(II), but form stable complex with nitrogen containing EDTA (**Equation 2.18**) and derivatives of 8-hydroxyquinolines. It has a high affinity for oxygen donors such as oxalates, polyphosphates and polyols (glycerol and sugar)[82] as expected with its relatively high oxidation state.

$$[Fe(H_2O)_6]^{3+}_{(aq)} + EDTA^{4-}_{(aq)} \longrightarrow [Fe(EDTA)]^{-}_{(aq)} + 6H_2O_{(l)} \qquad \textbf{2.18}$$

Titanium (IV) forms complexes which can be 4 to 6 coordinated with the most common coordinating been 6 coordinated due to titanium's ability to expand its coordination environment. Titanium (IV) forms stable complexes with oxygen donor ligands such as hydroquinone, thynol, chlorophenol and hydroxybenzoic acid.[84,81]

Table 2.12: Oxidation states and stereochemistry of iron and titanium[73,81]

Oxidation state	Coordination number	Geometry	Examples
Fe^0, Ti^0	5	Trigonal bypyramidal	$Fe(CO)_5$
	6	Octahedral	$Ti(CO)_6$
Fe^{II}, Ti^{II}, d^2	4	Tetrahedral	$FeCl_2(PPh_3)_2$, $(\eta\text{-}C_5H_5)_2Ti(CO)_2)$
	6	Octahedral	$[Fe(H_2O)_6]_2^+$, $TiCl_2$
Fe^{III}, Ti^{III}, d^1	3	Trigonal, planar	$Ti[N(SiMe_3)_2]_3$
	4	Tetrahedral	$FeCl_4^-$
	5	Trigonal bypyramidal	$FeCl_5^{3-}$,$TiBr_3(NMe_3)_2$
	6	Octahedral	$Fe(acac)_3$, $Ti(H_2O)_6^{3+}$
	7	Pentagonal bipyramidal	$[FeEDTA(H_2O)]^-$
	8	Dodecahedral	$Fe[(I\text{-norbornyl})_4]$
Fe^{IV}, Ti^{IV}, d^0	4	Tetrahedral	$[Fe(NO_3)_4]^-$ (only in solid oxides), $TiCl_4$
	5	Trigonal bipyramidal	$[TiOCl_2(NMe_3)_2]$
	6	Octahedral	$[Fe(diars)_2Cl_2]^{2+}$,$Ti(acac)_2Cl_2$,
	7	Pentagonal bipyramidal	$[TiCl(S_2CNMe_2)_3]$

2.5.5 Organometallic complexes

Titanium and iron form numerous organometallic complexes with σ-and π donor ligands. Ferrocene (dicyclopentadienly iron) is easily recognised as an orange powder complex formed by the reaction between cyclopentadiene and iron (**Equation 2.19**). Its structure was first published by Pauson [$Fe(\sigma\text{-}C_5H_5)_2$] and later rediscovered/ re-characterized by G Wilkinson as a π-sandwich structure.[83] Iron with zero oxidation state (Fe(0)) is favoured for iron catalysis since the metal in this low

83 Astruc, D., Organometallic Chemistry and Catalysis, pp.7-8 (2007)

oxidation state can form more reactive iron complexes compared to those which are five to six coordinated. It can also form carbonyl compounds which are stable, the most common being five-coordinated pentacarbonyl ($(Fe(CO)_5)$ complex.[84,76]

$$2NaC_5H_5 + FeCl_2 \longrightarrow Fe(C_5H_5)_2 + 2NaCl \qquad \textbf{2.19}$$

The organotitanium complexes can form both metal-carbon π-bond as well as metal-carbon σ-bonds. Ti-C π-bond metal complexes include $Ti(CH_3)Cl_3$, $Ti(C_6F_5)Cl_3$ and $Ti(CH_2Ph)_4$. Complexes containing Ti-C σ-bonds on the other hand are formed by cyclopentadienyl ($C_5H_5^-$) anion (or derivatives) and the most common complex is the $(C_5H_5)_2TiCl_2$ compound which is red in colour and is mostly used as a starting reagent to synthesize other organotitanium complexes. Complexes containing both ligands are also known such as $Ti(CH_2Si(Me)_3)_2(C_5H_5)_2$.[83] More recently these titanium organometallic compounds have been explored as potential catalysts and for the potential synthesis of other organic compounds due to the high abundance and the low intrinsic toxicity of titanium.[85]

2.6 Applications and uses of Titanium and Iron

A large percentage of titanium dioxide produced is used as pigment in the paint, plastic and paper industry.[4] By 1970s the new discovery of TiO_2-based materials prompted research in the nanotechnology field to find new methods for the synthesis of the nanostructured TiO_2 materials with UV/Vis applications. Titanium is also extensively used for photocatalysis, photovoltaic cells and sensors.[86] Titanium and its different alloys found wide application, ranging from the military aerospace to the jewellery industry (**Figure 2.14, Table 2.13**). In biomedicine, titanium alloys compete with stainless steel and cobalt-base alloy (vitalism) as implant devices (replacing unsuccessful hard tissues) due to their high bio-compatibility, non-toxicity as well as

84 Plietker B.(ed), Iron Catalysis in Organic Chemistry: Reaction and Applications, pp.1,2,5 (2008)

85 Petasis, N.A. and Hu, Y.H., Current organic chemistry, Volume 1, No.3, pp.249-250 (1997)

86 Bavykim, D.V. and Walsh, F.C., Titanate and Titania Nanotubes: Synthesis, Properties and Applications, pp.2-6 (2010)

their ability to resist corrosion. Specific implants include artificial hearts, artificial knee joints and bone plates.[87]

Iron recovered from the smelting process is used for steel production. Iron recovered from other processes has also been recovered and used at a smaller scale for production of water treatment (iron chloride), in fertilizers and in animal food (ferrous sulphate heptahydrate).[8]

Figure 2.14: Applications of titanium metal.[88]

87 Elias, C.N., Lima, J.H.C., Valiev, R. and Meyers, M.A., Biological application of titanium and its alloys, *Journal of the Minerals, Metals, and Materials, Society,* **60**(3), p.46 (2008)

Table 2.13: Applications of titanium in different fields[88,48]

Field	Application
Aerospace	Jet engines, airframes, fuel tanks
Chemical and industrial plant	Catalysis, pumps and valves, chemicals and seawater pipes
Medicine	Surgical implants and devices, dental implants, pacemaker cover
Sports	Golf clubs, baseball bats, bike frames
Architecture	Roofing (The Guggenheim museum in Spain)
Automotive	Springs, bolts, exhaust systems
Jewellery and Accessories	Watches, rings, photo frames

2.7 Conclusion

Titanium's unique properties which include its good biocompatibility and high strength-to-weight ratio earn this element its popularity and is underlined by its wide application in different industries. Interestingly, it is one of the most abundant elements on the planet, but its conventional extraction process from its primary sources is expensive making high grade titanium slag production with methods such as Benelite and Becher process excessively expensive. This high production cost necessitates the development of new or alternative beneficiation production processes for titanium beneficiation. With the above-mentioned in mind, this study was mainly aimed at developing cost-effective dissolution, analytical and separation procedures for processing of titanium. These include the development of accurate, precise and robust analytical procedures as part of good quality control as well as for accurate determinations of titanium (and iron as major and common impurity) in different matrices.

88 Titanium uses, [Assessed 15-02-2016]. Available from: http://metalpedia.asianmetal.com/metal/titanium/application.shtml

3 Dissolution and separation of titanium and iron: Literature review

3.1 Introduction

Ilmenite is a major source of both titanium and iron and it is often commercially beneficiated for the production of pure TiO_2 using a combination of physical and chemical processes. Separation techniques range from gravitation and magnetic separations to hydrometallurgical processes such as solvent extraction. Some of these processes are energy demanding, costly and time consuming (**Chapter 2**). Hydrometallurgical processes rely on the complete dissolution of the mineral for both the separation and also the accurate quantification of the mineral constituents at different stages of the beneficiation process. The complete dissolution of ilmenite mineral has been a challenge for many researchers and hundreds of articles and patents reporting on successful dissolution methods have been published.[89] This chapter reviews some of the research done on the dissolution of ilmenite using acid digestion, flux fusion and microwave acid assisted digestion. The discussion also includes separation techniques such as precipitation, ion exchange and solvent extraction. Finally the chapter also reviews different analytical techniques which are used for the quantification of titanium and iron in natural and synthetic matrices.

89 Biswas, K.R., Karmak, A.K. and Ara, J., Baking of ilmenite on Koistening with sulphuric acid by leaching with dilute sulphuric acid solution, *International Conference on Computer, Communication, Chemical, Materials and Electronic Engineering*, pp.31-34 (2016)

3.2 Dissolution of titanium and iron containing minerals

3.2.1 Acid /base dissolution technique

Ilmenite is moderately resistant to most of the mineral acids under normal conditions and dissolution procedures often make use of elevated temperature or many hours of stirring. The mineral is commonly digested using HCl or H_2SO_4 at elevated temperatures. Several researchers have extensively studied the dissolution of ilmenite using these two acids and investigated the effect of different experimental parameters such as particle size, temperature, mechanical activation[90] and acid concentration on the rate and extend of dissolution. Unlike the grinding of the ore with the aim to reduce the particle size, mechanical activation is used to induce phase transformation, structural defects and change surface characteristics with the aim to enhance the dissolution of the minerals.[91]

Jonglertjunya and Rubcumintara[92] dissolved an ilmenite sample using 8.0 M H_2SO_4 and 6 hours of stirring and reported 64 % Fe and 57 % Ti in the filtrate. Sasikumar *et al*[90] digested ilmenite in 9.2 M H_2SO_4 at 120 ºC and recovered 84 % Fe and 41 % Ti in the filtrate. In a different study Sasikumar *et al*[93] dissolved Orissa ilmenite using 9.4 M H_2SO_4 at 95 ºC and obtained 90 % Fe and 65 % Ti in the filtrate.

90 Sasikumar, C., Rao, D.S., Srikanth, S., Mukhopadhyay, N.K. and Mehrotra, S.P., Dissolution studies of mechanically activated Manavalakurichi ilmenite with HCl and H_2SO_4, *Hydrometallurgy*, 88, pp.154-69 (2007)

91 Kumar, S., Alex, T.C. and Kumar, R., Mechanical activation of solids in extractive metallurgy, [Accessed 07-09-2016]. Available from: http://eprints.nmlindia.org/5844/1/51-56.PDF

92 Jonglertjunya, W. and Rubcumintara T., Titanium and iron dissolution from ilmenite by acid leaching and microbiological oxidation techniques, *Asia-Pacific Journal of chemical Engineering*, pp.323-33 (2013)

93 Sasikumar, C., Rao, D.S., Srikanth, S., Mukhopadhyay, N.K. and Mehrotra, S.P., Effect of mechanical activation on the kinetics of sulphuric acid leaching of beach sand ilmenite from Orissa, India, *Hydrometallurgy*,75, pp.189-204 (2004)

Haverkamp *et al*[94] used 32 % HCl at 60 - 90 ºC at a molar ratio of 2:1 ($HCl:FeTiO_3$) and leached approximately 90 % of both Fe and Ti. In another study, Habib *et al*[95] digested the mineral using 6.0 M HCl at 110 ºC and reported recoveries of 53.5 % Ti and 60 % Fe and they improved their own dissolution method by using a mixture of HCl and methanol (6.0 M:0.5 M) at its boiling temperature and they dissolved 91 % Ti and 95 % Fe in the sample. In another study Habib *et al*[96] also investigated the dissolution of an ilmenite sample with 6.0 M HCl and ethanol or phenol (both 6.0 M:0.5 M) and they dissolved approximately 88 % Ti and 95 % Fe with the ethanol mixture while the phenol mixture produced recoveries of 81 % Ti and 85 % Fe.

Mehdilo and Irannajad[97] studied the ilmenite sample from the Qara-aghaj deposit (North West of Iran). The ore sample (Hard rock) was subjected to gravity and magnetic separation to recover an ilmenite mineral (**Table 3.1**). The ilmenite concentrate was then converted to titanium slag using the carbo-thermal reduction smelting process (coke and Na_2CO_3) in a DC electronic arc furnace (see **Chapter 2, Section 2.3.3**). The two elements were leached from the slag using HCl and dilute H_2SO_4 at 95 ºC and using a solid to liquid ratio of 1:4. Results indicated that 91 % TiO_2 was leached into HCl while H_2SO_4 leached 86.8 % TiO_2 under the similar experimental conditions **(Table 3.1**).

94 Haverkamp, R.G., Kruger, D. and Rajashekar, R., Digestion of New Zealand ilmenite by hydrochloric acid, *Hydrometallurgy*, 163, pp.198-203 (2016)

95 Habib, M. A., Biswas, R.K., Ali, M.R. and Hasan, A.K.M., Leaching of non-treated ilmenite by HCl-CH_3OH-H_2O mixture and its kinetics, *Indian Journal of Chemical Technology*, 13, pp.53-56 (2016).

96 Habib, M.A., Biswas, R.K., Sarkar, P.K. and Ahmed, M., Leaching of ilmenite by mixed solvent and their kinetics, *Bangladesh Journal of Scientific and Industrial Research*, 38, pp.1-12 (2003)

97 Mehdilo, A. and Irannajad, M., Iron removing from titanium slag for synthetic rutile production, *Physicochemical Problems of Mineral Processing*, **48**(2), pp.425-439 (2012)

Table 3.1: Quantitative results of the Ti concentrates obtained from the titanium slag treated with different acid analysed with XRF[97]

Composition, %	Ore sample	Ilmenite	Titanium slag	Ti slag Leaching	
				H_2SO_4	HCl
TiO_2	9.0	44.5	72.7	86.8	91.0
Fe_2O_3	34.4	46.1	7.8	1.87	0.61
MnO	0.41	0.83	0.97	0.57	0.62
MgO	15.0	3.76	3.21	2.79	2.11
SiO_2	27.4	2.76	5.24	4.6	3.28
Al_2O_3	3.1	0.58	2.90	1.02	0.22
CaO	5.9	0.61	1.08	1.04	0.58
P_2O_5	2.9	0.52	--	--	--
V_2O_5	0.14	0.26	0.30	0.22	0.18
Na_2O	0.25	--	0.20	--	--
K_2O	--	--	4.22	-	--
Total	**98.5**	**99.73**	**99.28**	**99.63**	**99.51**

--Not determined
SO_3 in H_2SO_4 —0.51%, Cl in HCl— 0.38 %

Biswas and Mondal[98] studied the digestion of ilmenite ore using different mineral acids such as HCl, $HClO_4$, HF, H_2SO_4 and HNO_3. In the study it was found that the 5.5 M HF was the most successful in dissolving the mineral sand. After 5 hours of digestion using a solid to liquid ratio (S/L) of 0.05 g/mL and at its boiling point, recoveries of 81 % Ti and 26 % Fe were obtained. Andrade *et al*[99] reported the complete dissolution of ilmenite mineral using phosphoric acid digestion. A 0.1 g of ilmenite sample was dried before at 120 ºC and reacted with phosphoric acid (85 %) at 230 ºC.

98 Biswas, R.K. and Mondal, M.G.K., A study on the dissolution of ilmenite sand, *Hydrometallurgy*, 17, pp.385-390 (1987)

99 Andrade, J.B., Nunes, G.S., Veiga, M.P., Costa, S., Ferreira, S.L.C., Amorim, M.M. and Reis, S.T., Spectrophotometric and inductive coupled plasma determination of titanium in ilmenites after rapid dissolution with phosphoric acid, *Talanta*, 44, pp.165-168 (1997)

Sasikumar *et al*[90] studied an ilmenite sample obtained from Manavalakurichi which was first mechanically activated and then subjected to acid dissolution. The maximum dissolution of Fe and Ti in 9.2 M H_2SO_4 solution at 120 ºC was 84 and 41 % respectively. These results were lower compared to their study using Chatrapur Indian ilmenite ore which dissolved 90 % Fe and 65 % Ti using identical experimental conditions. In the same study, Sasikumar *et al*[90]also investigated Manavalakurichi ilmenite ore leaching using 11.5 M HCl at 100 ºC and dissolved 46 % Ti and 95 % Fe. Li *et al*[100] investigated the acid leaching of a mechanically activated ilmenite sample from Panzhihua using 50 % H_2SO_4 100 ºC and reported 82.1 % dissolution of the starting material.

The use of caustic digestion followed by acid dissolution for ilmenite dissolution has also been studied.[13] Nayl and Aly[101] decomposed an ilmenite mineral using a 70 % KOH solution at a ratio of 1:5 (solid: liquid) and at 150 ºC for 3 hours with constant stirring. The KOH reacted with the ilmenite to form potassium titanate ($K_4Ti_3O_8$) and iron oxide. The dissolution of this mixture was subsequently investigated with H_2SO_4, HCl and $C_2O_4H_2$. The oxalic acid dissolution (80 % wt) produced recoveries of 73 % Fe and 93 % Ti and the study indicated that the elemental recoveries increased with an increase in acid concentration. The HCl (9.0 M) dissolution at a ratio of 1:5 (acid:liquid), at 120 ºC and 2 hours of constant stirring produced recoveries of 91 % Ti and 96 % Fe. The 6 M H_2SO_4 dissolution at a ratio of 11:1 (acid: liquid), at 150 ^oC and 2.5 hours of stirring produced recoveries of 91 % Ti and 94 % Fe. Subagja *et al*[102] decomposed the ilmenite using KOH at 150 ºC and constant stirring for 120 min. The decomposition step was subsequently followed by acid leaching using 75 % H_2SO_4 solution. They reported the recoveries of 85 % Ti and 30 % Fe.

100 Li, C., Liang, B. and Guo, L., Dissolution of mechanically activated Panzhihua ilmenite in dilute sulphuric acid, *Hydrometallurgy*, 89, pp.1-10 (2007)

101 Nayl, A.A. and Aly, H.F., Acid leaching of ilmenite decomposed by KOH, *Hydrometallurgy*, 97, pp.86-92 (2009)

102 Subagja, R., Andriyah, L. and Lalasari, L.H., Decomposition of ilmenite from Bangka island-Indonesia with KOH solutions, *Asian Transactions on Basic and Applied Science*, **3**(2), pp.59-64 (2013)

Nayl *et al*[103] also reacted a titanium slag sample with NH_4OH (4 M) at 150 ºC to form ammonium titanate ($(NH_4)_2TiO_3$. The product of this decomposition reaction was dissolved in hot water at 70 ºC and constant stirring of 2.5 hours. The filtrate which was obtained was dried and calcinated at 350 ºC for 4 hours. The calcined solid was washed with HCl (3.0 M), water and dried at 120 ºC. An XRD analysis of this product indicated that it contained 99.8 % TiO_2 and less than 0.1 % of Fe and SiO_2. Xue *et al*[104] reacted a titanium slag (55.1 % Ti and 0.90 % Fe) sample with NaOH (60 % wt) at temperature between 400 to 475 ºC at atmospheric pressure. The undissolved material was washed with water and subsequently reacted with HCl under reflux. 99.3 % Ti, 0.060 % Fe, 0.068 % SiO_2 and less than 0.05 % of Al_2O_3 and MnO recoveries were reported.

3.2.2 Flux fusion digestion and dissolution

From the above discussion it is apparent that the acid dissolution is a promising dissolution technique, but in many cases does not achieve complete sample dissolution. Flux fusion on the other hand has been reported to be highly successful in the complete dissolution of the ilmenite. Felman[105] fused an ilmenite sample with lithium borate ($Li_2B_4O_7$) at 950 ºC and achieved a complete sample digestion in 20 minutes. The resultant melt was dissolved in a solution of 3 % HNO_3 and 2.5 % tartaric acids. Premaratne and Rowson[106] fused an ilmenite with $KHSO_4$ at 800 ºC and achieved a complete sample digestion. The melt dissolved completely in a 20 % H_2SO_4 solution. Radhamani *et al* [107] used phosphate fusion on synthetic ilmenite

103 Nayl, A.A., Ismail, I.M. and Aly, H.F., Ammonium hydroxide decomposition of titanium slag, *Hydrometallurgy*, 98, pp.196-200 (2009)

104 Xue, T., Wang, L., Qi, T., Chu, J.M., Qu, J. and Liu, C., Decomposition kinetics of titanium slag in sodium hydroxide system, *Hydrometallurgy*, 95, pp.22-27 (2009)

105 Felman, C., Behaviour of Trace refractory minerals in lithium metaborate fusion-acid dissolution procedure, *Analytical Chemistry*, **55**(14), pp.2451-2453 (1983)

106 Premaratne, W.A.P.J. and Rowson, N.A., Microwave assisted dissolution of Sri Lankan ilmenite: extraction and leaching kinetics of titanium and iron metals, *Journal of Science of the University of Kelaniya Sri Lanka*, 9, pp.1-14 (2014)

107 Radhamani, R., Mahanta, P.L., Murugesan, P. and Chakrapani. G.J., Novel fusion method for direct determination of uranium in ilmenite, rutile, columbite, tantalite and xenotime minerals by laser induced fluorimetry, *Journal of Radioanalytical and Nuclear Chemistry*, **285(**2), pp.287-292 (2010)

(48.60 % TiO_2, 47.90 % FeO) and rutile (> 90 % TiO_2) samples. The samples were fused with sodium di-hydrogen phosphate and di-sodium hydrogen phosphate (1:1) in a temperature between 700 and 850 ºC. The resulting melts were dissolved in water and 92 % ilmenite and 102 % rutile were recovered.

3.2.3 Microwave acid-assisted digestion

Microwave acid-assisted dissolution has several advantages compared to convention acid dissolution methods. These include combining high pressure and temperature to completely dissolve a sample and also results to a smaller degree in samples contamination (see **Chapter 4, Section 4.2.3**). Premaratne and Rowson[106] investigated the dissolution of an ilmenite sample from Sri Lanka using 12.2 M H_2SO_4 (25 mL, 0.2 g) and microwave conditions of 600 W, 120 ºC and 2 hours digestion time and obtained recoveries of 74.2 % Ti and 71.3 % Fe. Tripathi and Chattopadhyay[108] digested titanium containing minerals using HNO_3:HCl:HF (2:2:1) acid mixture applying microwave conditions of 600 W for 17 minutes. After digestion, 5 % boric acid was added and the solution was allowed to evaporate on a hot plate to reduce the volume to about 5 mL before diluting to with H_2O to 100 mL. Their report indicated the dissolution of more than 99 % of Ti and Fe. In another study[109] a soil samples from the National Institute of Standard and Technology (NIST) was digested in a microwave using a mixture of HNO_3:HCl:HF (2 mL, 6 mL, 2 mL). Average recoveries of 95.6 % Ti and 99.3 % Fe were reported.

108 Tripathi, A. and Chattopadhyay, P., Digestion of titanium bearing geologic materials involving microwaves, *Annali di Chimica*, 97, pp.1047-1064 (2007)

109 McDonald, D. and Amarin, A., Direct determination of Cu, Fe, Mn, P, Pb and Ti in HF acid-digested soils using the Agilent 4200 Microwave Plasma- Atomic Emission Spectrometer, Agilent Technology, pp.1-7 (2015)

3.3 Separation of Ti and Fe in ilmenite

Separation of elements with similar chemical and physical properties is a challenge in hydrometallurgical processing.[110] Therefore, the separation of titanium and iron in ilmenite using cost effective procedures has attracted considerable attention from researchers. The sections of the chapter focus on the hydrometallurgical separation of titanium and iron in ilmenite, titanium slag and synthetic mixtures.

3.3.1 Precipitation

Mahmoud *et al*[111] dissolved an ilmenite sample (20 g) in 20 % HCl and added 0.01 g iron powder with stirring under reflux for 5 hours. The slurry was filtered and the solid titanium precipitated was washed with 3 % HCl and dried at 110 ºC and followed by calcination at 900 ºC. Quantitative results indicated that 90 % TiO_2 was recovered and only 0.8 % Fe_2O_3 co-precipitated in the process. Lasheen[112] also separated titanium and iron in ilmenite using concentrated HCl (12 M) after the reductive leaching using metallic iron as reductant. Iron metal powder (6%) was added to the sample solution at 1:3 ratio (solid: liquid) and refluxed for 8 hours. About 89 % TiO_2 and 6.7 % Fe_2O_3 were recovered in the filtrate. Vasquez and Molina[113] treated an ilmenite sample in a furnace at different temperatures (700, 800, 900 and 1050 ºC) prior to its separation and leaching with 20 wt % HCl. Metallic iron was added to the reaction with stirring. At 700 ºC, 88 % of Fe was extracted with less than 10 % co-extraction of Ti.

110 Nete, M., Separation and purification of niobium and tantalum from synthetic and natural compounds, PhD. Thesis, University of the Free State, p.40 (2013)

111 Mahmoud, M.H.H., Afifi, A.A.I. and Ibrahim, I.A., Reductive leaching of ilmenite ore in hydrochloric acid for preparation of synthetic rutile, *Hydrometallurgy*, 73, pp.99-109 (2004)

112 Lasheen, T.A.I., Chemical beneficiation of Rosetta ilmenite by direct reduction leaching, *Hydrometallurgy*, 76, pp.123-129 (2005)

113 Vasquez, R. and Molina, A., Leaching of ilmenite and pre-oxidized ilmenite in hydrochloric acid to obtain a high grade titanium dioxide, *Metal*, 5, pp.13-15 (2008)

Baba *et al*[114] removed 85.4 % of ilmenite ore with acid leaching using 2.0 M HCl solution at 80 ºC. Ammonia (3.0 M) was added which precipitated 97.6 % of iron. The titanium which remained in solution was recovered by solvent extraction using 1.5 M TBP in kerosene and subsequently stripped with 0.1 M HCl. Quantitative results indicated that 96.6 % Ti was recovered in a single stage step.

Kigashi *et al*[115] decomposed an ilmenite sample using the nitrofluor process. The sample was reacted with a HF-NO_2 azeotrope and boiled at 52 ºC. A light green precipitate was observed after 2 hours of boiling. The precipitate was determined to contain 50 % iron while the filtrate contained 93 % of titanium. Both metals were considered to form nitrosylium penta(or hexa) fluoro complexes (**Equation 3.1 and 3.2**) but the subsequent decomposition of $NOFeF_4$ lead to the formation of insoluble FeF_3. After 140 hours of stirring approximately 99 % of Ti and less than 5 % of Fe were recovered in the filtrate.

$$TiO_2 + 6NO + 6F \longrightarrow (NO)_2TiF_6 + 2NO + 2NO_2 \qquad \textbf{3.1}$$

$$Fe_2O_3 + 8NO + F^- \longrightarrow 2NOFeF_4 + 3NO + 3NO_2 \qquad \textbf{3.2}$$

Wang *et al*[116] prepared $Ti(SO_4)_2$ by dissolving TiO_2 in concentrated H_2SO_4 at 120 ºC. Iron sulphate ($Fe_2(SO_4)_3$) was subsequently added to generate the Ti^{4+}/Fe^{3+} mixture of a 1:10 mole ratio. The acidity of the solution was adjusted using NaOH while disodium ethylenediammine tetra-acetate (EDTA) was added to prevent the precipitation of Fe^{3+}. The titanium hydroxide which precipitate from the hydrolysis of $Ti(SO_4)_2$ was calcined at 900 ºC for 2 hours. The analytical results indicated that Ti hydrolysis increase with an increase in pH (**Figure 3.1**) and up to 99.9 % TiO_2 recoveries were recorded in the isolated products.

114 Baba, A.A., Adekola, F.A. and Arodola, O.A., Simultaneous recovery of total iron and titanium from ilmenite ore by hydrometallurgical processing, *Association of Metallurgical Engineers of Serbia*, **18**(1), pp.67-78 (2012)

115 Kigashi, A., Okada, K., Ohkawa, A. and Nakamura, Y., The recovery of titanium from ilmenite by Nitrofluor process, *The Research Institute of Mineral Dressing and Metallurgy*, pp.201-212 (1969)

116 Wang, M., Woo, K.D., Kim, I.Y., Woo, K.I. and Sui, Z., Separation of Fe^{3+} during hydrolysis of TiO^{2+} by addition of EDTA, *Hydrometallurgy*, 89, pp.319-322 (2007)

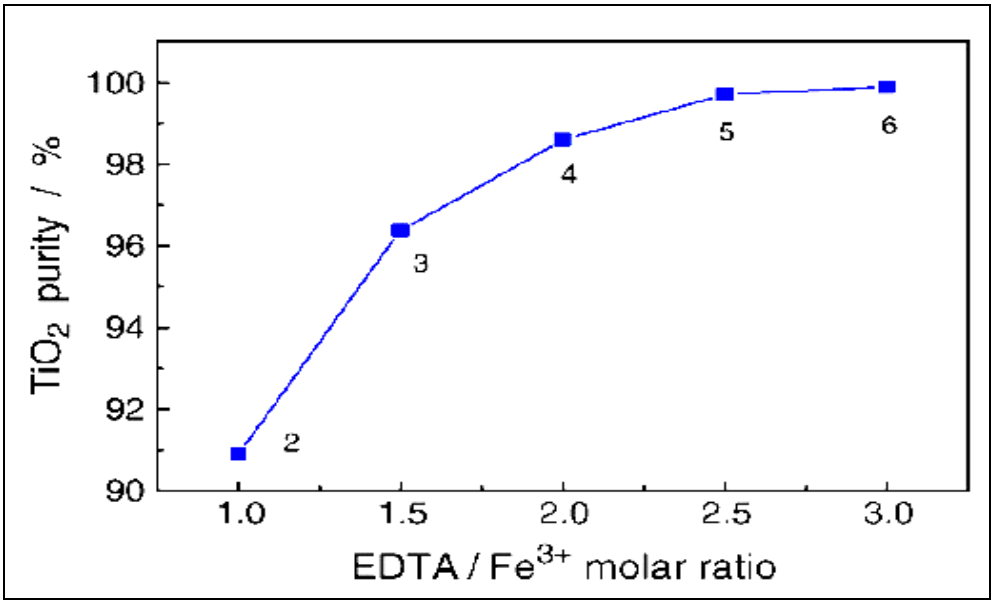

Figure 3.1: Increase in TiO_2 due to an increase in EDTA /Fe^{3+} molar ratio.

3.3.2 Solvent extraction

Solvent extraction has become an important technique for the separation of titanium and iron due to its ability to produce cleaner separations with reduced waste and easy recycling of waste. Extractants which have been investigated thus far include numerous organophosphorous compounds (DEHPA, EHEHPA, Cyanex 272, Cyanex 302) acids,[117,118,119,125] neutral organophosphorus (TBP, TOPO, TRPO, Cyanex 923) [120,121,122,125] compound and different amines (Alamine 336, Aliquat 336).[125]

117 Islam, M.F. and Biswas, R.K., The solvent extraction of Ti(IV),Fe(III) and Mn(II) from acidic sulfate—acetate medium with bis-(2-ethylhexyl)-phosphonic acid in benzene, *Journal of Inorganic Nuclear Chemistry*, 43, pp.1929–1933 (1981).

118 Islam, F., Rahman, H. and Ali, M., Solvent extraction separation study of Ti(IV), Fe(III) and Fe(II) from aqueous solutions with di-(2-ethylhexyl)- phosphoric acid in benzene. *Journal of Inorganic Nuclear Chemistry*, 41, pp.217–221 (1971).

119 Deep, A., Malik, P. and Gupta, B., Extraction and separation of Ti(IV) using Thiophosphinic acids and its recovery from ilmenite and red mud, *Separation Science and Technology*, **36**(4), pp.671-685 (2001)

120 Seyfi, S. and Abdi, M., Extraction of titanium (IV) from acidic medium by tri-n-butyl phosphate in kerosene, *Minerals Engineering*, **22**(2), pp.116-118 (2009)

121 Shibata, J. and Kurihara, Y., A study on separation and purification process of high purity titanium oxide, *Kagaku Kogaku Ronbunshu,* 18, pp.521–527 (1992)

Saji *et al*[123] extracted Fe from titania waste (waste chloride liquor, 2 M HCl) using a mixture of TBP and MIBK (70:30 vol %). Wang *et al*[124] extracted 97 % Fe from a 9.35 M HCl ilmenite solution using MIBK with no titanium co-extraction. In another study Wang *et al*[124] separated Ti and Fe from an ilmenite sample using 0.2 mol/L TRPO in xylene. Approximately 90 % Fe and 30 % Ti were extracted into the TRPO/xylene mixture from a 2 M HCl solution. Hao *et al*[125] extracted titanium from H_2SO_4 solution using 25 % (v/v) TRPO-kerosene system. This process proved to be tedious and required a multi-stage extraction process and they extracted 96 % Ti with 7 % Fe co-extraction. When the extraction process was conducted in a N_2 atmosphere the co-extraction of Fe decreased to 1 %. Remya and Reddy[122] also studied the separation of titanium and iron in a synthetic waste sample using a 4 mol/L HCl solution in the presence of TRPO dissolved in kerosene and which also contained 10 % isodecanol. In this study Ti, Fe and V were selectively extracted into the TRPO/kerosene/isodecanol system and thereby separated from Mg, Al, Cr and Mn which remained in the aqueous solution. Ti was selectively back-extracted from the organic phase under different acid condition (2.5 M HCl) and thus separated it from the Fe and V in the solvent.

Silva *et al*[126] separated Ti and Fe from ilmenite in a sulphuric acid solution using bis-(2-ethylhexyl) phosphoric acid (D2EHPA) at 1:1 (v/v) ratio. A two step extraction process recovered 99.4 % Ti with 15.9 % Fe co-extraction. The co-extracted Fe was selectively back extracted using 4.5 mol/L H_2SO_4 and in excess of 99.5 % of this co-

122 Remya, P.N. and Reddy, M.L., Solvent extraction separation of titanium, vanadium, iron from simulated waste chloride liquors of titanium minerals processing industry by trialkylphosphine oxide cyanex 923, *Journal of Chemical Technology and Biotechnology,* 79, pp.734-741 (2004)

123 Saji, J., Studies on liquid-liquid extraction separation of valuable metals from titania waste, PhD. Thesis, Cochin University of Science and Technology, pp.32-77 (2002)

124 Wang, X., Liang, B., Lu, L.W.P., Li, C., Wu, P. and .Ju, W., Simultaneous oxidation and extraction of iron from simulated ilmenite hydrochloric acid leachate, *Hydrometallurgy*,129-130, pp.105-111 (2012)

125 Hao, X., Lu, L., Liang, B., li, C., Wu, P. and Wang, J., Solvent extraction of titanium from the simulated ilmenite sulfuric acid leachate by trialkylphosphine oxide, *Hydrometallurgy*, pp.113-114, (2012)

126 Silva, G.C., Cunha, J.W.S.D., Dweck, J. and Afonso, J.C., Liquid-liquid extraction of iron and titanium by bis-(2-ethyl-hexyl) phosphoric acid (D2EHPA), *Minerals Engineering*, 21, pp.416-419 (2008)

extracted Fe was recovered thereby achieving more than 99 % Ti and Fe purity. Singh and Dhadke[127] separated titanium from iron using D2EHPA in toluene from $HClO_4$ solution. Ti was then selectively back extracted from the organic phase using 3 % H_2O_2.

In another study, Borsalani *et al*[128] extracted Ti from HCl solution using 2-ethylhexyl phosphonic acid mono-2-ethylhexyl ester (EHEHPA) dissolved in kerosene. This mixture extracted 93 % Ti with 49.8 % Fe co-extraction. Fontana *et al*[129] also studied the extraction of titanium and iron extraction in EHEHPA from an HCl solution. Their results indicated that approximately 90 % was extracted together with 20 to 67 % Fe in the presence of 1 M HCl solution using 0.5 M EHEHPA. Saji and Reddy[130] managed to successfully separate Ti and Fe from 0.2 M HCl solution using 0.2 M bis (2,4,4-trimethylpentyl) phosphinic acid (BTMPPA) in kerosene. Quantitative results indicated that 99.9 % of Ti moved into the organic phase and no Fe co-extraction observed.

3.3.3 Ion exchange

The successful separation of Ti and Fe has also been reported using ion exchange technique using both anionic and cationic resins. Yang and Pin[131] dissolved a Ti/Fe rock sample using a mixture of $HF:HNO_3:HClO_4$ and concentrated HCl and then separated Ti and Fe using a synthetic Levextrel aliquat 336 anion exchanger. Ti was

127 Singh, R.K. and Dhadke, P.M., Extraction and separation of titanium (IV) with D2EHPA and PC-88A from aqueous perchloride acid solutions, *Journal of Serbian Chemical Society*, **67**(7), pp.507-521 (2002)

128 Borsalani, A., Ghahremani, H., Seyfi, S. and Abdi, M.A., Solvent extraction of tetravalent titanium from chloride and nitrate solutions by 2-ethylhexyl phosphonic acid mono-2-ethylhexyl ester (EHEHPA) in Kerosene, *Der Chemica Sinica*, **2**(6), pp.204-211 (2011)

129 Fontana, D., Kulkarni, P. and Pietrelli, L., Extraction of titanium (IV) from acidic media by 2-ethylhexyl phosphonic acid mono-2-ethylhexyl ester, *Hydrometallurgy*, 77, pp.219-225 (2005)

130 Saji, J. and Reddy, M.L.P., Selective extraction and separation of titanium(IV) from multivalent metal chloride solutions using 2-ethylhexyl phosphonic acid mono-2-ethylhexyl ester, *Separation Science and Technology*, **38**(2), pp.427-441 (2003)

131 Yang, X. and Pin, C., Separation of hafnium and zirconium from Ti and Fe rich geological materials by extraction chromatography, *Analytical Chemistry*, 71, pp.1706-1711 (1999)

eluted first with 10 M HCl (10 mL) followed by Fe with 1 M HNO_3 (10 mL) at a flow rate of 0.36 mL/min. Recoveries in excess of 99 % Fe and 95 % Ti were obtained. Kurt *et al*[132] also successfully separated Ti and Fe from HCl solution using the Dowex-1 anion exchanger. Elution of Fe was accomplished with a 1 M HCl solution while Ti was eluted with 9.1 M HCl.

Strelow *et al*[133] separated Fe and Ti from a synthetic mixture dissolved in HCl/$HClO_4$ solution using the AG50W-X8 sulfufonate polystyrene cation exchange resin. Ti was eluted with a 15 mL mixture of 0.5 M H_2SO_4 and 0.05 % H_2O_2 while the Fe was eluted with 20 mL mixture containing 0.20 M HCl and 55 % acetone. Both elements were quantitatively recovered. Qureshi *et al*[134] used a tantalum antomonate resin to separate V, Fe and Ti. In their study the V was eluted first with 0.1 M HNO_3 (80 mL) followed by the elution of the Fe with 1 M HNO_3 (25 mL) and finally the Ti was eluted with 2 M H_2SO_4 + H_2O_2 (9:1, 60 mL). Fe and Ti recoveries of 105 % and 100 % were reported.

Das and Pobi [135] separated Ti, Fe and Al from bauxite and clay using a synthetic N-benzoyl-N-phenylhydroxyamine resin (BPHA-resin) after digesting the samples with a Na_2CO_3 flux. The resin was washed with Na_2SO_4 at a pH 2.5 followed by the sorption of the metal ions. Elution of Ti was accomplished with 12 mL of 0.5 M H_2SO_4 solution at a flow rate of 0.5 mL/min. Due to the same pH sorption properties of Al and Fe a fluoride masking agent was subsequently added to the column to prevent simultaneous elution Fe and Al. Fe was subsequently eluted with 25 mL 2 M HCl

132 Kurt, A., Nelson, K.F. and Smith, G.W., Anion-exchange studies.IX: Adsorbability of a number of metals in hydrochloric acid solution, *The Journal of Physical Chemistry*, pp.11-17 (1985)

133 Strelow, F.W.E., Liebenberg, C.L. and Victor, A.H., Accurate Determination of Ten Major and Minor Elements in Silicate Rocks Based on Separation by Cation Exchange Chromatography on a Single Column, *Analytical Chemistry*, **46**(11), pp.1409-13 (1947)

134 Qureshi, M., Gupta, J.P. and Sharma, V., synthesis of reproducible and chemically stable Tantalum Antimonate: Quantitative Separation of VO^{2+}-Al^{3+}-Ti^{4+}, $V0^{2+}$-Fe^{3+}-Ti^{4+}, and UO_2^{2+}-Ti^{4+}, *Analytical Chemistry*, **45**(1), pp.1901-1905 (1973)

135 Das, J. and Pobi, M., Separation of titanium, iron and aluminium on a chelating resin with benzoylphenylhydroxylamine group and application to bauxite and clay, *Fresenius Journal of Analytical Chemistry*, 336, pp.578-581 (1990)

while the Al was finally eluted with 50 mL of 4 mol/L H_2SO_4 solution. The results from this study are reported in **Table 3.2**.

Table 3.2: Quantitative results after the separation of Ti, Fe and Al in different samples using the BPHA-resin[135]

Sample	Compound	Reported value (%)	Found (%)[b]	Recovery (%)
Bauxite (B.A.S)	Al_2O_3	51.2[a]	50.9	99.4
	Fe_2O_3	17.5	16.9	96.5
	TiO_2	2.25	2.18	96.8
Bauxite (I.A.C)	Al_2O_3	49.1[a]	48.6	98.9
	Fe_2O_3	13.5	13.0	96.2
	TiO_2	10.0	9.92	99.2
Bentonite clay (SINP)	Al_2O_3	24.14	23.9	99.0
	Fe_2O_3	6.85	6.2	90.5
	TiO_2	1.74	1.7	97.7

[a] By difference, [b] Mean of triplicate analysis

3.4 Analytical techniques

Accurate determination of the analytes at all the stages of sample preparation is of utmost importance to assess the success of an experimental procedure, for quality control purposes as well as for mass balance. This section of the chapter is a literature review of analytical techniques used for the determination of Ti/Fe in different natural and synthetic samples. Some of the analytical techniques used by previous researchers in this field are briefly described and analytical results are reported if they were recorded. Both the wet chemical methods and direct analysis of solid samples are discussed.

3.4.1 Spectroscopic techniques

3.4.1.1 Solution analysis

Spectrophotometric techniques are still the most widely used methods for routine analysis as they are cheap, accurate and easy to use.[136] From literature review several methods are reported that were used for the determination of titanium and iron. For iron analysis, reagents such as 1,2-dihydroxybenzene-3,5-disulfonic acid, ferrozine and 2,2-dipyridine were used for spectrophotometric determination.[137] For titanium analysis hydrozones (isonicotinoyl hydrazine, 2,4-dihydroxybenzaldehyde and phenyl-2methyl-3-hydroxy-4-pyridone) and 1,2-cyclohecanedione were commonly used during the spectrophotometric determination of the element.[138] Interference of other elements is usually eliminated by addition of a masking agent such as thiosulphate, ascorbic acid, thiorea, oxalate and tartrate.[139,140]

Ferreira *et al*[141] developed a fast spectrometric method to determine Ti in geological samples using 3,4-dihydroxybenzoic acid (DHB). DHB react with titanium to form a yellow complex with an absorption maximum at 380 nm. The limit of detection for Ti analysis using this technique was determined to be 2.3 ng/mL. Absorption measurements for this Ti complex are accomplished in a pH range of 4 - 5.

136 Srilalitha, V*.,* A new spectrophotometric method for the determination of trace amounts of titanium(IV*), Physics, Chemistry and Technology*, **8**(1), pp.15-24 (2010)

137 Zannat, T. and Ahmed, M.J., A simple and rapid spectrophotometric method for the determination of iron in environmental, biological, pharmaceutical, food and soil samples using 1,2-dihydroxybenzene-3,5-disulfonic acid, *European Journal of Chemistry*, **5**(1), pp.101-100 (2014)

138 Suvarapu, L.N., Seo, Y.K. and Baek, S.O., Spectrophotometric Determination of Titanium(IV) by Using 3,4-Dihydroxybenzaldehydeisonicotinoyl- hydrazone(3,4- DHBINH) as a Chromogenic Agent, *Chemical Science Transaction*, **1**(1), pp.171-179 (2012)

139 Sumathi, G. and Reddy, T.S., Determination of titanium (IV) with 2-hydroxy-1-naphthaldehyde-p-hydroxybenzoic hydrozone using direct and derivative spectrophotometry, *International Journal of Innovative Science, Engineering and Technology*, **2**(10), pp.147-154 (2015)

140 Babaiah, O., Rao, K., Reddy, T. and Reddy, V.K., Rapid, selective, direct and derivative spectrophotometric determination of titanium with 2,4-dihydroxybenzaldehyde isonicotinoyl hydrazone, *Talanta*, **43**(4), pp.551-58 (1996)

141 Ferreira, S.L.C., De Araujo, N.M.L., Matos, R.C., Torres, A.L. and Costa, A.C.S., Fast spectrophotometric determination of titanium in rocks with 3,4-dihydroxybenzoic acid, *Mikrochemica Acta*, 122, pp.95-99 (1996)

Interference from iron, which has the absorption maxima at 380 and 570 nm, was eliminated by converting Fe(III) to Fe(II) using ascorbic acid as a reducing agent. This method was compared to a conventional method which uses hydroxylamine hydrochloride as masking agent and the comparison between the results are reported in **Table 3.3**. The student t-test showed no significant difference in the two methods at 95 % confidence level and the results were found to be satisfactorily accurate and precise (RSD < 1 %).

Table 3.3: Comparison of the of different methods used to determine titanium in geological samples[141]

Standards	Fast method[a]	Conventional method	Value certified
Clay 1	0.27 ± 0.01	0.28 ± 0.01	0.26
Andesite	0.84 ± 0.01	0.85 ± 0.02	0.87
Bentonite	1.26 ± 0.01	1.33 ± 0.02	1.28
Basalt	1.33 ± 0.02	1.33 ± 0.04	1.30
Bauxite	2.77 ± 0.03	2.81 ± 0.01	2.78

[a] — 95% confidence interval

Rudometkina and Ivanov[142] developed a UV-Vis spectrometric method for the quantitative determination of titanium and iron in complex samples such as minerals and alloys. Their method involve sample digestion using a mixture of 4 % HF and H_2SO_4 (1:1) and a dropwise addition of HNO_3. The residual sample was digested by flux fusion using Na_2CO_3 and $Na_2B_4O_7$ (1:1). 2 mL of 10 % tartaric acid was added to the combined solution and the pH was adjusted to 4.2-4.3 using 1 M NH_3 solution. Both Fe and Ti in solution were then complexed with EDTA. The Fe(III)-EDTA complex has an absorption maximum at 365 nm and is stable over a pH range of 2.7-6. The calibration curve obeyed beers law in the 0.008 to 0.09 mg/mL concentration range with a molar absorption coefficient of 1030 $L.mol^{-1}.cm^{-1}$. Ti (IV)-EDTA complex also absorb at 365 nm but is stable over the pH range of 3.2 - 7 and has a molar absorption coefficient of 1070 $L.mol^{-1}.cm^{-1}$. A linear Beer's law plot was observed

142 Rudometkina, T.F. and Ivanov, V.M., Spectrometric determination of macro quantities of iron and titanium in real-world objects, *Moscow University Chemistry Bulletin*, **66**(5), pp.315-317 (2011)

within the 0.006 – 0.08 mg/mL concentration range. This method was applied to ilmenite, magnetite, ferrosilicium for Fe quantification and ferrosilicate, rutile and ilmenite for TiO_2 quantification. The concentrations of titanium and iron which were obtained were compared to the results obtained using other techniques and the results are shown in (**Table 3.4**).

Table 3.4: Determination of Ti and Fe in different samples with UV-Vis and the alternative method[112]

Minerals and alloys used	Content	Found[a]	Alternative method
Fe (%)			
Ilmenite	31.4 ± 0.2	31.5 ± 0.4	--
Magnetite	52.8 ±0.1	52.8 ± 0.3	--
Ferrosilicium	28 ± 30	27.7 ± 0.2	--
TiO_2 (%)			
Ilmenite	--	16.1 ± 0.2	16.2 ± 0.1**
Rutile	--	90.2 ± 0.4	91.1 ± 0.6*
Ferrotitanium	71.2 ± 0.1	71.4 ± 0.3	--

[a] Number of replicates = 5(Fe),3 (TiO_2) confidence level P=0.95
**Determined by photometric procedure with diantipyrylmethane,
* Determined by titration with EDTA
--Not determined

Andrade *et al*[99] analysed an ilmenite sample with ICP-OES after its dissolution using H_3PO_4 (**Section 3.2.1**). The wavelengths at 259.9 nm and 334.9 nm were selected for analysis of Fe and Ti respectively and the sample contained 12.14 % TiO_2 and 38.2 % FeO. Radhamani *et al*[143] who decomposed an ilmenite sample using sodium di-hydrogen orthosphate and di-sodium hydrogen orpthophosphate (1:1) as flux (**Section 3.2.2**) used ICP-OES to study the composition of synthetic ilmenite and rutile. The ICP-OES results were validated by comparing the newly obtained results

143 Radhamani, R., Murugesan, P., Premadas, A. and Srivasva, P.K.A., Novel rapid method for preparation of sample solution for chemical characterisation of titanium minerals by atomic spectrometry, *Talanta*, **71**(5), pp.1932-1938 (2007)

with those obtained using atomic absorption spectroscopy (AAS) for the same sample (**Table 3.5**).

Table 3.5: Comparison of ICP-OES and AAS results for synthesised rutile and ilmenite[143]

Oxide	Synthetic mixture of Rutile			Synthetic mixture of ilmenite		
	Content (mg)	Found (mg)		Content (mg)	Found (mg)	
		ICP-OES	AAS		ICP-OES	AAS
TiO_2	90.0	90.2	89.5	45	45.5	44.3
Fe_2O_3	5.0	4.90	4.5	45	44.8	44.9
MnO_2	1.5	1.51	1.48	1.5	1.5	1.56
MgO	1.5	1.45	1.44	1.5	1.51	1.48
V_2O_5	1.5	1.45	1.49	1.5	1.48	1.50
Cr_2O_3	1.5	1.52	1.43	1.5	1.55	1.45

The microwave digestion method developed by Tripathi and Chattopadhyay[108] **(Section 3.2.3**) was applied to different titanium containing minerals (**Table 3.6**) and the concentrations of the elements in the mineral samples were subsequently determined with ICP-OES. The ICP-OES results were compared to those obtained using UV-Vis spectroscopy, which was used as in this study as a reference method. Excellent agreement between the elemental recovery of the two methods and the certified values of standard reference materials were obtained and indicated that the digestion procedure could reliably be used for sample preparation for the accurate determination of Ti in different minerals.

Table 3.6: Titanium concentration (%) in various samples using ICP-OES and UV-Vis[108]

Sample	Titanium dioxide (%, wt/wt)		
	UV-Vis[a]	ICP-OES[a]	Certified value
Titanium dioxide (SRM-154b)	99.55 (0.16, 0.16)	99.29 (0.1, 0.12)	99.74
Rutile (IGS-32)	92.12 (0.24, 0.26)	92.35 (0.10, 0.11)	95.51
Ilmenite (IGS-31)	54.42 (017, 0.32)	54.33 (0.06, 0.10)	54.74
Tropical soil (SAu-1)	1.72 (0.02,1.10)	1.74 (0.01, 0.86)	1.80
Columbite (IGS-33)	1.72 (0.03, 1.92)	1.75 (0.02, 1.20)	1.74
Basalt (BIR-1)	0.96 (0.01, 0.73)	0.95 (0.01, 0.63)	0.96
Stream Sediments (STSD-4)	0.74 (0.01, 1.61)	0.75 (0.02, 2.27)	0.76
Granite (G-2)	0.47 (0.01, 2.13)	0.46 (0.01, 3.04)	0.48

[a] Number of replicate —10 (mean, standard deviation, % RSD)

Hirata *et al*[144] developed a quantification method using on-line pre-concentration ion exchange chromatography to increase the sensitivity of Ti, Fe, Cr and Al for analysis with ICP-OES. A sample was buffered with 0.5 M ammonium acetate at pH 3.8 and pumped through a column at 6.0 mL/min and eluted with HNO_3 (2 M) to the ICP-OES nebulizer at 3.0 mL/min using a flow injection analysis system. The FIA-ICP system yielded a linear calibration curve and the relative standard deviation for peak heights of 10 ug/L and 20 are reported in (**Table 3.7**). The detection limits were calculated and compared to those obtained using ICP-OES. The signal peak height gives detection limits of at least 1 order of magnitude better (in most cases, 30-fold better) than conventional ICP analysis.

144 Hirata, S., Umezaki, Y. and Ikeda, M., Determination of chromium (III), titanium, vanadium, iron(III) and aluminium by inductively coupled plasma atomic emission spectroscopy with an on-line preconcentrating ion exchange column, *Analytical Chemistry*, **58**(13), pp.2602-2060 (1986)

Table 3.7: Precision, linearity and signal enhancement for the online pre-concentrating FIA-ICP system[144]

Element	Concentration µg/L	RSD (%) n = 5	Linear range, µg/L	Signal enhancement[a] (fold increase peak height)
Al	20	3.5	2.0 - 100	34
Cr (III)	10	4.0	0.2 - 100	113
Fe (III)	10	4.4	0.1 - 100	52
Ti(V)	10	2.3	0.1 - 100	68

[a] Sample rate—17 samples/h with 180s load times.

3.4.1.2 Direct solid analysis

Klepka *et al*[145] studied the composition of a Norway ilmenite sample using XRD. Three different phases were identified, namely ilmenite ($FeTiO_3$, 89 %), hematite (Fe_2O_3, 9 %) and enstatite ($MgSiO_3$, 5 %). These phases covered 89 % of the mineral with 11 % determined as oxide of trace elements such as Al, Mg, Si, Ca and V. Samal *et al* [146] studied ilmenite, titanium slag and metalized ilmenite (ilmenite heated at 1200 ºC) for their compositional phases. The natural ilmenite sample was found to possess one phase ($FeTiO_3$) while the metalized ilmenite showed distinct iron oxide and titanium oxide phases. The titanium slag showed 4 different phases, namely $Fe_3Ti_3O_{10}$, TiO_2, Fe and Fe_2O_3. When the titanium slag was heated the phase composition changed from anatase (TiO_2) to rutile (TiO_2).

Vasquez and Molina[113] studied the effect of oxidising an ilmenite sample in a furnace at different temperatures (700, 800, 900 and 1050 ºC) prior to separation using HCl leaching (**Section 3.3.1**). The oxidized ilmenite was studied using XRD before and after acid leaching (**Figure 3.2**). The results indicated a decrease in iron content as

145 Klapka, M., Lawniczak-Jablonska, K. and Jablonski, M., Combined XRD, EPMA and X-ray absorption study of ilmenite used in pigment production, *Journal of Alloys and Compounds*, 401, pp.281-288 (2005)

146 Samal, S., Mohapatra, B.K., Mukherjee, P.S. and Chatterjee, S.K., Integrated XRD, EPMA, and XRF study of ilmenite and titanium slag used in pigment production, *Journal of Alloys and Compounds*, 474, pp.484-489 (2009)

indicated by the disappearance of the hematite peaks (**Figure 3.2, b**) after acid leaching.

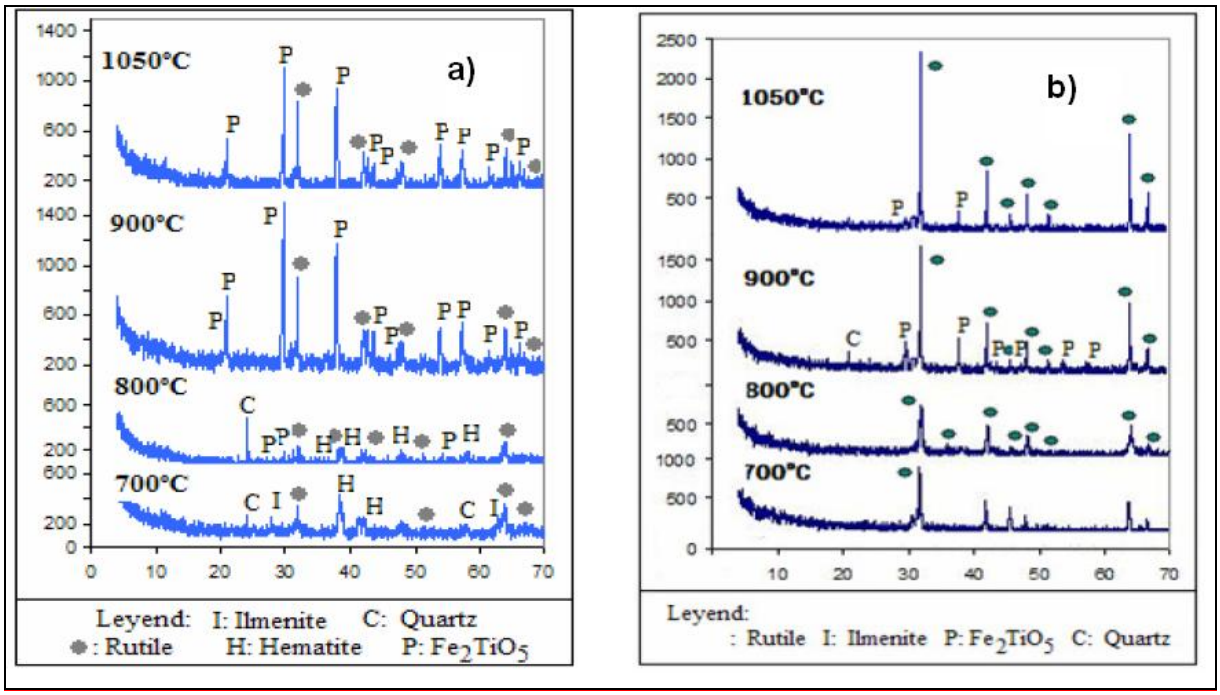

Figure 3.2: XRD spectrum of a) ilmenite oxidized at different temperatures and b) the product obtained after leaching ilmenite which was pre-oxidized.[113]

Mehdilo and Irannajad[97] analysed the ilmenite sample from Qara-aghaj (**Paragraph 4, Section 3.2.1**) using XRD to determine the major mineral phases. The results revealed that the sample contained TiO_2 (anatase and rutile), $Fe_2Ti_3O_9$, Ti_2O_5 and FeO. The concentrations of the different elements were determined using XRF and are reported in **Table 3.1**.

Swanepoel[147] reacted an ilmenite sample with 30 % bituminous coal at 1325 ºC in a nitrogen atmosphere (**Equation 3.2**) and the product was characterised by SEM and EDX analyses. The SEM results indicated an iron globule attached to nitride ilmenite and the results were confirmed using EDX with estimated elemental mass percentage of 69.00 % Ti, 17.77 % Fe, 11.98 % C and 1.26 % Al (**Figure 3.3, A**). It is also important to note that not all the globules in the product are iron (**Figure 3.3, B**) but the Fe particle was also analyse by EDX showing elemental composition; C 63.60

147 Swanepoel, J.J., Process development for removal of Nitrided ilmenite, M.Eng Thesis, University of Pretoria, pp.15-23 (2010)

%, Si 0.68 %, Ti 4.71 % and Fe 30.92 %. The high carbon concentration observed (63.60 %) was due to the carbon coating on the Fe particle. The major composition of the sample were also determined to be TiN (51.45 %), α-Fe (93.70 %), Fe_3C (6.50 %) and TiO_2 (2.35 %) using XRD analysis.

$$FeTiO_{3(S)} + 3C_{(s)} + N_2 \longrightarrow TiN_{(s)} + 3CO_{(l)} + Fe_{(s)} \quad \textbf{3.3}$$

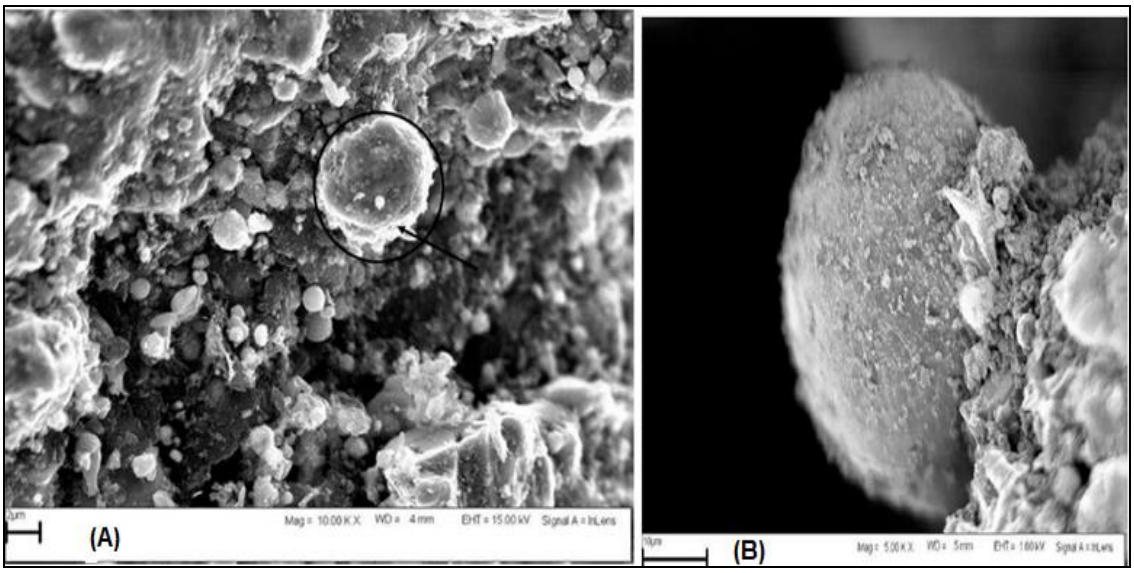

Figure 3.3: A) An ilmenite nitride sample with Fe particle, B) Fe particle attached to a nitride ilmenite sample.

Samal *et al*[146] also studied the natural ilmenite, metallised ilmenite and titanium slag samples using SEM and EDX. SEM results indicated that the ilmenite sample was elongated with some fine cracks in the mineral. The metalized ilmenite which was also analysed by EPMA had distinct Ti, Fe phases with traces of V. Titanium slag appeared irregular with small cracks and holes and contained small globules of Fe. The EDX analysis also indicated that the weighed percentage of Fe decreased from ilmenite (22.65 %) to titanium slag (5.27 %) whereas Ti concentration increased from ilmenite (23.28 %) to titanium slag (32.91 %).

3.5 Characterization techniques

Other analytical techniques which have been used include infrared spectroscopy and CHNS elemental analyses. These techniques are mainly used in the chemical elucidation of compounds formed during synthesis, composition determination and/or for quality control at different stages of mineral processing.

During the separation processes, several researchers (**Section 3.3.1**) have used IR for structural elucidation of the Ti and Fe type complexes formed during the process.[122,123] Reyma *et al*[148] synthesised the hydrozone complex for effective solvent extraction of Ti and Fe. The 3-phenyl-4-acyl—isoxazolones (HFBPI) were reacted with $FeCl_3$ and $TiCl_4$ in acetyl acetone. IR spectroscopy was used to characterise the different products obtained. The IR spectrum showed a shift in C=O stretching frequency from 1702 to 1607 cm^{-1} for $Fe(PBI)_3$ and 1620 in Ti-HFBPI and the strong band observed at 2600 cm^{-1} in the free ligand disappeared in the newly formed Ti and Fe complexes, indicating the successful chelation of the metal and the ligand which were then extracted into the xylene.

Saji *et al*[149] demonstrated the complexation of $TiCl_4$ with bis(2,4,4-tris-methylpentyl) phosphinic acid (cyanex 272) (**Figure 3.4).** The IR spectrum indicated that the stretching frequency shifts for P=O in the Ti(IV)-cyanex complex from 1170 to 1014 cm^{-1} compared to the free cyanex 272 and this indicated the involvement of the P=O oxygen bond in the metal-ligand coordination. The P-OH vibration was observed at 958 cm^{-1} both in the ligand and the metal-ligand complex. The titanium was then extracted into cyanex 272 in xylene and was then separated from a synthetic mixture of Ti(IV) (2.5×10^{-3} M) and Fe(III) (0.5×10^{-3} M). More than 99.9 % of the titanium was extracted and no Fe(III) was co-extracted.

148 Remya, P.N., Pavithran, R. and Reddy, M.L.P, 3-Phenyl-4acyl-5-isoxazolones as reagents for the solvent extraction separation of Titanium(IV) and Iron(III) from multivalent metal chloride solutions, *Solvent Extraction and Ion Exchange*, **22**(3), pp.473-490 (2004)

149 Saji, J., Saji, J.K. and Reddy, M.P.L., Liquid-liquid extraction of tetravalent titanium from acidic chloride solution by Bis(2,4,4-trimethylpentyl) phosphinic acid, *Solvent Extraction and Ion Exchange*, **18**(5), pp.877-894 (2000)

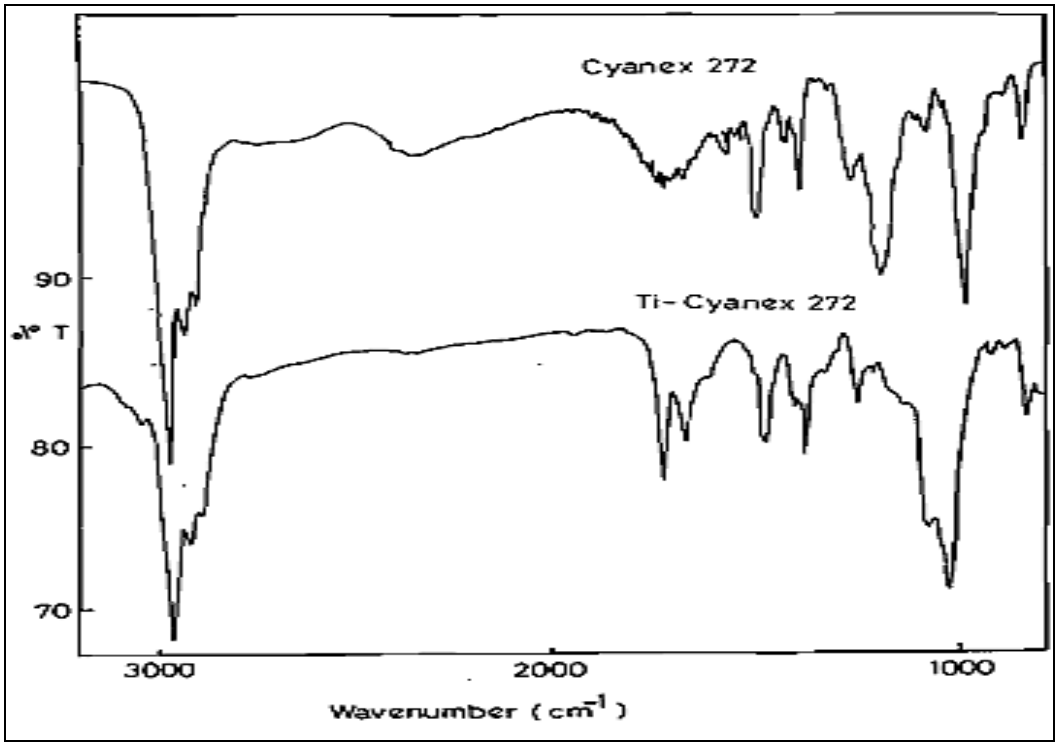

Figure 3.4: The IR spectra of cyanex and Ti(IV)-cyanex complex.

CHNS elemental analysis was also used for the characterisation of different Ti and Fe complexes. Carmalt *et al*[150] synthesised titanium thiolate complexes by reacting $TiCl_4$ with different ligands which include 2-mercaptopyridine, 4-ter-butylpyridine 2-mercaptopyrimidine and 4-ter-butylpyridine, $TiCl(SC_5H_4N)_3$ and $TiCl(SC_4H_3N_2)_3$ were obtained. The elemental composition of the products was determined using a CHNS analysis and the data was as follow (%): $TiCl(SC_5H_4N)_3$ calculated C 43.5, H 2.9, N 10.2; found C 43.7, H 2.7, N 10.7 %; for $TiCl(SC_4H_3N_2)_3$ calculated C 47.4, H4.9, N14.7; found C 47.7, H 5.1, N14.1 %.

Xu *et al*[151] synthesised a pyridine-2,3,5,6-tetracarbonylxylato-bridge Fe(III) complex ($K[Fe(H_2pdtc)_2$) that contains K^+ as counter ion. This complex was isolated after the reaction between $Fe_2(SO_4)_3 \cdot 7H_2O$, pyridine-2,3,5,6-tetracarboxylic acid and KOH

150 Carmalt, C.J., Peter, E.S., Parkin, I.V. and Tocher, D.A., Synthesis and characterisation of titanium pyridine and pyrimidine-thiolates and their applications as precursor to titanium disulfide, *Polyhedron*, **26**(1), pp.43-48 (2007)

151 Xu, W., Lin, J.L., Zhu, H.L., Hu, F.H. and Zheng, Y.Q., Synthesis, crystal structure and magnetic properties of iron (II) pyridine-2,3,5,6-tetracarboxylate complex, *Zeitschrift für Naturforschung*, 66b, pp.465-470 (2011)

under ambient conditions (**Equation 3.4**). Elemental analyses of the complex indicated a successful complexation as the theoretical and experimental composition of C, H and N in ($K[Fe(H_2pdtc)_2$) were in excellent agreement: C 35.96 (35,74), H 1.01(0.80), N 4.66(4.52) %.

$$Fe_2(SO_4)_3 + 4H_4pdtc + 2KOH \longrightarrow 2K[Fe(H_2pdtc)_2] + 3H_2SO_4 + 2H_2O \qquad \textbf{3.4}$$

In another study Yau *et al*[152] synthesised a hydrazone complex with Ti and Fe and characterised them using elemental analysis as reported in **Table 3.8.**

Table 3.8: Elemental analysis data for Ti and Fe hydrazone complexes

Complex	C (%)	H (%)	N (%)
HCMANBH	54.09 (53.26)	3.34(3.04)	11.98(11.12)
Ti-HCMANBH	37.89 (38.32)	3.01 (3.42)	8.17 (8.38)
Fe-HCMANBH	38.81 (39.10)	2.83 (3.08)	8.11 (8.55)

Found (Calculated)
HCMANBH= 2-hydroxy-5-chloro-4-methylacetophenone-4nitrobenzylhydrazone.

3.6 Conclusion

From the above discussions it is apparent that many analytical determinations of titanium containing minerals have been performed. Flux fusion turned out to be the most successful technique for the complete dissolution of the mineral followed by microwave acid assisted digestion, especially in the presence of HF. Interestingly addition of organic solvents such as ethanol, methanol and phenols in a conventional acid leaching (see **Section 3.3.1**) significantly improved the dissolution of both Ti and Fe with this technique which is otherwise the least successful compared to flux fusion

152 Yau, S.R., Yaul, A.R., Pethe, G.B. and Aswar, A.S., Synthesis and characterization of transition metal complex with N,O-Chelating hydrazone Schiff base ligand, *American-Eurasian Journal of Scientific Research*, **4**(4), pp.229-234 (2009)

and microwave dissolution methods. Although flux fusion is a highly successful technique for the complete dissolution of Ti containing minerals it has several disadvantages which include the cross contamination of the sample by the flux and potential loss of volatile elements. The use of HF on the other hand can result in environmental pollution and is also the most corrosive acid for digestion.

This literature studies also show that successful separations of Ti and Fe were accomplished with solvent extraction technique. Both Ti and Fe were easily extracted by organic extractants in H_2SO_4 or HCl matrices and the separation of the two elements was achieved by the selective striping of either Ti or Fe under different acidic conditions. Other separation techniques which have been studied and have shown different levels of success and include ion exchange and selective precipitation.

From the above discussions it also appear that ICP-OES is the most preferred analytical technique for the accurate quantification of Ti, Fe and other elements in minerals and synthetic samples. This may be due to the several advantages the ICP-OES (**Chapter 4**) has over other techniques such as UV-Vis and XRF and these include its low detection limits, wider linear range and the ability to handle complex mineral matrices better (compared to ICP-MS which is affected by totally dissolved solids). The studies have also shown that IR and CHNS elemental analysis can be used to successfully identity and characterise Ti and Fe compounds.

4 Selection of analytical techniques

4.1 Introduction

Hydrometallurgical processing of minerals always entails four essential steps, namely i) dissolution and homogenization of the sample, ii) proper identification of the mineral constituents, iii) the accurate determination of their concentrations and iv) the separation and isolation of individual constituents. The first step in mineral processing include the crushing, grinding or even moulding of the mineral into pellets followed by the dissolution and homogenization of the samples using different techniques (wet ashing) such as flux fusion, microwave digestion and open vessel acid digestion. Qualitative and quantitative analyses are usually accomplished using different analytical techniques such as ICP-OES, ICP-MS, AAS (for wet analysis), SEM-EDS, XRD and XRF (for solid analyses). Separations are commonly accomplished using techniques such as flotation, ion exchange, solvent extraction and selective precipitation.

This chapter gives details on the principles and techniques used in the dissolution of the ilmenite sample and the separation of the major constituents therein. The chapter also cover the instrumentals and techniques that are commonly used for the quantification and characterisation of products during the mineral (ilmenite) processing.

4.2 Sample dissolution methods

Sample preparation is a fundamental step in the mineral processing process and in chemical analysis. For wet chemical analysis the sample preparation involves the complete dissolution of the solid sample to afford the total complete quantification and characterization of the sample.[153] Although numerous reports have been published on the successful dissolution of ilmenite (see **Chapter 3**), the common challenge during this step is finding a digestion method which allow for the subsequent separation of the constituents (mainly Ti and Fe) using rapid and economical routes. In this study conventional acid dissolution, flux fusion and microwave acid assisted digestion techniques were investigated to identify the most promising dissolution technique for the complete dissolution of ilmenite sample or which allowed for the quantitative leaching of the major elements, Ti and Fe from the mineral.

4.2.1 Conventional acid digestion method

Acid leaching using conventional methods such as heating the sample/acid mixture on a hot plate with constant stirring is the most common and oldest digestion procedure in mineral processing (see **Chapter 3, Section 3.2.1**). The procedure generally involved mixing of a solid sample and a mineral acid such as HNO_3, HCl, H_2SO_4 or HF (**Table 4.1)** or an acid mixture such as H_2SO_4/HF**.** This digestion technique is often affected by other experimental parameters such as the sample constituents and the degree of pulverization or milling.[154] This method of sample decomposition is usually less successful compared to flux fusion and microwave assisted digestion techniques. However, acid mixtures containing HF have been proved to be highly effective in the dissolution of numerous mineral samples at elevated temperatures which contain silicate minerals.[153] The literature study[155] also

153 Chao, T.T. and Sanzolone, R.F., Decomposition techniques, *Journal of Geochemical Exploration*, 44, pp.65-106 (1992)

154 Dulski, T.R., A Manual for the Chemical Analysis of Metals, pp.70-89,95-107,411-413 (1996)

155 Nete, M., Koko, F., Theron, T., Purcell, W. and Nel, J.T., Primary beneficiation of tantalite using magnetic separation and acid leaching, *International Journal of Minerals, Metallurgy and Materials*, **21**(12) pp.1154-1159 (2014)

indicated that acids such as H_2SO_4 can selectively dissolve certain mineral from the mineral matrix and thereby achieving their separation from the rest of the elements.

Table 4.1: Different mineral acids used for sample dissolution[153,154,156]

Acid	Uses
HF	Digest oxides of Ti, Na, Ta and Zr, sulphides, silicates.
HCl	Dissolves carbonates, borates, phosphates, sulphates except barite.
HNO_3	Oxides, sulphides, selenides, arsenides and carbonates readily.
H_2SO_4	Decompose monazite, sulphides, oxides, carbonates and hot concentrated acid dissolves most organic compounds.
H_3PO_4	Sulphides, oxides, silicates and carbonates.
Aqua regia ($3HNO_3$:1HCl)	Decomposes sulphides, arsenides Mo and W minerals.

All acid dissolution procedures have the advantage of less sample contamination compared to flux fusion techniques (flux impurities). However, the maximum temperature of the dissolution step is limited by the boiling point of the mineral acid used and there is the possibility of the loss of volatile elements.[154,157] Fumes from the boiling acids can also lead to seriously air contamination if digestion is carried out in open vessels. In addition, acids such as HF and $HClO_4$ are hazardous and dangerous to work with. $HClO_4$ is very explosive while HF is toxic and corrosive to humans and equipment (require the use of plastic glassware). Other acids such as HNO_3 and HCl are difficult to handle and corrosive to the disposal equipment and the environment.[153,158,159]

156 Kenkel, J., Analytical Chemistry Technicians, 3rd edition, pp.26-28 (2002)

157 Decomposing and Dissolving the Sample, [Accessed 14-10-16]. Available from : http://www.cengage.com/resource_uploads/downloads/0495558281_371363.pdf

158 Mitra, S., Sample Preparation Techniques in Analytical Chemistry, pp.231-237 (2003)

4.2.2 Flux fusion method

Flux fusion is commonly used for minerals, slags and alloys which are resistant to acid attack under normal conditions. In this method a sample is mixed homogeneously with a salt (excess) and the mixture is fused at temperatures which exceed the melting point of the salt (flux). The molten mixture obtained is then dissolvent in a suitable solvent such as water, acid or a base. The improved efficiency of this dissolution method compared to acid digestion is due to the high temperatures needed to produce molten salts (≥ 200 ºC) and the high ionic concentrations (ion liquids) while acid digestion is often limited by the boiling point of the respective acid. The successful dissolution of a mineral with flux fusion depends on several factors which include i) the acid-base properties of the sample and the fluxing agent, (acidic minerals are often more soluble in basic fluxes)[160] ii) the melting point of the flux salt to produce an ionic liquid (often referred to as molten salts at high temperatures); and iii) the flux:sample weight ratio. In this process the flux acts as a solvent and the dissolution of the sample is therefore governed by the solubility such as the saturation point of the solution.[153,160] **Table 4.2** Contains a list of some of the commonly used fluxes together with the samples they are useful on.

159 Kuboyana, K., Sasaki, N., Nakagome, Y. and Katoaka, M., Wet Digestion, Analytical Chemistry, 360, pp.184-191 (2005)

160 Nete, M., Separation and Purification of Niobium and Tantalum from synthetic and Natural compounds, PhD. Thesis, The University of the Free State, pp.59-58,64-79 (2013)

Table 4.2: Common fluxes used for decomposition of metals and minerals[153,154]

Flux	Melting point (ºC)	Crucible	Uses
$LiBO_2$	850	Pt, Au	Minerals, soils, and slags
NaOH or KOH	318	Pt, Au, Zr	Silicon carbide and silicates
Na_2O_2	1000	Fe, Ni	Platinum alloys, Sn, Cr and Zr minerals
$K_2S_2O_7$	495	Pt, porcelain	Metal oxides
Na_2CO_3	Decomposes	Pt, Ni, Zr	Silicates, phosphates and sulphates
NH_4I	> 300 (starts to sublime)	Porcelain	Si-minerals, REE, oxides

Although mineral dissolution by flux fusion is normally very successful, some disadvantages may include sample contamination due to the addition of impurities from the flux. Some of these fluxes which contain the easily ionisable elements (EIEs, alkali and earth alkali elements) negatively affect the analysis of the target elements. For example, the Li and Na found in $LiBO_3$ and $NaBO_3$ change the flame properties of ICP-OES instrument while borate on the other hand may precipitate as boric acid (especially in high acidic solutions) which can co-precipitate some of the analytes and thereby reducing their concentration in solution.[159] The boric acid precipitation or any other precipitate formation can also result in the clogging of the ICP nebulizer.[161] In addition, the high salt concentrations may results in negative matrix effects such as ICP torch clogging due to the solid deposition during the evaporation step and can reduce the analyte signal intensities. Dilution of the sample can also result in the reduction of the analyte signal (to levels below the LOD) which can affect the accuracy of the results.[162,163]

161 Dean, J., Practical Inductively Coupled Plasma Spectroscopy, p.29 (2005)

162 Van de Wiel, H.J., Determination of elements by ICP-AES and ICP-MS, National Institute of Public Health and the Environment, pp.15-19 (2003)

163 Massaro, E. J., Handbook of Human Toxicology, pp.18-19 (1997)

4.2.3 Microwave digestion

Microwave dissolution was introduced in the mid 1970's and thereafter many researchers developed mineral dissolution methods associated with energy conservation using this technique. Microwave assisted digestion has gained popularity in recent years due to advantages such as clean dissolutions, improved safety and little or no loss of volatile compounds leading to highly reliable elemental analysis.[164,165,166] In this technique digestions are carried out in closed vessels which are transparent to the microwave energy and the uniform and direct heating of the sample (see **Figure 4.1**) leads to shorter digestion times. Microwave instruments are mostly used for digestion of pure metals, metal oxides and minerals.

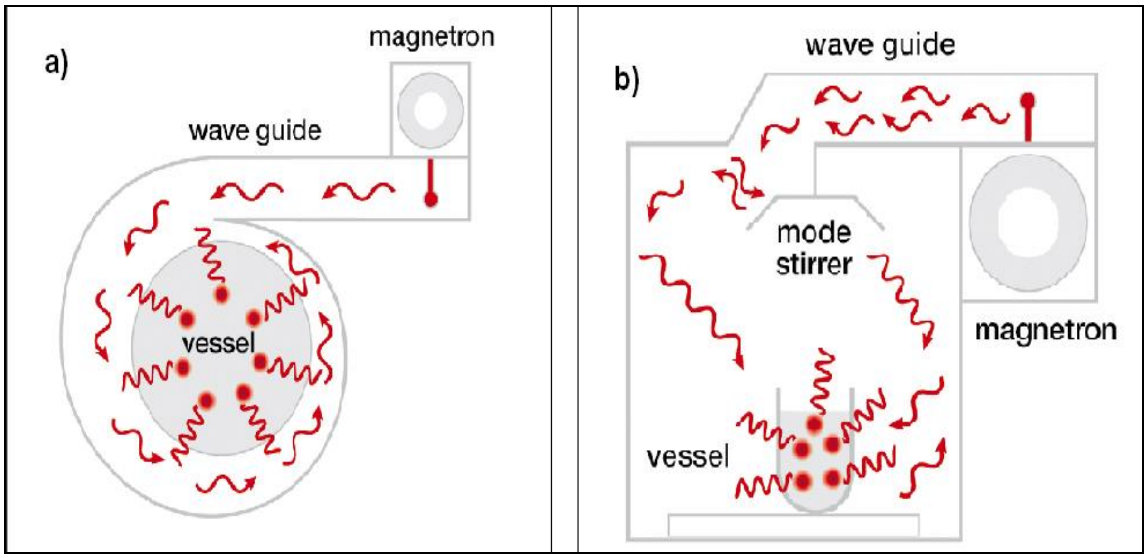

Figure 4.1: Schematic presentation of microwave system a) Single mode apparatus, b) Multi-mode apparatus.[167]

164 Haque, K.E., Microwave energy for mineral treatment processes- a brief review, *International Journal of Mineral Processing*, **57**(1), pp.1-24 (1999)

165 Panias, D. and Krestous, A., Use of microwave energy in metallurgy, 1st International conference on Advances in Mineral Resource Management and Environmental Geotechnology, AMIREG, pp.215-220 (2004)

166 Hassan, N.M., Rasmussen, P.E., Zlotorzynska, V.C. and Chen, H., Analysis of environmental samples using microwave assisted acid digestion and inductive coupled plasma mass spectrometry: Maximizing total element recoveries, *Water Air Soil Pollution*, 178, pp.323-334 (2007)

167 Instrument types/Microwave reactors, [Accessed 03-10-16]. Available from: http://www.this-is-synthesis.com/mainnav/crash-course/instrument-types/

The primary disadvantage of microwave digestion is the fast rate of the sample heating which may result in uncontrollable exothermic reactions that can lead to the explosions within the equipment. The digestion tubes can also crack due to build-up of pressure and increase in temperature.[168] It is therefore extremely important to carefully select the appropriate solvents for the digestion of different solid samples. The selection criteria should include the following; i) the solvent should not react with the digestion vessels (HF attacks quartz and borosilicate vessels), ii) the selected solvent should not react violently with the sample under the set microwave conditions (e.g. digestion of organic samples with HNO_3)[157] and iii) the solvent should not be an explosive hazard, e.g. $HClO_4$ can easily explode under pressure.[169] Other disadvantages include the limited amount of sample that can be digested at a time due to the microwave vessel design.[168]

4.3 Separation techniques

The next step in the hydrometallurgical processing of minerals after dissolution entails the separation and isolation of the individual mineral elements or pure metal compounds. In analytical chemistry successful separation entails the isolation of the analyte from an interfering component. The following sub-sections discuss some of the separation techniques which were investigated in this study for the separation of Ti from Fe present in the ilmenite.

4.3.1 Selective precipitation

Precipitation is a separation method based on the difference in solubility of the different components in solution.[170] Precipitation results from the supersaturation (surpassing the K_{sp} of the specific compound) of a solution at equilibrium. The effect of this process leads to nucleation where a number of particles, atoms or ions join

168 Benefits of Microwave Digestion over Open Acid Digestions, [Accessed 19-11-2016]. Available from: http://lab-training.com/2014/01/19/benefits-of-microwave-digestion-over-open-acid-digestions/

169 Luque de Castro, M.D. and Luque Garcia, J.L., Acceleration and Automation of Solid Sample Treatment, pp.212-214 (2002)

together forming a stable solid (nuclei) resulting in crystal growth.[171,172] Von Weimarn[171] described the precipitation process as a relative supersaturation (RSS) reaction represented by **Equation 4.1**

$$RSS = (Q-S)/S \qquad \textbf{4.1}$$

where Q is the solutes actual concentration and S is the solutes concentration at equilibrium. Precipitation is more likely to occur by particle growth. The particle sizes of the precipitate are increased by decreasing the RSS value and a high RSS ratio indicates formation of precipitation with small particles and high rate of nucleation. Essentially precipitate is the condition that exists in solution which has a small RSS value predicting particle growth as a crystalline solid. This is mostly done by increasing the S value and decreasing the Q value.[171,173] The particle size of the precipitate is largely influence by reagent concentration, temperature, solubility (K_{sp}) and the rate of reaction.

The selective precipitation technique is used more often for isolation than for separation purposes. For effective separation, the precipitate which is formed should have a low solubility (compared to the other chemical species in solution) and it should be easy to separate from the solution. Additionally, only one element should precipitate with no or the minimum co-precipitation of other elements in solution under a certain set of experimental conditions. The solubility of a product is often facilitated by controlling the conditions of the reaction leading to precipitate formation. The heterogeneous equilibrium reaction during precipitation is presented by **Equation 4.2** and the solubility of the precipitate can be determined by the calculation of its solubility product (K_{sp}) as indicated by **Equation 4.3**.[171,173]

170 Marozenko, Z. and Baloerzak, M., Separation, Preconcentration and Spectrometry in Inorganic Analysis, pp.12-17 (2000)

171 Christian, G. D., Analytical Chemistry, 5th edition, pp.145-152,158-161,506,485-492 (1991)

172 Skoog, D.A., West, D.M., Holler, F.J. and Crouch S.R., Fundamental of Analytical Chemistry, 9th edition, pp.773-781,43-50,281-287,865-871,849 (2014)

173 Precipitation Gravimetry, [Accessed 22-10-2016]. Available from: http://chem.libretexts.org/Textbook_Maps/Analytical_Chemistry_Textbook_Maps/Map%3A_Analytical_Chemistry_2.0_(Harvey)/08%3A_Gravimetric_Methods/8.2%3A_Precipitation_Gravimetry

$$AB_{(s)} \overset{Ksp}{\rightleftharpoons} A^{+}_{(aq)} + B^{-}_{(aq)} \quad \textbf{4.2}$$

$$K_{sp} = [A^{+}][B^{-}] \quad \textbf{.4.3}$$

Precipitation can be accomplished using both organic and inorganic precipitants. The organic precipitants (**Table 4.3**) are mostly chelating agents and have the advantage of giving a precipitate that has low solubility in water.[171]

Table 4.3: Some of the commonly used organic precipitants[174,175]

Name	Formula	Example of ions precipitated
8-hydroxyquinoline	C_9H_7ON	Fe^{3+}, Zn^{2+}
Dimethylglygoxime	$C_4H_7O_2N_2$	Ni^{2+}, Pd^{2+}
Anthranilic acid	$C_7H_7NO_2$	Cu^{2+}, Zn^{2+}, Cd^{2+}
Cupferron	$C_6H_9N_3O_2$	Fe^{3+}, V^{4+}, Cu^{2+}, Ti^{4+}
Tetraphenylarsonium chloride	$C_{24}H_{20}AsCl$	MoO_4^-, WO_4^-

Precipitation reactions are usually carried out under mild conditions such as room temperature and low acidity (due to pH dependence of most precipitating agents). However, separations by this technique are affected by co-precipitation reactions through surface adsorption, mixed-crystal formation and/or occlusion. Other disadvantages include filtering small colloidal particles as they settle with difficulty at the bottom of the solution. Crystalline particles on the other hand are usually larger in size and are easily separated from the solution and the rest of the elements by filtration. The precipitating agent should also be selective towards the target elements.[171,172]

174 Chapter 5 Titrimetry and Gravimetry [Accessed 11-10-2016]. Available from: http://kczx.hnu.cn/G2S/Template/View.aspx?courseId=5&topMenuId=128478&action=view&type=&name=&menuType=1&curfolid=156679

175 Sivasankar, B., Engineering Chemistry, p.283 (2008)

4.3.2 Solvent extraction

Solvent (liquid-liquid) extraction is a separation technique in which chemical species are separated based on their different solubility properties between two immiscible liquids. This technique is one of the most widely used hydrometallurgical methods for separation of metals and it has been extensively studied in Ti and Fe separation. The method is easy to use and can extract both major and trace elements in a sample with high separation efficiency.

A solute is distributed between two immiscible liquid phases during the shaking of the liquid mixture (**Equation 4.4**). The extent to which a solute is distributed between the solvents is determined by calculating the distribution coefficient (K_D) which is the ratio of its concentrations in the two phases. For example, a large K_D value in **Equation 4.4** would imply a successful extraction of solute A into the organic solvent. The total extraction of the solute is also determined by a distribution ratio (D) given in **Equation 4.5**.[171]

$$K_D = \frac{[A]_{org}}{[A]_{aq}} \qquad \textbf{4.4}$$

$$D = \frac{\sum A_{org}}{\sum A_{aq}} \qquad \textbf{4.5}$$

Metal ions are mostly extracted as metal chelates under specific pH conditions. Generally, the reactions leading to a successful extraction of metals involve the conversion of a metal ion of interest, with chelating, to an organic-like molecule which is more soluble in the organic than in aqueous solvent. Separation can be achieved by the selective extraction of a target element or by collective extraction of all the elements followed by the selective back-extraction under different experimental conditions. The general extraction mechanism of metal ions is illustrated in **Figure 4.2** and the extraction of metal chelates is indicated in **Equation 4.6** with the equilibrium constant (D) given by **Equation 4.7**. These chelates are often insoluble in

water and result in precipitation but are soluble in organic solvents such as hexane, toluene and chloroform.[171]

$$M^{n+}_{(aq)} + nHX_{(org)} \overset{D}{\rightleftharpoons} MX_{n(org)} + nH^{+}_{(aq)} \qquad \textbf{4.6}$$

with

$$D = \frac{[MX_n]_{org}[H^+]^n_{aq}}{[M^{n+}]_{aq}[HX]^n_{org}} = K_D \frac{[H^+]^n_{aq}}{[HX]^n_{org}} \qquad \textbf{4.7}$$

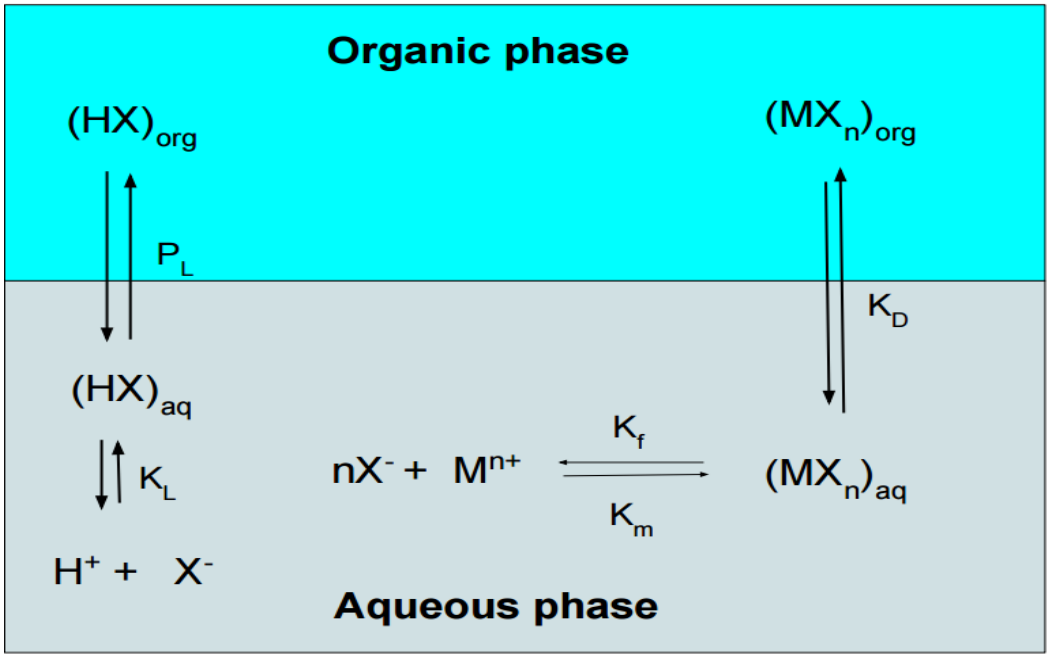

Figure 4.2: General extraction of metal ions.

The extraction of metal ion M^{n+} in **Figure 4.2** can be summarised in four steps indicated by **Equations 4.8** to **Equation 4.15**.

$$HX_{(aq)} \overset{P_L}{\rightleftharpoons} HX_{(org)} \qquad \textbf{4.8}$$

with

$$P_L = \frac{[HX]_{org}}{[HX]_{aq}} \qquad \textbf{4.9}$$

where P_L= the distribution constant of chelating agent between the two immiscible layer.

$$MX_{n(aq)} \overset{K_D}{\rightleftharpoons} MX_{n(org)} \qquad \textbf{4.10}$$

with

$$K_D = \frac{[MX_n]_{org}}{[MX_n]_{aq}} \qquad \textbf{4.11}$$

where K_D= the distribution constant of metal chelate between the two immiscible layer.

$$HX_{(aq)} \overset{K_L}{\rightleftharpoons} H^+_{(aq)} + X^-_{(aq)} \qquad \textbf{4.12}$$

with

$$K_L = \frac{[H^+]_{aq}[X^-]_{aq}}{[HX]_{aq}} \qquad \textbf{4.13}$$

where K_L= the distribution constant of chelating agent in the aqueous layer

$$MX_{n(aq)} \overset{K_m}{\rightleftharpoons} M^{n+}_{(aq)} + nX^-_{(aq)} \qquad \textbf{4.14}$$

with

$$K_m = \frac{[M^{n+}]_{aq}[X^-]^n_{(aq)}}{[ML_n]_{aq}} \qquad \textbf{4.15}$$

where K_m= the distribution constant of metal chelate in a aqueous phase

Equation 4.11 divide by **4.15** and **Equation 4.13** divide by **4.19** can be expressed as:

$$\frac{[MX_n]_{org}}{[M^{n+}]_{aq}} = \frac{K_D}{K_m}[X^-]^n_{aq} \qquad \textbf{4.16}$$

$$[X^-]_{aq} = \frac{K_L}{P_L} \times \frac{[HX]_{org}}{[H^+]_{aq}} \qquad \textbf{4.17}$$

$[X^-]_{aq}$ in **Equation 4.16** can be substituted in to **Equation 4.17** and expressed as:

$$D = \frac{[MX_n]_{org}[H+]^n{}_{aq}}{[M^{n+}]_{aq}[HX]^n{}_{org}} = K_D \frac{[H^+]^n{}_{aq}}{[HX]^n{}_{org}} \qquad \textbf{4.18}$$

since (see **Equation 4.4**)

$$K_D = \frac{[MX_n]_{org}}{[MX_n]_{aq}} \qquad \textbf{4.19}$$

It is important to note that **Equations 4.7** and **4.18** are identical. The extraction ratio (D) can thus also be presented as a combination of individual processes/equilibrium reactions as illustrated in **Figure 4.2** where

$$D = \frac{K_D K_L{}^n}{K_m P_L{}^n} \qquad \textbf{4.20}$$

The kind, and size of the influence of the different equilibrium reactions (**Equation 4.8, 4.10, 4.12 and 4.14**) on the D value can now be calculated/predicted using this expression.

The distribution ratio can also be expressed as

$$D = K_D \left(\frac{1}{1 + K_b / [H^+]} \right) \qquad \textbf{4.21}$$

If the acid dissociation constant, K_a, and mass balance of the acid species ($[HA]^T$) are taken into account.

From **Equation 4.21**, D is directly proportional to $[H^+]$ and it is equal to K_D at $[H^+] >> K_b$.

The efficiency of the separation is determined by a separation factor (α, **Equation 4.22**) and the separation is considered feasible if α > 1.[176]

$$\alpha = \frac{K_{D(A)}}{K_{D(B)}} \qquad \textbf{4.22}$$

Separation of metal ions using solvent extraction is affected by two main factors, namely; the selection of the chelating agents and solvent selection. The chelating agent should form stable complexes with the metal ion of interest under favourable conditions used during the extraction.[160] In addition, the metal ion should be highly soluble in the one solvent (usually water phase) while the newly formed compound should be very soluble in the second immiscible solvent. Solvent selection is also important and depends on factors such as, the distribution coefficient, solvent capacity and selectivity.[177] The extracting solvents should have low boiling point (easy to evaporate for ICP-OES analysis), low viscosity and show distinct separation phases.[160] Some of the most commonly used solvents in the study of separation of titanium and iron are presented in **Table 4.4.**

Table 4.4: Some common organic solvents used in the extraction of Ti and Fe

Solvent	Density, g/mL	Solubility in H_2O, %
Methyl isobutyle ketone (MIBK)	0.802	1.90 % at 20 ^oC
Tributyl phosphate (TBP)	0.97	6.4
Kerosene	0.819	0.095
Xylene	0.861	Insoluble

176 Solvent Extraction, [Accessed 06-11-2016]. Available from: http://userpages.umbc.edu/~dfrey1/ench445/regular.pdf

177 CHAPTER-2 SOLVENT EXTRACTION, [Accessed 07-11-2016]. Available from: http://www.gonuke.org/acad/Solvent%20extraction.pdf

Although solvent extraction is a common technique used on a large scale in the industry, some of its disadvantages include the fact that it is time consuming and labour intensive. Solvents used may also be lost in the aqueous layer either by mixing or dissolution and this factor largely depend on the solubility of the solvent used in combination with water. Emulsion formation between the two layers can also occur during the extraction and it is often difficult to break.[178,179]

4.3.3 Ion exchange chromatography

Ion exchange is also very useful separation technique in mineral processing. The technique has advantages which include its low capital cost, mild separation conditions and widespread application in different fields.[180] Ion exchange chromatography is particularly used to separate inorganic ions based on their different ionization or charged properties. The technique consists of the stationary solid and the mobile phases. Stationary phase is normally a polystyrene type organic resin with ionic sites where the metal or polyatomic ions of metals are exchanged and separated from each other is accomplished as they are washed from the resin with a mobile solvent. Ions are separated according to their i) mobility through the resin, ii) different affinities for the resin and iii) size and charges. The distribution of each metal between the stationary and the mobile phases can be calculated as indicated in **Equation 4.23**.[160]

$$K_s = \frac{[X]_m}{[X]_s} \qquad \textbf{4.23}$$

where K_s is the distribution coefficient between the stationary and the mobile phase at equilibrium, $[X]_m$ is the concentration of component X in the mobile phase at equilibrium and $[X]_s$ is the concentration of component X in the stationary phase at

178 Marsden, J.O. and House, C.L., The Chemistry of Gold Extraction, 2nd edition, p.358 (2006)

179 Principled of Extraction (Overview), [Accessed 06-11-2016]. Available from: http://www.chemistry.sc.chula.ac.th/course_info/2302548/Wk3.pdf

180 Acikara, O.B., Ion-Exchnage Chromatography and its Applications, InTech, pp.32-(2013)

equilibrium. A large K_s value indicates that a solute will be retained by a stationary phase.[172]

The retention factor (k) describes the migration of species in the column and it is expressed as indicated by **Equation 4.24.** The retention factor value > 1 indicate a successful separation.

$$k = \frac{t_r - t_0}{t_o} \qquad \textbf{4.24}$$

where t_r is retention time (the degree in which the molecule remains in the column) and is t_0 is the time required for mobile phase to pass through a column (dead time). The extend of the separation of the two different species (A and B) during extraction can also be expressed by separation factor (α) as described in **Equation 4.25**.[172]

$$\alpha = \frac{k_B}{k_A} \qquad \textbf{4.25}$$

This parameter describes how well solute B can be separated from solute A In a column where k_B is the retention factor of a strongly retained solute B and k_A is the retention factor of the more eluted solute A. A separation factor, α > 1 indicates successful separation.[172]

The efficiency of a column for a separation of any pair of elements can be affected by the length as this determines the number of theoretical plates (N) (**Equation 4.26** or **4.27)** and the larger the value of N the better the separation.[172]

$$N = 16\left(\frac{t_r}{w}\right)^2 \qquad \textbf{4.26}$$

$$N = 5.54\left(\frac{t_r}{w_{1/2}}\right)^2 \qquad \textbf{4.27}$$

where w is the width of the peak and t_r is the retention time. Other parameters include the flow rate of the mobile phase, volume of the eluent and the type and the length of a column.[171,172]

Resins are classified according to the charge of their functional groups namely cation and anion exchangers. In addition, depending on the functional group substituent on the stationary phase and the charge on the resin they can be strong or weak exchangers.[160] There are two types of resins which are used in ion exchange separation namely cation and anion exchangers. Cation exchangers can be strongly or weakly acidic while anion exchangers are also classified as strong base or weak base exchangers. Weak ion exchangers (anion and cation) are restricted to narrow pH range activities compared to strong ion exchanges which have a wide pH range.[171]

Different counter ions such as Na^+ (cation resin) and Cl^- (anion resin) have different interacting (ion interactions) strength with a resin during the extraction process. The lower the selectivity of a resin, the more readily it will be exchanged with another ion. To improve the selectivity of the resin, counter ions such as Li^+, Br^- and SO_4^{2-} are used. The particle size of a resin is also important which refers to the size of the solid support. The particle sizes often have an impact on the resolution and not the selectivity. Large particles, allow high flow rate and low resolution. Smaller particles provide high resolution but low flow rate.[181]

4.4 Quantification and characterization techniques

Spectrometric techniques such as nuclear magnetic resonance (NMR), X-ray diffraction and X-ray fluorescence are the most widely used techniques for characterization of both synthetic and natural samples. These techniques are generally easy to operate and most of them provide low running costs. In mineral processing atomic spectroscopic techniques such as inductively coupled plasma

181 Principles of Ion Exchange Chromatography, [Accessed 06-11-16]. Available from: http://www.bio-rad.com/en-za/applications-technologies/liquid-chromatography-principles/ion-exchange-chromatography

(ICP-OES and ICP-MS) and atomic absorption (AAS) are the most favoured methods due to their high sensitivity (low detection limits), multi-elemental analysis capabilities (ICP) as well as high selectivity.[172,182]

In the following sections attention will be given to the techniques which were used in this study and include discussions on the working principles, advantages and disadvantages of techniques such as ICP-OES which was extensively used for the characterization of ilmenite ore during the digestion and separation steps. Discussions will also include the basic principles of infrared (IR) spectroscopy and CHNS micro-element analysis and scanning electron microscope (SEM-EDS) which were also used in this study.

4.4.1 Inductively coupled plasma optical emission spectrometry (ICP-OES)

Inductively coupled optical emission spectroscopy (ICP-OES) was first commercialized in 1974 and is currently one of the most popular analytical techniques.[183] The instrument allows for highly specific elemental analysis with low levels of interference by impurities, its plasma source is extremely stabile, it has the ability to excite numerous elements for simultaneous elemental analyses and it is very easy to operate.[184] The analysis in this technique is based upon the excitation of the outer (valence) electrons of the different elements in a solution in a RF discharged environment (extremely high temperature) and the subsequent emission of photons by these atoms or ions as they return to lower energy states.[183]

Sample introduction entails transporting of sample from the original solution (normally water) to the peristaltic pump and the sample is injected into the capillary tube to the nebulizer where the high pressured argon gas breaks the liquids into droplets of various sizes (aerosol) (**Figure 4.3**). The aerosol created within the nebulizer is transported through the spray chamber where the larger droplets which are formed

182 Atomic spectroscopy, [Accessed 06-11-2016]. Available from: http://www.andor.com/learning-academy/atomic-spectroscopy-atomic-absorption,-emission-and-fluorescence-techniques

183 Boss, C.B. and Fredeen, K.J., Concepts, Instrumentation and Techniques in Inductively Coupled Plasma Optical Emission Spectrometry, 3rd edition, pp.1-7,2-12 (1997)

184 Cazes, J. (ed), Analytical Instrumentation Handbook, 3rd edition, pp.57-74 (2004)

during the aerosol formation are filtered away to ensure that the pulses that occur within the ICP during nebulisation, are smoothed. The smaller droplets of the aerosol are carried into the plasma (about 1 - 5% of the sample introduced into the nebulizer is transported into the plasma) while 95 - 99% of the sample is drained into the waste container. The aerosol is carried into the plasma where atoms of ions are desolvate, vaporize, atomize, ionize and excited.[183,185]

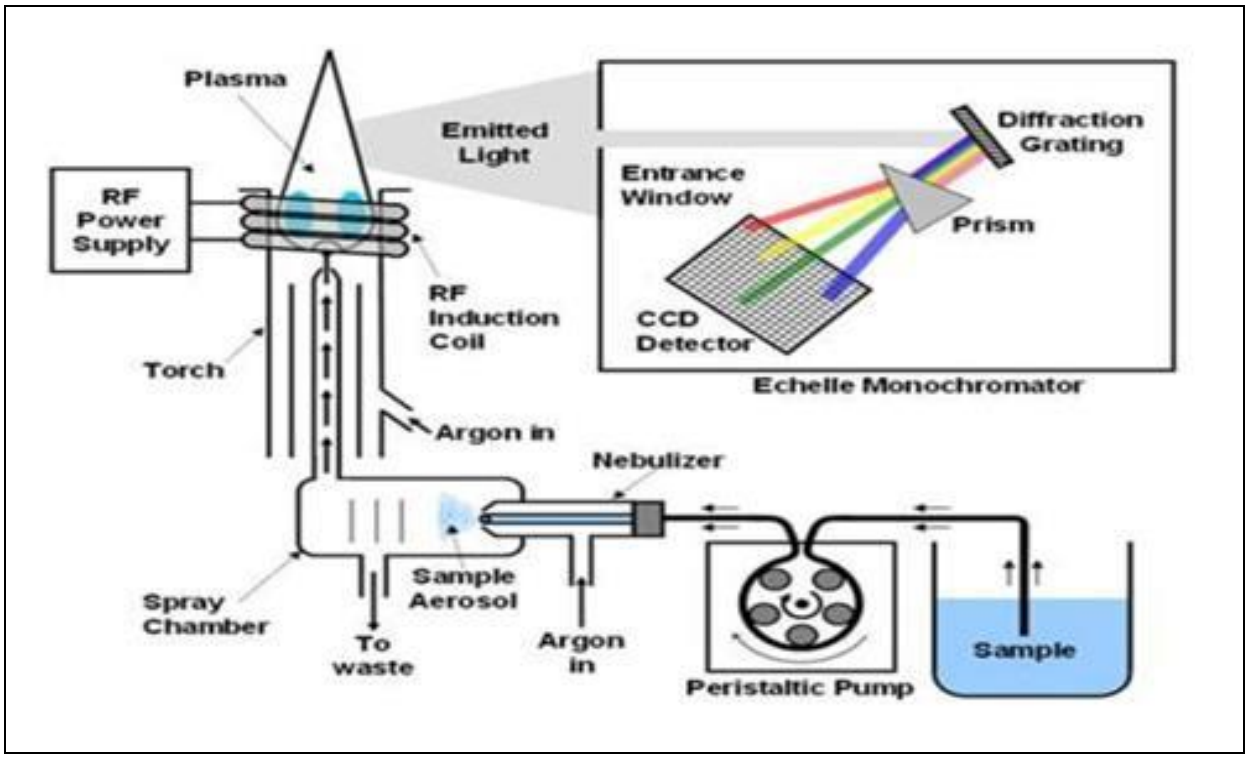

Figure 4.3: Sample introduction into ICP-OES with major components of the instrument.[186]

The plasma torch (**Figure 4.4**) is one of the most important components of the ICP-OES and consist of three concentric tubes that control the argon gas flow in the equipment and is needed for i) plasma flow, ii) the auxiliary flow and iii) the nebulizer flow. The plasma flow, keeps the quartz wall of the torch cool while the auxiliary flow reduces the carbon formation during organic sample analysis on the tip of the injector tube and finally the nebulizer flow carries the sample to the plasma.[183,185]

185 Ghosh, S. and Prasanna, V., L., Inductively coupled plasma-optical emission spectroscopy: A review, *Asian Journal of Pharma Press*, **3**(1), pp.24-33 (2013)

186 Inductively coupled plasma-optical emission spectrometer (ICP-OES), [Accessed 22-08-2016]. Available from: http://www.rohs-cmet.in/content/icp-oes

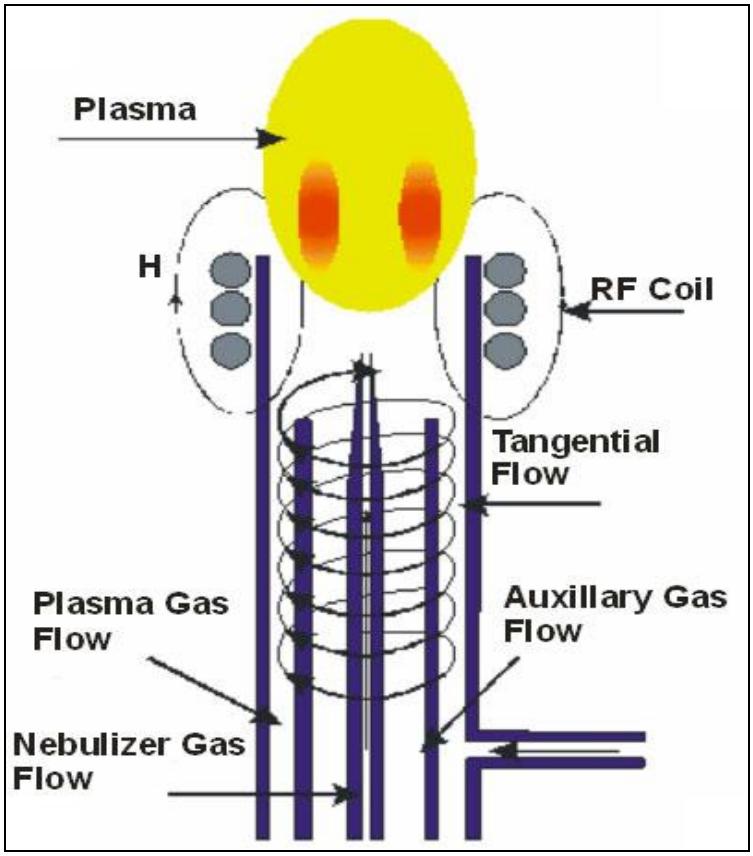

Figure 4.4: Schematic diagram of an inductively coupled plasma torch.[187]

A water-cooled induction coil surrounds the top of the plasma tube and it is powered by radio frequency generator (RF) which radiates 0.5 - 2 kW of power at 27.12 MHz and generates a magnetic field (labelled H in **Figure 4.4**). As the argon flows through the three concentric tubes of the torch, a spark is created by a Tesla coil within the equipment, producing a stream of electrons and Ar^+, cation (**Equation 4.28**) which move in the opposite direction within the magnetic field. This opposite flow of different charged species cause a lot of friction which translate to a lot of heat generation. These electrons induce further ionization of argon gas molecules due to the numerous highly kinetic energetic collision with other atoms to sustain the plasma discharge with high temperature ranging from 6000 to 10, 000 K.[184,185]

$$Ar \longrightarrow Ar^+ + e^- \qquad \textbf{4.28}$$

187 Comparison between ICP-MS and ICP-OES spectrometric techniques, [Accessed 01-09-2016]. Available from: http://lab-training.com/2014/10/11/comparison-icp-ms-icp-oes-spectrometric-techniques/

The next step after the sample molecules has been desolvated, vaporised and atomised, involves the excitation and ionization. When the activated electrons return to the ground state, they emit light at a specific wavelength which is unique for every element on the periodic table. A monochromator detects the emitted radiation and the individual wavelengths are arranged for identification and quantification of all the elements in the sample. A set of or combination of specific wavelength is characteristic for a specific element which give qualitative sample information while the intensities of the emission lines are used for quantitative data about a sample.[184]

Although ICP-OES has proved to be an highly effective for identifying and quantifying different kinds of inorganic samples it is an expensive instrument to run (argon gas is required) and has poor tolerance to organic solvents.[188] Sample preparations require completely sample dissolution for analyses while solutions obtained by flux fusion dissolution usually requires dilution due to the high salt content (see **Section 4.2.2**) to minimize the nebulizer blocking. Samples with complex elemental matrixes may also result in spectral interference can overlap while matrix effect from easily ionised elements also occurs. Some acids used for sample preparation such as HF attacks the plasma torch and destroy the instrument.[189]

4.4.2 Scanning electron microscope with Energy dispersive spectroscopy (SEM-EDS)

The scanning electron microscope with energy dispersive spectroscopy (SEM-EDS) is based upon surface analysis to determine the properties of solid chemical compounds. Sample preparation often involves sputter coating of non-conducting materials using an electro-conductive thin film such as carbon, gold, graphite and platinum.[190] In SEM, the backscattered electron images (BSE) gives compositional information about the sample based on different elemental atomic numbers and their

188 Scott, R.A. and Lukehart, C.M., Applications of Physical Methods to Inorganic and Bioinorganic Chemistry, p.206 (2007)

189 Elemental Analyses by ICP-AES, [Accessed 28-11-2016]. Available from: http://www.ncm.unn.ru/files/2015/11/applecture212.pdf

190 Balazsy, A.T. and Eastop, D., Chemical principles of textile conservation, Routledge, p.397 (2011)

distribution while “Energy Dispersive Spectroscopy” (EDS) enables the identification of the elements and their relative concentrations.

A SEM uses a beam of electrons focused to scan over an area of a surface of a solid sample to create an image of the material.[191] The interaction between the electron beam and the sample surface leads to the release of energetic favourable electrons from the sample (**Figure 4.5, a**) and the different patterns resulting from this interaction give different kinds of information about the sample. The secondary electrons produced by the SEM images, backscattered electrons (BSE) and diffracted backscattered electrons (EBSD), give information about the crystal structures and mineral orientations while the photons (characteristic X-rays) are used for elemental analysis and continuum X-rays.[192]

When a sample is irradiated with the electron beam, the electrons in the inner shell are excited and removed from the core of the electron configuration, creating the electron hole which is now filled by the cascading of electrons from the outer or high energy shells (**Figure 4.5**, **b**). The difference in energy between the higher and the lower energy shell is characteristic/unique for all the elements and the energy is detected as characteristic X-rays.[193] SEM-EDS has the ability to provide both qualitative and semi quantitative elemental information of chemical compounds except for the samples containing the lighter elements such as H, He and Li.[194]

191 Scanning Electron Microscope, [Accessed 09-12-2016]. Available from: http://www.nanoscience.com/technology/sem-technology/

192 Valenzuela-Muniz, A. M., ABC’s of Electrochemistry series Materials Characterization techniques: SEM and EDS, Center for Electrochemical Engineering Research, 2011, [Accessed 27-06-2017]. Available from: https://www.ohio.edu/engineering/ceer/research/upload/sem-edx.pdf

193 Zhou, W., Apkarian, R.P., Wang, Z.L. and Joy, D.,(ed) Scanning Microscopy for Nanotechnology,: Techniques and Applications, p.7 (2006)

194 Newbury, D.E. and Ritchie, N.W.M., Is Scanning electron microscope/energy dispersive x-ray spectrometry (SEM/EDS) Quantitative?, Scanning, **35**(3), pp.141-168 (2013)

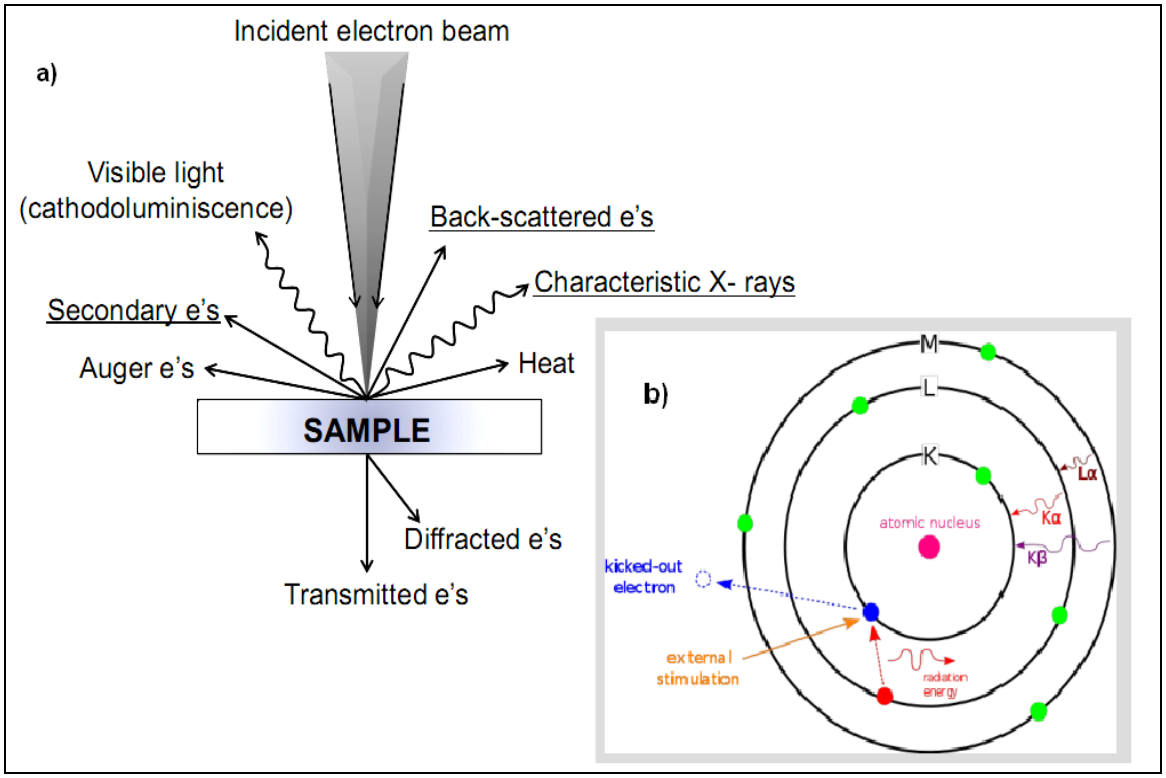

Figure 4.5: a) Interaction of the sample with incident electron beam and b) production of characteristic X-rays.[192]

X-ray photons generated by the inner-shell ionization escape the sample to the detector where the x-rays of different elements are separated into individual energy spectra. Electron-hole pairs are created in the Si(Li) detector (most commonly used detector in EDS instruments). A basic EDS system consists of 3 components, a X-ray detector, a pulse processor and a computer system (**Figure 4.6**). The newly generated X-rays create a small current which is converted into a voltage pulse. The charged pulse created in this process is proportional to the energy of incoming X-rays and are amplified to reflect the energy of the detected X-ray. The voltage pulses are then converted into a signal which is processed by the computer system.[195,196] The produced spectral peaks are unique to an individual element (qualitative information)

195 SEM Introduction: an Overview of Scanning Electron Microscope, [Accessed-06-11-2016]. Available from: http://www.understanding-cement.com/sem-introduction.html

196 Williams, D.B., Goldstein, J.I. and Fiori, C.E., Principle of X-Ray Energy –Dispersive Spectrometry in the Analytical Electron Microscope, pp.123-125 (1986)

and the peak heights correspond to the energy level of the x-rays emitted (quantitative information).[197]

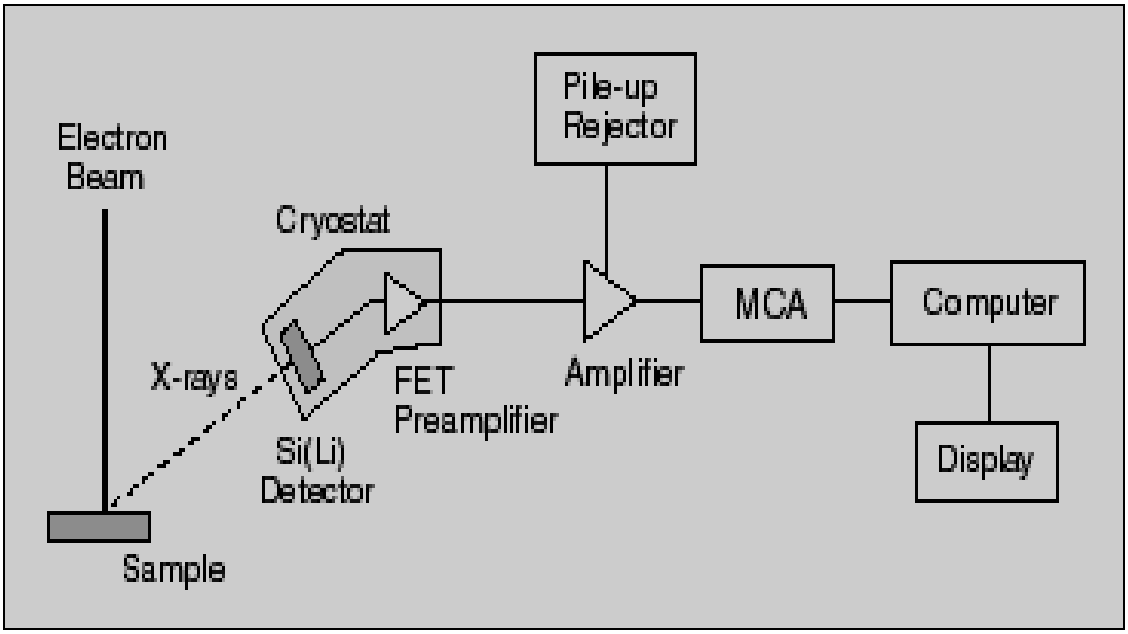

Figure 4.6: The basic principles of SEM-EDS Instrumentation.[198]

This technique (SEM-EDS) requires less sample preparation as the samples are analyzed as solid which is a big advantage especially for analysis of refractory minerals (such as ilmenite and zircon) which are usually resistant to chemical attack and difficult to dissolve. Other advantages include the small amount of sample to complete the analysis as well as the non-destructive nature of the analysis which makes the samples reusable for other purposes. However, the strict requirement for the sample to be in solid for analysis using SEM-EDS also means the technique has limited applications. Other disadvantages include its inability to detect elements with low atomic numbers (H, He, Li and Be) as well as spectral overlap between different elements (for example, Mn K_β overlaps with Fe_α and Ti K_β overlaps with V K_α) and can affect the accuracy of the results.[197,199]

197 Energy Dispersive Spectroscopy, [Accessed 01-10-2016]. Available from: file:///C:/Documents%20and%20Settings/uvp/My%20Documents/Downloads/EKB_Energy_Dispersive_Spectroscopy_LR%20(5).pdf

198 A Basic Understanding of SEM and EDS, [Accessed 06-11-2016]. Available from: http://www.forensicevidence.net/iama/sem-edxtheory.html

199 Wavelength dispersive (WDXRF) and energy dispersive (EDXRF) X-ray fluorescence, [Accessed 06-11-16]. Available from: http://slideplayer.com/slide/5313093/

4.4.3 Infrared (IR) spectroscopy

IR is a useful technique for the characterization of both organic and inorganic compounds with the exception of oxygen, nitrogen and chlorine. The IR region in the electromagnetic spectrum (**Figure 4.7**) lies between the UV-Vis and microwave region and is divided into near IR, mid-IR and Far-IR regions. The mid-infrared region is the most commonly used for chemical characterization due to its fine structure information (stronger line strength) for qualitative information.[154]

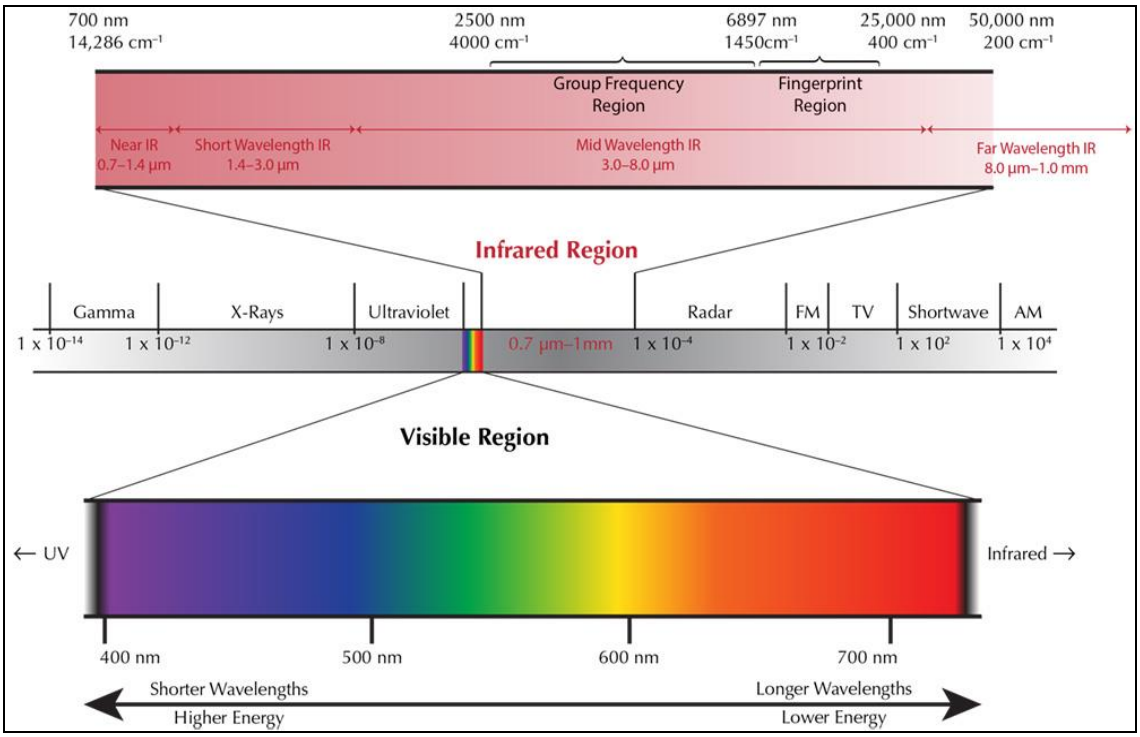

Figure 4.7: The electromagnetic spectrum with IR region wavelengths.[200]

During analysis the emitted IR radiation is absorbed by the molecule and the increase in energy results in the increase in molecule bond vibration (amplitude). The newly absorbed energy lead to bond deficiency, resulting in either stretching or bending at different frequencies for kinds of chemical bonds. Bending vibration involves a change in the angle between two atoms due to the energy that is absorbed while stretching vibration involves the change in bond length. Non-polar

200 Introduction to infrared spectroscopy, [Accessed 22-08-2016]. Available from: http://www.lotusgemology.com/index.php/library/articles/294-ftir-in-gem-testing-ftir-intrigue-lotus-gemology

molecules such as Cl_2, N_2 and Br_2 do not absorb radiation due to their non-coupling interaction with IR waves. When the frequency of a molecular vibration corresponds to the frequency of IR radiation absorbed, the IR spectrum is obtained.[201,202]

When a molecule absorbs the IR radiation, the electronic dipole moment of the molecule changes during the vibration action as the bonds expand and contract. There are two types of molecular vibrations, namely stretching and bending vibration (**Figure 4.8**). Stretching vibrations can also be either symmetric or asymmetric and the bending vibrations can be rocking scissoring, wagging or twisting.[203]

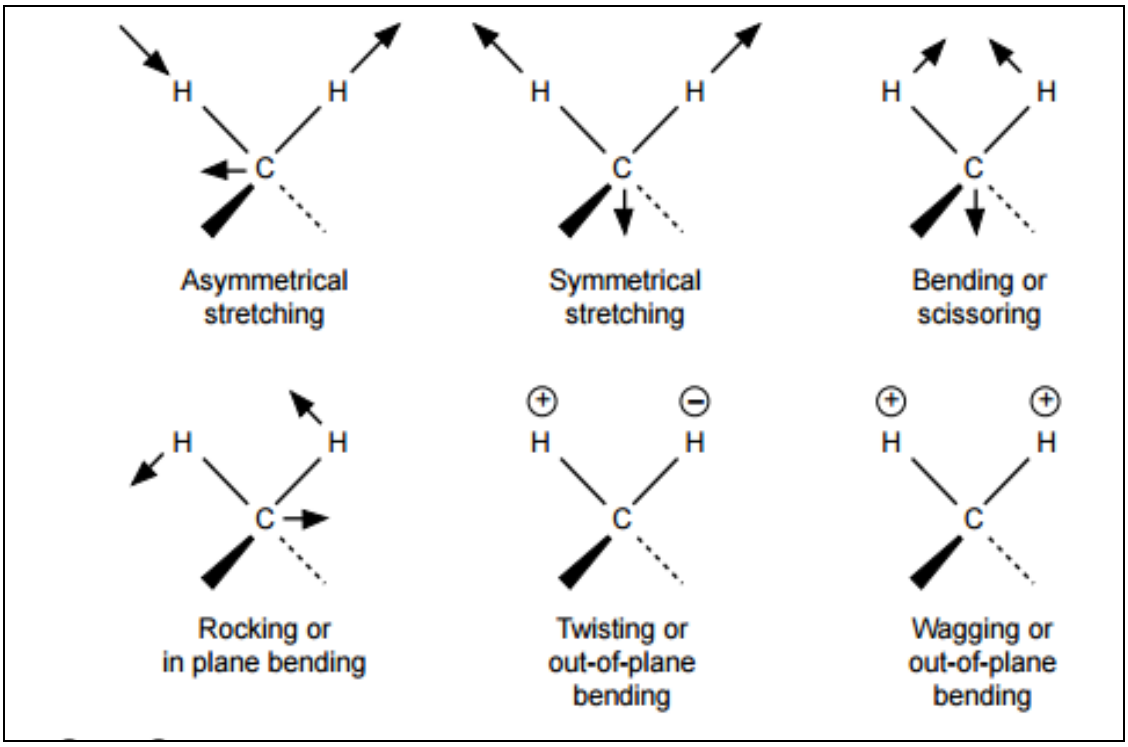

Figure 4.8: Different types of molecular vibrations.[204]

The IR spectrum is simple to interpret and is reliable to assigning different chemical compounds or functional groups with this technique. The spectrum also gives

201 Rouessac, F. and Rouessac, A., Chemical Analysis: Modern Instrumentation Methods and Techniques, 2nd edition, pp.207-240 (2007)

202 Mohan, J., Organic spectroscopy: Principles and Application, 2nd edition, pp.8-9 (2002)

203 Stuart, B.H., Infrared Spectroscopy: Fundamentals and Applications, pp.1-2,5-11 (2004)

204 Infrared spectroscopy, [Assessed 27-10-2016]. Available from: file:///C:/Documents%20and%20Settings/uvp/My%20Documents/Downloads/MCT3%20Infrared%20(1).pdf

information about the structure, purity and symmetry of a compound under study.[201] Some of the most frequently used functional groups are listed in **Figure 4.9** with their correlation frequencies.

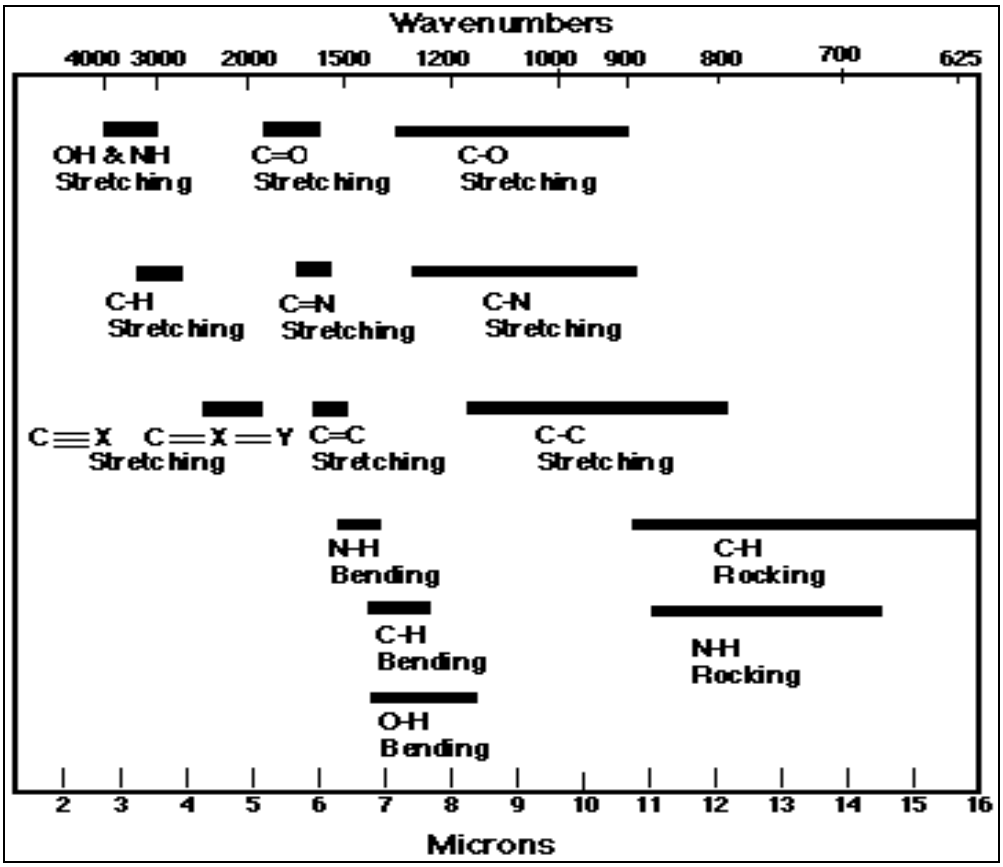

Figure 4.9: Common functional groups with their characteristic vibration modes.[205]

4.4.4 CHNS micro-analyser

CHNS micro-analyser is used for the accurate determination of carbon, hydrogen and nitrogen and sulphur in organic or organometallic compounds.[206]. The method involves the weighing a small sample in an oxidisable tin capsules, the subsequent

205 Infrared Spectroscopy, [Accessed 03-11-2016]. Available from: http://www.wag.caltech.edu/home/jang/genchem/infrared.htm

206 Etherington, K.J., Rodger, A. and Hemming, P., CHN microanalysis-a technique for the 21st century, Lab Plus International, pp.26-27 (2001)

burning of such sample in a high temperature furnace under a constant flow of helium stream and high purity oxygen.[207]

The basic setup of the most common elemental analyser is illustrated in **Figure 4.10**. The equipment is calibrated first with high purity standards (with known quantities of C, H, N and S) such as acetanilide and ehylendiamineteraacetic acid (EDTA). The sample is burned (decomposed) in high purity oxygen environment in to the combustion chamber at 950 ºC and which convert the chemical compound into their respective and the newly formed gases (CO_2, N_2, H_2O and SO_2). These combustion products (gases) are then transported by the carrier gas (helium) to a column containing high purity copper turning which removes excess O_2 and converts nitrogen to nitrogen oxide. These gases are then passed through the thermal conductor to IR detectors where they are quantified.[208]

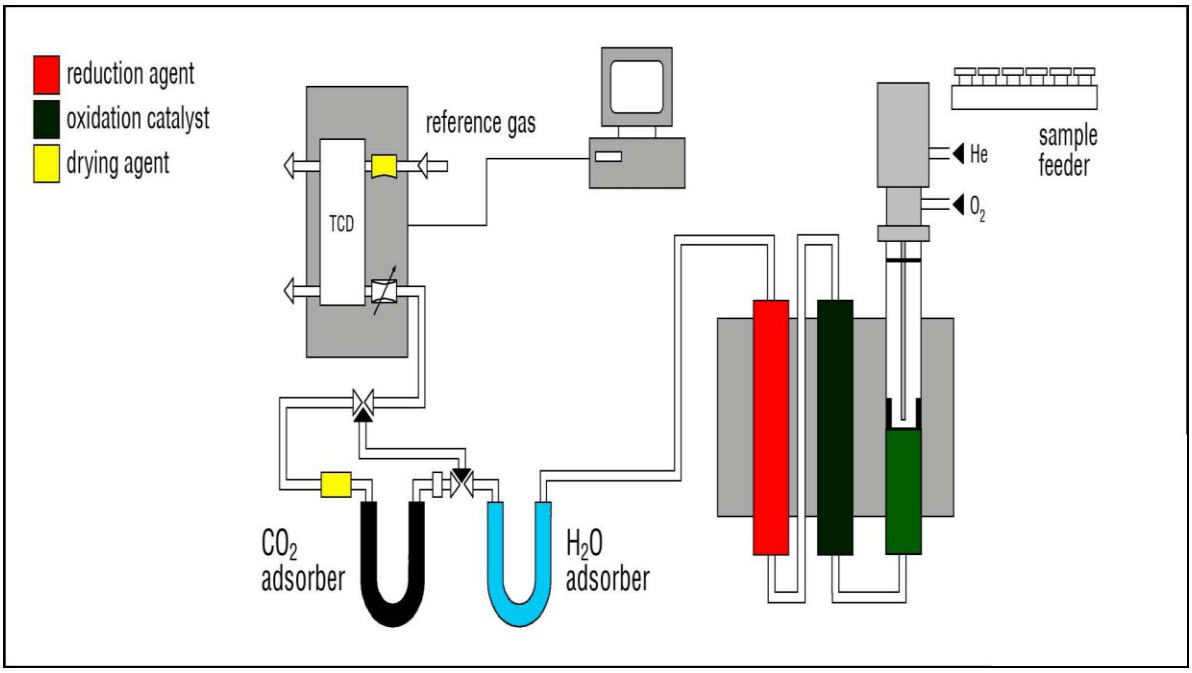

Figure 4.10: The basic set-up of CHN microanalyser.[209]

207 Gunaraj, V., Proceedings of the International Conference on Emerging Technologies in Intelligent System and Control, p.525 (2005)

208 Thompson, M.(ed), CHNS Elemental Analysers, *AMC Technical Briefs,* No.29, Volume 4, The Royal Society of Chemistry, 2008

209 Vario MACRO CHN, [Accessed 08-10-16]. Available from: http://jdelement.com/ProductShow.asp?ID=121

CHNS microanalysis is a straightforward technique requiring only a small amount of sample to complete the analysis, with easy sample preparation operations and is highly precise and accurate results. The instrument is automated and allows the simultaneous determination of C, H and N under the same conditions.[206] However, the instrument is very expensive and the analyses are destructive to the sample nature.

4.5 Conclusion

The principle behind open beaker acid digestion, flux fusion and microwave which are used in this study, were discussed in this chapter. Applicable separation methods such as selective precipitation, solvent extraction and ion exchange methods which were used in the beneficiation of ilmenite were also discussed. All the qualitative and quantitative analyses in this study were accomplished using ICP-OES. SEM-EDS was also used to determine the major elements in the ilmenite mineral and their percentages. It is important to note that most of the instrument selection or application was guided by the availability or accessibility of the instruments for this study. The separated and newly isolated titanium and iron compounds were also characterised using IR and CHNS elemental analysis.

5 Dissolution and analysis of titanium and iron containing samples

5.1 Introduction

The first step in the ilmenite beneficiation process is the development of a method that can completely dissolve the Ti and Fe compounds within the mineral prior to the hydrometallurgical separation. Acid leaching using either HCl or H_2SO_4 at elevated temperatures (1000 to 1100 ºC) (see **Chapter 2, Section 2.3.3.2**) is the most common ilmenite dissolution method and has extensively been studied (see **Chapter 2, Section 2.3.3.2** and **Chapter 3**). However, this procedure produce large volume of acid waste and it was decided to develop alternative dissolution methods which will also produce products that allowed for subsequent separation of Ti and Fe in the mineral.

The focus of this part of the study is the development of sample preparation procedures and the accurate determination of Fe and Ti in pure (metals and inorganic) compounds in ilmenite. The main aim in this part of the study was to develop a relatively less energy demanding dissolution method for ilmenite using techniques such as flux fusion and microwave digestion. The developed dissolution techniques were then evaluated for the subsequent isolation or separation of Ti from Fe in the dissolved ilmenite mineral (see **Chapter 6**) using different separation techniques.

5.2 Experimental procedures

5.2.1 Reagents and equipments

All chemicals and reagents used in this study are listed in **Table 5.1** indicating their purity and the supplier.

Table 5.1: Chemicals used to conduct the experiment

Chemical	Formula	Purity	Supplier
Nitric acid	HNO_3	65 %	Merk
Sulphuric acid	H_2SO_4	98 %	Sigma-Aldrich
Orthophosphoric acid	H_3PO_4	85 %	Merk
Hydrochloric acid	HCl	32 %	Merk
Titanium standard	Ti	2 % HNO_3/HF	Merk
Silicon standard	Si	HNO_3/HF	Merk
Multi element standard	Fe, Mg, Mn, Al	HNO_3^*	Merk
Titanium powder	Ti	99.7 %	Sigma-Aldrich
Fe metal powder (90 mesh)	Fe	--	--
Titanium tricloride	$TiCl_3$	15 %	--
Iron chloride	$FeCl_3 \cdot 6H_20$	99 %	Merk
Ammonium bifluoride	$NH_4 \cdot HF_2$	--	Merk
Potassium fluoride	KF	--	Riedel-de haen
Sodium tetraborate	$Na_2B_4O_7$	99 %	Sigma -Aldrich
Lithium metaborate	$LiBO_2$	> 98 %	Sigma -Aldrich
Sodium bicarbonate	Na_2CO_3	99 %	Riedel-dehaen
Potassium pyrosulphate	$K_2S_2O_7$	97.5 %	Saarchem
Sodium phosphate dibasic	NaH_2PO_4	≥ 99 %	Sigma-Aldrch
Sodium phosphate monobasic	Na_2HPO_4	99 %	PAL Chemicals
Methanol	C_2H_5OH	≥ 99.9 %	Sigma-Aldrich

-- Information not supplied, * 23 elements in dilute nitric acid

A Shimadzu AW320 electronic balance certified under ISO 9001 requirements was used to accurately weigh all samples to 0.1 mg at 20 ± 3 ºC. A Tescan VEGA3 SEM with an Oxford X-Max^N EDS operating with SEM electronics, was also used for quantification of ilmenite mineral. All the sample solutions prepared in this study were quantitatively transfer between and into the analytical apparatus using a Brand Transferpettes type (1.0 mL and 10.0 mL) or Lasec micro-pipettes (100 µL - 1000 µL). Schott Duran (grade (A)) beakers and volumetric flasks (100.0, 200.0, 250.0 and 500.0 mL) were used during sample preparations. All the glassware which was used in this study was cleaned by soaking them in 55 % HNO_3 (10.0 mL) for 24 hours followed by a thorough rinsing with ultra-pure water prior to use. The ultra-pure water (conductivity = 0.001 mS/cm) were prepared with an ultra-reverse osmosis system from ADJ traders and were used for in all solution preparations for analysis. Qualitative and quantitative analysis of Ti and Fe samples in solution were performed with a Shimadzu ICPS-7510 ICP-OES sequential plasma spectrometer under constant experimental conditions which are presented in **Table 5.2**. All analysis were done in triplicate with the reported significant figures based on the standard deviation of three different analysis.

Table 5.2: ICP-OES operational conditions for of Ti and Fe analysis.

Parameter	Condition
RF power	1200 W
Coolant gas flow	14.0 L/min
Plasma gas flow	45 L/min
Carrier gas flow	0.7 L/min
Auxiliary gas flow	0.5 L/min
Sample introduction method	Peristaltic pump
Spray chamber	Glass cyclonic
Type of nebuliser	Concentric

5.2.2 Sample background

The ilmenite sample used in this study was obtained from the Namakwa Sands Mine in the Western Cape of South Africa. The mineral was used without further grinding or crushing.

Figure 5.1: The ilmenite mineral sand used in this study.

5.2.3 Preparation of the calibration standards for ICP-OES analysis

The calibration standard solutions were prepared from 1000 mg/L Ti and Si standards as well as multi- element standard solution containing Fe, Mn, Mg, and Al. All the inductively coupled plasma- optical emission spectroscopy (ICP-OES) standard solutions were prepared by adding appropriate volume of 1000 ppm of the multi-standards to 100.0 mL volumetric flask to obtain elemental concentrations ranging between 0.5 and 10.0 which were used to construct the calibration curves for the different elements using ICP-OES. To each volumetric flask 10.0 mL of appropriate acid (H_3PO_4, H_2SO_4, HNO_3 and HCl and *aqua regia*) was added and filled to the mark with ultra-pure water. The blank solution was prepared by adding 10.0 mL of appropriate acid to 100.0 mL volumetric flask and diluting to the mark. A qualitative analyses of the dissolved ilmenite samples also indicated the presence of Mn, Mg, Al and Si. The quantitative analysis of the Ti and Fe were performed at 334.941 nm and 238.204 nm. The other elements in the ilmenite sample were quantified using the analytical lines given in **Table 5.3.**

Table 5.3: Selected wavelengths for different elements analysed in ilmenite[210]

Element	Wavelength (nm)
Fe	238.204
Ti	334.941
Mn	293.930
Mg	202.582
Si	252.851
Al	394.403

5.2.4 Determination of limit of detection and quantification (LOD and LOQ's)

The limit of detection (LOD) and limit of quantifications (LOQ) were determined in different acid matrices and calculated according to **Equations 5.1**

$$\text{LOD} = \frac{s}{\text{m}} \times 3.3 \qquad \textbf{5.1}$$

where *s* is the standard deviation of 10 replicates[211] of the blank intensity measurements and m is the slope of the standard calibration curve. The LOQ was calculated a factor (10 times) higher than the LOD value[172] and are reported in **Table 5.4**.

210 Winge R.K., Fassel V.A., Peterson V.J. and Floyd M.A., Inductively coupled Plasma-Atomic Emission spectroscopy, an atlas of spectral information, 20, pp.262-286 (1985)

211 Shrivastava, A. and Gupta, V.B., Method for the determination of limit of detection and limit of quantitation of the analytical methods, *Chronicles of Young Scientists*, **2**(1), pp.21-25 (2011)

Table 5.4: Calculated LOD and LOQs for Ti and Fe

Element	Standard deviation (*s*)	Slope (m)	LOD (ppm)	LOQ (ppm)
H_3PO_4 (85%)				
Ti	0.00234	1.8277	0.0039	0.0389
Fe	0.0014	0.4476	0.0093	0.0932
H_2SO_4 (98%)				
Ti	0.0034	1.8006	0.0056	0.0565
Fe	0.0004	0.3179	0.0035	0.0354
HNO_3 (65%)				
Ti	0.0034	1.2056	0.0097	0.0975
Fe	0.0019	0.6978	0.0030	0.0296
HCl (32%)				
Ti	0.0033	0.6900	0.0142	0.1412
Fe	0.0007	0.0154	0.1278	1.2779
HNO_3:HCl (1:3)				
Ti	0.0030	1.3628	0.0066	0.0661
Fe	0.0005	0.7321	0.0021	0.0212

5.2.5 Dissolution and analysis of Ti and Fe samples

5.2.5.1 Quantification of Ti and Fe in inorganic compounds

0.05 g of $FeCl_3 \cdot 6H_2O$ was accurately weighed to 0.1 mg and dissolved in 10.0 mL of distilled water and filled to the mark in a 100.0 mL volumetric flask. A 1.0 mL aliquot of this solution was quantitatively transferred to different 100.0 mL volumetric flasks. To each flask 10.0 mL of different acid (HCl, *aqua regia*, HNO_3, H_2SO_4 and H_3PO_4) was added and filled to the mark with distilled water. The diluted solutions were then analysed using ICP-OES and the results are presented in **Table 5.5.**

For the titanium analysis, a 1.0 mL aliquot of $TiCl_3$ (0.0113 M) was quantitatively transferred into a 100.0 mL volumetric flask and filled to the mark with distilled water. A 1.0 mL aliquot of this solution was quantitatively transferred to different 100.0 mL volumetric flasks. To each flask 10.0 mL of desired acid (HCl, *aqua regia*, HNO_3, H_2SO_4 and H_3PO_4) was quantitatively transferred and filled to the mark with distilled water. The diluted solutions were analysed using ICP-OES and the results are presented in **Table 5.5.**

Table 5.5: Quantification of Ti and Fe in $TiCl_3$ and $FeCl_3 \cdot 6H_2O$ using ICP-OES

Sample	Mass weighed (g)	Theoretical metal concentration (ppm)	% Recovery (*s*)	(% RSD)
H_3PO_4				
Ti	0.0558 - 0.0562	5.4005	103.6(5)	0.46
Fe	0.011 - 0.0109	1.0434 - 1.0744	103(2)	1.67
H_2SO_4				
Ti	0.0565 - 0.0571	5.4005	105.2(6)	0.56
Fe	0.011 - 0.0109	1.0372 - 1.0785	103(2)	1.91
HNO_3				
Ti	0.0524 - 0.054	5.4005	98(1)	1.460
Fe	0.0108 - 0.0109	1.063 - 1.0744	101.5(9)	0.90
HCl				
Ti	0.0524 - 0.0540	5.4005	98(1)	1.46
Fe	0.0106 - 0.0114	1.0764 - 1.0888	102(1)	0.10
Aqua regia				
Ti	0.053 - 0.0554	5.4005	100(2)	2.36
Fe	0.0105 - 0.011	1.033 - 1.0764	100(4)	3.47

*Average of three analysis

5.2.5.2 Dissolution of Ti and Fe powder by open beaker digestion

0.1 g Samples of titanium and iron powders with mass of approximately 0.1 g were accurately weighed to 0.1 mg and added to 10.0 mL of different mineral acids, namely H_3PO_4, H_2SO_4, HNO_3, HCl, and *aqua regia*. The mixtures were heated for 3 hours at temperatures well-below the boiling points of the different acids (60 ºC for HCl, HNO_3 and *aqua regia*, 150 ºC for H_2SO_4 and 200 ºC for H_3PO_4) with constant stirring. Visual inspection indicated the complete sample dissolution in H_2SO_4 and H_3PO_4 for both the Ti and Fe metal. Incomplete dissolution was observed for HNO_3, HCl and *aqua regia* for both the Ti and Fe metal powders. The reaction mixtures with the incomplete dissolution were filtered and the filtrates were quantitatively transferred to 100.0 mL volumetric flask to allow from metal dissolution quantification. In all the cases the acidity of these solution were adjusted to match those of the standard solutions matrixes and the volumetric flasks were filled to the mark with ultra-pure water. All the solutions were analysed using ICP-OES and the results are presented in **Table 5.6.**

Table 5.6: Recoveries of Ti and Fe from pure metals dissolution using bench top acid digestion

Sample	Mass weighed (g)	% Recovery	(% RSD)
H_3PO_4 (200 ºC)			
Ti	0.0999 - 0.1008	105.4(6)	0.63
Fe	0.0971 - 0.1019	97(1)	1.25
H_2SO_4 (150 ºC)			
Ti	0.0996 - 0.1001	104.4(3)	0.99
Fe	0.1004 - 0.1007	98(1)	0.38
HNO_3 (60 ºC)			
Ti	0.1002 - 0.1008	0.183(9)	0.52
Fe	0.100 - 0.1019	72(1)	1.92
HCl (60 ºC)			
Ti	0.1002 - 0.1008	45.2(3)	0.83
Fe	0.1004 - 0.1017	96.6(6)	0.72
Aqua regia (60 ºC)			
Ti	0.10013 - 0.1005	0.192(6)	0.32
Fe	0.0993 - 0.1008	95.0(1)	1.07

*Average of three analysis

5.2.5.3 Dissolution of ilmenite with open- beaker digestion

Ilmenite samples of approximately 0.1 g (accurately weighed to 0.1 mg) were quantitatively transferred to 100.0 mL beakers and 10.0 mL of different acids were added to these samples namely H_2SO_4, H_3PO_4, HNO_3, HCl and *aqua regia*. The mixtures were heated at 60 ºC (HCl, HNO_3 *and aqua regia*), 200 ºC (H_2SO_4) and 150 ºC (H_3PO_4). The filtrate mixtures were prepared similar to **Section 5.2.4.1** for ICP-OES analysis and the results are given in **Table 5.7.**

Table 5.7: Quantification of ilmenite sample in different mineral acids

M_xO_y (%)	*Aqua regia*	HCl	HNO_3	H_2SO_4	H_3PO_4
Fe_2O_3	0.285(2)	2.51(2)	0.25(1)	20.2(2)	46.8(3)
TiO_2	0.03308(5)	1.28(3)	0.0517(5)	34.8(1)	38.4(3)
Mn_3O_4	--	0.035(3)	--	0.8(4)	0.25(1)
SiO_2	--	0.0847(7)	0.057(8)	1.6(2)	0.28(8)
MgO	0.1202(5)	0.03888(1)	0.0685(3)	0.101(4)	0.325(8)
Al_2O_3	0.0120(5)	0.091(8)	0.0428(3)	0.7(2)	0.153(3)
Total % mass	**0.43**	**4.03**	**0.46**	**58.19**	**86.19**

* Average of three replicates
-- Not identified

5.2.5.4 Flux fusion dissolution of ilmenite

5.2.5.4.1 Dissolution of ilmenite using different fluoride salts as fluxes

Approximately 0.1 g aliquots (accurately weighed to 0.1 mg) of the ilmenite samples were mixed homogenously mixed with the fluoride salts ($NH_4.HF_2$ and KF) at different ratios (1:10 and 1:20 mass ratio) as illustrated in **Table 5.8**. The $NH_4{\cdot}HF_2$/ilmenite fusion was investigated at 200 ºC for different digestion times of 30 min and 60 min. Both the 30 and 60 min heating periods indicated incomplete sample digestion (by visual inspection) with a white amorphous melt that partially dissolved in water. The KF/sample mixture was digested at different fusion times of 30 and 60 min at a temperature of 950 ºC. The resultant brown amorphous type melt was a dissolved in 1.0 M H_2SO_4[160] and both these fluxes showed incomplete dissolution under the cited experimental conditions. The remaining sample solids were separated from the

solution by filtration and the filtrate was quantitatively transferred to a 100.0 mL volumetric flask. 10.0 mL H_2SO_4 was added to the filtrate solution to match the standard sample matrices and filled to the mark with water. The final solutions were analysed using ICP-OES and the results are given in **Table 5.8**.

Table 5.8: ICP-OES results for $NH_4.HF_2$ and KF fusion with ilmenite

M_xO_y (%)	$NH_4 \cdot HF_2$		KF	
	1:10, 30 min	**1: 20, 60 min**	**1:10, 30 min**	**1: 20, 60 min**
Fe_2O_3	31.8(5)	31.9(8)	30.(1)	24.6(5)
TiO_2	36.0(3)	35.5(4)	37(2)	38.8(3)
Mn_3O_4	1.39(2)	0.91(2)	1.00(1)	0.96(5)
SiO_2	--	--	--	--
MgO	0.319(7)	0.32(2)	0.37(3)	0.35(1)
Al_2O_3	0.72(6)	0.85(3)	0.73(5)	0.596(2)
Total % mass	**69.87**	**69.56**	**69.88**	**65.28**

* Average of three replicates
--Not determined

5.2.5.4.2 Dissolution of Ilmenite with $K_2S_2O_7$ and Na_2CO_3 as fluxes

Approximately 0.1 g of ilmenite sample was homogeneously mixed with 1.0 g each of $K_2S_2O_7$ and Na_2CO_3 and fused at 800 and 900 ºC for 30 min respectively. The obtained amorphous solids were dissolved in 10.0 mL of 1.0 M H_2SO_4. Visual inspection indicated that the samples were incompletely dissolved. The undissolved solids were separated from the acids by filtration and the filtrates were quantitatively transferred to 100.0 mL volumetric flasks. The solutions acidity were adjusted to match the of standards solutions and were subsequently diluted with water. The results of an ICP-OES analysis are presented in **Table 5.9.**

Table 5.9: ICP-OES results after fusion of ilmenite with $K_2S_2O_7$ and Na_2CO_3

M_xO_y (%)	$K_2S_2O_7$	Na_2CO_3
	800 ^oC, 30 min	900 ^oC, 30 min
Fe_2O_3	25.5(1)	21.6(4)
TiO_2	31.8(7)	19.1(6)
Mn_3O_4	0.41(1)	0.68(4)
SiO_2	0.55(3)	1.73(8)
MgO	0.2(2)	0.26(2)
Al_2O_3	0.2(2)	0.5(5)
Total % mass	**58.70**	**44.49**

* Average of three replicates

5.2.5.4.3 Dissolution of ilmenite using borates and $Na_2HPO_4/NaH_2PO_4{\cdot}H_2O$ as fluxes

Approximately 0.1 g of ilmenite (accurately weighed to 0.1 mg) was mixed with 1 g each of $Na_2B_4O_7$ and $LiBO_2$ (1:10 sample:flux mass ratio). The mixtures were then fused at 1000 ºC for 30 minutes. The obtained yellowish melts were dissolved in 10.0 mL H_2SO_4 (95 - 97 %), heated to at 50 ºC and constant stirred overnight. To prevent any boric acid precipitation, 40 mL of methanol was slowly added to the acid/sample mixture during dissolution of the melt to allow the evaporation of borax.[212] These solutions were each transferred to a 100.0 mL volumetric flask and filled to the mark with ultra-pure water. 1.0 mL aliquot of each solution was pipetted to a 100.0 mL volumetric flask to which 10.0 mL H_2SO_4 was added to ensure matrix matching with the standard solutions. The solutions were analysed using ICP-OES and the results are given in **Table 5.10.**

In another fusion method, 0.1 g of ilmenite was accurately weighed (accurately to 0.1 mg) and mixed with 0.8 g Na_2HPO_4 and 0.8 g $NaH_2PO_4{\cdot}H_2O$ (1:16 mass ratio). The

212 Nete, M., Dissolution and Analytical characterization of tantalite ore, niobium metal and other niobium compounds, M.Sc Thesis, The University of the Free State, p. 72 (2009)

mixture was fused at 800 ºC for 30 min which formed a glassy melt in the process. The melt easily dissolve in water and the solution was quantitatively transferred to 100.0 mL volumetric flask, 5.0 mL H_3PO_4 (85 %) was added to the mixture and filled to the mark with water. The solution was analysed using ICP-OES and the results are presented in **Table 5.10**.

Table 5.10: ICP-OES results after fusion with borates and phosphate flux

M_xO_y (%)	**$Na_2B_4O_7$**	**$LiBO_2$**	**$Na_2HPO_4/NaH_2PO_4{\cdot}H_2O$**
	1000 ^oC, 30 min	**1000 ^oC, 30 min**	**800 ^oC, 30 min**
Fe_2O_3	56.5(2)	55.1(3)	55.9(5)
TiO_2	46.3(5)	47.7(5)	49(2)
Mn_3O_4	1.46(5)	1.25(1)	1.36(8)
SiO_2	1.45(6)	1.471(9)	1.6(1)
MgO	0.477(3)	0.401(9)	0.297(9)
Al_2O_3	1.18(3)	1.13(2)	0.61(2)
Total % mass	**107.50**	**107.34**	**109.03**

* Average of three replicates

5.2.6 Quantification of ilmenite sample with SEM-EDS

An ilmenite sample was send to the University of the Free State (Qwa-Qwa Campus) for the semi-quantitative and qualitative analysis using scanning electron microscope-energy dispersive spectroscopy (SEM-EDS). The EDX spectrum of the ilmenite sample is given in **Figure 5.2** as well as the quantitative of the elements which were detected in the sample and these results are reported in **Table 5.13.**

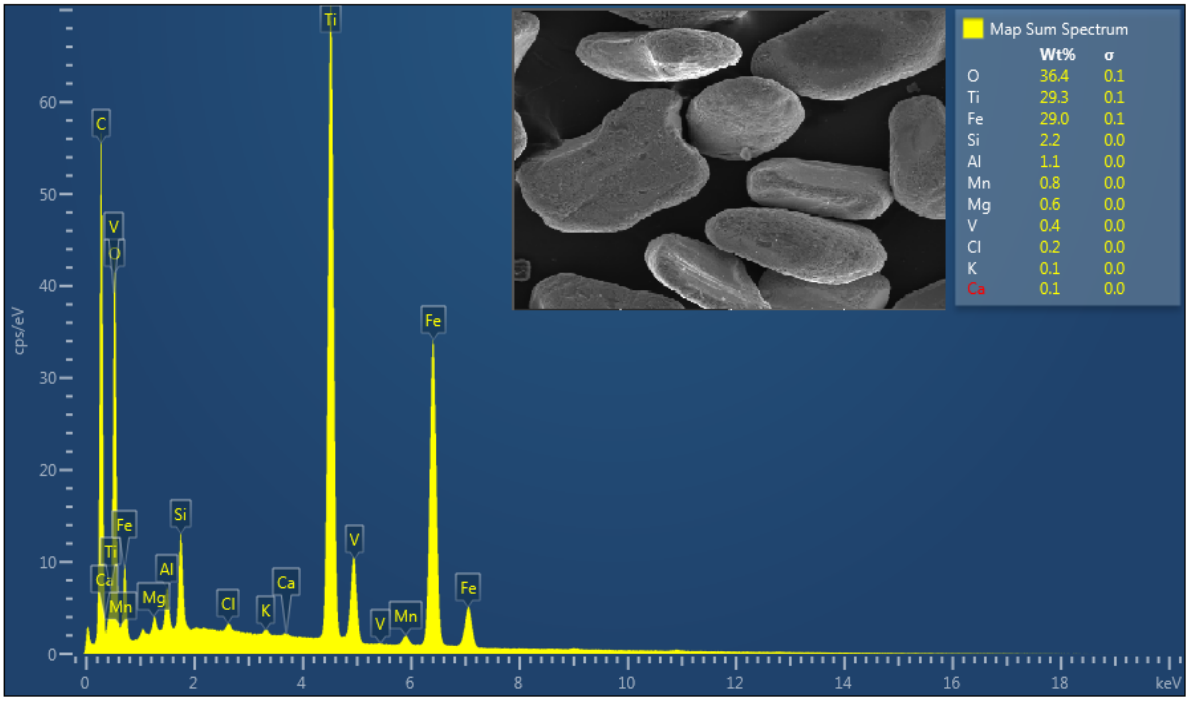

Figure 5.2: The EDX spectrum of the sample as well as the concentration of the different elements in the sample.

5.3 Results and Discussion

5.3.1 LOD and LOQ

The LODs and LOQs of Ti and Fe were first determined prior to the ICP-OES analysis of the numerous elements in the different samples. The LODs were determined in the different mineral acids (**Table 5.4**) at 334.941 nm and 259.940 nm analysis lines for Ti and Fe respectively due to their high degree of sensitivity. The LOD for Ti varied between 0.0039 and 0.0142 ppm while that of Fe from 0.0021 - 0.127 ppm. The LOQs for the two elements were also calculated as indicated in **Section 5.2.3** (ten times the LODs). The low LODs for the two elements (in the part per billion range) indicated that both the two elements can be detected and quantified at very low concentrations and these results are comparable to those reported in the literature (see **Table 5.11**).[106,162]

Table 5.11: Comparison of the LODs for the Fe and Ti in different studies

Element	*This study	*Tantalite[155]	*PDZ[213]
Ti	0.0039	0.0015[a]	8.88 x 10^{-5} [a]
Fe	0.0021	0.0035	0.00109

* H_2SO_4
[a] 336.121 nm

5.3.2 Dissolution and quantification (validation) of Ti and Fe in different samples

5.3.2.1 Quantification of Ti and Fe in inorganic salts

Different acids used in this study were used to quantify Ti and Fe in $TiCl_3$ and $FeCl_3.6H_2O$ using ICP-OES. The results obtained in **Table 5.10** indicated excellent quantification of Ti and Fe with recoveries of Ti ranging from 98(1) to 105.2(2) % while that of Fe ranged from 100(4) to 103(2) %. These results clearly indicate the compatibility of ICP-OES in the analysis of Ti and Fe in pure metals and the mineral ilmenite at the selected experimental conditions such as wavelength selection, matrix matching and the calibration curve.

5.3.2.2 Dissolution and quantification of Ti and Fe in pure metal samples

The dissolution of the pure Ti and Fe metal samples was initially investigated using open beaker acid digestion. Visual inspection of the resultant reactions mixture after the dissolution of the two metal samples indicated the complete dissolution with concentrated H_2SO_4 and H_3PO_4 at elevated temperatures (150 ºC and 200 ºC). ICP-OES quantification indicated Ti recoveries in both acids of were 104.4(3) % and 105.4(6) % while that of Fe were 98(1) % and 97(1) % respectively. The dissolution of the same metal powders in HNO_3, HCl and *aqua regia* produced poor Ti recoveries of 0.183(9) %, 0.192(6) % and 45.2(3) %. The Fe metal/acid reactions on the other hand also indicated the incomplete dissolution with HNO_3 as acid with an average recovery of 72(1) %, while visual inspection indicated better dissolution in *aqua regia* and HCl with recoveries of 95.0(1) % and 96.6(6) % respectively.

213 Lotter, S.J., Identification and quantification of impurities in zircon, PDZ and other relevant zirconium products, MSc thesis, The University of the free state, pp.8-91 (2008)

5.3.2.3 Dissolution and quantification of Ti and Fe in ilmenite

The dissolution of the ilmenite was also investigated using the same acids at different temperatures (ranging between 60 to 150 ºC depending on the type of acid) which are identical to those acids which were used to evaluate for the dissolution of Ti and Fe metal powders. The results in this part of the study showed similar dissolution trends for both Ti and Fe in H_3PO_4 and H_2SO_4 (see **Table 5.12**), although the recoveries indicated the incomplete dissolution in the mineral sample. Sasikumar *et al*[90,93] obtained 84 % Fe and 41 % Ti dissolution in ilmenite while in another study obtained 90 % Fe and 65 % Ti dissolution (see also **Chapter 3, Section 3.2.1**). In their study, the mineral samples were mechanically activated and they also observed that the difference in the dissolution is affected by weathering. In this study the mineral sand was not grinded or reduced to a specific size. Andrade *et al*[99] reported a complete leaching of Ti and Fe in ilmenite using H_3PO_4 under similar experimental conditions of 230 ºC.

Table 5.12: Ti and Fe recoveries after dissolution of ilmenite using different mineral acids

Acid	TiO_2		Fe_2O_2	
	Mean (SD)	**% RSD**	**Mean (SD)**	**% RSD**
Aqua regia	0.03308(5)	0.027	0.285(2)	0.10
HCl	1.28(3)	0.40	2.51(2)	0.86
HNO_3	0.0517(5)	1.52	0.25(1)	0.69
H_2SO_4	34.8(1)	1.65	20.2(2)	1.37
H_3PO_4	38.4(3)	1.11	46.8(3)	1.25

Although HCl showed a similar dissolution trend (to metal powders), the recoveries were extremely low while HNO_3 and aqua regia were almost completely ineffective in the leaching or the dissolving of these elements in the ilmenite mineral (**Table 5.12**). Habib *et al*[95] studied the leaching of ilmenite using 6.0 M HCl at 110 ºC with a solid to liquid ratio mole ratio of 0.02 g/mL under reflux conditions. Their results indicated that 53.5 % Ti and 60 % Fe were leached from the mineral under these experimental

conditions. Haverkamp *et al*[94] dissolved up to 90 % of both Ti and Fe in ilmenite at 60 - 90 ºC with 32 % (w/w) HCl at a mole ratio of 2:1 (HCl: $FeTiO_3$) under reflux conditions applied for 7 minutes. Results obtained in this study on the other hand indicated the partial to unsuccessful dissolution of these elements (Ti and Fe) when using the five different acids as a dissolving reagent. This may be due to different experimental parameters such as sample particle sizes and poor temperature control since in this study was conducted in an open uncontrolled environment.

5.3.3 Effect of different flux on ilmenite digestion

Different fluxes were evaluated for the flux fusion digestion of ilmenite mineral. Dissolution with fluoride fusion ($NH_4{\cdot}HF_2$ and KF), $K_2S_2O_7$ and Na_2CO_3 showed the incomplete dissolution of the mineral (see **Table 5.8** and **Table 5.9**). Complete dissolution of the mineral was however observed using $Na_2B_4O_7$, $LiBO_2$ and NaH_2PO_4:Na_2HPO_4 (see **Table 5.10**) with the total recoveries of 107.5 %, 107.34 % and 109.03 % respectively. The higher than expected recoveries may be attributed to the addition of impurities present in the salts or to the high sodium and lithium content (EIE influence of flame temperature). These results indicate that the strong basic fusion salts (borates and phosphates) are successful in the dissolution of ilmenite compared to more acidic fusion fluxes such as fluorides and potassium pyrosulphates (**Table 5.13**).[214]

214 Theron, T.A., Nete, M., Venter, J.A., Purcell, W. and Nel, J.T., Dissolution and quantification of tantalum- containing compounds: Comparison with niobium. *South African Journal of Chemistry*, 64, pp.173-178, (2011)

Table 5.13: Comparison of the quantitative results obtained from the dissolution of ilmenite using different flux reagents

Flux	Fusion Temperature (^oC)	Solvents	Results
Na_2CO_3	900	1.0 M H_2SO_4	Incomplete
$K_2S_2O_7$	800	H_2SO_4	Incomplete
$LiBO_2$	1000	H_2SO_4	**Complete**
$Na_2B_4O_7$	1000	H_2SO_4	**Complete**
$NH_4{\cdot}HF_2$	200	H_2O	Incomplete
KF	950	1.0 M H_2SO_4	Incomplete
NaH_2PO_4:Na_2HPO_4 (1:1) mixture	800	H_2O	**Complete**

5.3.4 Sample characterization using SEM-EDS

The ilmenite sample was also characterised using SEM-EDS and the results obtained in this study indicated the presence of 38.5 wt % of O_2, Ti (27.8 wt %), Fe (27.27 wt %) and Si (3 wt %) as major elements (see **Figures 5.1 and Table 5.14**). Doubrovine[215] studied the chemical composition of the titanomagnetite using SEM-EDS and his results indicated the presence of 14.5 % Ti, 50.6 % Fe and 31.2 % O_2 as major elemental content. The presence of C in **Figure 5.3** may be due to the carbon coating during sample preparation. Other elements which were observed in trace quantities in the ilmenite include Cl, K, Al, Mg and Mn (**Table 5.14**).

215 Doubrovine, P., Quantitative X-ray Microanalysis of Fe-Ti Oxides Using Energy-Dispersive Spectrometry, [Accessed 05-05-2017]. Available from; http://www.optics.rochester.edu/workgroups/cml/opt307/spr04/pavel/

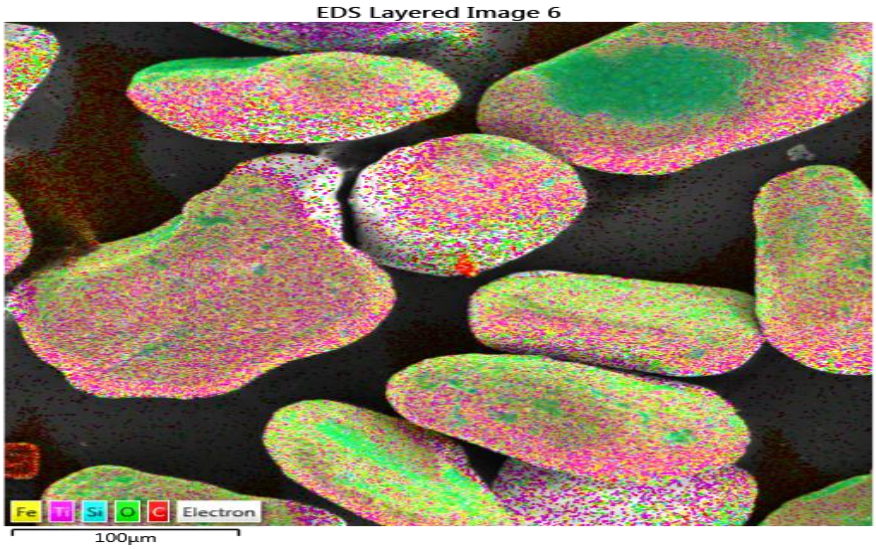

Figure 5.3: SEM-EDS Layered image with Major elements in the ilmenite sample

5.3.4.1 Evaluation of SEM-EDS for quantification analysis

The ability of SEM-EDS to provide reliable quantitative analysis results for the ilmenite constituents was evaluated by comparing it with those obtained using ICP-OES analysis. It is important to note that only the ICP-OES results in which the sample was completely dissolved were used for comparison with the SEM-EDS results. For this comparison, both the ICP-OES and SEM-EDS results are represented as percent metals and the results are given in **Table 5.14**

Table 5.14: Comparison of elemental content in ilmenite using EDS and ICP-OES quantification.

Analyte*	SEM-EDS	NaH_2PO_4:Na_2HPO_4	$LiBO_2$	$Na_2B_4O_7$
O	38.5 (2)	--	--	--
Fe	27(2)	39.1(6)	38.54(3)	39(1)
Ti	27(2)	29.(1)	28.6(5)	27(1)
Si	3.0(8)	2.6(4)	0.690(8)	0.71(8)
Al	0.9(6)	0.32(2)	0.62(2)	0.630(3)
Mg	0.8(2)	0.180(8)	0.29(1)	0.288(2)
Mn	0.7(1)	0.98(7)	0.901(1)	1.05(4)
K	0.3(1)	--	--	--
Cl	0.13(6)	--	--	--

* Analysis in triplicate
--Not detected

A graphic presentation of the results obtained with ICP-OES from the complete sample dissolution methods using flux fusion ($LiBO_2$, $Na_2B_4O_7$ and phosphate flux) and those obtained with SEM-EDS and the results are shown in **Figure 5.4**. Generally, there is good correlation between the SEM-EDS and ICP-OES results, especially for the elements with high concentrations that are present in the sample. It is only the Fe concentrations obtained from the SEM-EDS evaluation which is lower than those obtained using ICP-OES (see **Figure 5.4**). The results for poor iron analysis may be attributed to the fact that SEM-EDS is a surface sensitive technique which requires that samples be electrically conductive and more importantly, homogeneously mixed during sample preparation for accurate analysis.[216] The agreement between the two sets of results becomes even worse as the elemental content within the mineral decreases. The SEM-EDS analysis for Mg, Mn, Al, Si Cl and K showed poor compatibility with the ICP-OES results and the relative standard deviation for these elements ranged from 15.75 to 60.92 %. This can be attributed to very high LOD values (1000 - 3000 ppm)[217]cited for in SEM-EDS analysis, indicating that the quantification of these elements is close or below the detection limit to afford the poor quantification which is observed. A possible explanation for relatively poor analytical results obtained with SEM-EDS could be attributed to the type and the particle size of the sample used during the analysis. Large quantities of particles should be analysed to ensure that the good representative elemental quantities for the sample is obtained and it would also reduce the analytical error, while different particle sizes may also lead to different quantities reported for the element present in the selected particles.[218] For example Haley *et al*[218] analysed 100 particles in their study of estuarine and obtained accurate Al, Fe, Mg, Si, Ca and K analysis. The ICP-OES analysis of the flux fusion solutions in this study produced % RSDs in the order of 5 %, with the exception of Si whose % RSD was 13.45 %.

216 Kuisma-Kursula, P., Accuracy, precision and detection limits of SEM-WDE, SEM-EDS and PIXE in the multi-elemental analysis of medieval glass, *X-ray Spectrum*, 29, pp.119-118 (2000)

217 Energy Dispersive Spectroscopy on the SEM: A Primer, [Accessed 28-02-2007]. Available from; http://www.charfac.umn.edu/instruments/eds_on_sem_primer.pdf

218 Haley, S.M., Tappin, A.D, Bond, P.R. and Fitzsimons, M.F., A comparison of SEM-EDS with ICP-AES for the quantitative elemental determination of Estaurine particles, *Environmental Chemistry Letters*, 4, pp.235-238 (2006)

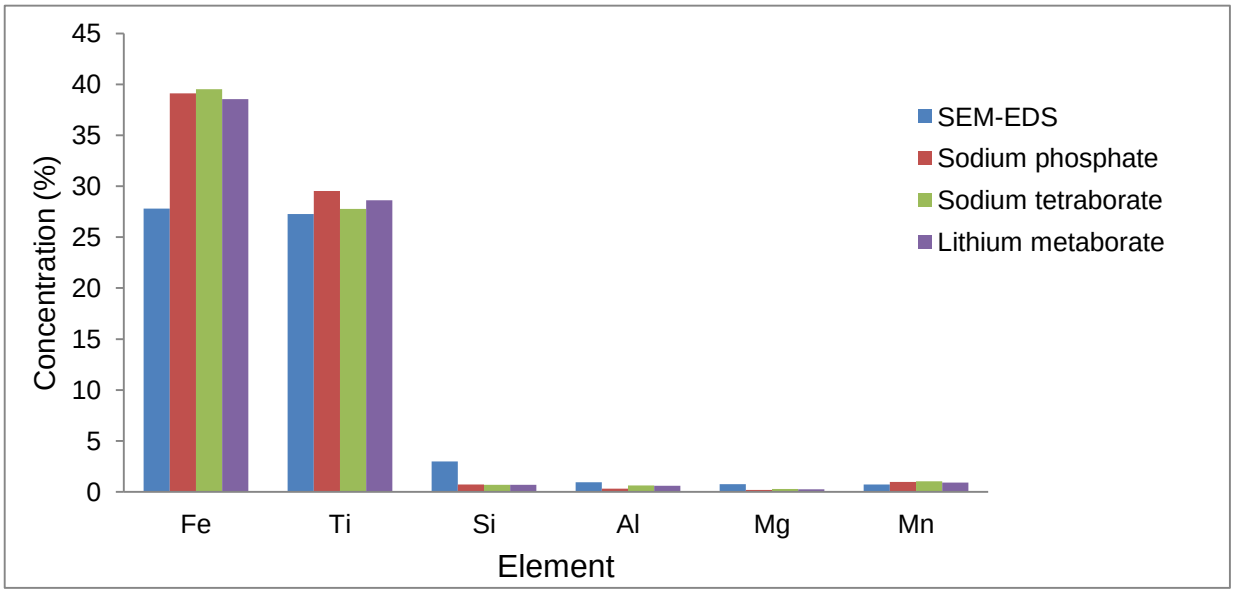

Figure 5.4: Quantitative analysis of Ilmenite sample using wet analysis and dry analysis.

Although SEM-EDS analysis usually suffers from the poor sensitivity as an analytical technique, this technique has other unique advantages above other techniques such as the ability to detect and estimate the concentration of non-metals such as Cl and O, and the alkali elements such as K which is traditionally difficult to analyse using ICP-OES.

5.4 Conclusion

The acid dissolution of Ti and Fe powder in open beaker using H_2SO_4 and H_3PO_4 as acids proved to be very effective with the complete dissolution of the metal samples and very good Ti and Fe percent recoveries were obtained. The successful dissolution conditions developed for the metal powders were then evaluated for the dissolution of the ilmenite mineral. These acid dissolution digestions were however not very successful and incomplete dissolution was achived with both acids. However, H_3PO_4 slighly outperformed H_2SO_4 as acid and 34.79 % TiO_2 and 19.50 % Fe_2O_3 compare to H_2SO_4 (38.39 % Ti and 45.25 % Fe). HCl, HNO_3 and *aqua regia* were also inverstigatedas possible dissolution agents but they were highly unsuccessful with very poor recoveries of both elements using these acids. Flux fusion dissolution of the ilmenite was also inverstigated using a number of fluxes.

ilmenite was completely dissolved using $Na_2B_2O_7$, $LiBO_2$, and sodium phosphate mixture ($Na_2HPO_4/NaH_2PO_4 \cdot H_2O$) as fluxes. The mineral was also characterised using SEM-EDS for qualitative and semi-quantitative analysis. The ability of SEM-EDS to provide reliable quantitative results was evaluated by comparing the results with those obtained using ICP-OES. Relatively good agreement, especialy for the elements with higher concentrations in the mineral sample, was obtained with the exception in Fe analysis. The comparison indicated that the elements in minor quantities namely Al, Mn, and Mg were at least in the same order of magnitue in recovery.

6 Separation of titanium and iron in ilmenite mineral

6.1 Introduction

Ilmenite usually contains Ti and Fe as major elements with minor amounts of Mn, Al, Si and Mg as trace elements. The overall aim of this study was to investigate different hydrometallurgical separation techniques which include selective precipitation, solvent extraction and ion exchange as possible beneficiation processes for ilmenite (see **Chapter 1**, **Section 1.3**). The first step in all hydrometallurgical separation processes entails the development of experimental conditions for the complete dissolution of the mineral samples and in this case it was accomplished with borate and phosphate fluxes as described in **Section 5.2.5.4.3** (see **Chapter 5**). The different separation techniques which were investigated in this study, concentrated on the dissolved mineral samples in a phosphate matrix. The phosphate flux melt (see **Chapter 5, Section 5.2.5.3.3**) easily dissolved in H_2O and thus allowed for the easy manipulation/control of the acid/base concentrations during the solvent extraction and selective precipitation processes.

The separation process development concentrated on Ti and Fe as the major elements in the mineral, but the analytical process also allowed for the tracking of the other minor elements. The flow diagram in **Figure 6.1** summarizes the different routes and chemicals used in the separation steps developed for ilmenite in this study.

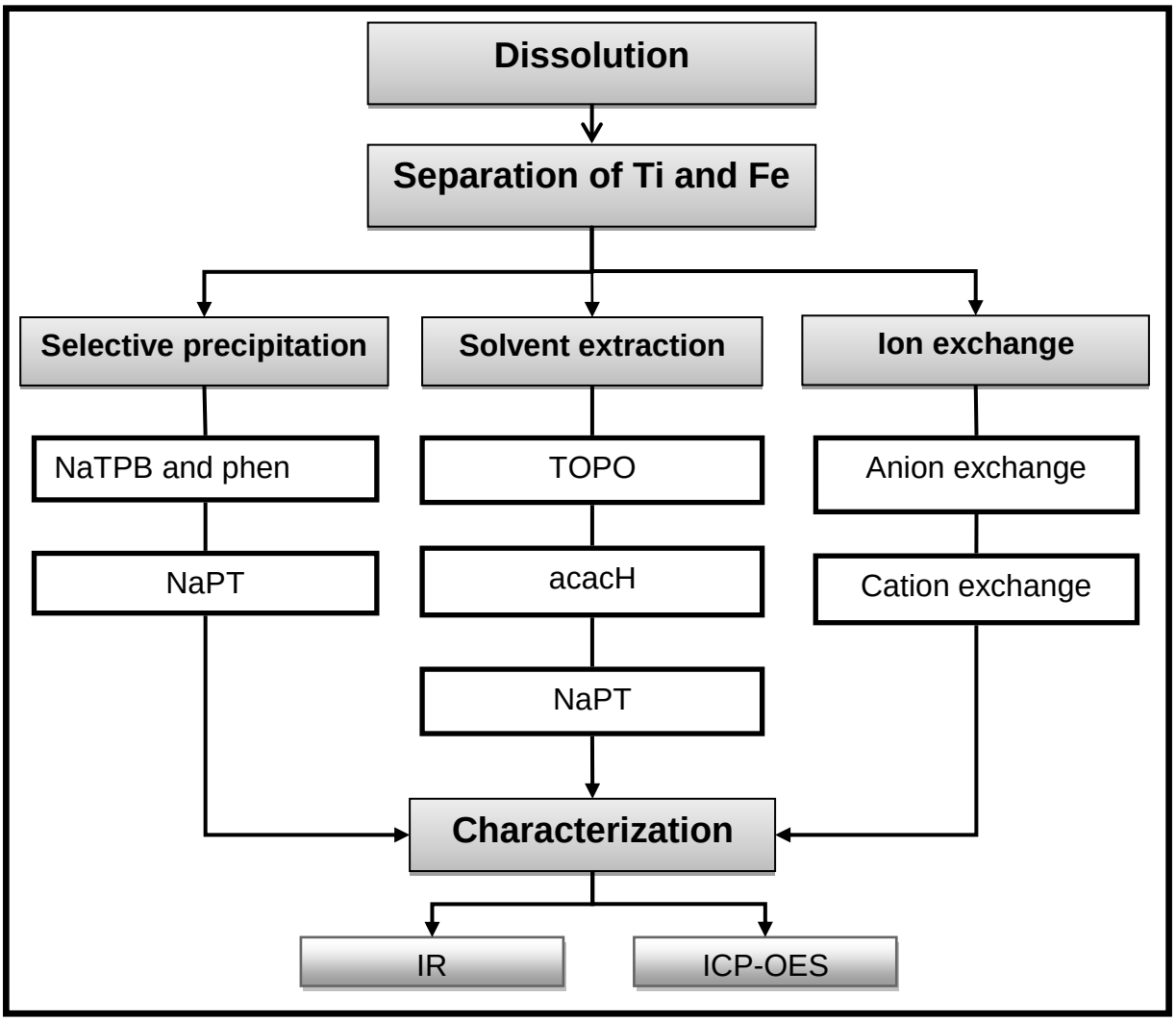

Figure 6.1: Flow diagram indicating the general procedure to separate Ti and Fe in ilmenite.

6.2 Experimental methods

6.2.1 Reagents and equipment

A Shimadzu ICPS-7510 ICP-OES sequential plasma spectrometer (see **Table 5.2**) was used for the quantitative and qualitative analysis of Ti and Fe after every separation step. A Digilab Scimitar series spectrometer was used to characterize the isolated compounds after the different separation stages. Ultra-pure (conductivity = 0.001 mS/cm) water was used throughout the study. All chemicals and commercial reagents were used without further purification. The chemicals used in this part of the study are listed in **Table 6.1**.

Table 6.1: List of reagents with their purities and suppliers.

Chemical	Formula	Purity	Supplier
Ammonium iron(II) sulphate	$FeH_{20}N_2O_{14}S_2$	99 %	Glassworld
Titanium tricloride	$TiCl_3$	15 %	--
Hydrogen peroxide	H_2O_2	--	Merk
Phenantroline (phen)	$C_{12}H_8N_2$	--	Glassworld
Sodium tetraphenyl borate (NaTPB)	$C_{20}H_{20}BNa$	≥ 99.5 %	Sigma-Aldrich
2-Mercaptopyridine N-oxide sodium salt (NaPT)	C_4H_4NNaOS	≥ 96 %	Sigma-Aldrich
Acetylacetone (acacH)	$C_5H_8O_2$	99.5 %	Sigma-Aldrich
Trioctylphosphine oxide (TOPO)	$C_{24}H_{51}OP$	> 97 %	Fluka chemika
Ethanol	CH_3OH	99.5 %	Merck
Methyl isobutyl ketone (MIBK)	$C_6H_{12}O$	99 %	Saarchem
1-Octanol	$C_8H_{18}O$	99.5 %	Sigma-Aldrich
Kerosene	$C_{12}H_{26}$	--	Sigma-Aldrich

-- Not supplied

6.2.2 Preparation of ICP-OES calibration solutions and measurements

Multi-element calibration standard solutions were prepared from 1000 mg/L Ti/Si stock solutions as well as a 1000 mg/L multi-element stock solutions containing Fe, Mn, Al, and Mg by adding appropriate volumes in 100.0 mL volumetric flask to prepare 0.5, 1.0, 3.0, 5.0 and 10.0 mg/L concentrations. Three sets of standard solutions were prepared with different acid matrices to ensure matrix matching. All the standard solutions contained 10.0 mL of either H_2SO_4, H_3PO_4 or HCl and diluted to the mark with ultra-pure water. The blank solution was prepared similar to the standard and sample solutions by adding 10.0 mL of the appropriate acid (or the fused phosphate melt solution) in 100.0 mL volumetric flask to match the standards and sample solutions to ensure matrix matching and then diluting to the mark with ultra-pure water.

6.2.3 Selective precipitation of Fe and Ti in different matrices

The selective precipitation of Ti and Fe in the dissolved ilmenite sample was investigated using a combination of phenantroline (phen) and sodium tetraphenylborate (NaTPB) as well as the sodium mecarptopyridine N-oxide salt (NaPT). Initially the possible precipitation of Ti and Fe with the phen/NaTPB combination was evaluated with pure titanium trichloride and ammonium iron (II) sulphate and then applied it to the ilmenite. During the NaPT study, the selective precipitation was only investigated using ilmenite for the possible Ti/Fe separation.

6.2.3.1 Selective precipitation of Fe

6.2.3.1.1 Selective precipitation of Fe with NaTPB and phenantroline

Approximately 0.1 g (accurately weighed to 0.1 mg) of ammonium iron (II) sulphate was dissolved in 5 mL of water and transferred into a 100.0 mL volumetric flask and filled to the mark. A 1.0 mL aliquot of these solution was quantitatively transferred into a 100 mL beaker and mixed homogenously with 0.2 g of phenantroline (dissolved in 5 mL ethanol) (1:1, Fe:phen ratio) forming a red colored solution. Sodium tetraphenyl borate (NaTPB, see **Figure 6.3**) solution (0.2 g dissolved in 5.0 mL of ethanol) was added to the red solution and precipitation formation was observed. The red precipitate was separated using centrifugation and dissolved in 10.0 mL of H_2SO_4 with heating (65 ºC). To the filtrate 10.0 mL of H_2SO_4 was added for the matrix matching with the standard solutions and filled to the mark with water in a 100.0 mL volumetric flask. The experiment was repeated with different ratios of Fe:phen (1:3 and 1:5) and all the solutions were analyzed with ICP-OES and the results are presented in **Table 6.2**

Table 6.2: Total Fe Recovery after precipitation with NaTPB and phen

Sample ratio (Fe:phen)	% Recovery		Total % mass
	Precipitate	Filtrate	
1:1	55(5)	73(3)	128(3)
1:3	99(5)	25.3(6)	125(6)
1:5	82(8)	24(5)	127(4)

Average of n=3 measurements

6.2.3.1.2 The effect of NaTPB and phenantroline on the total Fe recovery

The results obtained in **Section 6.2.3.1** indicated total % recovery of Fe far in excess of a 100 % when Fe content in the precipitate and the filtrate is added together. The study was expanded to determine the effect of the presence (or not) of phen, NaTPB, and a combination of phen and NaTPB on the total Fe recovery. Three sets of different solutions were prepared in 100.0 mL beakers and to each solution a 1.0 mL aliquot of the Fe solution prepared in **Section 6.2.3.1** were added. To the first beaker, 0.2 g of phen dissolved in 5 mL of ethanol (1:1, Fe:phen) was added and a red solution was obtained. To the second beaker 0.2 g of NaTPB dissolved in 5 mL ethanol (1:3, Fe:NaTPB,) was added forming a white precipitate. To the third beaker, both phen and NaTPB (Fe:phen:NaTPB, 1:1:3) were added which resulted in the formation of a red precipitate. The precipitate which formed in both last two beakers were isolated using a centrifuge and subsequently dissolved in 10.0 mL of H_2SO_4 and heated at 100 ºC with constant stirring. The acidity of the filtrate solutions (or supernatant solution separated from the precipitate by decantation) in the second and third beakers and the solution in the first beaker (containing only Fe and phen) was adjusted by adding 10.0 mL H_2SO_4. All solutions were quantitatively transferred to a 100.0 mL volumetric flask and filled to the mark with water. The influence of the ligands on the Fe recoveries was tested by comparing the analytical results of a free Fe solution to those of Fe/phen, Fe/NaTPB, and Fe/ phen/NaTPB. A 1.0 mL aliquot of Fe solution was also acidified with 10.0 mL H_2SO_4 and filled to the mark in a 100.0 mL volumetric flask. All the solutions were analyzed with ICP-OES and the results are presented in **Table 6.3.**

Table 6.3: The recovery of Fe in the presence of phen, NaTPB and a combination of phen and NaTPB

Sample	% Fe recovery	
	Precipitate	**Filtrate**
Fe	--	104.1(2)
Fe and phen	--	84.4(8)
Fe and NaTPB	108.1(4)	9.9(2)
Total % mass	**118.0(2)**	
Fe, phen and NaTPB	96.9(7)	19.2(3)
Total % mass	**116(1)**	

-- Not observed, Average of n=2

6.2.3.1.3 Improvement in the percentage Fe recovery

The experiment was repeated (similar to **Section 6.2.3.1.1** in a 1:1 ratio (Fe:phen) to try and improve the recovery percentage (in excess of 100 % for **Section 6.2.3.1.1**). The isolated precipitate was dried by placing it in an oven at 100 ºC for 5 min and then re-dissolved in a 10.0 mL of H_2SO_4 and heated at 100 ºC with constant stirring. The acidity of the filtrate (supernatant solution separated from the precipitate by decantation) was adjusted by adding 10.0 mL H_2SO_4. All the solutions were transferred to a 100.0 mL volumetric flask and filled to the mark with water and the results are presented in **Table 6.4**.

Table 6.4: Total Fe recovery after precipitation with NaTPB/phen and the drying of the precipitate

Sample analysis	% Recovery		Total % mass
	Precipitate	**Filtrate**	
1	46.02	62.99	109.03
2	45.24	53.95	99.20
3	45.38	57.71	103.10
Mean	*45.5(4)*	*58(5)*	*104(5)*
% RSD	*0.92*	*7.80*	*4.77*

6.2.3.2 Selective precipitation of Ti

6.2.3.2.1 Selective precipitation of Ti with NaTPB and phenantroline

A 1.0 mL aliquot of $TiCl_3$ was mixed homogeneously with H_2O_2 (10.0 mL) and quantitatively transferred to a 100.0 mL volumetric flask and filled to the mark with water. A 1.0 mL aliquot of the solution was mixed with 0.2 g of phen (dissolvent in 5.0 mL ethanol) in a beaker. No colour change was observed with the addition of phen to Ti solution, suggesting that no reaction took place between the two reagents even after the phen concentration was increased (1:3, Ti:phen). It was therefore decided to stop any further Ti-phen variation due the absence of any observable reaction.

In the next step, the study investigated the possible precipitation reaction between Ti and sodium tetraphenylborate (NaTPB). A 1.0 mL aliquot of the Ti solution was also mixed with 0.2 g of NaTPB dissolved in 5.0 mL ethanol (1:3, Ti:NaTPB). A yellow precipitate immediately formed upon the mixing the two solutions. The precipitate was separated by centrifugation and re-dissolved in 10.0 mL of H_2SO_4 at 100 ºC with constant stirring. The acidity of the filtrate (supernatant solution separated from the precipitate by decantation) was adjusted by adding 10.0 mL H_2SO_4. All the solutions were analyzed using ICP-OES and the results are presented in **Table 6.5**.

Table 6.5: Total Ti recovery after NaTPB precipitation

Sample ratio	% Recovery		Total % mass
	Precipitate	Filtrate	
1.1	38.3(2)	69(7)	107(7)
1.3	94(8)	14(7)	108(1)

Average of n=2

6.2.3.3 Precipitation separation of Ti and Fe in ilmenite

6.2.3.3.1 Selective precipitation of Ti and Fe in ilmenite with NaTPB and phenantroline

The next step was to investigate the possible separation of Ti and Fe in the mineral ilmenite using NaTPB and phen. A 1.0 mL aliquot of the phosphate fused ilmenite sample prepared in **Section 5.5.3.1** (see **Chapter 5**) was mixed with 0.01 g of phen dissolved in 5 mL ethanol (1:1, Fe:phen). To the solution 0.2 g of NaTPB dissolved in

5.0 mL of ethanol was added forming a colourless crystalline precipitate. The precipitate was filtered and dissolved in 10.0 mL of H_2SO_4 and heated at 100 ºC with constant stirring. 10.0 mL of H_2SO_4 was also added to the filtrate (supernatant solution separated from the precipitate by decantation) to adjust the acidity. All the solutions were quantitatively transferred to a 100.0 mL volumetric flask and analysed using ICP-OES. The results are presented in **Table 6.6**

Table 6.6: Total Ti and Fe recoveries in ilmenite after NaTPB/ phen precipitation

Ratio(Fe: phen)	samples	% Recovery	
		Ti	Fe
1:0.5	Filtrate	0.0	0.0
	Precipitate	89.7(9)	101.1(2)
Total % mass		**89.7(9)**	**101.1(2)**
1:3	Filtrate	81(1)	140(7)
	Precipitate	35(10)	25.1(9)
Total % mass		**116(10)**	**165(8)**
1:5	Filtrate	82(4)	74(10)
	Precipitate	46(26)	12(10)
Total % mass		**173(21)**	**113(10)**

Average of n=3 measurements

6.2.3.4 Selective precipitation of Ti and Fe in ilmenite with NaPT

The possible selective precipitation of Ti and Fe in ilmenite was investigated using 2-mercaptopyridine N-oxide sodium salt (NaPT, see **Figure 6.4**). 0.02 g (0.000137 mol) NaPT (accurately weighed to 0.1 mg) was dissolved in 5.0 mL of water. A 1.0 mL aliquot of phosphate fused ilmenite sample solution (see **Chapter 5**, **Section 5.5.3.1)** was added to the NaPT solution. The resultant solution turned dark purple followed by a purple precipitate formation which left the supernatant liquid colorless. The pH of the solution after mixing the reagents was found to be 9.00. The dark purple precipitate was separated from the solution by centrifugation and decantation. The precipitate was re-dissolved by addition of 5.0 mL of concentrated HCl and

quantitatively transferred to a 100.0 mL volumetric flask. The filtrate was also acidified with 5.0 mL of HCl for acid matrix matching and diluted to the mark with water in a 100.0 mL volumetric flask. The standard solutions were also prepared similar to the prepared solutions for matrix matching and analyzed using ICP-OES. The process was performed in triplicate and the results are presented in **Table 6.7** (see also **Figure 6.5** and **Figure 6.6**).

Table 6.7: Total Ti and Fe recoveries in ilmenite after NaPT precipitation

Samples	**% Recovery**	
	Ti	**Fe**
Precipitate	0.0	102.74
Filtrate	98.59	0.0
Total % mass	**98.59**	**102.74**
Precipitate	0.0	105.17
Filtrate	100.62	0.0
Total % mass	**100.62**	**105.17**
Precipitate	0.0	102.73
Filtrate	99.60	0.0
Total % mass	**99.60**	**102.73**
Mean	***99.60(1)***	***103(1)***
% RSD	***1.02***	***1.36***

Average of n=3 measurements

6.2.3.4.1 IR analysis of the ilmenite product precipitate obtained after NaPT addition

The ilmenite precipitate obtained in **Section 6.2.3.4** and the NaPT compound (starting material) were characterised with IR spectroscopy and the spectra is shown in **Figure 6.2** with the most important stretching frequencies listed in **Table 6.8.**

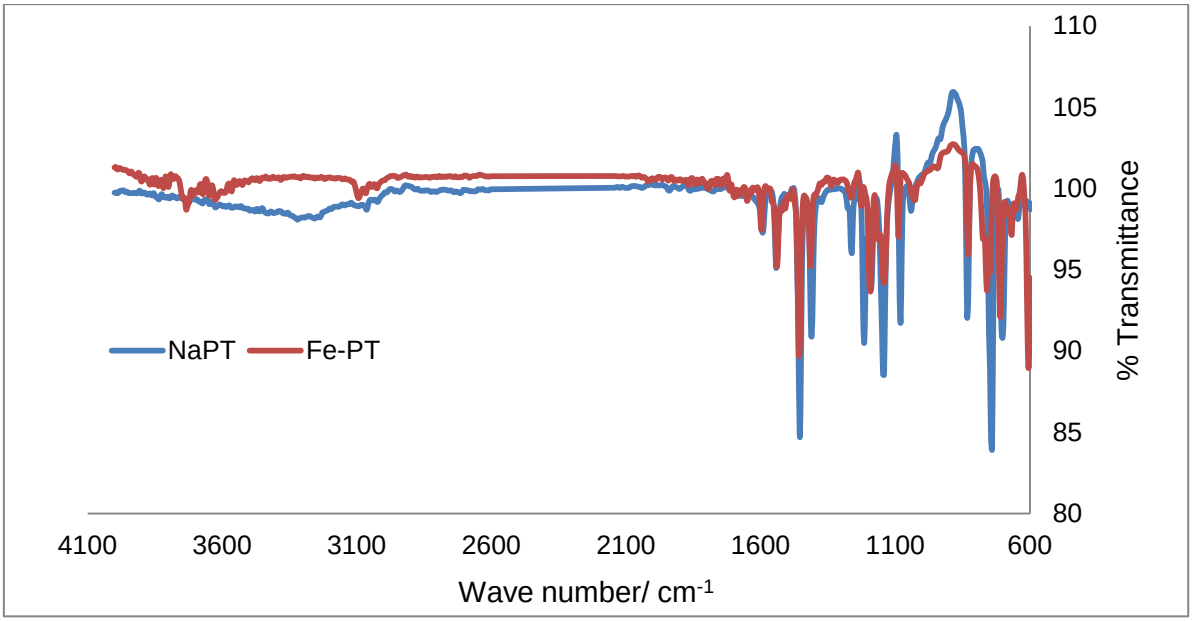

Figure 6.2: The IR spectra of NaPT and Fe-PT precipitate.

Table 6.8: The IR stretching frequencies of NaPT and Fe-PT

Compound	NaPT	Fe-PT
ν (C-S)	1143.8	1142.1
ν (C=S)	742.3	710.0
δ(N-O)	832.0	829.4
ν (N-O)	1204.3	1183.7

6.2.4 Solvent extraction separation of Ti and Fe in ilmenite

The next step in the investigation involved the possible solvent extraction separation of Ti and Fe present in a phosphate fused ilmenite sample which was prepared in **Section 5.5.3.1** (see **Chapter 5**). The extraction process was investigated using three different complexing/chelating agents namely sodium mercaptopyridine N-oxide (NaPT, see **Figure 6.4**), tri-octylphosphine oxide (TOPO, see **Figure 6.8**) and acetylacetone (acacH, see **Figure 6.8**) in different acids which included HCl, H_2SO_4 and H_3PO_4. The extracting solvents investigated include kerosene, methyl isobutyl ketone (MIBK) and 1-octanol.

6.2.4.1 Extraction of Ti and Fe in ilmenite with TOPO in kerosene

6.2.4.1.1 Extraction of Ti and Fe with TOPO in HCl medium

A 1.0 mL aliquot of the phosphate ilmenite sample prepared in **Section 5.5.3.1** was mixed with 5.0 mL HCl solution of desired concentration (~2.0 to ~8.0 M) in a separation funnel. 10.0 mL of TOPO (0.2 g, 0.0052 mol) dissolve in kerosene was added to the separating funnel and the mixture was shaken for 10 min. The aqueous phase was collected in a 100 mL beaker. The organic phase was back extracted with two portions of 10.0 mL ultra-pure water and the water portions were collected in another 100 mL beaker. All the solutions were heated to 60 ºC to evaporate any dissolved organic solvents in the aqueous layer. The solutions were allowed to cool to room temperature, transferred to 100.0 mL volumetric flask, acidified to match the blank and standard matrices and filled to the mark with water. The solutions were analyzed using ICP-OES and the results are given in **Table 6.9** (see **Figure 6.9** and **Figure 6.10**) with the acidity in the aqueous solution adjusted after dilution.

Table 6.9: Extraction of Ti and Fe with TOPO in kerosene using HCl acidic medium

[HCl] (M)	Aqueous phase		Organic phase	
	% Recovery		% Recovery	
	Ti	Fe	Ti	Fe
1.7	97(2)	98(2)	0.8(1)	2(2)
3.3	97.8(8)	47.7(7)	0.8(8)	50(4)
6.7	81(7)	0.00109(1)	22(6)	99.0(8)

Average of n=3 measurements

6.2.4.1.2 Extraction of Ti and Fe with TOPO in H_2SO_4 and H_3PO_4

A 1.0 mL aliquot of phosphate ilmenite sample prepared in **Section 5.5.3.1** was mixed with 5.0 mL H_2SO_4 solution of desired concentrations (~2.0 to ~8.0 M) in a separation funnel. 10.0 mL of TOPO solution (0.2 g, 0.00052 mol dissolve in kerosene) was added and the mixture was shaken for 10 min. The extraction procedure was performed similar to **Section 6.2.4.1.1** and the resultant solutions were heated to evaporate all the organic solvents, cooled to room temperature, acidified and filled to the mark with water in a 100.0 mL volumetric flask. All solutions

were analyzed with ICP-OES and the results are given in **Table 6.10** (see **Figure 6.11** and **Figure 6.12**). The extraction process was also repeated with H_3PO_4 solutions at different concentrations (2.0 to 8.0 M) and the results are presented in **Table 6.11**.

Table 6.10: Extraction of Ti and Fe with TOPO in kerosene using H_2SO_4

$[H_2SO_4]$ (M)	Aqueous phase		Organic phase	
	% Recovery		% Recovery	
	Ti	Fe	Ti	Fe
1.7	100(6)	104(2)	0.0	0.0
3.3	100(2)	105.4(8)	0.0	0.7(1)
6.7	52(4)	99(6)	48(4)	0.32(6)

Average of n=3 measurements

Table 6.11: Extraction of Ti and Fe with TOPO in kerosene using H_3PO_4

$[H_3PO_4]$ (M)	Aqueous phase		Organic phase	
	% Recovery		% Recovery	
	Ti	Fe	Ti	Fe
1.7	98(1)	100.4(8)	0.0	0.0
3.3	95(4)	95(6)	6(5)	5(7)
6.7	98(4)	99.6(1)	0.9(1)	0.0

Average of n=2 measurements

6.2.4.2 Solvent extraction of Ti and Fe with acacH as a ligand

6.2.4.2.1 Extraction of Ti and Fe with acacH in HCl medium

A 1.0 mL aliquot of the phosphate sample was mixed with 5.0 mL HCl of desired concentration (~0.1 to ~8.0 M) in a separation funnel. The acacH solution (1.0 mL, 0.0974 mol) and 10.0 mL of MIBK were added and the mixture was shaken for 10 min and allowed to stand for 15 min for complete liquid phase separation. The aqueous phase was collected in a 100 mL beaker. The organic phase was back extracted with two portions of 10.0 mL distilled water. All the solutions were heated at

60 ºC to evaporate any dissolved organic solvents in a 100 mL glass beaker. The solutions were allowed to cool to room temperature, acidified transferred to 100.0 mL volumetric flask, acidified to match the blank and standard matrices and filled to the mark with water. The solutions were analyzed using ICP-OES and the results are given in **Table 6.12** (see **Figure 6.13** and **Figure 6.14**) with the acidity in the aqueous solution adjusted after dilution. The extraction process was also conducted using 1-octanol (see **Figure 6.15** and **Figure 6.16**) as the extracting solvent.

Table 6.12: The extraction of Ti and Fe with acacH in HCl medium using 1-octanol and MIBK

[HCl] (M)	Aqueous phase		Organic phase	
	% Recovery		% Recovery	
	Ti	Fe	Ti	Fe
	1-octanol			
#0.07	100(4)	99.9(1)	0.0	0.0
#0.7	98(1)	100(2)	0.0	0.0
*1.4	102(3)	101(3)	0.0	0.0
*3.0	64(1)	75(4)	35(3)	23(1)
*6.0	82(5)	102(1)	19(6)	0.04(2)
	MIBK			
*1.4	97(1)	76.5(2)	1(2)	22.5(2)
*3.0	92(4)	0.0209(4)	7(2)	100(2)
*6.0	98(6)	0.15(4)	0.7(2)	99(3)

*Average of n=3 measurements, #Average of n=2 measurements

6.2.4.2.2 Extraction of Ti and Fe in H_2SO_4 and H_3PO_4 medium using MIBK and 1-octanol

A 1.0 mL phosphate fused ilmenite sample prepared in **Section 5.5.3.1** was mixed with 5.0 mL H_2SO_4 of desired concentration (~2.0 M to ~6.0 M) and 1.0 mL of acacH (1.0 mL, 0.0974 mol). The extraction procedure was performed similar to **Section 6.2.4.1.1** and the resultant solutions were heated to evaporate all the organic solvents, cooled to room temperature, acidified and filled to the mark with water in a 100.0 mL volumetric flask. All solutions were analyzed with ICP-OES and the results

are given in **Table 6.13**. The extraction process was also repeated with H_3PO_4 solutions using 1-octanol and MIBK as extracting solvents at different concentrations (~2.0 to ~ 6.0 M) and the results are presented in **Table 6.14**.

Table 6.13: The extraction of Ti and Fe in with acacH in H_2SO_4 medium

$[H_2SO_4]$ (M)	Aqueous phase		Organic phase	
	% Recovery		% Recovery	
	Ti	Fe	Ti	Fe
	1-octanol			
1.4	94(6)	97.9(2)	6(6)	0.7(1)
3.0	86(3)	101(2)	13(4)	0.0
6.0	20.5(5)	96.1(7)	81(1)	9(1)
	MIBK			
1.4	102(2)	99(4)	0.0	0.0
3.0	104.5(1)	103(3)	0.0	0.0
6.0	99(4)	99(3)	5(6)	6(5)

Average of n=3 measurements

Table 6.14: The extraction of Ti and Fe in with acacH in H_3PO_4 medium

$[H_3PO_4]$ (M)	Aqueous phase		Organic phase	
	% Recovery		% Recovery	
	Ti	Fe	Ti	Fe
	1-octanol			
1.4	103.4(5)	99.8(8)	0.0	0.0
3.0	98(1)	99(1)	2(1)	0.8(1)
6.0	89(1)	99(1)	10(1)	2(2)
	MIBK			
1.4	99(5)	99(3)	3(4)	3(4)
3.0	96(2)	97(2)	3(1)	3.0(5)
6.0	93(3)	97(3)	5(6)	3(1)

Average of n=2 measurements

6.2.4.2.2.1 Extraction of Ti and Fe in HCl medium

The results obtained in **Section 6.2.4.1** indicated the positive extraction of both Ti and Fe with acacH at higher acidic condition. The extraction of these elements was also investigated without the addition of acacH. A 1.0 mL aliquot of ilmenite phosphate sample was mixed with 5.0 mL HCl solution (~2.0 M to ~8.0 M). The acidic solution was shaken for 10 min and extracted with 10.0 mL of MIBK (or 1-octanol, **Table 6.15**). The extraction and back procedures were performed similar to **Section 6.2.4.1.1** and the resultant solutions were heated to evaporate any dissolved organic solvent, cooled to room temperature, acidified and filled to the mark with water in a 100.0 mL volumetric flask. All solutions were analyzed with ICP-OES and the results are given in **Table 6.15** (see **Figure 6.17** and **Figure 6.18**).

Table 6.15: Extraction of Ti and Fe from HCl solutions without acacH

[HCl] (M)	Aqueous phase		Organic phase	
	% Recovery		% Recovery	
	Ti	Fe	Ti	Fe
	1-octanol			
1.4	99(1)	103.4(6)	0.0	0.0
3.0	99(2)	1.9(2)	6(1)	97(4)
6.0	88(2)	0.8(1)	15(2)	101(1)
	MIBK			
1.4	99(2)	101.3(5)	0.0	0.3(5)
3.0	101(8)	0.6(9)	0.9(9)	105(3)
6.0	103(5)	0.035(7)	3(1)	104(2)

Average of n=3 replicates

6.2.4.2.2.2 Extraction of Ti and Fe in H_2SO_4 and H_3PO_4 medium (without acacH)

The extraction process was also investigated in H_3PO_4 and H_2SO_4 medium (without the presence of acacH) using MIBK and 1-octanol as the extracting solvents. The extraction procedure was performed similar to **Section 6.2.4.1.1** and the resultant solutions were heated to evaporate any dissolved organic solvents, cooled to room temperature, acidified and filled to the mark with water in a 100.0 mL volumetric flask.

All solutions were analyzed with ICP-OES and the results are given in **Table 6.16** and **Table 6.17**.

Table 6.16: Extraction of Ti and Fe in H_2SO_4 medium with MIBK and 1-octanol as extracting solvents

[H_2SO_4] (M)	**Aqueous phase**		**Organic phase**	
	% Recovery		**% Recovery**	
	Ti	**Fe**	**Ti**	**Fe**
	1-octanol			
1.4	97(3)	102(.7(9)	6(1)	2(3)
3.0	63(9)	100.3(9)	34(2)	7.8(8)
6.0	83(2)	68(6)	21(3)	32(7)
	MIBK			
1.4	101(2)	100.4(4)	0.0	0.0
3.0	97(2)	96.8(1)	1.6(2)	6.1(7)
6.0	92(3)	98(1)	13(3)	7.6(5)

Average of n=3 measurements

Table 6.17: Extraction of Ti and Fe in H_3PO_4 mediums with MIBK as the extracting solvents.

[H_3PO_4] (M)	**Aqueous phase**		**Organic phase**	
	% Recovery		**% Recovery**	
	Ti	**Fe**	**Ti**	**Fe**
1.4	100(1)	102(1)	0.0	0.0
3.0	99(1)	103(1)	1.1(1)	0.0
6.0	100(1)	101(2)	0.65(1)	0.08(1)

Average of n=3 measurements

6.2.4.3 Extraction of Ti and Fe with NaPT as chelating compound

6.2.4.3.1 Extraction of Ti and Fe with NaPT in HCl medium

A 1.0 mL aliquot of the phosphate fused ilmenite sample prepared in **Section 5.5.3.1** was mixed with 5.0 mL HCl of desired concentration (~0.1 to ~6.0 M). The NaPT solution (0.02 g, 0.00137 mol in 10.0 mL H_2O) and 10.0 mL of MIBK were added to the separating funnel. The mixture was shaken for 10 min and then allowed to stand for 15 min to allow for the complete liquid phase separation. The aqueous phase was collected in a 100 mL beaker. The organic phase was back extracted with two portions of 10.0 mL H_2SO_4 (6.0 M). All the solutions were then heated at 60 ºC to evaporate any dissolved organic solvents in a 100 mL glass beaker. The solutions were allowed to cool to room temperature, quantitatively transferred to 100.0 mL volumetric flask, acidified to match the blank and standard matrices and filled to the mark with water. The final solutions were analyzed using ICP-OES and the results are given in **Table 6.18** (see **Figure 6.19** and **Figure 6.20**) with the acidity of the aqueous solution adjusted after dilution The experiment was also conducted using 10.0 mL of 1-octanol as the extracting solvent (see **Table 6.18**, **Figure 6.21** and **Figure 6.22**).

Table 6.18: Extraction of Ti and Fe with NaPT in HCl medium using MIBK and 1-octanol as the extracting solvents

[HCl] (M)	Aqueous phase		Organic phase	
	% Recovery		% Recovery	
	Ti	Fe	Ti	Fe
	1-octanol			
0.05	97.8(2)	0.04(6)	0.46(4)	91.3(6)
1.0	93(1)	0.8(3)	6(3)	98(3)
2.0	79(1)	2.2(4)	24(9)	95.9(3)
3.0	85(6)	10(5)	15(3)	93(5)
	MIBK			
0.05	98(5)	0.011(6)	0.74(6)	99.4(6)
1.0	100(2)	0.2(4)	0.0071(1)	100(4)
2.0	101(1)	2(1)	0.9(1)	97(1)
3.0	98.3(8)	0.5(2)	0.0076(1)	97(2)

Average of n=3 measurements

6.2.4.3.2 Extraction of Ti and Fe with NaPT in H_2SO_4 and H_3PO_4 medium

A 1.0 mL phosphate fused ilmenite aliquot prepared in **Section 5.5.3.1** was mixed with 5.0 mL H_2SO_4 of desired concentration (~2.0 to ~6.0 M). The NaPT solution (0.02 g, 0.00137 mol in 10 mL H_2O) and 10.0 mL of MIBK were added to a separating funnel. The mixture was shaken for 10 min and allowed to stand for 15 min for complete liquid phase separation. The solutions were prepared similar to **Section 6.2.4.3.1** and heated to evaporate any dissolved organic solvents, cooled to room temperature, acidified and filled to the mark with water in a 100.0 mL volumetric flask. All solutions were analyzed with ICP-OES and the results are given in **Table 6.19**. The extraction was also studied in H_3PO_4 media using MIBK and 1-octanol as the extracting solvents and the results are presented in **Table 6.20** (see **Figure 6.23** and **Figure 6.24**).

Table 6.19: The extraction of Ti and Fe with NaPT in H_2SO_4 solution using MIBK and 1-octanol as the extracting solvents

[H_2SO_4] (M)	**Aqueous phase**		**Organic phase**	
	% Recovery		**% Recovery**	
	Ti	**Fe**	**Ti**	**Fe**
	1-octanol			
1.0	100.1(1)	0.0	0.0	99(7)
2.0	99(3)	0.45(1)	0.9(1)	95.5(1)
3.0	103(1)	6(2)	0.029(5)	96(2)
	MIBK			
1.0	103(2)	0.0	0.0	99(1)
2.0	99(2)	0.01(3)	2(3)	101(3)
3.0	101(1)	0.5(2)	0.19(8)	98(2)

Average of n=3 measurements

Table 6.20: The extraction of Ti and Fe with NaPT in H_3PO_4 solution using MIBK and 1-octanol as the extracting solvents

$[H_3PO_4]$ (M)	Aqueous phase		Organic phase	
	% Recovery		% Recovery	
	Ti	Fe	Ti	Fe
	1-octanol			
1.0	103(2)	0.02(2)	1.6(3)	103(3)
2.0	99.7(5)	0.03(3)	1.3(1)	100(2)
3.0	98(1)	0.01(5)	4.7(3)	98(5)
	MIBK			
1.0	104(1)	0.01(3)	0.012(2)	99(3)
2.0	99(2)	0.07(8)	0.011(1)	102.4(8)
3.0	104(4)	4(1)	0.15(2)	96(1)

Average of n=3 measurements

6.2.5 Ion exchange separation of Ti and Fe in phosphate matrix

The final part of the study involved the investigated of the separation of Ti and Fe in ilmenite using ion exchange chromatography. The study involved the investigating of both cation and anion exchange resins (weak and strong) presented in **Table 6.21** to determine the adsorption and separation behavior of these two elements in a phosphate matrix **Section 5.5.3.2** (see **Chapter 5**).

Table 6.21: Types of cationic and anionic resins used for the separation of Ti and Fe

Resins	Functional group	Ionic form	Type of resin
Cation exchanger			
Dowex Marathon C Hydrogen	Sulphonic acid	H^+	Strong acidic
Clinobrite Zeolite	--	--	Weakly acidic
Amberjet 1200H	Sulphonic acid	H^+	Strong acidic
Amberlite IR-130C	Sulphonate	Na^+	Strong acidic
Anion exchanger			
Amberlite IRA-900	Trimethyl ammonium	Cl^-	Strong basic
Amberlite IRA-402	Trimethyl ammonium	Cl^-	Strong basic
Dowex marathon WBA	Polyamine	$-NH_2$	Weak basic
Dowex 66 free base	Polyamine	$-NH_2$	Weak basic
Dowex 1x4	Trimethyl ammonium	Cl^-	Strong basic

--Information not supplied

6.2.5.1 Separation of Ti and Fe using cation exchange resins

6.2.5.1.1 Separation of Ti and Fe with cationic resins by H_3PO_4

This section describes the possible separation of the Ti and Fe in the ilmenite using the weak acidic Clinobrite zeolite resin as well as the strong acidic resins such as Amberjet 1200H, Amberlite IR-130C and Dowex C-hydrogen. All resins were individually mixed with water to form a slurry which was transferred into a 20 x 1.2 cm column. A 5.0 mL aliquot of a phosphate sample solution (prepared in **Chapter 5**, **section 5.5.3.2**) was transferred into the column and subsequently eluted with 10.0 mL solution H_3PO_4 (1.0 and 10.0 M) at a flow rate of 0.8 mL/min. The effluent was collected in a 100.0 mL volumetric flask, diluted to the mark with water and analyzed with ICP-OES. The results obtained are presented in **Table 6.22** (see **Figure 6.26**).

Table 6.22: % Recovery of Ti and Fe from the column separated on weak acidic and strong basic resins with H_3PO_4

$[H_3PO_4]$ (M)	#Zeolite		#Amberjet 1200H		#Amberlite IR-130C		*Dowex C-hydrogen	
	Ti	Fe	Ti	Fe	Ti	Fe	Ti	Fe
1.0	88(2)	100(7)	104.(2)	83(2)	97(2)	90(1)	103.5(7)	100.3(3)
10.0	103(6)	102(5)	98(6)	85(2)	97(4)	104(7)	--	--

#Average of n=2 replicates,* Average of n=3 replicates, -- Not determined

6.2.5.1.2 Separation of Ti and Fe with cationic resins by HCl elusion

Elution with a dilute H_3PO_4 solution for both weak and strong cation exchange resins in **Section 6.2.5.1.1** indicated no separation between Ti and Fe (see also **Figure 6.26**). In the next step, the separation on cation exchange resins was repeated with HCl as the eluent. The columns were prepared similar to **Section 6.2.5.1.1** and the elution was carried with 1.0 M HCl and 10.0 M HCl solutions using both weak and strong cation exchange resins. The ICP-OES analysis results are presented in **Table 6.23**.

Table 6.23: % Recovery of Fe and Ti from the column separated on weak acidic and strong basic resins with HCl

[HCl] (M)	Amberlite 1R 130C		Zeolite		Amberjet 1200H	
	Ti	Fe	Ti	Fe	Ti	Fe
1.0	93(2)	88(3)	98.5(3)	101(3)	107(1)	99.5(6)
10.0	98.3(2)	98(9)	--	--	102(4)	104.5(6)

--Not determined
Average of n=2 replicates

6.2.5.2 Separation of Ti and Fe using anion exchange resins

6.2.5.2.1 Separation of Ti and Fe using strong anionic resins

In the next step, the separation of Ti and Fe was investigated using the anion exchange resins (Amberlite IRA-900 and Amberlite IRA-402) as stationary phase and H_3PO_4 and HCl solutions as mobile phases. A glass column was packed with a resin as indicated in the above sections (see **Section 6.2.5.1.1**) and prepared for elution and separation of Ti and Fe. A 5.0 mL aliquot of phosphate sample solution (prepare in **Chapter 5, Section 5.5.3.2**) was transferred into the column and subsequently eluted with different concentrations of H_3PO_4 (0.5 to 10.0 M). The elution procedure was performed on the strong anion exchange resins. The effluent was collected in 100.0 mL volumetric flask and the acidity of the solutions was adjusted to match the standard solutions matrix. The solutions were diluted with water and analyzed using ICP-OES. The quantitative results obtained indicated no elution of both Ti and Fe at 0.5 M and 1.0 M H_3PO_4 in both resins. At 3.0 M and 5.0 M only Fe was eluted from the column while Ti was still strongly retained/adsorbed under these experimental conditions. Titanium was only eluted at high HCl concentration (equal or above 5.0 M [Cl^-]) (see **Figure 6.30**) and the analytical results are presented in **Table 6.24**.

Table 6.24: % Recovery of Ti and Fe using strong basic Amberlite IRA-900 and Amberlite IRA-402 resins

[PO_4^{3-}] (M)	**Amberlite IRA-900**		**Amberlite IRA-402**	
	Ti	**Fe**	**Ti**	**Fe**
0.5	0.0	0.0	0.0	0.0
1.0	0.0	0.0	0.0	0.0
3.0	0.0	63(9)	0.0	51(13)
5.0	13.37(5)	81(15)	5.88(1)	68(4)
10.0	74(5)	72(2)	62(2)	72(2)

Average of n=3 measurements

The results in **Table 6.24** indicated the elution of significant amount of Fe in the column with Ti strongly retained at 3.0 and 5.0 M. The possible elution of Ti from the above columns was further investigated by sequential elution of the same columns

(where no Ti was eluted) with 10.0 mL portions of 5.0 M HCl in a 100.0 mL volumetric flask, diluted to the mark with water and analyzed with ICP-OES. The results obtained are presented in **Table 6.25**.

Table 6.25: Elution of Fe with 5.0 M HCl from the different resins after the initial eluted with different H_3PO_4 concentrations

Initial $[PO_4^{3-}]$(M) in Fe elution	Amberlite IRA-900		Amberlite IRA-402	
	Ti	Fe	Ti	Fe
3.0	89(10)	0.0	90.9(2)	0.0
5.0	93(5)	1.20(15)	87.0(1)	0.88(4)
10.0	--	--	--	--

--Not determined

6.2.5.2.2 Separation of Ti and Fe using different anionic Dowex anionic resins

The potential separation of Fe and Ti present in ilmenite using strong anionic resins were observed in **Section 6.2.5.2.1** As such, the study was expanded to include more anionic resins which involved both weak and strong resins. The elution procedure was repeated as indicated in **Section 6.2.5.2.1** Fe was eluted from the column with different concentrations of PO_4^{3-} (~0.5 to ~10.0 M) and the analytical results are presented in **Table 6.26**.

Table 6.26: Separation of Ti and Fe using different Dowex anionic resins by elution with H_3PO_4

$[PO_4^{3-}]$ (M)	Dowex Marathon WBA		Dowex 66 free base		Dowex 1X4	
	Ti	Fe	Ti	Fe	Ti	Fe
0.5	0.0	0.0	0.0	0.0	0.0	0.0
1.0	0.0	0.0	0.0	0.0	0.0	0.0
3.0	0.91 (1)	103.46(1)	0.0	106.4(5)	0.0	97.3(6)
5.0	1.19(3)	96(1)	0.0	96(9)	8.32(3)	84(3)
10.0	100(5)	102(2)	100(3)	103(3)	101(3)	100(3)

Average of n=3 measurements

The results in **Table 6.26** indicated the successful elution of Fe from the column while Ti was still strongly retained at 3.0 and 5.0 M [PO_4^{3-}]. The elution of Ti from the above columns were further investigated by sequential elution of the same columns with 10.0 mL portions of HCl solution (5.0 M) in a 100.0 mL volumetric flask, diluted to the mark with water and analyzed with ICP-OES. The results obtained are presented in **Table 6.27** (see **Figure 6.30**).

Table 6.27: Elusion of Ti with 5.0 M HCl in different Dowex resins

Initial [PO_4^{3-}] (M) in Fe elution	Dowex Marathon WBA		Dowex 66 free base		Dowex 1X4	
	Ti	Fe	Ti	Fe	Ti	Fe
3.0	99.1(1)	0.54(1)	103(4)	0.0	97.3(6)	0.0
5.0	100.8(3)	0.23(1)	100(1)	0.0	84(3)	1.57(3)
10.0	--	--	--	--	--	--

Average of n=3 measurements, -- Not determined

6.3 Results and Discussions

6.3.1 Selective precipitation of Ti and Fe

6.3.1.1 Selective precipitation of Ti and Fe with phenantroline and sodium tetraphenyl borate

In this study the selective precipitation of Ti and Fe was first investigated with $(NH_4)_2Fe(SO_4)_2{\cdot}6H_2O$ and $TiCl_3$ salts of known purity. $(NH_4)_2Fe(SO_4)_2{\cdot}6H_2O$ react with phenantroline (phen) forming the well-known red coloured $[Fe(phen_3)]^{2+}$complex in solution (see **Equation 6.1**). The addition of sodium tetraphenyl borate (NaTPB, see **Figure 6.3**) as anion to the $[Fe(phen_3)]^{2+}$ solution resulted in the precipitate of the Fe complex (see **Table 6.2** and **Equation 6.2**). The analytical results obtained indicated a Fe recovery of up to 99(5) % for the dissolved precipitate at a Fe:phen ratio of 1:3 (see **Table 6.2**). However, the filtrate indicated an additional 25.3(6) % Fe, resulting in an unacceptable Fe recovery of 125.3(6) %. This inaccurate mass balance of Fe prompted further investigations into experimental as well as analytical procedures.

$$Fe^{2+} + 3phen \underset{}{\overset{k_1/k_{-1}}{\rightleftharpoons}} [Fe(phen)_3]^{2+} \qquad \textbf{6.1}$$

where $k_1=6.55x10^4M^{-1}s^{-1}$ and $k_{-1}=9.28x10^{-5}M^{-1}s^{-2}$ **219**

$$[Fe(phen)_3]^{2+} + 2NaTPB \rightleftharpoons [Fe(phen)_3](TPB)_2 + 2Na^+ \qquad \textbf{6.2}$$

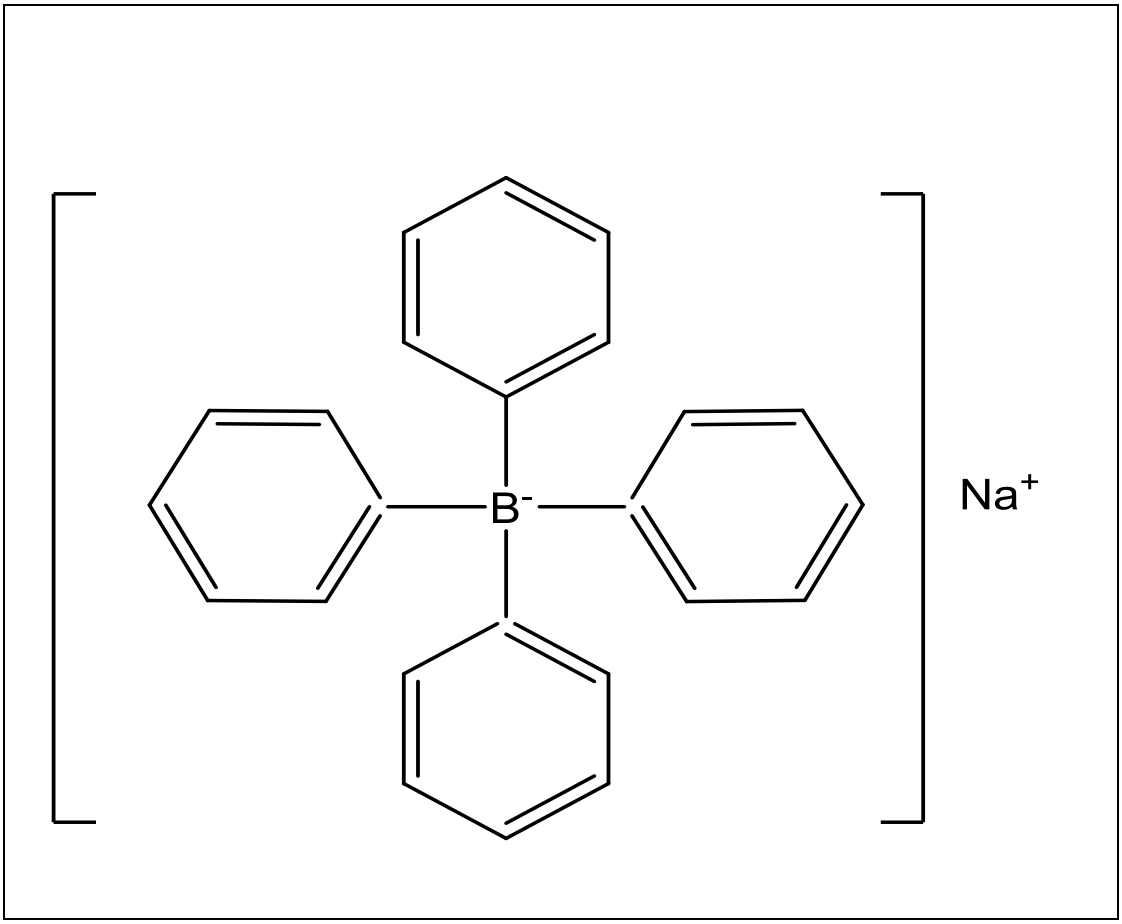

Figure 6.3: The chemical structure of sodium tetraphenyl borate sodium salt (NaTPB).

The study then shifted to determine the effect of both the phen and the NaTPB salts (anion) in the possible improvement of the analytical result. These results (see **Table 6.3**) clearly indicated high % Fe recoveries with increase in both the (phen and the

219 Adhikamsetty, R.K., Gollapalli, N.R., and Jonnalagadda, S.B., Complexation Kinetics of Fe^{2+} with 1,10-phenanthroline forming ferroin in acidic solutions, *International Journal of Chemical Kinetics*, 40, pp.515-523 (2008)

NaTPB) concentrations. A possible reason with the further increase in recovery can be attributed to an equilibrium shift to the right according to **Equation 6.1** (Le Chaterlier's principle) with the formation of large amount of $[Fe(phen)_3]^{2+}$ while the additional amount of NaTPB also resulted in an equilibrium shift to the right, producing more precipitation formation. Another possibility[220] for the higher Fe recovery may be due to high carbon content in ICP-OES resulting in a change in (higher) plasma continuum background (see **Figure 4.4, Chapter 4**) which enhances the signal to background ratio and causes spectral interferences. Another possibility is that of a carbon enhancement effect on elements such as Fe and Ti with the ionization potentials between 9 and 12 eV. Grindlay *et al*[221] studied a number of elements such as As and Se and observed that the enhancement of the carbon can cause an increase of up to 23 % on the emission signal. However the higher than expected Fe recovery can also be attributed to 'wet' samples. In the final step in this part of the study, the Fe-precipitate was dryed at 100 ºC for 5 min. This action reduced Fe recovery within the acceptable % recoveries (104(5) %) (see **Table 6.4**).

The first step in Ti analysis was to oxidize $Ti(III)Cl_3$ to $Ti(IV)Cl_4$ with H_2O_2 addition to change its oxidation state to prevent any co-reaction with Fe^{3+} present in solution (in ilmenite). The addition of phenantroline to the Ti solution resulted in no observable color change and thus leading to the assumption that no chemical reaction took place between $TiCl_4$ and phenantroline (see **Equation 6.3**). The subsequent addition of NaTPB on the other hand resulted in formation of a yellow precipitate (see **Equation 6.4**). At 1:1 Ti/NaTPB ratio, 38.3(3) % of Ti was precipitated with 76(2) % remaining in solution. Increasing the Ti/NaTPB ratio to 1:3 also increased the Ti precipitation to 94(8) %.

$$Ti^{4+} + phen \rightleftharpoons \text{No reaction} \qquad \textbf{6.3}$$

$$Ti^{4+} + 4NaTPB \rightleftharpoons \mathbf{Ti(TPB)_4} + 4Na^{+} \qquad \textbf{6.4}$$

220 Flores, E.M.M., Microwave-Assisted Sample Preparation for Trace Element Determination, pp. 254-256 (2014)

221 Grindlay, G., Gras, L., Mora., J. and de Loos-Vollebregt, M.T.C., Carbon-related matrix effects in inductively coupled plasma atomic emission spectroscopy, *Spectrochimica Acta Part B: Atomic Spectroscopy,* 63, pp.234-243 (2008)

6.3.1.1.1 Selective precipitation of ilmenite with NaTPB and phenantroline

The overall aim of the study was to separate Ti and Fe in ilmenite and in this part of the study the selective precipitation using NaTPB and phen was attempted. The idea was that the introduction of phen to afford the $[Fe(phen)_3]^{2+}$ complex would introduce enough chemical differences between the two elements (Ti and Fe) to allow for their separation with the addition of the large organic TPB^- anion. The results in **Table 6.2** and **Table 6.5** however indicated the simultaneous precipitation of both elements present in ilmenite after the iron complexation with phen and the addition of TPB^-. At Fe:phen ratio of 1:3, 35(10) % of Ti was co-precipitated with 25.1(9) % Fe while at 1:5 ratio 45(26) % Ti was co-precipitated with 12(10) % Fe. This observation can easily be explained when all the experimental results obtained in this study are considered. The results reported in **Table 6.3** and **Table 6.5** indicated that Fe is completely recovered as the phen complex (higher) in the presence of TBP^-, and also in the presence of only TBP^- as anion, while Ti precipitated completely in the presence of NaTPB, Chemically it points to the simultaneous action of all three reactions (**Equation 6.1**, **6.2** and **6.4**) and hence no separation (see **Equation 6.5**).

$$Fe^{2+} + Ti^{3/4+} + 3phen + 8NaTPB \rightleftharpoons [Fe(phen)_3](TPB)_2 + Ti(TPB) + Ti(TPB)_{3/4} + 8Na^+ \quad \textbf{6.5}$$

The results obtained in **Table 6.6** at Fe: phen ratio of 1:3 and 1:5 also indicated the inaccurate total mass balance for both Ti and Fe analysis (113(10) to 165(9) total mass %) and these can be attributed to the possible effects mentioned in **Section 6.3.1.1** (carbon effect) with large percentage recovery of Fe and Ti observed in the filtrate.

6.3.1.2 Selective precipitation of Ti and Fe in ilmenite with NaPT

The failure to selectively separate Ti and Fe with the phen complex formation and precipitation approach prompted the use of the sodium salt of 2-mercaptopyridine N-oxide (NaPT, see **Figure 6.4**) as complexation or chelating agent. Surprisingly, the addition of NaPT to the dissolved ilmenite solution immediately led to a color change, from colorless to dark blue, followed by the formation of dark purple precipitate which settled very easily on the bottom of the glass container. Dissolution of the dark blue precipitate and subsequent analyses of both the precipitate and the initial filtrate (see

Table 6.7) indicated the successful separation of the Fe and the Ti with Fe an average recovery of 104(1) % in the blue precipitate, while Ti remained unreactive in the filtrate with 99.60(1) % Ti recovered. The results are graphically illustrated in **Figure 6.5** and **Figure 6.6**.

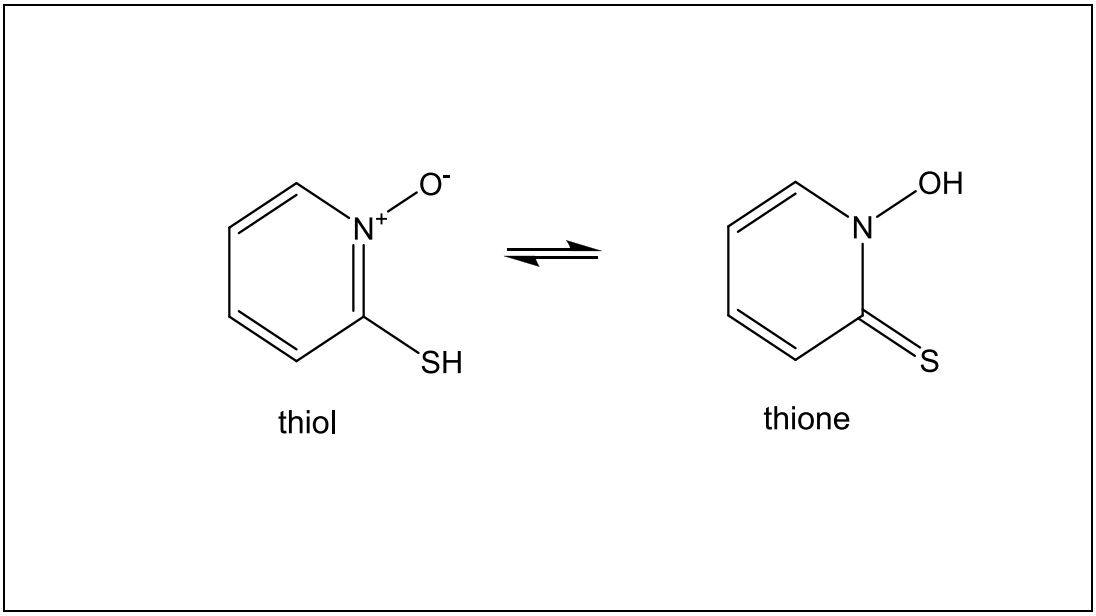

Figure 6.4: Tautomeric forms 2-mercaptopyridine N-oxide.

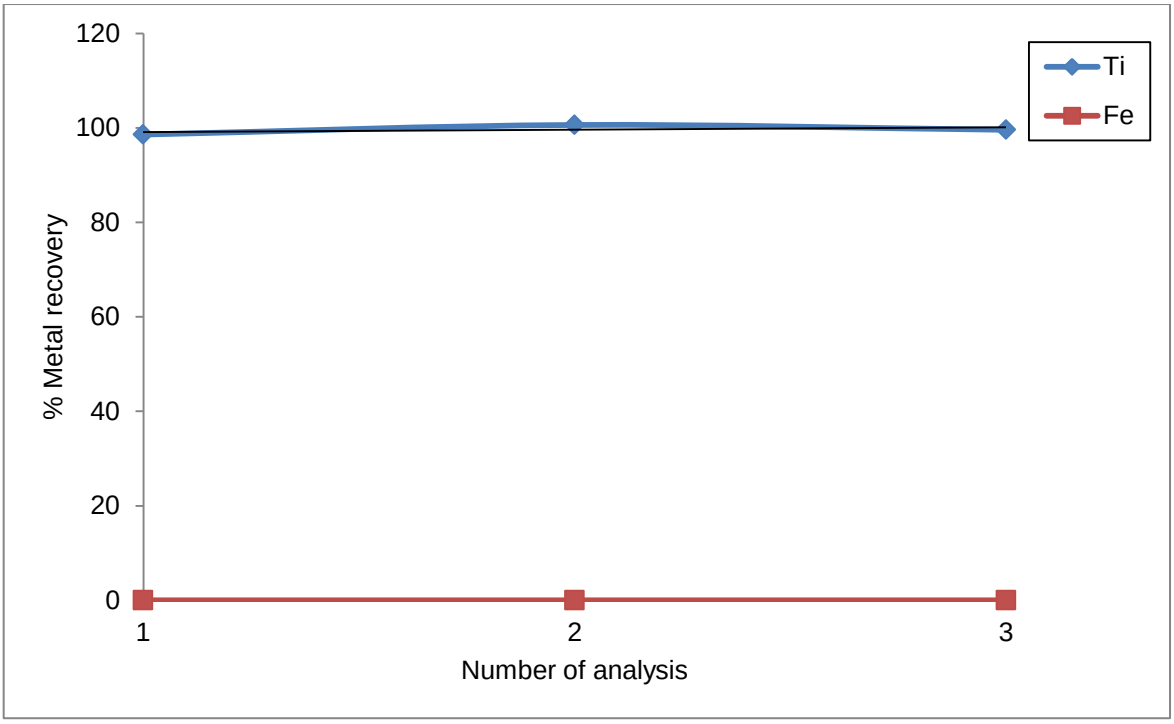

Figure 6.5: Recovery of Ti and Fe in the filtrate using NaPT.

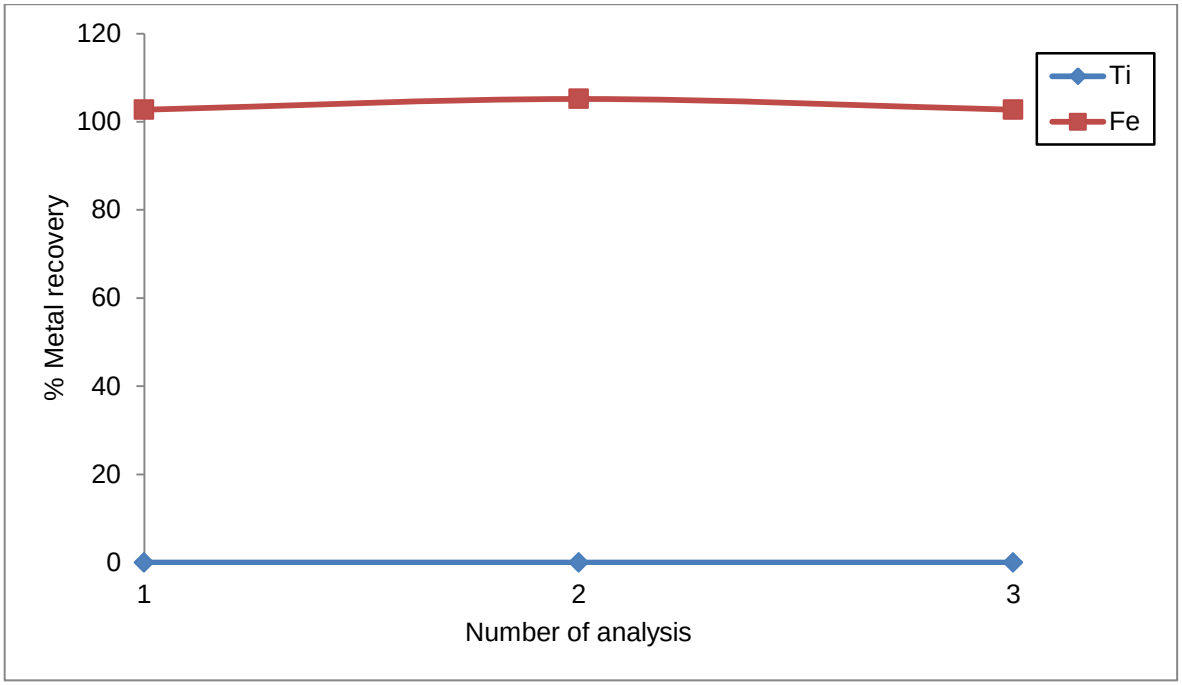

Figure 6.6: Recovery of Ti and Fe in the precipitate using NaPT.

According to literature, the NaPT act as a thione (see **Figure 6.4**) and forms the stable water insoluble $[Fe(C_5H_4NOS)_3]$ complex with Fe^{3+} binding through the N-oxide oxygen atom and thiolate sulpher atom at a pH of 9 (see **Figure 6.7**, **Equation 6.6** to **6.8**). It is also known that the NaPT reacts with ferrous or ferric iron in a wide pH range of (2 to 6) forming a stable complex.[222,223,224]

$$Fe^{3+} + 3NaPT \rightleftharpoons [Fe(PT)_3] + 3Na^{+} \quad \textbf{6.6}$$

$$Fe^{2+} + 2NaPT \rightleftharpoons [Fe(PT)_2] + 2Na^{+} \quad \textbf{6.7}$$

$$Ti^{3+} + NaPT \rightleftharpoons \text{No reaction} \quad \textbf{6.8}$$

222 Parajon-Costa, B.S., Gonzalez-Baro, A.C. and Baran, E.J., Electrochemical and spectroscopic behaviour Bis(2-mercaptopyridine-N-oxide) oxovanadium (IV), *Zeitschrift fur anorganische und allgemeine Chemie*, 628, pp.1419-1424 (2002).

223 Mohamed, A., Makhyoun, R.A. and Palmer, A.A., The Ni(II) of 2-hydroxy-pyridine-N-oxide 2-isothionate: Synthesis, Charecterization, Biological Studied, and X-ray Crystal structure using (1) Cu Kα Data and (2) Synchrotron data, *Journal of Material Science & Nanotechnology,* **2**(1), pp.1-11 (2014)

224 Dalziel, J.A. and Thompson, M., The gravimetric determination of Iron by the homogeneous precipitation of the tris(2-thiopyridine-N-oxide) Iron(II) Complex, *Analyst*, 89, pp.707-712 (1964)

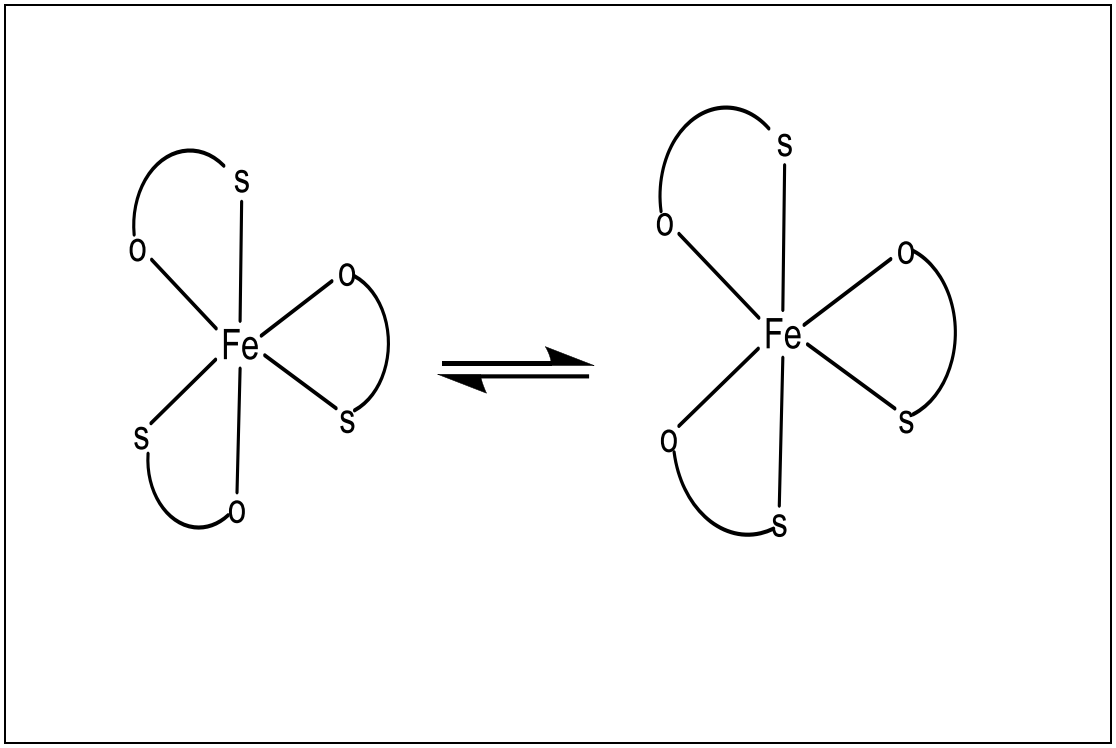

Figure 6.7: The five membered Fe(III) thione complex after the reaction with HP^{-}.[224]

Very interesting, the analytical results obtained from the results indicate that Ti (3+ or 4+) does not react with NaPT. A possible reason that Fe react successfully with NaPT is the presence of sulphur atom in the chelate molecule which renders the ligand a moderate base (hard base/base theory) and it is well known that Fe react very easily with moderate bases such as S^{2-}, NH_3 and CN^{-} but that the 3+ and 4+ oxidation state of Ti require hard bases to react and therefore the absence of any notable reaction between Ti and the chelating agent. In conclusion it can be said that the two main elements present in ilmenite was quantitatively separated with NaPT.

6.3.1.2.1 Infrared analysis

The important IR stretching frequencies of the product obtained after the Fe and NaTP reaction are listed in **Table 6.8**. The stretching frequency at 1143.8 cm^{-1} which was observed in the free ligand spectrum (see **Figure 6.7**) is assigned to C=S vibrations. The same peak was also observed in the Fe-PT precipitate but in the product the band was shifted to a lower frequency of 1142.1 cm^{-1}. The C-S peak of the thiol group (see **Figure 6.4**) at 702 cm^{-1} in the free ligand is also shifted to 710 cm^{-1} in the precipitate product. The 832.0 and 1204.3 cm^{-1} band are assigned to the δ(N-O) and ν (C-N) group in the free ligand spectrum shifted from 829.4 and 1183.7

cm-1 in the precipitate The shift in C-S and N-O stretching frequencies and several other frequencies which include ν(C=C) at 1595.181 and ν(C=N) at 1539 cm^{-1} which also shifted in the precipitate indicates the possible formation of a new compound between Fe and NaPT ligand.

According to literature, the ν(N-O) occur between 880 and 830cm^{-1}[225] while the C-S absorption in pyridine derivatives occur between 1160 and 1130 cm^{-1}[226]. Parajon-Costa *et al*[222], synthesised $VO(NaPT)_2$ and observed the shift in the ν(N-O) and δ(N-O) upon metal complex from 1205 to 1188 cm^{-1} and 833 to 829 cm^{-1} respectively.

6.3.2 Solvent extraction of Ti and Fe using different complexing agents and solvents

The next step in this investigation concentrated on the possible solvent extraction separation of the two main elements in ilmenite. The study involved different coordinating agents, which include TOPO, acacH (see **Figure 6.8**) as well as NaPT (see **Figure 6.4**) which was used for the elective precipitation of the Fe in the mineral sample. The different immiscible solvents used in the study include kerosene, 1-octanol and MIBK.

225 Karayannis, N.M., Metal complexes of aromatic amine N-oxides, *Coordination Chemistry Reviews*, **11**(2), pp.93-139 (1973)

226 Chen, X., Hu, Y., Wu, D., Weng, L. and Kang, B., Synthesis and electrochemistry of some transition metal complexes with 2-mercaptopyridine n-oxide and crystal structure of Bis(2-mercaptopyridine n-oxide) nickel(II), *Polyhedron*, **10**(23/24), pp.2651-2657 (1991)

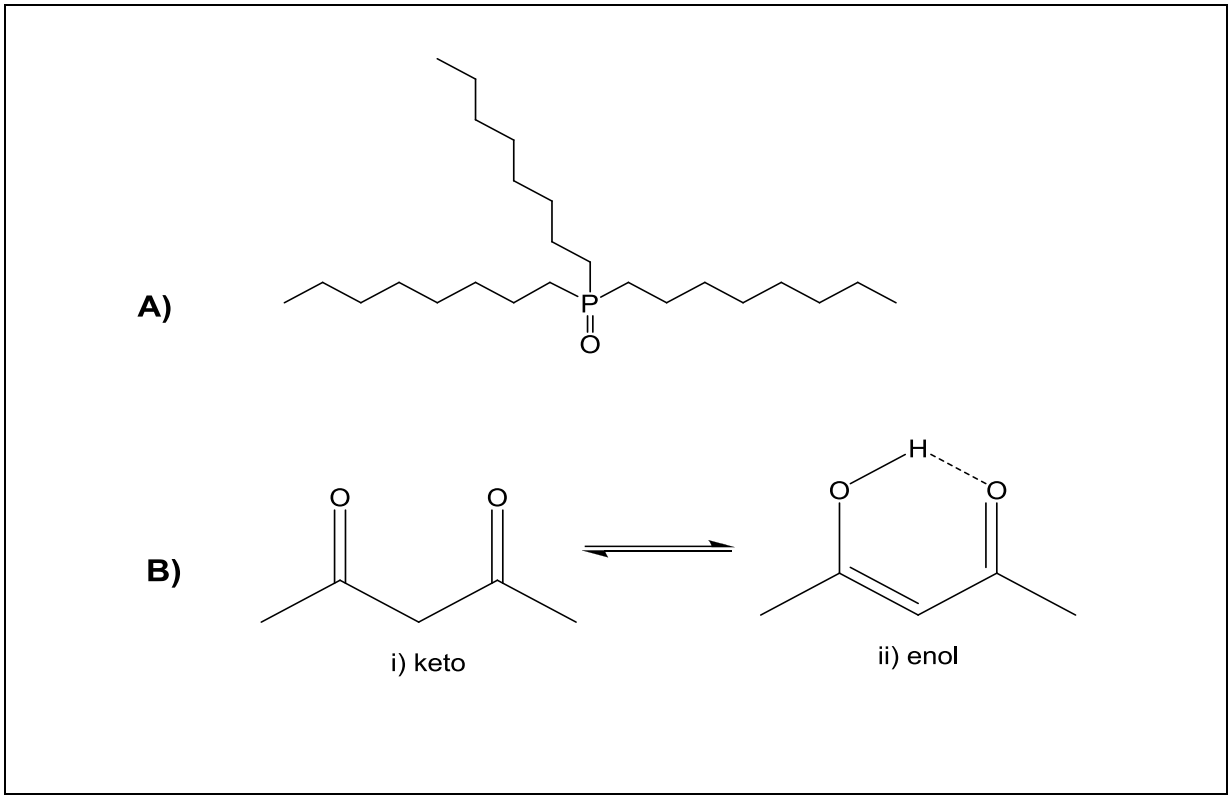

Figure 6.8: The chemical structures of coordinating ligands; A) trioctylphenylphosphate (TOPO) and B) acetylacetone(acacH)**.**

6.3.2.1 Solvent extraction of Ti and Fe with TOPO-kerosene in different acids

The extraction of Ti and Fe using TOPO (see **Figure 6.8**) dissolved in kerosene was investigated in the presence of three different mineral acids. The analytical results reported in **Table 6.9** to **Table 6.11** clearly indicate that no or very little extraction of both the elements (0.8(1) and 2(2) % Fe and Ti respectively in the organic layer) took place at a lower acidity levels ([HCl] = 1.7 M) for all three acids, but an increase in the acid concentration clearly increased the selectivity of the extraction with a marked increase in [Fe^{2+}] recovery at 6.7 M with 99.0(8) % Fe present in the kerosene layer and the rest remaining in the aqueous layer (22(6) % Ti extracted at the same acid concentration) (see **Figure 6.9** and **Figure 6.10**). Literature studies[227] have indicated that the extraction of both Ti and Fe in HCl solutions using TOPO as the complexing agent in kerosene involves the following reactions (**Equations 6.9** and **6.10)**:

227 Mao., X.H. and Liu, D.J., Solvent extraction separation of titanium(IV) and iron(III) from acidic chloride solutions of trioctylphosphine oxide, *Asian Journal of Chemistry*, **25**(9), pp.4753-4756 (2013)

$$H^{+} + FeCl^{-}_{4(aq)} + TOPO_{(org)} \rightleftharpoons HFeCl_4 \cdot TOPO_{(org)} \quad \textbf{6.9}$$

$$Ti^{4+}_{(aq)} + 4Cl^{-}_{(aq)} + 2TOPO_{(org)} \rightleftharpoons TiCl_4 \cdot 2TOPO_{(org)} \quad \textbf{6.10}$$

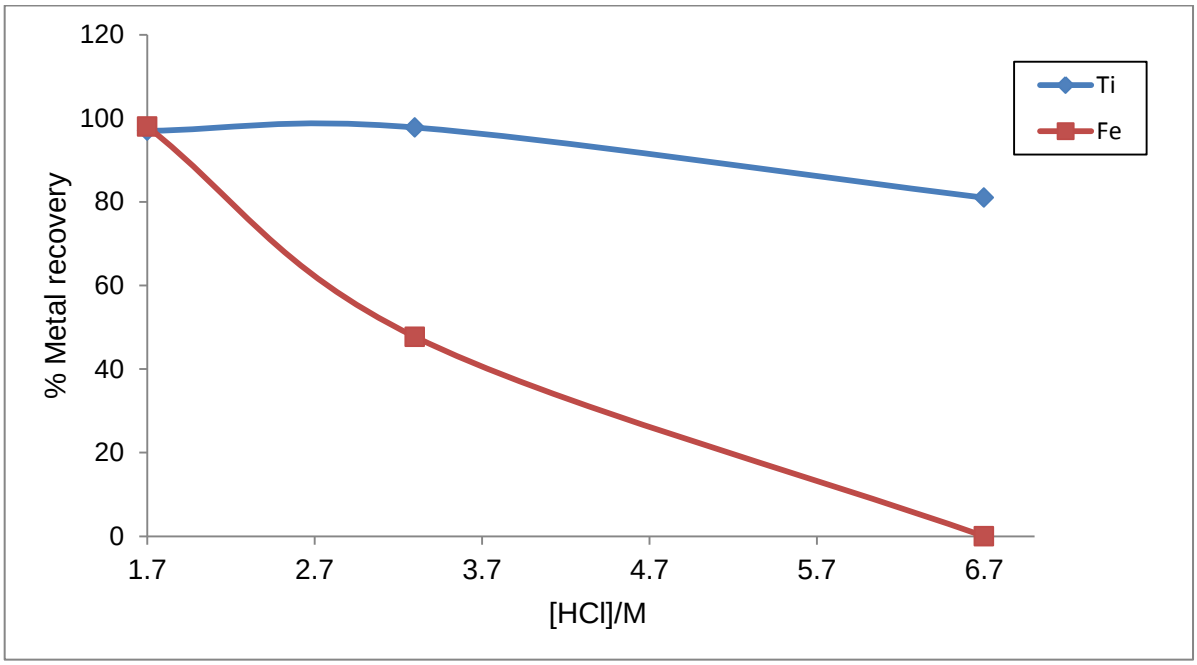

Figure 6.9: Ti and Fe recoveries in the aqueous solution from HCl medium using TOPO/kerosene.

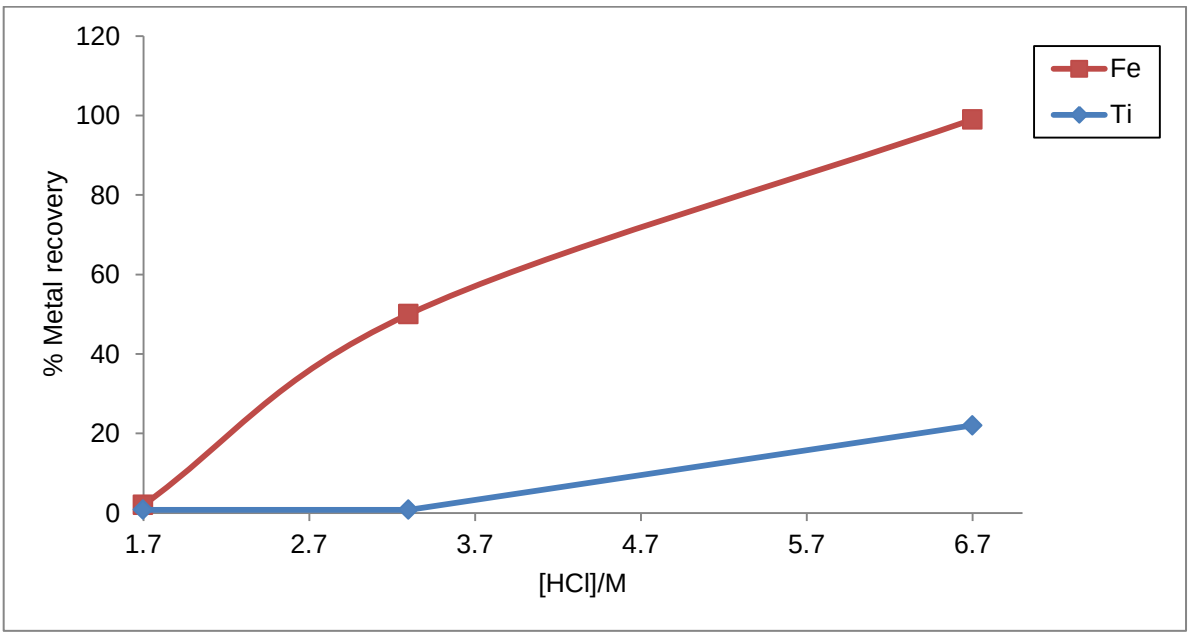

Figure 6.10: Ti and Fe recoveries in the organic extractant from HCl medium using TOPO/kerosene.

Very interesting however is that the extraction of the two elements reverse in order in the presence of H_2SO_4 with Ti being extracted into the organic layer (48(4) % of Ti with only 0.32 (6) % Fe) (see **Figure 6.11** and **Figure 6.12**). Finally no selectivity was observed in the presence of H_3PO_4 even at high concentrations (see **Table 6.11).** These results are in agreement with those reported by Shibata *et al*[228,229] who reported that both Ti and Fe can be extracted into the organic phase with an increase in HCl and H_2SO_4 concentrations.

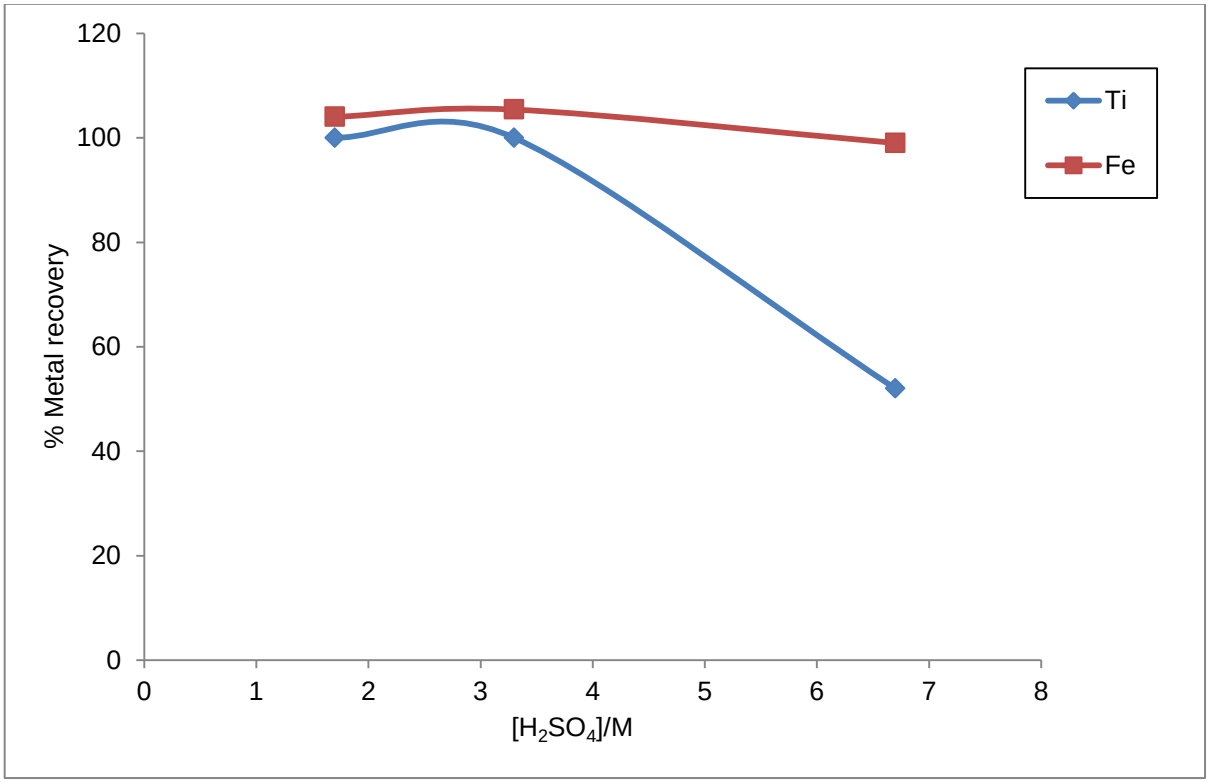

Figure 6.11: Ti and Fe recoveries in the aqueous solution in a H_2SO_4 medium using TOPO/kerosene.

228 Shibata, J. and Kurihara, Y., A study on separation and purification process of high purity titanium dioxide, *Kagaku Kogaku Ronbunshu,* 18(4), pp.521-527 (1992)

229 Shibata, J. Ohtomo, M. and Tanaka, K., Simultaneous countercurrent multistage extraction process for recovery of titanium, *Kagaku Kogaku Ronbunshu,* 19, pp.214-219 (1993)

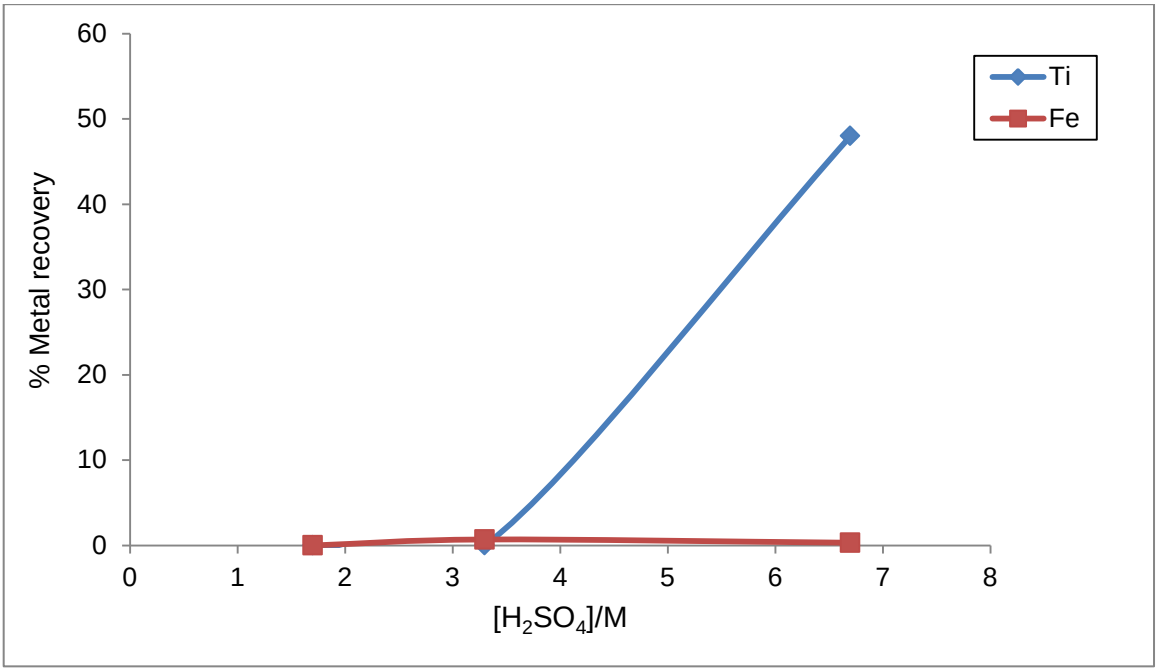

Figure 6.12: Ti and Fe recoveries in the organic extractant in a H_2SO_4 medium using TOPO/kerosene.

A possible explanation for the improved Ti extraction in a H_2SO_4 environment is the formation of a more stable or neutral $Ti(SO_4)_2$·TOPO compound (**Equation 6.11**), compared to $Fe(SO_4)/Fe_2(SO_4)_3$·TOPO compound (**Equation 6.12** and **13**). The success of TOPO as extraction/chelating reagent can be attributed (as was evident with the Fe/HCl extraction) to its high lipolicity and polarity. The dipolar phosphorous-oxygen bond in TOPO (see **Figure 6.8**) bind to the metal ion center while the long octyl group of the TOPO group impact organic characteristic to the metal compound to allow for its enhanced solubility in an organic such as kerosene. Successful organic solvent solubility therefore depends on the TOPO ligand to render organic properties to the metal center which depends on the charge and type of metal compound (1:1, 1:2 or 2:3) produced with SO_4^{3-} environment and the absence or limited protection renders the molecule water soluble.

$$Ti(SO_4)_{2(aq)} + TOPO_{(org)} \rightleftharpoons Ti(SO_4)_2 \cdot TOPO_{(org)} \qquad \textbf{6.11}$$

$$Fe(SO_4)_{(aq)} + TOPO_{(org)} \rightleftharpoons Fe(SO_4) \cdot TOPO_{(org)} \qquad \textbf{6.12}$$

$$Fe_2(SO_4)_{3(aq)} + TOPO_{(org)} \rightleftharpoons Fe_2(SO_4)_3 \cdot TOPO_{(org)} \qquad \textbf{6.13}$$

Both SO_4^{2-} and PO_4^{3-} are also re-known to be weak coordinating anions and both are regarded as hard bases. Recent studies also indicate that these anions tend to form polymeric anions with metal ions in their high oxidation state which are not conducive to the solvent extraction purposes (high degree of ionic or dipolar properties).

6.3.2.2 Solvent extraction of Ti and Fe with acacH

The relatively poor selectivity/separation that was obtained with TOPO prompted a search for an alternative, more selective ligand/organic solvent combinations. It was therefore decided to investigate the possible separation of Ti and Fe using acacH (see **Figure 6.8**) as a complexing agent. The study was conducted in the presence of different acids (0.07 to 6.0 M concentrations of HCl, H_2SO_4 and H_3PO_4) using MIBK and 1-octanol as the immiscible solvents. The analytical results reported in **Table 6.12** to **Table 6.14** indicated little of no metal extraction into the organic layer at low HCl concentration (0.07 to 1.4 M) with both MIBK and 1-octanol. Percentage Fe and Ti increased at higher acidic concentrations (3.0 and 6.0 M HCl with MIBK as extractant). However, Fe extraction increased rapidly in MIBK as solvent (see **Table 6.12**) and at 3.0 M HCl, 100(2) % Fe was extracted into the organic phase, while 92(4) % Ti remained in the aqueous phase. The same trend was also observed at 6.0 M with 99(3) % Fe extracted into the organic phase while 98(6) % of Ti was recovered in the aqueous phase (see **Figure 6.13** and **Figure 6.14**).

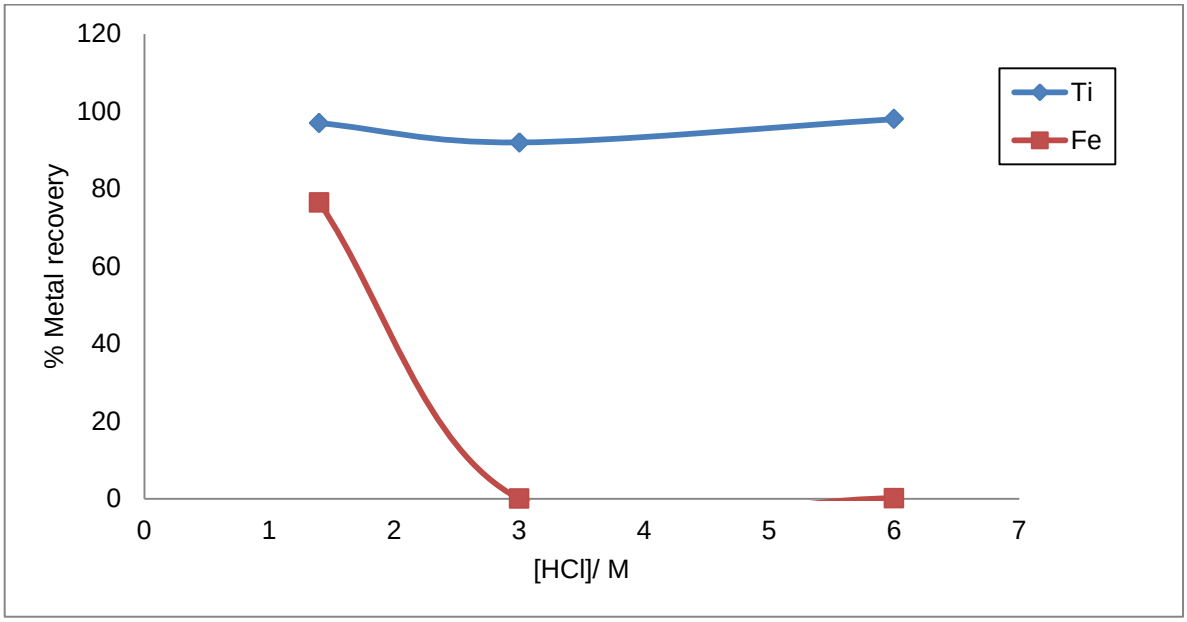

Figure 6.13: Ti and Fe recoveries in the HCl aqueous solution using acacH/MIBK.

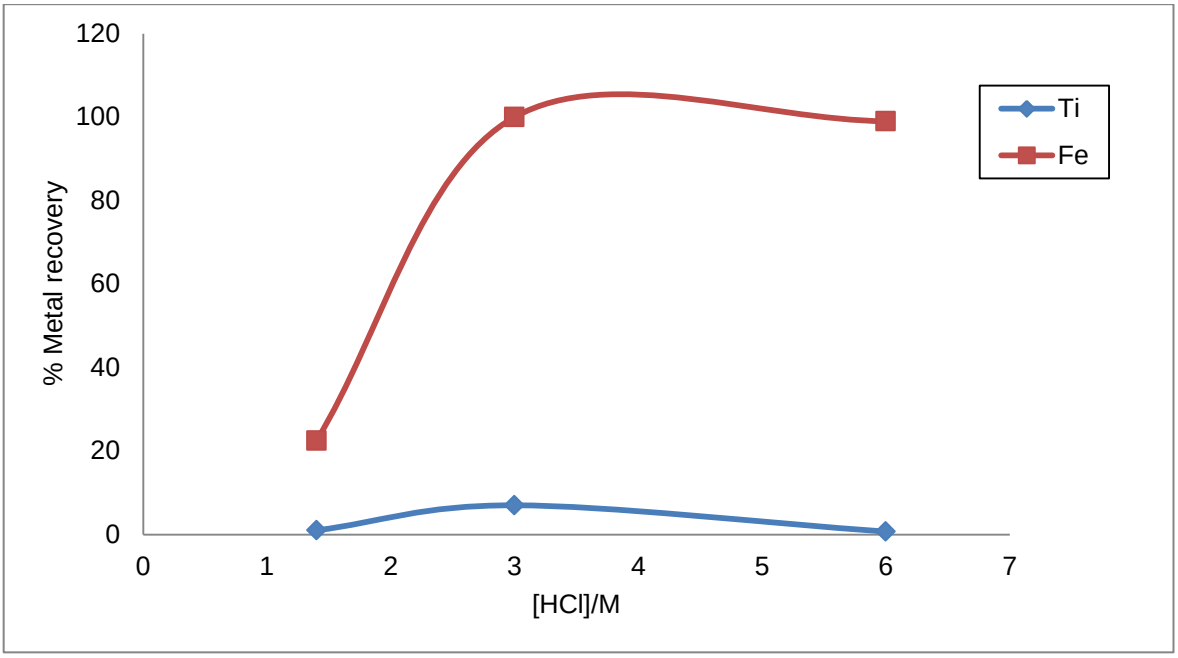

Figure 6.14: Ti and Fe recoveries in the organic phase after extraction with acacH/MIBK in HCl.

The extraction into 1-octanol was also first obtained at HCl concentration of 3.0 M, but it was the Ti compound which was preferentially extracted into the organic phase. The extraction was also characterized by poor selectivity and low elemental recoveries of the extracted species were obtained with 35(3) % Ti and 23(1) % of Fe co-extracted in to the organic phase. As HCl concentration was increased to 6.0 M, 19(6) % Ti and 0.04 % Fe recoveries were obtained in the organic phase (see **Figure 6.15** and **Figure 6.16**).

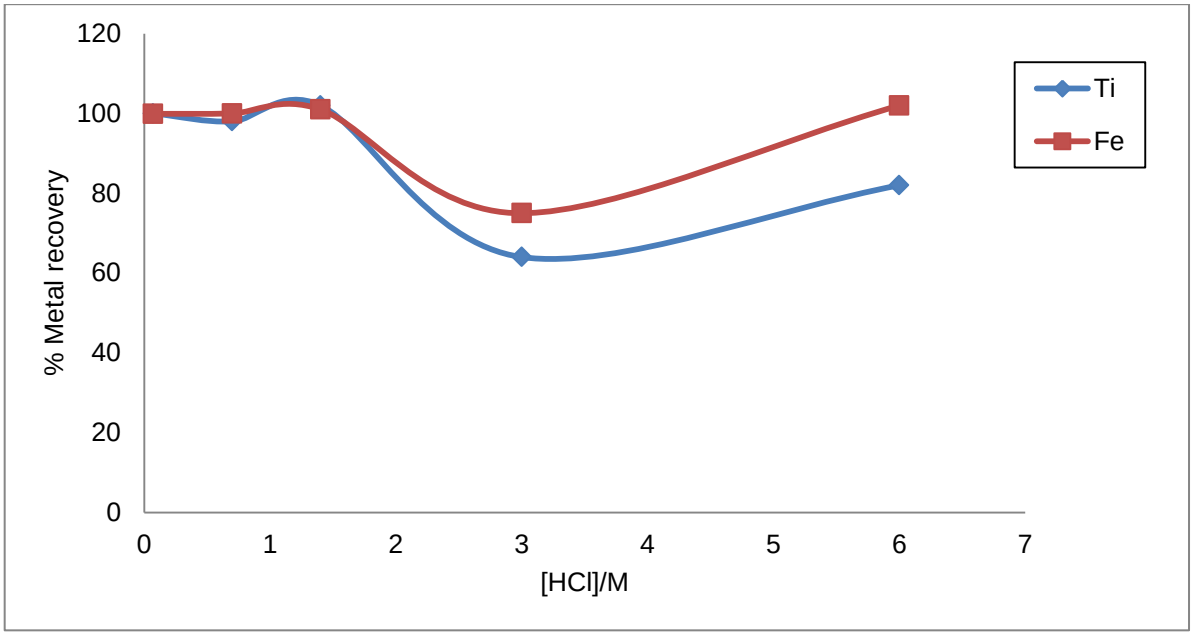

Figure 6.15: Ti and Fe recoveries in the aqueous solution in a HCl medium using acacH/1-octanol.

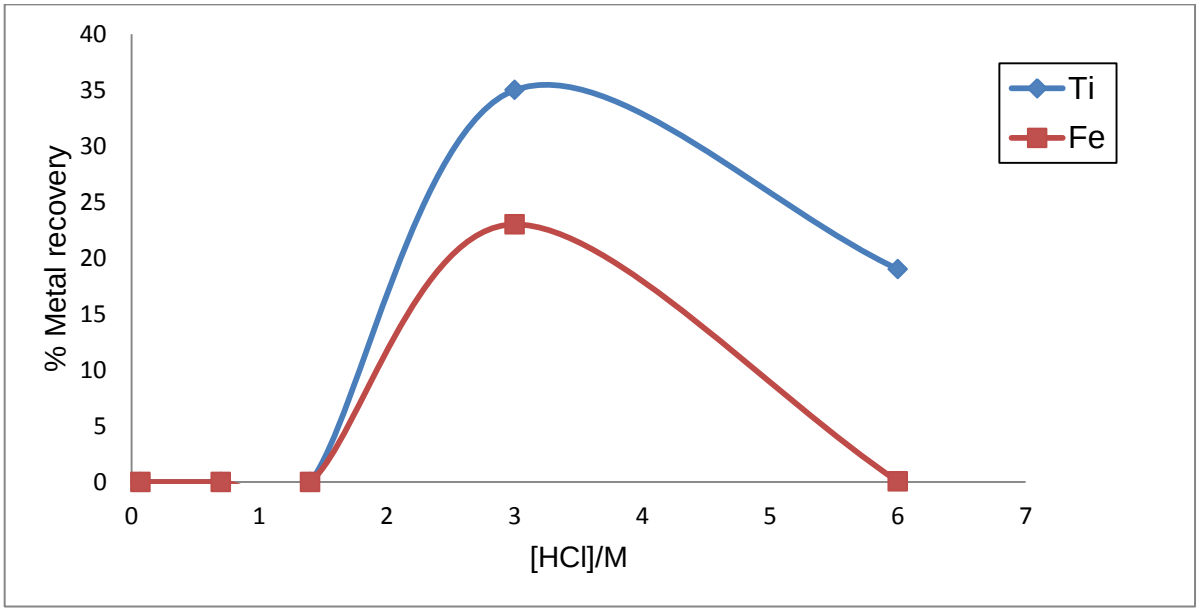

Figure 6.16: Ti and Fe recoveries in the organic solvent in a HCl medium using acacH/1-octanol.

The increase in Fe extraction into the organic layer at higher acidity levels are surprising and counter intuitive. An increase in acid concentration inevitably lead to a decrease in the $acac^-$ anion concentration (**Equation 6.14** and **6.15**) which can/should lead to lower metal recoveries.

$$Fe^{3+} + 3acac^{-} \rightleftharpoons Fe(acac)_3 \qquad \textbf{6.14}$$

$$-H^{+} \downarrow\uparrow +H^{+} \qquad \downarrow\uparrow$$

$$Fe^{3+} + 3acacH \rightleftharpoons Fe(acac)_3 + 3H^{+} \qquad \textbf{6.15}$$

A possible explanation for the increase in Fe is the formation of the Fe-acac^{-} -chloride compound at high HCl concentration which have substantial organic character.

The extraction of Ti or Fe was in the H_2SO_4 matrix was also unsuccessful using MIBK as the organic solvent. In 1-octanol and at high acid concentration, Ti was preferentially extracted into the organic phase compared to Fe. The extraction behaviour showed poor selectivity with 13(4) % Ti and 0.0 % Fe extracted in the organic phase at 3.0 M H_2SO_4. At 6.0 M, 81(1) % Ti and 9(1) % Fe were extracted into the organic phase (see **Table 6.13**). In H_3PO_4 medium no (or little) extraction was observed in the organic phase for both MIBK and 1-octanol solvents (see **Table 6.14**).

6.3.2.3 Solvent extraction of Ti and Fe in different acids (without acacH) using MIBK and 1-octanol

The unexpected increase in Fe extraction at high acidic concentrations was further investigated and the participation of acetylacetone (acacH) as complexing agent was questioned. AcacH normally functions better as a chelate under slightly basic conditions (see **Equation 6.14** and **6.15**) when the ligand is first deprotonated to increase its reactivity towards the metal center.

This compelled the investigation towards the extraction of these elements under the same experimental conditions, but this time without the addition of any complexing agents. The results obtained in this part of the study (see **Table 6.15**) showed the positive and selective extraction of Fe, thereby providing the evidence that the selective extraction of Fe in the previous study cannot be attributed to the presence or the participation of acacH in the extraction process (see **Figure 6.17** and **Figure 6.18**). According to literature[18] Fe is probably extracted from the HCl solution as a chloro-iron compound while Ti forms an oxychloro compound (see **Equations 6.16**

and **6.17**) which may have low solubility in organic phase. As the extraction process is very prominent at high acid concentration, it is possible that the increase in the Cl^- content results in the formation of $HFeCl_4$ which is easily extracted into MIBK (or 1-octanol) as in **Equation 6.18.** Mao X[227] studied the extraction of Fe^{3+} in HCl and observed that the increase in acid concentration also increases the extraction of Fe into the organic phase as $HFeCl_4 \cdot 2Decanol$.

$$Fe^{3+}_{(aq)} + 4Cl^-_{(aq)} + H^+_{(aq)} \rightleftharpoons HFeCl_{4(aq)} \qquad \textbf{6.16}$$

$$TiO^{2+}_{(aq)} + 2Cl^-_{(aq)} \rightleftharpoons TiOCl_{2(aq)} \qquad \textbf{6.17}$$

$$TiOCl_{2(aq)} + HFeCl_{4(aq)} + MIBK_{(org)} \rightleftharpoons HFeCl_4 \cdot MIBK_{(org)} + TiOCl_{2(aq)} \qquad \textbf{6.18}$$

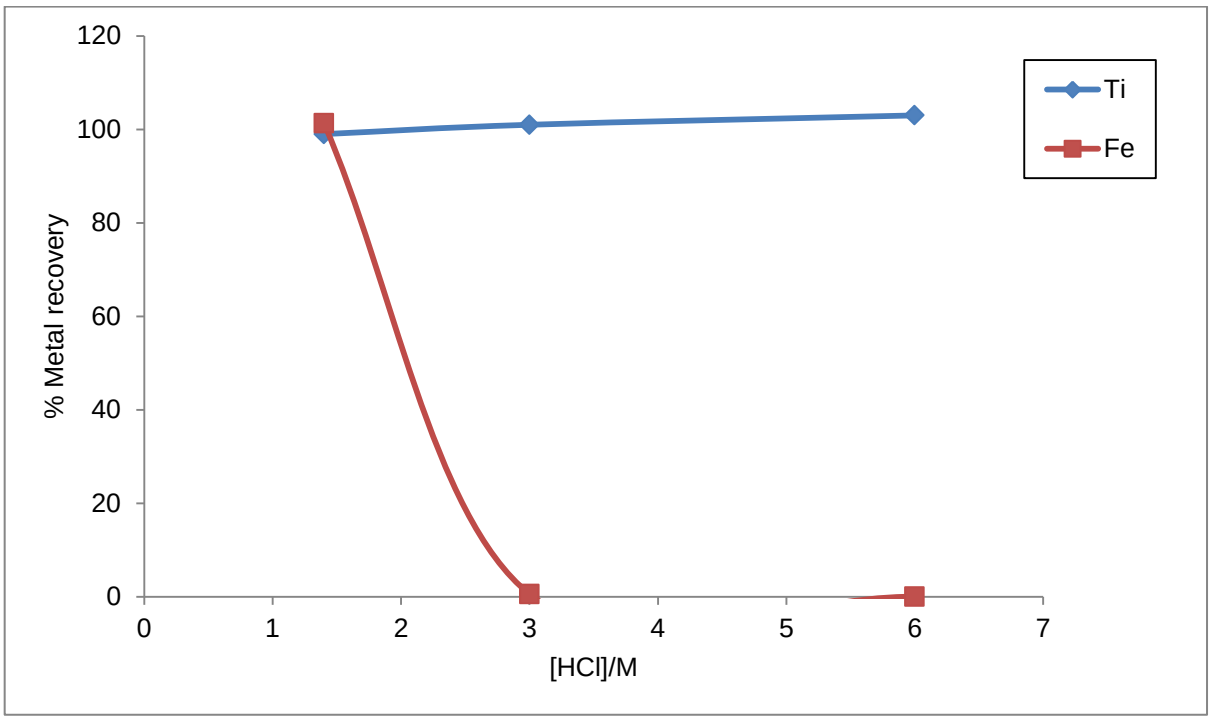

Figure 6.17: Ti and Fe recoveries in aqueous solution (without acacH) in a HCl medium using MIBK.

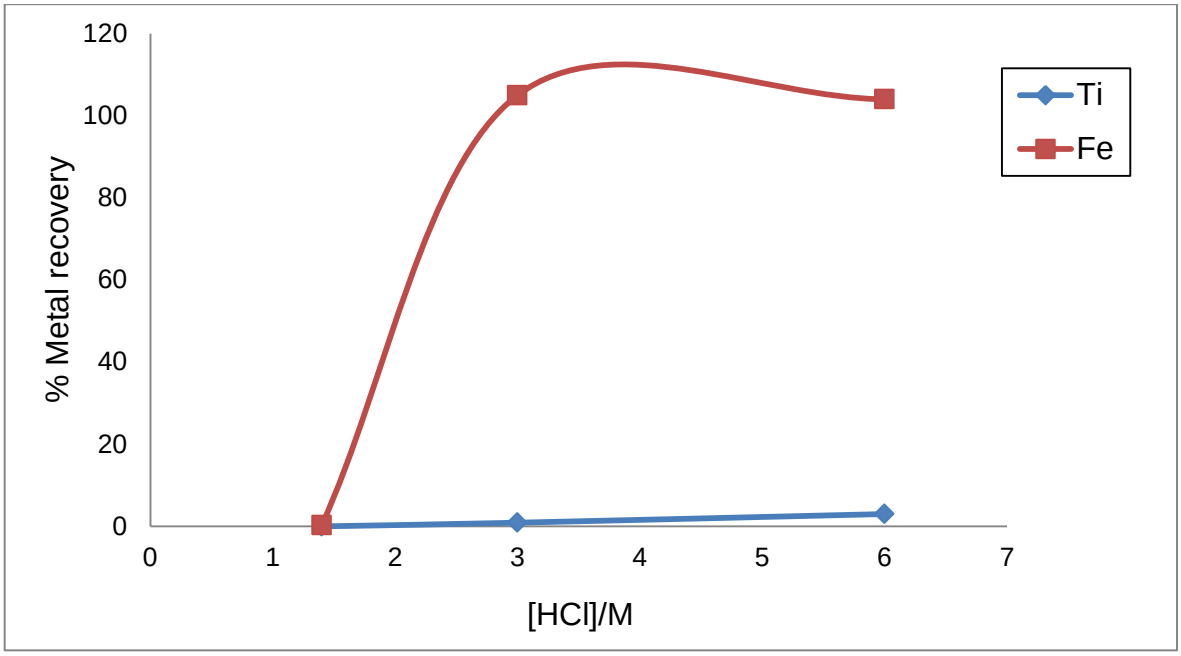

Figure 6.18: Ti and Fe recoveries in the organic extractant (without acacH) in a HCl medium using MIBK.

The extraction results obtained in H_2SO_4 and H_3PO_4 matrices also indicated poor selectivity with poor Ti and Fe extraction into the organic phases, similar to the results reported in **Section 6.2.4.2.2** when the extraction was investigated using the TOPO-kerosene system. In MIBK, both Ti and Fe remained in the aqueous phase with 97(2) % Fe and 96.8(1) % Ti present at 3.0 M H_2SO_4 while 92(3) % of Ti and 98(1) % Fe remained in the aqueous layer at 6.0 M H_2SO_4. In 1-octanol, no extraction was observed at 1.4 M but at 3.0 M H_2SO_4, 34(2) % of Ti and 7.8(8) % of Fe into the organic phase while at 6.0 M 21(3) % Ti was co-extracted with 32(7) % Fe in the organic phase. In H_3PO_4 medium little or no extraction of Ti and Fe was observed.

6.3.2.4 Solvent extraction of Ti and Fe with NaPT in different acids

Initial results obtained for the extraction separation of Ti and Fe using NaPT (see **Figure 6.4**) as a complexing agent in both the selective precipitation study and the solvent extraction (MIBK and 1-octanol) was afforded at low acid concentration. The extraction study was expanded to include [HCl] ranging between 0.05 and 3.0 M The results obtained in this study (**Table 6.18**, see also **Figure 6.19** and **Figure 6.20**) showed excellent recoveries of 99.4(6) % and 100(4) % Fe in MIBK for HCl concentration between 0.05 and 3.0 M and no Ti was extracted into the organic

phase under these conditions. A two-stage back-extraction using 6.0 M H_2SO_4 resulted in the re-dissolution of the precipitate and the total recoveries of 91.34 % Fe in 1-octanol and 99.41 % Fe in MIBK.

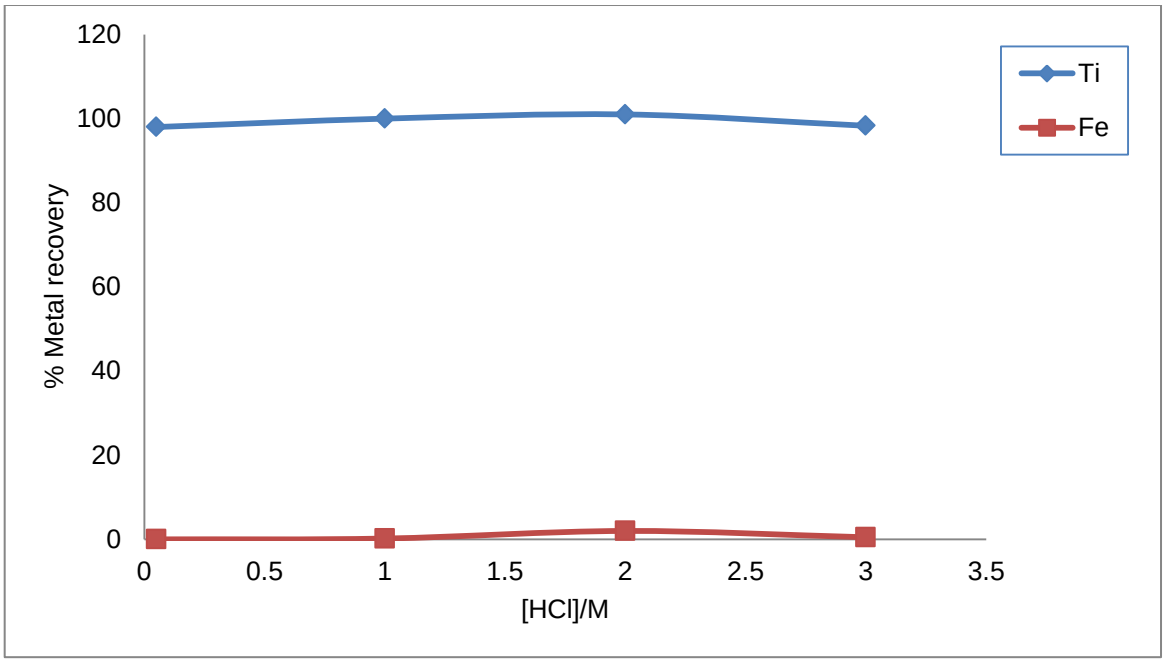

Figure 6.19: Ti and Fe recoveries in the aqueous solution in a HCl medium using NaTP/MIBK.

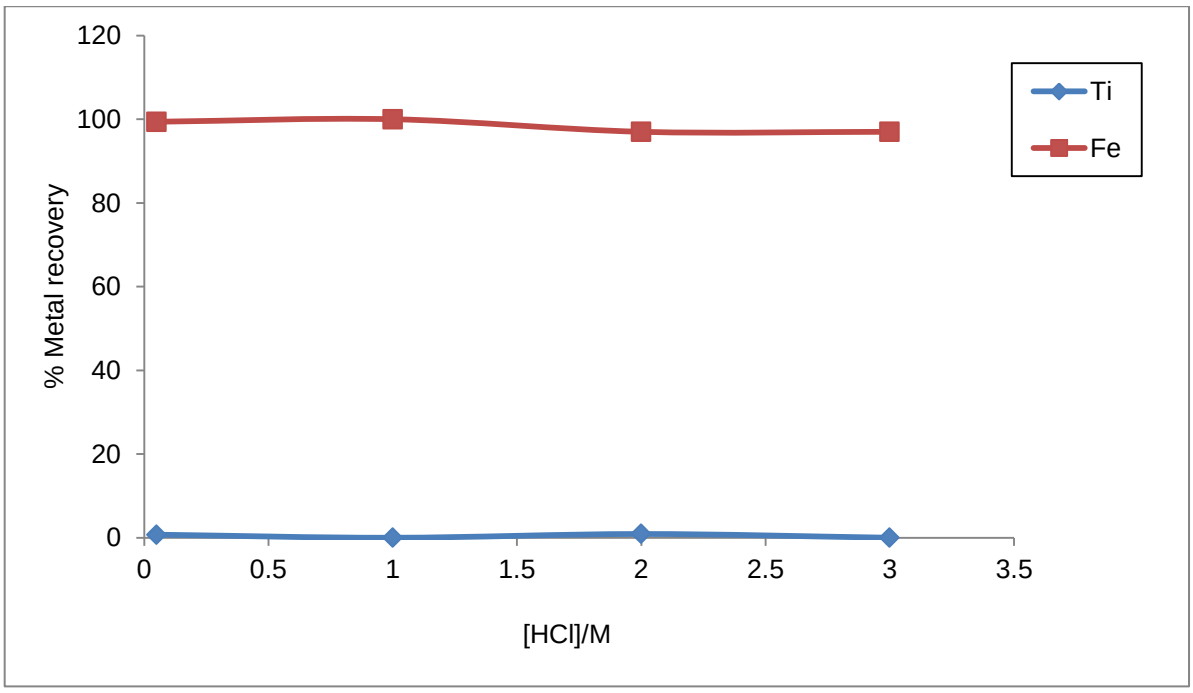

Figure 6.20: Ti and Fe recoveries in the organic extractant in a HCl medium using NaPT/MIBK.

These results point to the formation of a very stable Fe-PT complex, even at high [H^+]. The amount of HP^- needed for the complex formation decreases with an increase in [H^+] as indicated in **Equation 6.19**.

$$PT^- + H^+ \rightleftharpoons HPT \qquad \textbf{6.19}$$

pKa = 4.7 at 20 ºC in water[230]

For production formation **Equation 6.20** is possible;

$$Fe^{3+} + 3PT^- \rightleftharpoons Fe(PT)_3 \qquad \textbf{6.20}$$

The results obtained in this study indicate that enough PT^- is available for the complex formation at a [3 M H^+] to allow for the complete removal of Fe from the solution.

Extraction using 1-octanol also gave excellent Fe recoveries of 98(3) % at 1.0 M HCl but with co-extracted of 6(3) % Ti into the organic layer (**Table 6.18**, see **Figure 6.21** and **Figure 6.22**). Fe recoveries in the organic phase decreased with an increase in HCl concentration, pointing to the protonation of some of the PT^- bonded to the Fe metal center and hence a decrease in the amount of Fe in the organic layer. These results suggest that MIBK is a more suitable extractant compared to 1-octanol due to the high selectivity between Fe and Ti and good recoveries.

$$Fe(PT)_3 + H^+ \rightleftharpoons Fe(PT)_3 + Fe^{3+} + PT^- \qquad \textbf{6.21}$$

230 Ermolayeva, E. and Sanders, D., Mechanism of pyridine-induced membrane depolarization in neurospora crassa, *Applied and Environmental Microbiology*, pp.3385-3390 (1995)

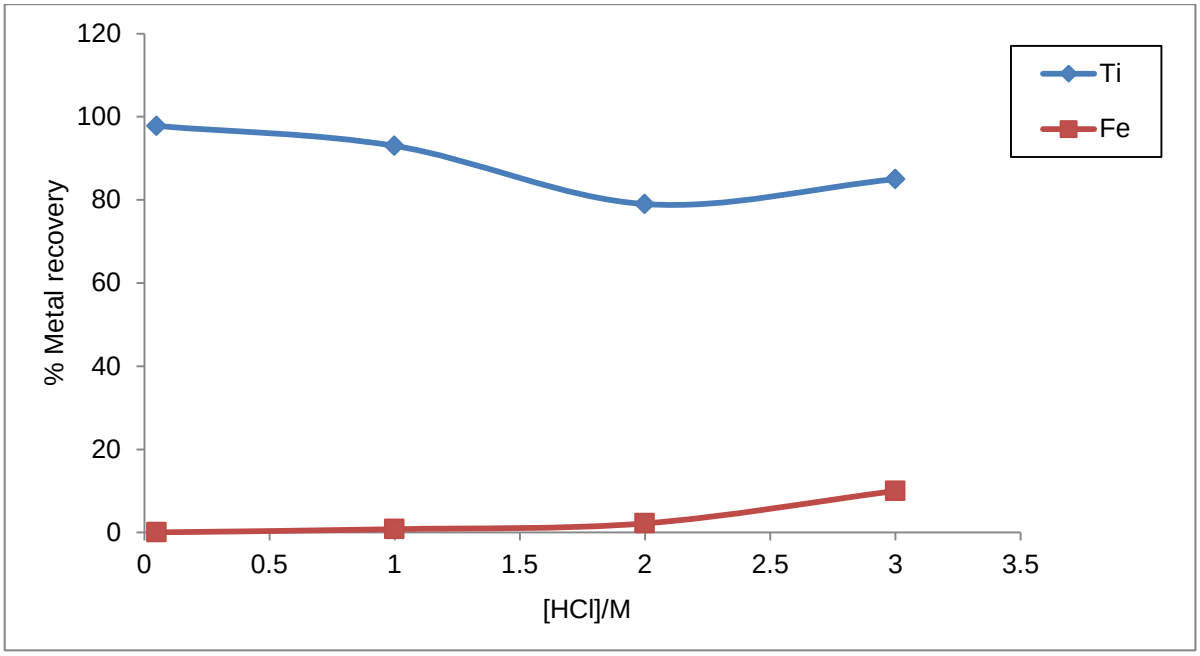

Figure 6.21: Ti and Fe recoveries in the aqueous solution in a HCl medium using NaTP/1-octanol.

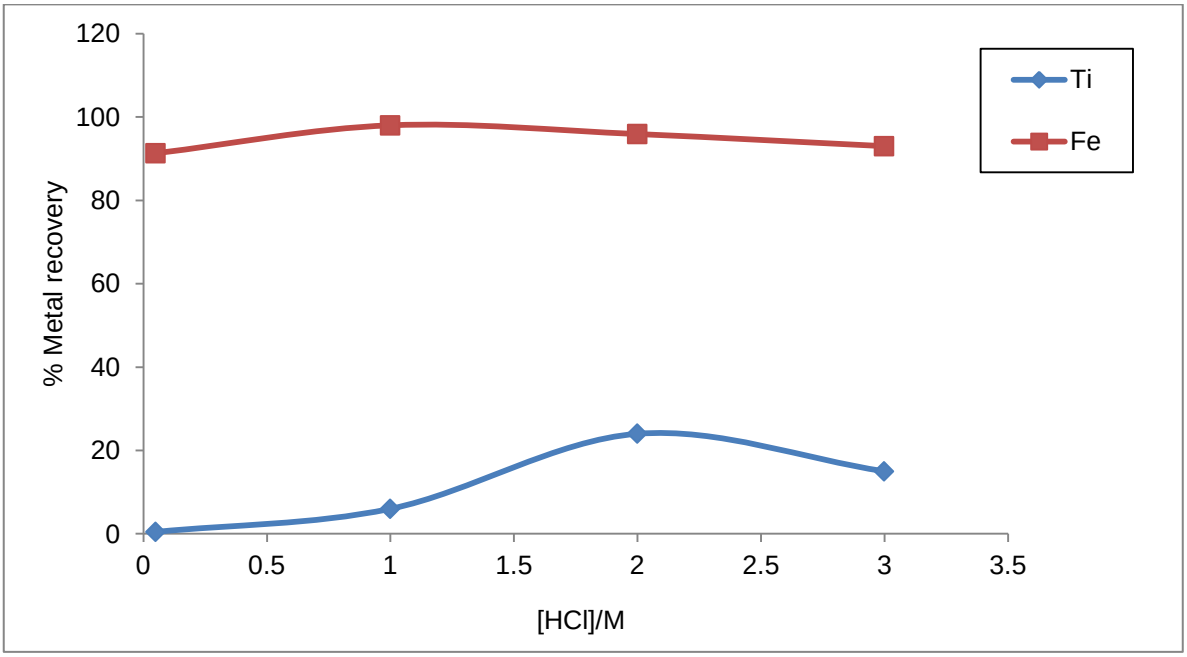

Figure 6.22: Ti and Fe recoveries in organic solution in a HCl media suing NaPT/1-octanol.

The solvent extraction using NaPT was also investigated in H_2SO_4 and H_3PO_4. Good separation of Ti and Fe was also observed with Fe extracted into MIBK and 1-octanol. The extraction of Fe into the organic phase was performed at 1.0 - 3.0M H_2SO_4 and H_3PO_4 concentration. In H_2SO_4 media, Fe recoveries ranged from 98(1)

% to 101(3) % in MIBK and 95(5) % to 99(7) % using 1-octanol. In H_3PO_4 media, the Fe recoveries ranged from 96(1) % to 102.4(8) % in MIBK (see **Figure 6.23** and **Figure 6.24**) and 98(5) % to 103(3) % in 1-octanol together with 1.3(1) % to 4.7(3) % Ti.

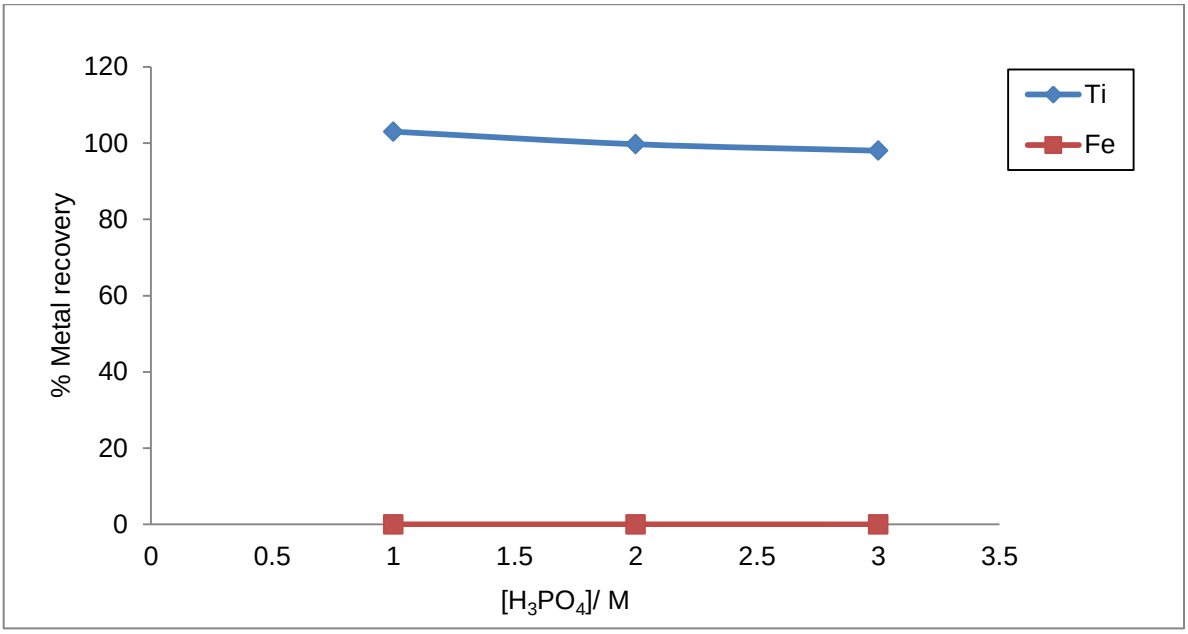

Figure 6.23: Ti and Fe recoveries in the aqueous solution in a H_3PO_4 medium using NaPT/1-octanol.

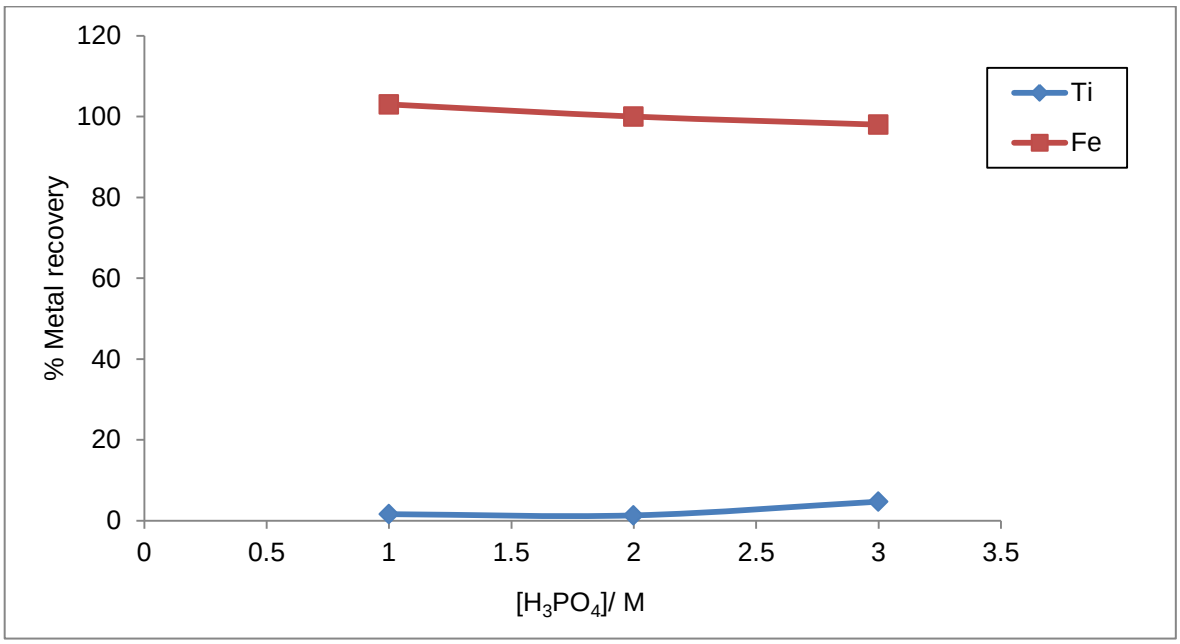

Figure 6.24: Ti and Fe recoveries in organic extracted in a H_3PO_4 medium using NaTP/1-octanol.

6.3.2.5 Separation parameters in the extraction of Ti and Fe

The final step in the solvent extraction study involved the evaluation of the separation parameters. The distribution ratio (D) and the separation factor (α) in **Section 6.3.2** were calculated using **Equation 4.26** and **Equation 4.22.** In HCl matrix, the distribution ratios for Fe were generally higher than those of Ti and thus leading to good separation factors which show favourable separations between these elements in both TOPO/kerosene and acacH/MIBK systems (see **Table 6.28** and **Table 6.29**). No or very poor separations were observed in acacH/1-octanol combination (see **Table 6.29**). It is also interesting to note a high dependence of this extraction on HCl concentrations (see **Table 6.29** and **Figure 6.25**) as this opens to determine the influence of chloride concentrations from other sources such as salts. The straight line curve observed in **Figure 6.25** clearly indicates that the extraction of Fe into MIBK depends on the increase in HCl concentration in the aqueous solution which is directly proportion to the separation factor.

Table 6.28: The distribution ratio and separation factor of Ti and Fe in HCl acidic medium using TOPO in kerosene

[HCl] M	Distribution ratio		Separation factor
	$D_{(Ti)}$	$D_{(Fe)}$	$\alpha_{Ti/Fe}$
1.6	5.0×10^{-1}	5.10×10^{-1}	1.02×10^{0}
3.3	7.70×10^{-3}	1.06×10^{0}	1.38×10^{2}
6.7	2.70×10^{-1}	9.12×10^{4}	3.33×10^{5}

Table 6.29: The distribution ratio and separation factor of Ti and Fe in HCl acidic medium using acacH in different organic solvents

[HCl] M	Distribution ratio		Separation factor
	$D_{(Ti)}$	$D_{(Fe)}$	$\alpha_{Ti/Fe}$
	1-octanol		
1.4	--	--	--
3.0	5.40×10^{-1}	3.10×10^{-1}	5.80×10^{-1}
6.0	2.30×10^{-1}	4.00×10^{-4}	1.70×10^{-3}
	MIBK		
1.4	1.30×10^{-2}	2.90×10^{-1}	2.30×10^{1}
3.0	7.20×10^{-2}	4.98×10^{3}	6.96×10^{4}
6.0	4.20×10^{-3}	6.55×10^{2}	1.57×10^{5}

--Complete separation

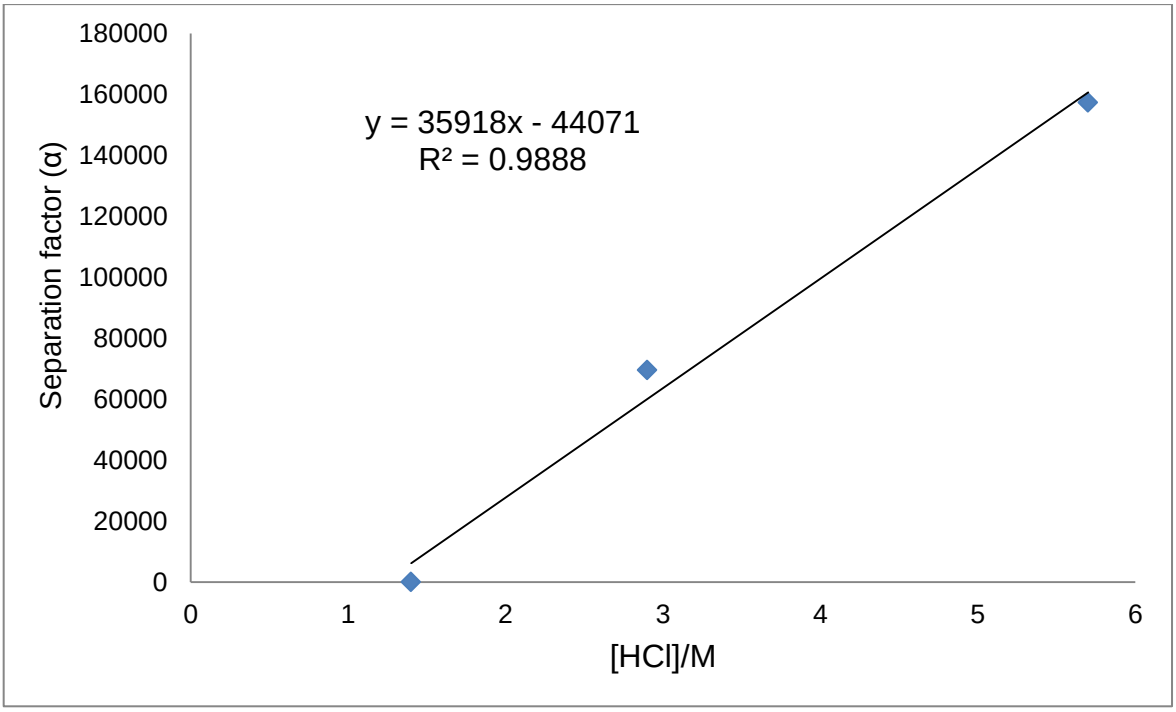

Figure 6.25: The plot of the separation factor v/s the HCl concentration using MIBK as a solvent.

In the extraction using HCl medium (**Figure 6.17**, see also **Table 6.15**) the results also showed the increase in Fe extraction as the HCl concentration increased and thus supporting the predicted formation of $TiOCl_2$ and $HFeCl_4$ (**Equation 6.16** and **Equation 6.17)**. The results in **Table 6.12** showed good separation between Ti and Fe with the separation factor increasing as a function of the acid concentration (see **Table 6.30**) in both solvents and these results are is in agreement with the results reported by White and Ross[231] which also showed an increase in the separation factor with an increase in acidic concentrations greater than 2.0 M HCl. There was no extraction of either Fe or Ti in H_2SO_4 and H_3PO_4 matrices.

Table 6.30: The distribution ratio and separation factor of Ti and Fe (no complexation reagents) in HCl acidic medium in different organic solvents

[HCl] M	Distribution ratio		Separation factor
	$D_{(Ti)}$	$D_{(Fe)}$	$\alpha_{Ti/Fe}$
	1-octanol		
1.4	0.0	0.0	0.0
3.0	6.00×10^{-2}	4.90×10^{1}	8.16×10^{2}
6.0	1.70×10^{-1}	1.19×10^{2}	7.03×10^{2}
	MIBK		
1.4	0.0	$3.00\ 10^{-3}$	--
3.0	9.00×10^{-3}	$1.84\ 10^{2}$	2.04×10^{4}
6.0	2.80×10^{-2}	$2.90\ 10^{3}$	1.05×10^{5}

--Not determined

The extraction ratio (D) in the two step back-extraction using 6.0 M H_2O_4 in the extraction of Ti and Fe using NaPT was also determined (see **Table 6.31.**).The Fe distribution ratio decreases with an increase in HCl concentration using 1-octanol as the extracting solvent. Both extractions in MIBK and 1-octanol show excellent separation factor (> 1).

231 White, J.C. and Ross, W.I, Separation by solvent extraction with Tri-octylphosphine oxide, Report NAS-NS 3102, US Atomic Energy Commission, pp.10-12,33-35 (1961)

Table 6.31: The distribution ratio and separation factor of Ti and Fe in HCl acidic medium using NaPT in different organic solvents

[HCl] M	Distribution ratio		Separation factor
	$D_{(Ti)}$	$D_{(Fe)}$	$\alpha_{Ti/Fe}$
	1-octanol		
0.05	4.70×10^{-3}	2.35×10^{3}	5.02×10^{5}
1.0	6.70×10^{-2}	1.18×10^{2}	1.75×10^{3}
2.0	3.10 x 10-^{1}	4.26×10^{1}	1.37×10^{2}
3.0	2.40×10^{-1}	8.85×10^{0}	3.70×10^{1}
	MIBK		
0.05	7.50×10^{-3}	9.21×10^{3}	1.23×10^{6}
1.0	6.93×10^{5}	4.35×10^{2}	6.29×10^{6}
2.0	9.50×10^{-3}	4.99×10^{1}	5.28×10^{3}
3.0	7.69×10^{5}	1.75×10^{1}	2.28×10^{6}

The same trend was also observed in H_2SO_4 and H_3PO_4. In H_2SO_4 (see **Table 6.32**), the results showed that the distribution ratio and the separation factor in both solvents (MIBK and 1-octanol) decrease with an increase in acid concentration. The results obtained in H_3PO_4 medium (see **Table 6.33**) also showed the increase in the distribution ratio and separation factor with acid concentration in 1-octanol (see **Table 6.33)**.

Table 6.32: The distribution ratio and separation factor of Ti and Fe in H_2SO_4 acidic medium using NaPT in different organic solvents

$[H_2SO_4]$ M	Distribution ratio		Separation factor
	$D_{(Ti)}$	$D_{(Fe)}$	$\alpha_{Ti/Fe}$
	1-octanol		
1.0	--	--	--
2.0	9.00×10^{-3}	2.14×10^{2}	2.37×10^{4}
3.0	2.80×10^{-4}	1.61×10^{1}	5.71×10^{4}
	MIBK		
1.0	--	--	--
2.0	2.20×10^{-2}	6.82×10^{3}	3.10×10^{5}
3.0	1.80×10^{-3}	1.79×10^{2}	1.02×10^{5}

--Complete separation

Table 6.33: The distribution ratio and separation factor of Ti and Fe in H_3PO_4 acidic medium using NaPT in different organic solvents

$[H_3PO_4]$ M	Distribution ratio		Separation factor
	$D_{(Ti)}$	$D_{(Fe)}$	$\alpha_{Ti/Fe}$
	1-octanol		
1.0	1.90×10^{-2}	3.50×10^{3}	2.70×10^{5}
2.0	4.80×10^{-2}	9.50×10^{3}	1.99×10^{5}
3.0	1.10×10^{-4}	9.83×10^{3}	8.63×10^{7}
	MIBK		
1.0	1.10×10^{-4}	1.40×10^{3}	1.32×10^{7}
2.0	1.50×10^{-3}	2.52×10^{1}	1.73×10^{4}
3.0	1.50×10^{-2}	4.38×10^{3}	2.81×10^{5}

6.3.3 Ion exchange separation of Ti and Fe using ion exchange chromatography

The final step in the study was to investigate the possible separation of Fe and Ti in ilmenite using ion exchange chromatography. Both cation and anion resins (see **Section 6.2.5.1**), including strong and weak, were investigated using different mineral acids or different acids concentration as mobile solvent.

6.3.3.1 Cationic exchange of Ti and Fe

Separation with cation-exchange resins (Dowex Marathon C Hydrogen, Clinobrite Zeolite, Amberjet 1200H and Amberlite IR-130C) indicated that both elements are poorly retained on both weak and strong resins (**Table 6.22** and **Table 6.23**, see also **Figure 6.26**) and were readily eluted simultaneously from the column using low concentrations of 0.1 M HCl and 0.1 M H_3PO_4 and an average elemental recoveries in excess of 90 % were reported. These results indicated poor elemental separation and the appearance of the two elements were close to dead time (t_0) which also suggested that the Fe and Ti products present in the phosphate matrix may be of an anionic nature.

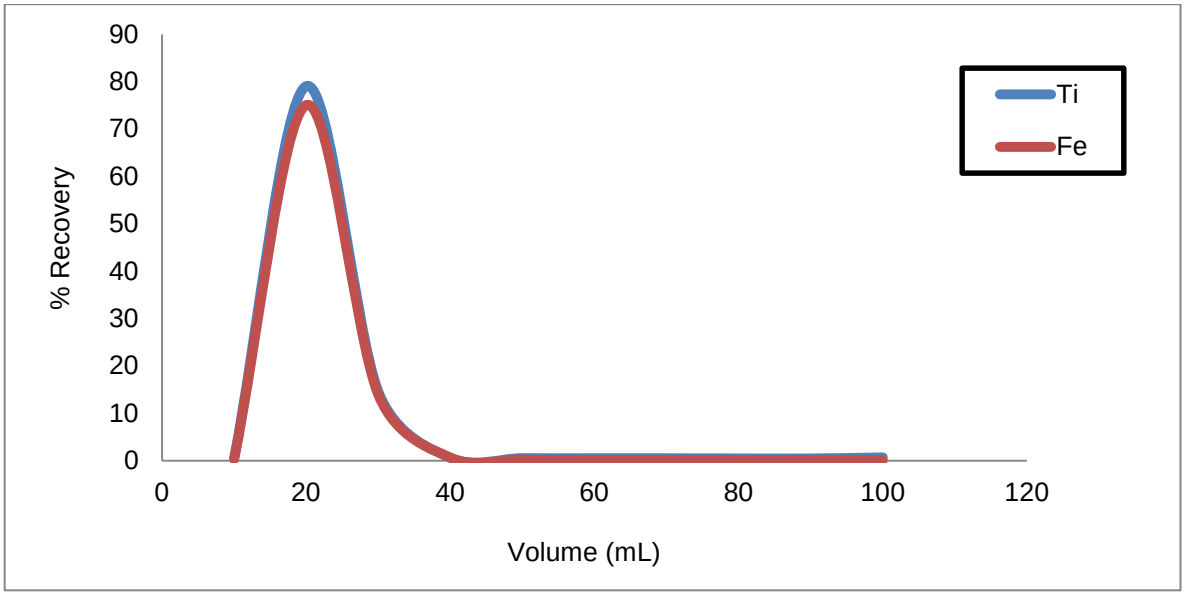

Figure 6.26: Elusion of Ti and Fe as a function of volume with 1.0 M H_3PO_4 at fixed flow rate of 1.7mL/min in Amberlite IR-130C.

6.3.3.2 Anion exchange of Ti and Fe

The next step involved the possible separation of the two elements using anion resins. The results obtained from the anion-exchange resin indicated the successful adsorption of both Ti and Fe on both the weak and strong resins. According to literature a successful adsorption of Ti onto the anionic exchange resin can be attributed to the formation of a strong titanium phosphate framework (see **Figure 6.31**) which has a strong anion exchange capacity.[232] Bhattacharyya and De[233] prepared a titanium phosphate ion exchange resin for separation elements such as Zr, Sc and Pb. Another study by Wang, X *et al*[234] has reported the successful isolation of two hydrated titanium compounds, $Ti(HPO_4)\ 2H_2O$ and $TiH_2(PO_4)_2{\cdot}2H_2O$ and this also could explain the successful adsorption and the anionic behavior of the titanium phosphate compound form during the dissolution of ilmenite using

232 Bhaumik, A. and Inagaki, S., Mesoporous titanium phosphate molecular sieves with ion exchange capacity, *Journal of American Society*,**123**(4), pp.691-696 (2001)

233 Bhattacharyya, D.K. and De, A., Adsorption of trace cations and the separation of Carrier-Free ^{95}Nb from ^{95}Zr, UX_1 from U and ^{45}Ca from ^{46}Sc on titanium phosphate column, *Journal of Radioanalytical and Nuclear Chemistry*, **83**(2), pp.309-318 (1984)

234 Wang, X., Yang, X. and Cai, Y., Novel flow-like titanium phosphate microstructures and their application in lead ion removal from drinking water, *Journal of Material Chemistry*, **A**(2), pp.6718-6722 (2014)

phosphate fluxes. No anionic iron phosphate could be found reported in the literature; however, it may be assumed that Fe compounds similar to those of Ti were also formed during the phosphate flux dissolution.

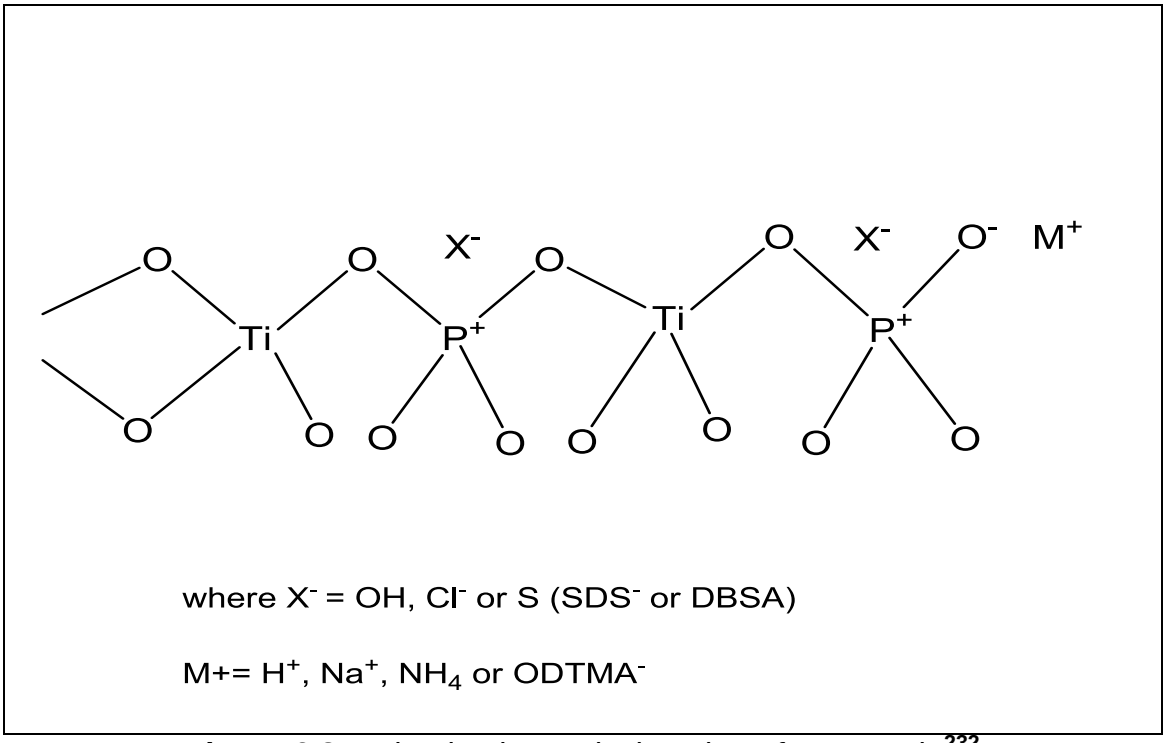

Figure 6.27: The titanium polyphosphate frame work.[232]

6.3.3.2.1 Elution of Ti and Fe from strong anion-exchange resins

The possible separation of the two elements initially involved the use of strong anion-exchange resins (Amberlite 900, Amberlite IRA-402, Dowex 1X4). Elution was investigated with acid concentrations ranging between 0.5 and 10.0 M H_3PO_4 as eluent, but positive results were only achieved at H_3PO_4 concentrations ≥ 3.0 M (see **Table 6.24**) and Fe was selectively eluted from the column. However, the Fe recoveries were generally poor and the lowest recoveries were obtained with Amberlite IRA-402 (51(13) %). The Fe recoveries were found to increase with an increase in H_3PO_4 concentration; however an increase to 5.0 M and 10.0 M also eluted Ti from the column. At 10.0 M H_3PO_4 almost equal amount of Fe and Ti were removed from the column, thereby compromising the initially separation of the two elements (see **Table 6.24**). It was then decided to investigate the use of different concentration of HCl (0.5 M and 5.0 M) as mobile solvent. The results obtained from this change indicated the successive elution of the two elements with Fe being the first eluted at 0.5 M HCl while Ti eluted at this acid concentration was characterized

by substantial tailing and 59.94 % Ti and 89.39 % Fe were recovered (see **Figure 6.28**).

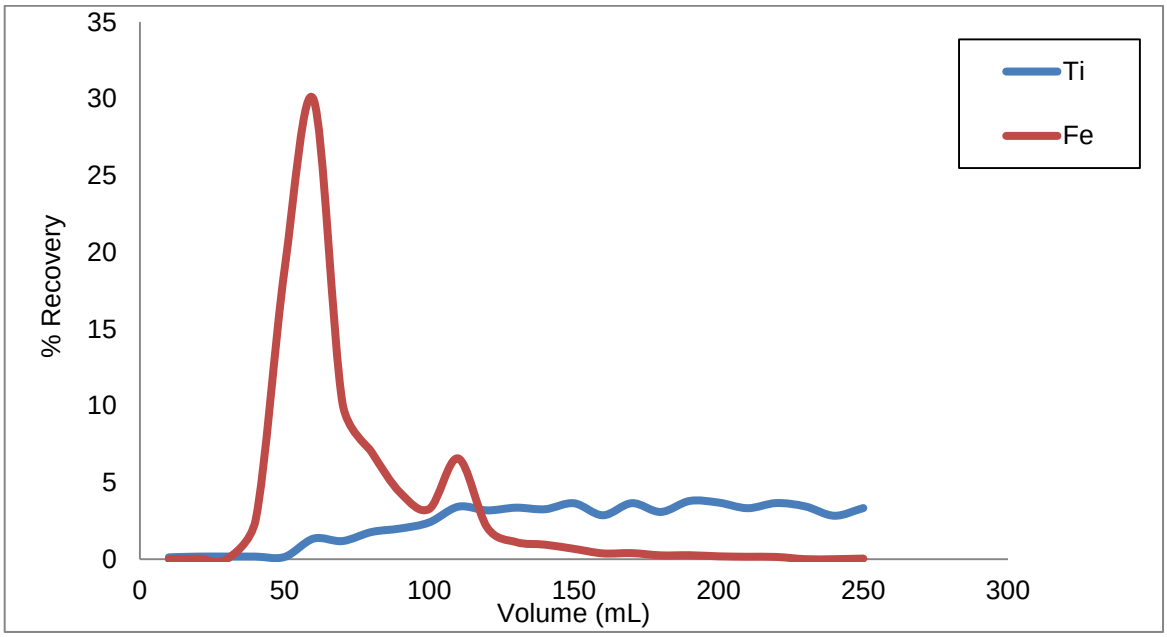

Figure 6.28: Elution of Ti and Fe with 0.5 M HCl in Dowex 1X4.

The next step involved the use of to 5.0 M HCl and the results obtained indicated improved Ti elusion, but unsatisfactory recoveries and separation between the two elements were obtained (see **Figure 6.29**).

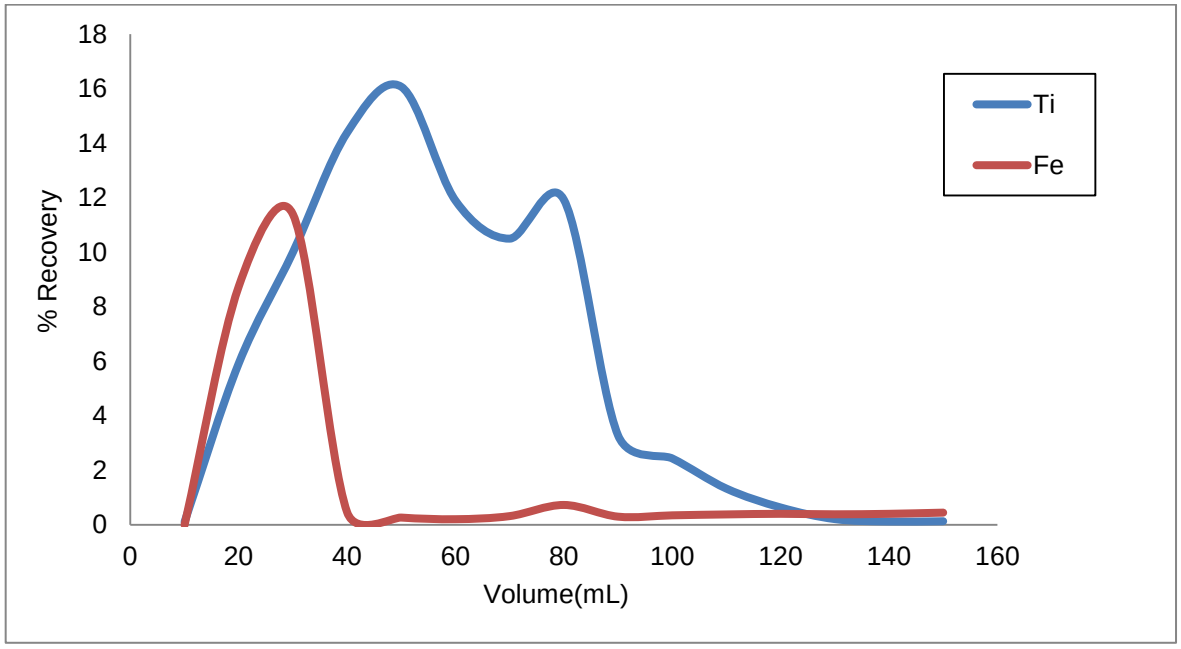

Figure 6.29: Elusion of Ti and Fe with 5.0 M HCl in Amberlite IRA-402.

The use of the Dowex 1x4 ion exchanger (see **Table 6.26** and **Table 6.27**) also separated the Ti and Fe using 3.0 M and 5 M H_3PO_4 However some occurred and 8.2 % Ti was co-extracted with the Fe. The remaining Ti in the column was further eluted with 5.0 M HCl. The elemental recoveries in Dowex 1x4 ion exchange resin were not quantitatively and 97.33(6) % Ti and 86.(3) % Fe in 3.0 M H_3PO_4 and 96(9) % Ti and 82(3) % Fe in 5.0 M H_3PO_4 were recovered.

6.3.3.2.2 Elution of Ti and Fe from weak anion-exchange resins

The results obtained from the elution of Ti and Fe using strong anionic exchange resins indicated that a 5.0 M H_3PO_4 is a suitable eluant for the selective elution of Fe while 5.0 M HCl appear to be the optimum acid concentration for Ti removal and recovery from the column.

The next step separation of Ti and Fe the sequential elution using HCl and H_3PO_4 on different weak basic ion exchange resins (Dowex Marathon WBA and Dowex 66 free base) (see **Table 6.26** and **Table 6.27**) was investigated. Results obtained in this study indicated a successful separation of the two elements (see **Figure 6.30** for Dowex marathon WBA resin) and Fe was eluted from the column with 5.0 M H_3PO_4 followed by Ti elution with 5.0 M HCl.

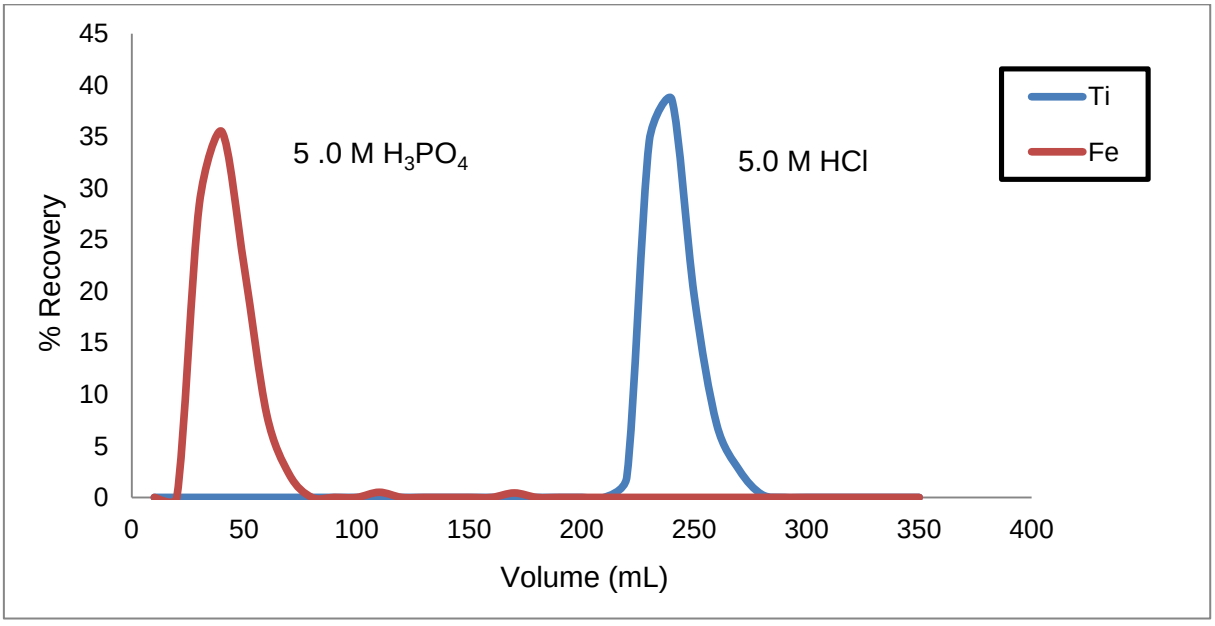

Figure 6.30: Elution of Ti and Fe as a function of volume using H_3PO_4 and HCl at a fixed flow rate of 1.7 mL/min in Dowex Marathon WBA resin.

The success of the separation depended heavily on the subsequence of the acid elusion, namely H_3PO_4 elution followed by HCl not vice versa. The elution results in this study suggest that although the Fe/Ti phosphate compounds are initially adsorbed on the anion exchange resin, the Fe/phosphate adsorption is weaker compared to the Ti/phosphate and is first eluted from the column. The stronger retained Ti/phosphate is then eluted with the HCl, probably to the enhancement formation of the Ti/phosphate in the presence of H_3PO_4 while the presence of the smaller Cl^- ions compete strongly for the exchange sites and is subsequently eluted.

The experiment was also conducted by elution with a change in acid order (HCl before H_3PO_4) but resulted in the co-elution of Ti and Fe with 30.67 % Ti co-eluted with Fe (see **Figure 6.31**).

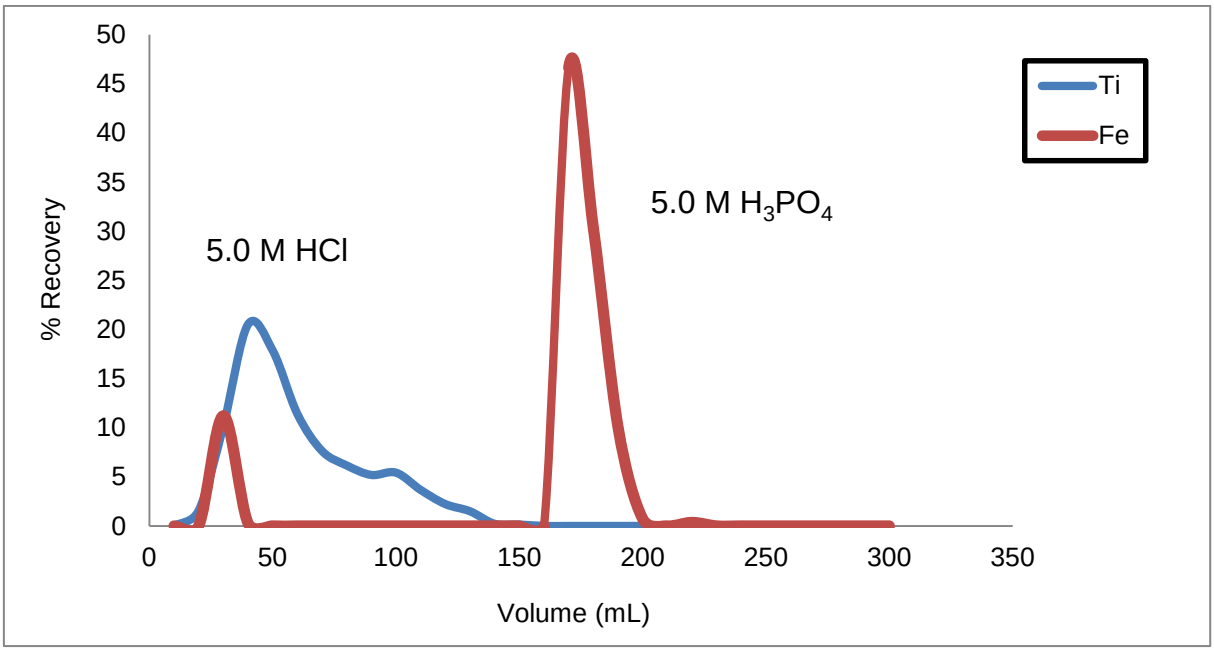

Figure 6.31: Elution of Ti and Fe with HCl prior H_3PO_4 elution at 5.0 M concentrations using Dowex Marathon WBA resin.

6.3.3.2.3 Quantitative parameters in anionic ion exchange

In conclusion, the semi-quantitative parameters of the columns were calculated. Parameters such as theoretical plates and height (N and H) were calculated according to **Equation 4.26** for all the strong and weak anionic resins used in this study. The retention factor (*k*) was also calculated using **Equation 4.24** and the separation factor (α) between Ti and Fe was calculated using **Equation 4.25**. The

column parameters in strong anionic resins are presented in **Table 6.34**. Using Amberlite 900 and Amberlite IRA 402 produced the highest Fe concentration between 30 and 50 mL while that of Ti ranged from 170 to 200 mL. In Dowex 1x4 ion exchange resin Fe was recovered between 30 and 40 mL while Ti between 200 and 240 mL.

Table 6.34: Column parameters for separation of Fe from Ti by eluting with 3.0 M and 5.0 M H_3PO_4 using Amberlite IRA-900, Amberlite IRA-402 and Dowex 1x4 ion exchange resin

$[PO_4^{3-}]$ (M)	Element	v(mL)	k	α	W(min)	N	H
Amberlite IRA-900							
3.0	Ti	183	29.55	**4.75**	100	74.48	0.27
	Fe	43	6.22	1.00	80	6.50	3.08
5.0	Ti	177	28.44	**6.24**	80	108.07	0.19
	Fe	33	4.56	1.00	100	2.46	8.12
10.0	Ti	40	5.67	**1.42**	70	7.24	2.76
	Fe	30	4.00	1.00	80	3.12	6.42
Amberlite IRA-402							
3.0	Ti	190	30.67	**6.73**	100	79.99	0.25
	Fe	33	4.56	1.00	50	9.85	2.03
5.0	Ti	180	29.00	**5.67**	100	71.80	0.28
	Fe	37	2.98	1.00	100	2.98	6.71
10.0	Ti	40	5.54	1.00	80	5.54	3.61
	Fe	10	7.23	1.00	70	7.24	2.76
Dowex 1x4 ion exchange resin							
3.0	Ti	237	38.44	**8.44**	100	124.12	0.16
	Fe	33	4.56	1.00	80	3.85	5.19
5.0	Ti	203	32.88	**5.80**	100	91.62	0.22
	Fe	40	5.67	1.00	120	2.46	8.12
10.0	Ti	40	5.67	**1.42**	50	14.18	1.41
	Fe	40	4.00	1.00	40	12.47	1.60

The column parameters were also calculated for the weak anionic resins and the results are presented in **Table 6.35.** For the Dowex Marathon WBA the highest Fe concentration eluted was observed between 40 and 50 mL using H_3PO_4 (3.0 and 5.0 M) while that for Ti was observed between 220 and 240 mL in HCl (5.0 M) at a flow rate at 1.7 mL/min. The same trend was also observed in Dowex free base 66 anionic resin.

Table 6.35: Column parameters for separation of Fe from Ti by eluting with 3.0 M and 5.0 M H_3PO_4 using Dowex Marathon WBA and Dowex 66 free base

$[PO_4^{3-}]$ M	Element	v (mL)	k	α	w(min)		H
Dowex Marathon WBA							
3.0	Ti	220	21.00	**3.38**	50	429.02	0.047
	Fe	43	6.22	1.00	50	16.64	1.20
5.0	Ti	227	36.78	**6.49**	80	177.90	0.11
	Fe	40	5.67	1.00	50	14.18	1.41
10.0	Ti	50	7.33	**1.67**	120	3.85	5.20
	Fe	30	4.00	1.00	50	7.98	2.51
Dowex 66 free base							
3.0	Ti	227	36.78	**6.49**	50	455.41	0.044
	Fe	40	5.67	1.00	70	7.23	2.76
5.0	Ti	223	36.22	**4.94**	40	69.78	0.029
	Fe	50	7.33	1.00	70	11.31	1.78
10.0	Ti	40	5.67	**1.42**	30	39.40	0.51
	Fe	30	4.00	1.00	50	7.98	2.51

6.4 Conclusion

This chapter described different techniques and results to separate the Fe and Ti in an ilmenite/phosphate matrix. Selective precipitation of Ti and Fe with phenantroline and sodium tetraphenylborate showed unsuccessful Ti and Fe separation and both metals collectively precipitated under the investigated experimental conditions. Selective precipitation of Fe with sodium mercaptopyridine N-oxide (NaPT) was

successfully achieved with 100 % precipitation of Fe while Ti remained in solution at low acidic concentrations.

The selective extraction of Fe in to the organic phase was studied using TOPO/kerosene, acacH/MIBK and acacH/1-octanol systems. The solvent extraction separation was investigated in different mineral acids matrices. The results showed similar extractions in the HCl matrix with the separation of Ti and Fe while no separation was accomplished in H_2SO_4 and H_3PO_4 in all the ligand/solvent systems. The results obtained from the extraction of Fe into the organic (MIBK) without the addition of acacH showed successful separation of Fe from Ti and thus indicating the possible non-participation of acacH in the Fe extraction. Selective extraction of Fe in the organic phase using NaPT was studied in acidic matrix. Successful extraction of Fe was accomplished in different mineral acids, H_2SO_4, H_3PO_4 and HCl. Analytical results showed that MIBK to be a more suitable extractant/organic solvent compared to 1-octanol.

Ion exchange was also investigated using both cationic and anionic exchange resins and successful separation was obtained using different anionic resins. The results obtained in this study indicated that Fe was solely eluted from the column using 3.0 M to 5.0 M H_3PO_4 and thus separated from Ti. Titanium was subsequently recovered from the resin with 5.0 M HCl elution. The results showed that a 10.0 M H_3PO_4 eluted both Ti and Fe from the column and therefore compromising the separation of these elements.

The aim of the study in this chapter (see **Figure 6.1**) was to obtain successful separation of Ti and Fe in the mineral ilmenite. The degree of success in this chapter (including **chapter 5**) can be summarised as in **Table 6.36**.

Table 6.36: Evaluation of success of various steps in beneficiation of Ti and Fe in ilmenite

Process	Parameters	Evaluation
Dissolution of ilmenite	Complete dissolution of sample	**>> 95%**
	Complete recovery of Ti and Fe with flux fusion	√√
Selective precipitation	Selective precipitation with phen and NaTPB	xx
	Selective precipitation with NaTP	√√
Solvent extraction	Separation of Ti and Fe with TOPO	√
	Separation of Ti and Fe with acacH	√√
	Separation of Ti and Fe with NaTP	√√
	Separation of Ti and Fe with no ligand in acidic medium	√√
Ion exchange	Cation exchange separation of Ti and Fe	xx
	Anion exchange separation of Ti and Fe	√√

√√**-** Successful to above 95 %, √**-** Successful below 90 %
xx -Not successful

7 Method Validation of the results

7.1 Introduction

Method validation is important in analytical laboratories for quality assurance and to see if the method that has been developed is suitable for its purpose. In this chapter we evaluated the results obtained in **Chapter 5** and **Chapter 6.** The validation parameters which were evaluated for Ti and Fe analysis using ICP-OES are listed in **Figure 7.1**.

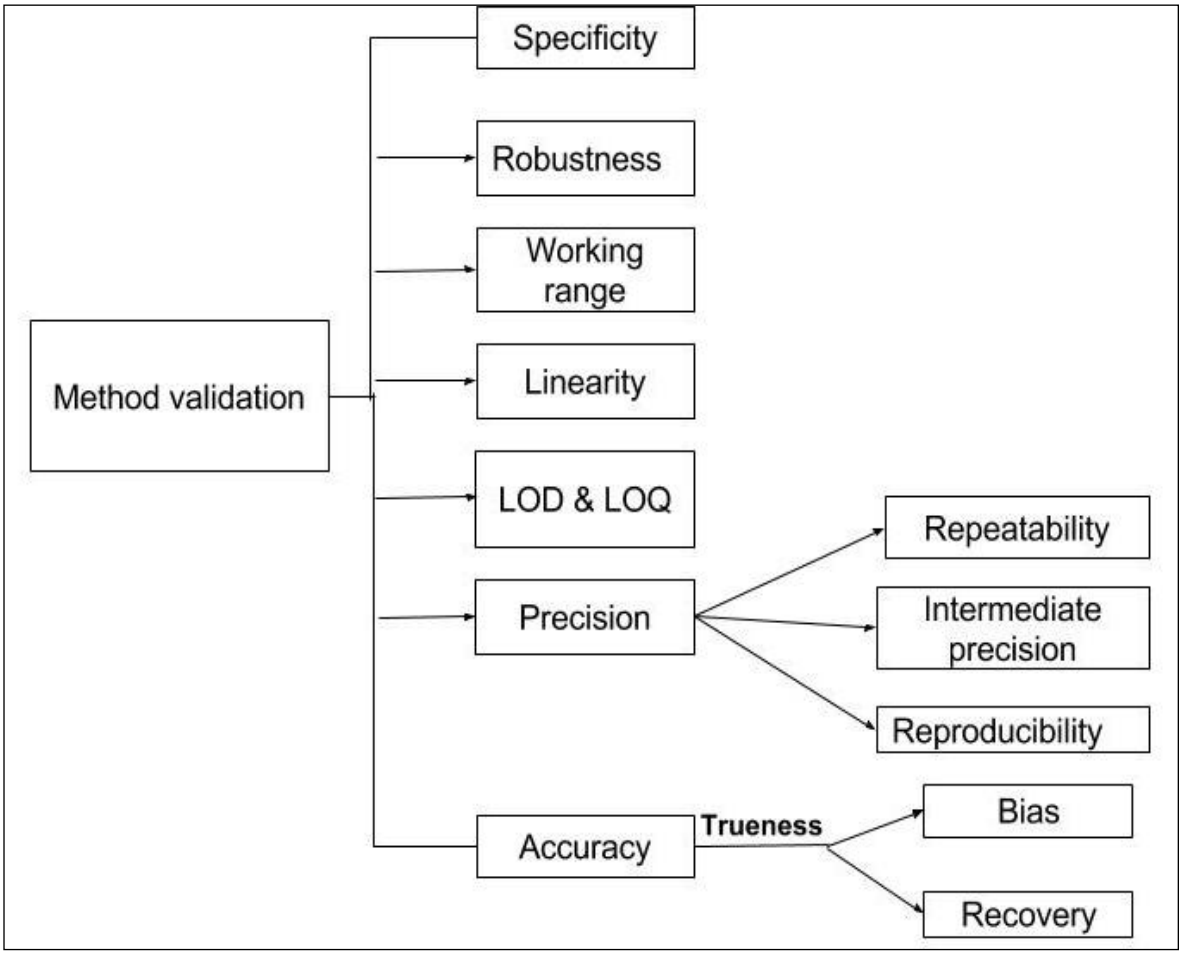

Figure 7.1: Method validation parameters evaluated in this study[235]

235 Bratinova, S., Raffael, B. and Simoneau, C., Guidelines for performance criteria and validation procedures of analytical methods used in controls of food, European Communities, pp.12,19,33-34 (2009)

In most of the cases the statistical was performed on at least 3 experimental replicates at a 95 % confidence level. The *t*-test was used to determine the accuracy and to accepted or rejected using the hypothesis criteria (t_{crit} -value used as ± 4.30 for three replicates with $t_{crit} < t < t_{crit}$, the hypothesis is accepted, **Equation 7.1**).

$$t = \frac{\bar{x} - \mu}{s/\sqrt{N}} \qquad \textbf{7.1}$$

where μ = The true mean value, N = The number of replicates and $\bar{x}$ = mean or average

The relative standard deviation (RSD) was calculated for 3 mean replicates using **Equation 7.3** and the standard deviation using **Equation 7.2**.

$$s = \sqrt{\frac{\sum_{i=1}^{N}\left(x_i - \bar{x}\right)^2}{N-1}} \qquad \textbf{7.2}$$

$$RSD = \frac{s}{\bar{x}} \times 100\% \qquad \textbf{7.3}$$

The calibration curve was used to evaluate the selectivity (S_m) and the specificity (S_b) with correlation coefficient (r) > 0.996 perceived as linear. All analysis were done in a working range of 0.5 to 10.0 ppm.

7.2 Validation in the dissolution and analysis of Ti and Fe samples

Table 7.1: Validation of Fe in $FeCl_3 \cdot 6H_2O$ in different acids using ICP-OES

Validation Criteria	Parameter	HCl	*Aqua regia*	HNO_3	H_2SO_4	H_3PO_4
Recovery	Mean % (*s*)	100(4)	102(1)	101.5(9)	103(2)	103(2)
Precision	RSD (%)	3.47	0.10	0.90	1.91	1.67
Linearity	R^2	1.0000	1.0000	0.9996	0.9990	0.9999
Sensitivity	slope	0.4458	0.4867	0.4799	0.4099	0.4783
Selectivity	S_m	0.3538	0.3947	0.3880	0.3175	0.3862
Specificity	S_b	0.2392	0.2668	0.2623	0.2146	0.2611
Error of Slope	Y-intercept	0.0105	0.0095	0.0084	0.0016	0.0140
t_{crit} at 95 % confidence interval		4.30				
t-value		0.37	1.56	7.89	25.50	17.26
Decision		Accept	Accept	Reject	Reject	Reject

Table 7.2: Validation of Ti in $TiCl_3$ in different acids using ICP-OES

Validation Criteria	Parameter	HCl	*Aqua regia*	HNO_3	H_2SO_4	H_3PO_4
Recovery	Mean % (*s*)	100(2)	98(1)	98(1)	105.2(6)	103.6(5)
Precision	RSD (%)	2.36	1.15	1.46	0.56	0.46
Linearity	R^2	0.9995	1.0000	0.9994	0.9999	0.9999
Sensitivity	slope	1.4683	1.4664	1.5498	1.1600	1.5465
Selectivity	S_m	1.3008	1.2987	1.3680	1.0212	1.3710
Specificity	S_b	0.8793	0.8779	0.9247	0.6903	0.9268
Error of Slope	Y-intercept	0.0264	0.0234	0.1116	0.0436	0.0389
t_{crit} at 95 % confidence interval		4.30				
t-value		-1.83	0.01	-0.03	0.10	0.06
Decision		Accept	Accept	Accept	Accept	Accept

Table 7.3: Validation of Ti, Fe in pure metals and ilmenite using *aqua regia*

Validation Criteria	Parameter	Ti metal	Fe metal	*Ilmenite	
				Ti	Fe
Recovery	Mean % (s)	0.1925(6)	98(1)	0.03308(2)	0.285(2)
Precision	RSD (%)	0.32	1.06	0.03	0.11
Linearity	R^2	0.9999	1.0000	0.9999	1.0000
Sensitivity	slope	1.3628	0.7321	1.3628	0.7321
Selectivity	S_m	1.2051	1.1465	1.2051	1.1465
Specificity	S_b	0.5592	0.5297	0.5592	0.5297
Error of Slope	Y-intercept	0.0224	0.0185	0.0224	0.0185
t_{crit} at 95 % confidence interval		4.30			
t-value		-282.82	-0.003	-9277.39	-326.9
Decision		Reject	Accept	Reject	Reject

*% metal oxide

Table 7.4: Validation of Ti, Fe in pure metals and ilmenite using HCl

Validation Criteria	Parameter	Ti metal	Fe metal	*Ilmenite	
				Ti	Fe
Recovery	Mean % (s)	45.2(4)	98.6(7)	1.289(2)	2.15(2)
Precision	RSD (%)	0.83	0.71	0.400	0.868
Linearity	R^2	0.9999	1.0000	0.9999	1.0000
Sensitivity	slope	1.3628	0.6900	1.3628	0.6900
Selectivity	S_m	1.2051	0.5844	1.2051	0.5844
Specificity	S_b	0.5592	0.2701	0.5592	0.2701
Error of Slope	Y-intercept	0.0224	0.0090	0.0224	0.0090
t_{crit} at 95 % confidence interval		4.30			
t-value		-0.25	-0.003	-15.79	-4328.00
Decision		Reject	Accept	Reject	Reject

*% metal oxide

Table 7.5: Validation of Ti, Fe in pure metals and ilmenite using HNO_3

Validation Criteria	Parameter	Ti metal	Fe metal	*Ilmenite	
				Ti	Fe
Recovery	Mean % (s)	0.1831(1)	72(1)	0.05146(5)	0.25(1)
Precision	RSD (%)	0.52	1.92	1.52	0.69
Linearity	R^2	0.9997	1.0000	0.9997	1.0000
Sensitivity	slope	1.2403	0.6978	1.2403	0.6978
Selectivity	S_m	1.0942	0.5917	1.0942	0.5917
Specificity	S_b	0.5077	0.2734	0.5077	0.2734
Error of Slope	Y-intercept	0.0156	0.0147	0.0156	0.0147
t_{crit} at 95 % confidence interval		4.30			
t-value		-181.39	-0.04	-106.41	-11.75
Decision		Reject	Reject	Reject	Reject

*% metal oxide

Table 7.6: Validation of Ti, Fe in pure metals and ilmenite using H_2SO_4

Validation Criteria	Parameter	Ti metal	Fe metal	*Ilmenite	
				Ti	Fe
Recovery	Mean % (s)	104(1)	102(5)	34.8(1)	20.2(2)
Precision	RSD (%)	1.01	5.27	1.65	1.37
Linearity	R^2	0.9981	1.0000	0.9981	1.0000
Sensitivity	slope	1.8018	0.3179	1.8018	0.3179
Selectivity	S_m	1.5953	0.1997	1.5953	0.1997
Specificity	S_b	0.6813	0.6237	0.6813	0.6237
Error of Slope	Y-intercept	-4.1959	-1.6219	-4.1959	-1.6219
t_{crit} at 95 % confidence interval		4.30			
t-value		0.007	0.0005	-11.75	-22.62
Decision		Accept	Accept	Reject	Reject

*% metal oxide

Table 7.7: Validation of Ti, Fe in pure metals and ilmenite using H_3PO_4

Validation Criteria	Parameter	Ti metal	Fe metal	*Ilmenite	
				Ti	Fe
Recovery	Mean % (s)	104(4)	98(1)	46.81(3)	38.4(4)
Precision	RSD (%)	3.68	1.26	1.11	0.41
Linearity	R^2	0.9998	0.9994	0.9998	0.9994
Sensitivity	slope	1.8435	0.4545	1.8435	0.4545
Selectivity	S_m	1.6321	0.4029	1.6321	0.4029
Specificity	S_b	0.7504	0.1589	0.7504	0.1589
Error of Slope	Y-intercept	-0.0005	0.0000	-0.00048	0.0000
t_{crit} at 95 % confidence interval		4.30			
t-value		0.01	-0.002	-3.72	-2.58
Decision		Accept	Accept	Accept	Accept

*% metal oxide

Table 7.8: Validation of Ti and Fe in ilmenite using $K_2S_2O_7$ and Na_2CO_3

Validation Criteria	Parameter	*$K_2S_2O_7$		*Na_2CO_3	
		Ti	Fe	Ti	Fe
Recovery	Mean % (s)	31.8(7)	25.5(1)	19.1(6)	21.6(4)
Precision	RSD (%)	3.74	5.56	5.90	2.96
Linearity	R^2	1.0000	0.9999	0.9989	0.9998
Sensitivity	slope	1.7210	0.1999	-0.0261	0.6001
Selectivity	S_m	1.5265	0.7313	1.5341	0.4972
Specificity	S_b	1.1293	0.5411	1.3322	0.4317
Error of Slope	Y-intercept	0.0286	0.0051	1.7289	-0.0070
t_{crit} at 95 % confidence interval		4.30			
t-value		-7.04	-6.84	-7.43	-15.17
Decision		Reject	Reject	Reject	Reject

* % metal oxide

Table 7.9: Validation of Ti and Fe in ilmenite using KF

Validation Criteria	Parameter	*1:10, 30 min		*1: 20, 60 min	
		Ti	Fe	Ti	Fe
Recovery	Mean % (s)	36.0(6)	31.8(5)	35.5(4)	31.9(8)
Precision	RSD (%)	7.04	6.88	1.29	2.94
Linearity	R^2	0.9986	0.9991	0.9986	0.9991
Sensitivity	slope	1.8556	0.1954	1.8556	0.1954
Selectivity	S_m	1.6510	0.6413	1.6510	0.6413
Specificity	S_b	1.1160	0.4335	1.1160	0.4335
Error of Slope	Y-intercept	0.0755	0.0079	0.0755	0.0079
t_{crit} at 95 % confidence interval		4.30			
t-value		-10049.00	-7774.70	-11261.00	--7510.50
Decision		Reject	Reject	Reject	Reject

*% metal oxide

Table 7.10: Validation of Ti and Fe in ilmenite using $NH_4{\cdot}HF_2$

Validation Criteria	Parameter	*1:20 (30 min)		*1: 20, 60 min	
		Ti	Fe	Ti	Fe
Recovery	Mean % (s)	37(2)	30.0(1)	38.8(3)	24.6(3)
Precision	RSD (%)	1.45	2.45	1.76	3.70
Linearity	R^2	0.9981	0.9991	0.9981	0.9991
Sensitivity	slope	-0.1582	0.7209	-0.1582	0.7209
Selectivity	S_m	2.0717	0.6126	2.0717	0.6126
Specificity	S_b	1.7990	0.5320	1.7990	0.5320
Error of Slope	Y-intercept	-0.6328	-0.0494	-0.6328	-0.0494
t_{crit} at 95 % confidence interval		4.30			
t-value		-3583.10	-5269.90	-15720.00	-14365.00
Decision		Reject	Reject	Reject	Reject

*% metal oxide

Table 7.11: Validation of Ti and Fe in ilmenite using borates

Validation Criteria	Parameter	*$Na_2B_4O_7$		*$LiBO_2$	
		Ti	Fe	Ti	Fe
Recovery	Mean % (s)	46.3(5)	56.5(2)	47.7(5)	55.1(3)
Precision	RSD (%)	1.72	3.54	1.87	0.90
Linearity	R^2	0.9994	0.9997	1.0000	0.9997
Sensitivity	slope	1.8128	0.2044	1.8128	0.2044
Selectivity	S_m	1.6120	0.0326	1.6120	0.0326
Specificity	S_b	1.0466	0.0220	1.0466	0.0220
Error of Slope	Y-intercept	0.0666	0.0078	0.0666	0.0078
t_{crit} at 95 % confidence interval		4.30			
t-value		-0.07	0.08	0.36	-0.03
Decision		Accept	Accept	Accept	Accept

*% metal oxide

Table 7.12 : Validation of Ti and Fe in $Na_2HPO_4/NaH_2PO_4{\cdot}H_2O$

Validation Criteria	Parameter	*Ti	*Fe
Recovery	Mean % (s)	49(2)	55.9(5)
Precision	RSD (%)	5.73	1.43
Linearity	R^2	1.0000	0.9990
Sensitivity	slope	1.9614	0.2146
Selectivity	S_m	1.7451	0.0669
Specificity	S_b	1.7451	0.0435
Error of Slope	Y-intercept	0.0382	0.0047
t_{crit} at 95 % confidence interval		4.30	
t-value		-0.10	0.00
Decision		Accept	Accept

*% metal oxide

7.3 Validation in separation of Ti and Fe in ilmenite mineral

Table 7.13: Validation of Fe salt in NaTPB and phen precipitate at different ratios

Validation Criteria	Parameter	1:1	1:3	1:5
Recovery	Mean % (s)	55(5)	99(5)	82(8)
Precision	RSD	10.45	5.64	10.12
Linearity	R^2	1.0000	1.0000	1.0000
Sensitivity	Slope	0.2167	0.2167	0.2167
Selectivity	s_m	0.0862	0.0862	0.0862
Specificity	S_b	0.4543	0.4543	0.4543
Error of Slope	y-intercept	-0.0474	-0.0474	-0.0474
Working range	Calibration curve	1.0-10.0 ppm		
t_{crit} at 95 % confidence interval		4.30		
t-value		-13.49	-0.31	-3.76
Decision		Reject	Accept	Accept

Table 7.14: Validation of Ti and Fe in ilmenite after NaTPB/phen precipitation

Validation Criteria	Parameter	1:0.5 (Fe/phen)		1:3 (Fe/phen)		1:5 (Fe/phen)	
		Ti	Fe	Ti	Fe	Ti	Fe
Recovery	Mean % (s)	89.7(9)	101.1(2)	35(10)	12.5(8)	46(5)	12(10)
Precision	RSD	0.96	0.17	31.47	6.98	11.21	112.83
Linearity	R^2	0.9998	1.0000	0.9998	1.0000	0.9998	1.0000
Sensitivity	Slope	1.5060	0.1575	1.5060	0.1575	1.5060	0.1575
Selectivity	s_m	1.3345	0.3447	1.3345	0.3447	1.3345	0.3447
Specificity	S_b	0.9021	0.2354	0.9021	0.2354	0.9021	0.2354
Error of Slope	y-intercept	0.1078	0.1575	0.1078	0.1575	0.1078	0.1575
t_{crit} at 95 % confidence interval		4.30					
t-value		-20.74	11.20	-10.30	-147.27	-18.13	-11.26
Decision		Reject	Reject	Reject	Reject	Reject	Reject

Table 7.15: Validation of Ti and Fe in NaPT precipitate

Validation Criteria	Parameter	Ti	Fe
Recovery	Mean % (s)	0.00	104(1)
Precision	RSD	0.00	1.36
Linearity	R^2	0.9998	1.0000
Sensitivity	Slope	0.8636	0.1800
Selectivity	s_m	1.2408	0.3739
Specificity	S_b	0.8387	0.1700
Error of Slope	y-intercept	0.1337	0.0315
Working range	Calibration curve	0.5-10 ppm	
t_{crit} at 95 % confidence interval		4.30	
t-value		--	0.1784
Decision		--	Accept

--Not determined

Table 7.16: Validation of Ti and Fe in TOPO/kerosene using HCl

Validation Criteria	Parameter	1.7 M		3.3 M		6.7 M	
		Ti	Fe	Ti	Fe	Ti	Fe
Recovery	Mean % (s)	0.8(1)	2(2)	0.8(8)	50(4)	22(6)	99.0(8)
Precision	RSD	173.21	147.36	109.91	8.16	28.20	0.85
Linearity	R^2	1.0000	0.9986	1.0000	0.9986	1.0000	0.9986
Sensitivity	Slope	1.1536	0.1830	1.1536	0.1830	1.1536	0.1830
Selectivity	s_m	1.7520	0.1330	1.7520	0.1330	1.7520	0.1330
Specificity	s_b	0.8130	0.0899	0.8130	0.0899	0.8130	0.0899
Error of Slope	y-intercept	0.1696	0.0069	0.1696	0.0069	0.1696	0.0069
t_{crit} at 95 % confidence interval		4.30					
t-value		-128.70	-69.43	-206.60	-20.79	-21.51	-2.031
Decision		Reject	Reject	Reject	Reject	Reject	Accept

Table 7.17: Validation of Ti and Fe in TOPO/kerosene using H_2SO_4

Validation Criteria	Parameter	1.7 M		3.3 M		6.7 M	
		Ti	Fe	Ti	Fe	Ti	Fe
Recovery	Mean % (*s*)	0.00	0.00	0.00	0.7(1)	48(4)	0.32(6)
Precision	RSD	0.00	0.00	0.00	173.21	9.49	173.21
Linearity	R^2	0.9996	0.9998	0.9996	0.9998	0.9996	0.9998
Sensitivity	Slope	2.4736	0.1980	2.4736	0.1980	2.4736	0.1980
Selectivity	s_m	2.2053	0.1932	2.2053	0.1932	2.2053	0.1932
Specificity	s_b	1.0233	0.1306	1.0233	0.1306	1.0233	0.1306
Error of Slope	y-intercept	0.3578	0.0042	0.3578	0.0042	0.3578	0.0042
t_{crit} at 95 % confidence interval		4.30					
t-value		--	--	--	-143.50	-19.70	-312.50
Decision		--	--	--	Reject	Reject	Reject

--Not determined

Table 7.18: Validation of Ti and Fe in the NaPT/MIBK using HCl

Validation Criteria	Parameter	0.05 M		1.0 M	
		Ti	Fe	Ti	Fe
Recovery	Mean % (*s*)	0.74(6)	99.4(6)	0.0071(1)	100(4)
Precision	RSD	86.62	0.64	173.21	4.78
Linearity	R^2	0.9993	0.9998	0.9993	0.9998
Sensitivity	Slope	1.5533	0.1631	1.5533	0.1631
Selectivity	s_m	1.3777	0.3610	1.3777	0.3610
Specificity	s_b	0.6393	0.2440	0.6393	0.2440
Error of Slope	y-intercept	-0.0961	0.0098	-0.0961	0.0098
t_{crit} at 95 % Confidence interval		4.30			
t-value		-269.80	-1.62	-143.00	0.08
Decision		Reject	Accept	Reject	Accept

Table 7.19: Validation of Ti and Fe in the NaPT/MIBK using HCl

Validation Criteria	Parameter	1.0 M		2.0 M	
		Ti	Fe	Ti	Fe
Recovery	Mean % (*s*)	0.9(1)	97(1)	0.0076(1)	97(2)
Precision	RSD	173.21	1.11	173.21	2.31
Linearity	R^2	0.9993	0.9998	0.9993	0.9998
Sensitivity	Slope	1.5533	0.1631	1.5533	0.1631
Selectivity	s_m	1.3777	0.3610	1.3777	0.3610
Specificity	s_b	0.6393	0.2440	0.6393	0.2440
Error of Slope	y-intercept	-0.0961	0.0098	-0.0961	0.0098
t_{crit} at 95 % Confidence Interval		4.30			
t-value		-103.10	-5.60	-13212.00	-2.34
Decision		Reject	Reject	Reject	Accept

Table 7.20: Validation of Ti and Fe in the NaPT/1-octanol using HCl

Validation Criteria	Parameter	0.05 M		1.0 M	
		Ti	Fe	Ti	Fe
Recovery	Mean % (*s*)	0.46(4)	91.3(6)	6(3)	98(3)
Precision	RSD	123.31	6.70	56.91	3.22
Linearity	R^2	0.9993	0.9998	0.9993	0.9998
Sensitivity	Slope	1.5533	0.1631	1.5533	0.1631
Selectivity	s_m	1.3777	0.3610	1.3777	0.3610
Specificity	s_b	0.6393	0.2440	0.6393	0.2440
Error of Slope	y-intercept	-0.0961	0.0098	-0.0961	0.0098
t_{crit} at 95 % Confidence Interval		4.30			
t-value		-304.97	-2.45	-45.87	-1.21
Decision		Reject	Accept	Reject	Accept

Table 7.21: Validation of Ti and Fe in the NaPT/1-octanol using HCl

Validation Criteria	Parameter	1.0 M		2.0 M	
		Ti	Fe	Ti	Fe
Recovery	Mean % (*s*)	24(9)	95.9(3)	15(3)	93(5)
Precision	RSD	35.54	0.38	23.47	5.59
Linearity	R^2	0.9993	0.9998	0.9993	0.9998
Sensitivity	Slope	1.5533	0.1631	1.5533	0.1631
Selectivity	s_m	1.3777	0.3610	1.3777	0.3610
Specificity	s_b	0.6393	0.2440	0.6393	0.2440
Error of Slope	y-intercept	-0.0961	0.0098	-0.0961	0.0098
t_{crit} at 95 % Confidence interval		4.30			
t-value		-14.94	-14.83	-39.43	-2.21
Decision		Reject	Reject	Reject	Accept

Table 7.22: Validation of Ti and Fe in the NaPT/MIBK using H_2SO_4

Validation Criteria	Parameter	1.0 M		2.0 M		3.0 M	
		Ti	Fe	Ti	Fe	Ti	Fe
Recovery	Mean % (*s*)	0.00	99(1)	2(3)	101(3)	0.19(8)	98(2)
Precision	RSD	0.00	1.34	147.00	3.15	46.19	2.30
Linearity	R^2	1.0000	0.9998	1.0000	0.9998	1.0000	0.9998
Sensitivity	Slope	1.5678	0.2874	1.5678	0.2874	1.5678	0.2874
Selectivity	s_m	1.3902	0.1798	1.3902	0.1798	1.3902	0.1798
Specificity	s_b	0.9397	0.1215	0.9397	0.1215	0.9397	0.1215
Error of Slope	y-intercept	0.1667	0.0539	0.1667	0.0539	0.1667	0.0539
t_{crit} at 95 % confidence interval		4.30					
t-value		--	-1.26	-52.87	0.71	-2005.00	-0.89
Decision		--	Accept	Reject	Accept	Reject	Accept

--Not determined

Table 7.23: Validation of Ti and Fe in the NaPT/1-octanol H_2SO_4

Validation Criteria	Parameter	1.0 M		2.0 M		3.0 M	
		Ti	Fe	Ti	Fe	Ti	Fe
Recovery	Mean % (*s*)	0.00	99(7)	0.9(1)	95.5(1)	0.029(5)	96(2)
Precision	RSD	0.00	7.84	136.45	0.13	173.21	2.77
Linearity	R^2	1.0000	0.9998	1.0000	0.9998	1.0000	0.9998
Sensitivity	Slope	1.5678	0.2874	1.5678	0.2874	1.5678	0.2874
Selectivity	s_m	1.3902	0.1798	1.3902	0.1798	1.3902	0.1798
Specificity	s_b	0.9397	0.1215	0.9397	0.1215	0.9397	0.1215
Error of Slope	y-intercept	0.1667	0.0539	0.1667	0.0539	0.1667	0.0539
t_{crit} at 95 % confidence interval		4.30					
t-value		--	-0.03	-140.50	-61.68	-3457.00	-2.52
Decision		--	Accept	Reject	Reject	Reject	Accept

--Not determined

Table 7.24: Validation of Ti and Fe in the NaPT/MIBK using H_3PO_4

Validation Criteria	Parameter	1.0 M		2.0 M		3.0 M	
		Ti	Fe	Ti	Fe	Ti	Fe
Recovery	Mean % (*s*)	0.012(2)	99(3)	0.011(1)	102.4(8)	0.15(2)	96(1)
Precision	RSD	173.21	3.61	173.21	0.86	164.87	1.66
Linearity	R^2	0.9988	0.9998	0.9988	0.9998	0.9988	0.9998
Sensitivity	Slope	1.6788	0.3228	1.6788	0.3228	1.6788	0.3228
Selectivity	s_m	1.0847	0.4092	1.0847	0.4092	1.0847	0.4092
Specificity	s_b	0.7332	0.2766	0.7332	0.2766	0.7332	0.2766
Error of Slope	y-intercept	0.0388	0.0266	0.0388	0.0266	0.0388	0.0266
t_{crit} at 95 % confidence interval		4.30					
t-value		-8431.00	-0.36	-8967.00	4.77	-690.80	-4.00
Decision		Reject	Accept	Reject	Reject	Reject	Accept

Table 7.25: Validation of Ti and Fe in the NaPT/1-octanol using H_3PO_4

Validation Criteria	Parameter	1.0 M		2.0 M		3.0 M	
		Ti	Fe	Ti	Fe	Ti	Fe
Recovery	Mean % (*s*)	1.6(3)	103(3)	1.3(1)	100(2)	4.7(3)	98(5)
Precision	RSD	18.33	2.81	104.82	2.11	6.42	5.92
Linearity	R^2	0.9988	0.9998	0.9988	0.9998	0.9988	0.9998
Sensitivity	Slope	1.6788	0.3228	1.6788	0.3228	1.6788	0.3228
Selectivity	s_m	1.0847	0.4092	1.0847	0.4092	1.0847	0.4092
Specificity	s_b	0.7332	0.2766	0.7332	0.2766	0.7332	0.2766
Error of Slope	y-intercept	0.0388	0.0266	0.0388	0.0266	0.0388	0.0266
t_{crit} at 95 % confidence interval		4.30					
t-value		-580.74	1.66	-126.30	0.73	-547.70	-0.46
Decision		Reject	Accept	Reject	Accept	Reject	Accept

Table 7.26: Validation of Ti and Fe in acacH/MIBK using HCl

Validation Criteria	Parameter	1.4 M		3.0 M		6.0 M	
		Ti	Fe	Ti	Fe	Ti	Fe
Recovery	Mean % (*s*)	1(2)	22.5(2)	7(2)	100(2)	0.7(2)	99(3)
Precision	RSD	149.34	4.26	33.70	1.74	41.00	3.74
Linearity	R^2	0.9998	1.0000	0.9998	1.0000	0.9998	1.0000
Sensitivity	Slope	1.7272	0.1800	1.7272	0.1800	1.7272	0.1800
Selectivity	s_m	1.5341	0.0002	1.5341	0.0002	1.5341	0.0002
Specificity	s_b	1.037	0.0001	1.037	0.0001	1.037	0.0001
Error of Slope	y-intercept	0.0535	0.0063	0.0535	0.0063	0.0535	0.0063
t_{crit} at 95 % confidence interval		4.30					
t-value		-93.79	-139.73	-72.76	-0.03	-1028.20	-0.30
Decision		Reject	Reject	Reject	Accept	Reject	Accept

Table 7.27: Validation of Ti and Fe in acacH/1-octanol using HCl

Validation Criteria	Parameter	1.4 M		3.0 M		6.0 M	
		Ti	Fe	Ti	Fe	Ti	Fe
Recovery	Mean % (*s*)	0.00	0.00	35(3)	23(1)	19(6)	0.04(2)
Precision	RSD	0.00	0.00	9.95	5.75	43.19	149.33
Linearity	R^2	0.9998	1.0000	0.9998	1.0000	0.9998	1.0000
Sensitivity	Slope	1.7272	0.1800	1.7272	0.1800	1.7272	0.1800
Selectivity	s_m	1.5341	0.0002	1.5341	0.0002	1.5341	0.0002
Specificity	s_b	1.037	0.0001	1.037	0.0001	1.037	0.0001
Error of Slope	y-intercept	0.0535	0.0063	0.0535	0.0063	0.0535	0.0063
t_{crit} at 95 % confidence interval		4.30					
t-value		--	--	-32.75	-98.27	-23.07	-9926.90
Decision		--	--	Reject	Reject	Reject	Reject

--Not determined

Table 7.28: Validation of Ti and Fe in acacH/MIBK using H_2SO_4

Validation Criteria	Parameter	1.4 M		3.0 M		6.0 M	
		Ti	Fe	Ti	Fe	Ti	Fe
Recovery	Mean % (s)	0.00	0.00	0.00	0.00	5(6)	6(5)
Precision	RSD	0.00	0.00	0.00	0.00	0.15	0.24
Linearity	R^2	0.9996	0.9998	0.9996	0.9998	0.9996	0.9998
Sensitivity	Slope	1.2368	0.3959	1.2368	0.3959	1.2368	0.3959
Selectivity	s_m	1.0911	0.3028	1.0911	0.3028	1.0911	0.3028
Specificity	s_b	0.7375	0.1405	0.7375	0.1405	0.7375	0.1405
Error of Slope	y-intercept	0.0329	-0.3183	0.0329	-0.3183	0.0329	-0.3183
t_{crit} at 95 % confidence interval		4.30					
t-value		--	--	--	--	-26.885	-30.169
Decision		--	--	--	--	Reject	Reject

--Not determined

Table 7.29: Validation of Ti and Fe in acacH/1-octanol using H_2SO_4

Validation Criteria	Parameter	1.4 M		3.0 M		6.0 M	
		Ti	Fe	Ti	Fe	Ti	Fe
Recovery	Mean % (s)	6(6)	0.7(1)	13(4)	0.0	81(1)	9(1)
Precision	RSD	73.02	141.42	36.38	0.0	1.53	15.10
Linearity	R^2	0.9996	0.9998	0.9996	0.9998	0.9996	0.9998
Sensitivity	Slope	1.2368	0.3959	1.2368	0.3959	1.2368	0.3959
Selectivity	s_m	1.0911	0.3028	1.0911	0.3028	1.0911	0.3028
Specificity	s_b	0.7375	0.1405	0.7375	0.1405	0.7375	0.1405
Error of Slope	y-intercept	0.0329	-0.3183	0.0329	-0.3183	0.0329	-0.3183
t_{crit} at 95 % confidence interval		4.30					
t-value		-35.79	-170.36	-30.07	--	-26.79	-109.55
Decision		Reject	Reject	Reject	--	Reject	Reject

--Not determined

Table 7.30: Validation of Ti and Fe in MIBK using HCl

Validation Criteria	Parameter	1.4 M		3.0 M		6.0 M	
		Ti	Fe	Ti	Fe	Ti	Fe
Recovery	Mean % (*s*)	0.00	0.3(5)	0.9(9)	105(3)	3(1)	104(2)
Precision	RSD	0.00	173.21	103.66	3.05	51.40	2.21
Linearity	R^2	0.9998	1.0000	0.9998	1.0000	0.9998	1.0000
Sensitivity	Slope	1.7272	0.1800	1.7272	0.1800	1.7272	0.1800
Selectivity	s_m	1.5341	0.0002	1.5341	0.0002	1.5341	0.0002
Specificity	s_b	1.037	0.0001	1.037	0.0001	1.037	0.0001
Error of Slope	y-intercept	0.0535	0.0063	0.0535	0.0063	0.0535	0.0063
t_{crit} at 95 % confidence interval		4.30					
t-value		--	-327.03	-187.07	3.00	-115.01	2.74
Decision		--	Reject	Reject	Accept	Reject	Accept

--Not determined

Table 7.31: Validation of Ti and Fe in 1-octanol using HCl

Validation Criteria	Parameter	1.4 M		3.0 M		6.0 M	
		Ti	Fe	Ti	Fe	Ti	Fe
Recovery	Mean % (*s*)	0.00	0.00	6(1)	97(4)	15(2)	101(1)
Precision	RSD	0.00	0.00	19.78	4.27	16.19	1.71
Linearity	R^2	0.9998	1.0000	0.9998	1.0000	0.9998	1.0000
Sensitivity	Slope	1.7272	0.1800	1.7272	0.1800	1.7272	0.1800
Selectivity	s_m	1.5341	0.0002	1.5341	0.0002	1.5341	0.0002
Specificity	s_b	1.0370	0.0001	1.0370	0.0001	1.0370	0.0001
Error of Slope	y-intercept	0.0535	0.0063	0.0535	0.0063	0.0535	0.0063
t_{crit} at 95 % confidence interval		4.30					
t-value		--	--	-138.68	-1.11	-60.56	0.70
Decision		---	--	Reject	Accept	Reject	Accept

--Not determined

Table 7.32: Validation of Ti and Fe in MIBK using H_2SO_4

Validation Criteria	Parameter	1.4 M		3.0 M		6.0 M	
		Ti	Fe	Ti	Fe	Ti	Fe
Recovery	Mean % (*s*)	0.00	0.00	1.6(2)	6.1(7)	13(3)	7.6(5)
Precision	RSD	0.00	0.00	13.43	10.65	21.33	6.32
Linearity	R^2	0.9996	0.9998	0.9996	0.9998	0.9996	0.9998
Sensitivity	Slope	1.2368	0.3959	1.2368	0.3959	1.2368	0.3959
Selectivity	s_m	1.0911	0.3028	1.0911	0.3028	1.0911	0.3028
Specificity	s_b	0.7375	0.1405	0.7375	0.1405	0.7375	0.1405
Error of Slope	y-intercept	0.0329	-0.3183	0.0329	-0.3183	0.0329	-0.3183
t_{crit} at 95 % confidence interval		4.30					
t-value		--	--	-784.88	-249.92	-55.096	-331.31
Decision		--	--	Reject	Reject	Reject	Reject

--Not determined

Table 7.33: Validation of Ti and Fe in 1-octanol using H_2SO_4

Validation Criteria	Parameter	1.4 M		3.0 M		6.0 M	
		Ti	Fe	Ti	Fe	Ti	Fe
Recovery	Mean % (*s*)	6(1)	2(3)	34(2)	7.8(8)	21(3)	32(7)
Precision	RSD	26.54	128.26	5.45	11.68	82.13	21.86
Linearity	R^2	0.9996	0.9998	0.9996	0.9998	0.9996	0.9998
Sensitivity	Slope	1.2368	0.3959	1.2368	0.3959	1.2368	0.3959
Selectivity	s_m	1.0911	0.3028	1.0911	0.3028	1.0911	0.3028
Specificity	s_b	0.7375	0.1405	0.7375	0.1405	0.7375	0.1405
Error of Slope	y-intercept	0.0329	-0.3183	0.0329	-0.3183	0.0329	-0.3183
t_{crit} at 95 % confidence interval		4.30					
t-value		-110.58	-66.81	-61.55	-181.74	-2.89	-16.60
Decision		Reject	Reject	Reject	Reject	Accept	Reject

Table 7.34: Validation of Ti and Fe in Dowex C-hydrogen cation resin at 3.0 M H_3PO_4

Validation Criteria	Parameter	Dowex C-hydrogen	
		Ti	Fe
Recovery	Mean % (s)	103.5(7)	100.3(3)
Precision	RSD	0.68	0.34
Linearity	R^2	0.9999	1.0000
Sensitivity	Slope	1.68863	0.186917
Selectivity	s_m	1.4974	0.1918
Specificity	s_b	0.6918	0.0865
Error of Slope	y-intercept	0.0218	0.0044
t_{crit} at 95 % confidence interval		4.30	
t-value		8.97	1.31
Decision		Reject	Accept

Table 7.35: Validation of Fe in strong basic Amberlite IRA 900, Amberlite IRA 402 and Dowex 1X4 ion exchange anionic resin at 3.0 M H_3PO_4

Validation Criteria	Parameter	Amberlite IRA 900	Amberlite IRA 402	Dowex 1X4
Recovery	Mean % (*s*)	63(9)	51(13)	86(3)
Precision	RSD	14.71	25.59	4.64
Linearity	R^2	0.9979	0.9979	0.9979
Sensitivity	Slope	0.2345	0.2345	0.2345
Selectivity	s_m	0.2865	0.2865	0.2865
Specificity	s_b	0.9465	0.9465	0.9465
Error of Slope	y-intercept	0.0380	0.0380	0.0380
t_{crit} at 95 % confidence interval		4.30		
t-value		-7.35	-6.35	-6.05
Decision		Reject	Reject	Reject

Table 7.36: Validation of Fe in strong basic Amberlite 900, Amberlite IRA 402 and Dowex 1X4 ion exchange anionic resin at 5.0 M H_3PO_4

Validation Criteria	Parameter	Amberlite IRA 900	Amberlite IRA 402	Dowex 1X4
Recovery	Mean % (*s*)	81(15)	68(5)	70(8)
Precision	RSD	18.78	6.83	10.90
Linearity	R^2	0.9989	0.9989	0.9989
Sensitivity	Slope	0.1943	0.1943	0.1943
Selectivity	s_m	0.2105	0.2105	0.2105
Specificity	s_b	0.0865	0.0865	0.0865
Error of Slope	y-intercept	0.0286	0.0286	0.0286
t_{crit} at 95 % confidence interval		4.30		
t-value		-2.15	-11.86	-6.68
Decision		Accept	Reject	Reject

Table 7.37: Validation of Ti and Fe in strong basic Amberlite IRA 900 and Amberlite IRA 402 resins at 10.0 M H_3PO_4

Validation Criteria	Parameter	Amberlite IRA 900		Amberlite IRA 402	
		Ti	Fe	Ti	Fe
Recovery	Mean % (*s*)	70.7(4)	73(3)	87.01(1)	68(5)
Precision	RSD	0.53	3.54	0.11	6.83
Linearity	R^2	0.9999	0.9998	0.9999	0.9998
Sensitivity	Slope	1.6890	0.2076	1.6890	0.2076
Selectivity	s_m	1.5404	0.1772	1.5404	0.1771
Specificity	s_b	0.9409	0.1080	0.9409	0.1080
Error of Slope	y-intercept	0.1468	0.0208	0.1468	0.0208
t_{crit} at 95 % confidence interval		4.30			
t-value		-136.58	-18.086	-233.59	-11.867
Decision		Reject	Reject	Reject	Reject

Table 7.38: Validation of Ti and Fe in strong basic Dowex 1X4 ion exchange anionic resin at 10.0 M H_3PO_4

Validation Criteria	Parameter	Dowex 1X4	
		Ti	Fe
Recovery	Mean % (*s*)	101(3)	101(3)
Precision	RSD	2.92	2.87
Linearity	R^2	0.9997	0.9997
Sensitivity	Slope	1.3755	0.1769
Selectivity	s_m	1.2430	0.1699
Specificity	s_b	0.5207	0.1038
Error of Slope	y-intercept	0.1559	0.0217
t_{crit} at 95 % confidence interval		4.30	
t-value		0.64	0.42
Decision		Accept	Accept

Table 7.39: Validation of Ti in Amberlite IRA 900 and Amberlite IRA 402 at 3.0 M and 5.0 M by elusion with 5.0 M HCl

Validation Criteria	Parameter	Amberlite IRA 900		Amberlite IRA 402	
		3.0 M	5.0 M	3.0 M	5.0 M
Recovery	Mean % (*s*)	80(10)	93(6)	85.5(2)	87.01(1)
Precision	RSD	13.64	5.62	0.28	0.11
Linearity	R^2	0.9999	0.9987	0.9999	0.9987
Sensitivity	Slope	1.9803	1.4866	1.9803	1.4866
Selectivity	s_m	1.7989	1.3463	1.7989	1.3463
Specificity	s_b	0.7535	0.5640	0.7535	0.5640
Error of Slope	y-intercept	0.2560	0.2120	0.2560	0.2120
t_{crit} at 95 % confidence interval		4.30			
t-value		-3.09	-2.28	-105.34	-233.59
Decision		Accept	Accept	Reject	Reject

Table 7.40: Validation of Ti in Dowex 1X4 ion exchange at 3.0 M and 5.0 M H_3PO_4 column by elusion with 5.0 M HCl

Validation Criteria	Parameter	Dowex 1X4 ion exchange	
		3.0 M	5.0 M
Recovery	Mean % (*s*)	82(4)	70(8)
Precision	RSD	4.69	10.90
Linearity	R^2	0.9996	0.9996
Sensitivity	Slope	0.1943	0.1943
Selectivity	s_m	0.2106	0.2106
Specificity	s_b	0.6957	0.6957
Error of Slope	y-intercept	0.0286	0.0286
t_{crit} at 95 % confidence interval		4.30	
t-value		-8.11	-6.68
Decision		Reject	Reject

Table 7.41: Validation of Fe in weak basic Dowex Marathon WBA and Dowex 66 free base at 3.0 and 5.0 M H_3PO_4

Validation Criteria	Parameter	Dowex Marathon WBA		Dowex 66 free base	
		3.0 M	5.0 M	3.0 M	5.0 M
Recovery	Mean % (*s*)	103(2)	96(2)	106.5(6)	96(9)
Precision	RSD	1.87	1.61	0.56	9.78
Linearity	R^2	0.9996	0.9978	0.9996	0.9978
Sensitivity	Slope	0.1943	0.1931	0.1943	0.1931
Selectivity	s_m	0.2106	0.2003	0.2106	0.2003
Specificity	s_b	0.6957	0.6559	0.6957	0.6559
Error of Slope	y-intercept	0.0286	4.8391	0.0286	4.8391
t_{crit} at 95 % confidence interval		4.30			
t-value		3.60	-4.13	18.84	-0.70
Decision		Accept	Accept	Reject	Accept

Table 7.42: Validation of Ti and Fe in weak basic Dowex Marathon WBA and Dowex 66 free base at 10.0 M H_3PO_4

Validation Criteria	Parameter	Dowex Marathon WBA		Dowex 66 free base	
		Ti	Fe	Ti	Fe
Recovery	Mean % (*s*)	97(3)	102(3)	100(3)	103(3)
Precision	RSD	3.13	3.20	3.15	3.19
Linearity	R^2	0.9997	0.9997	0.9997	0.9997
Sensitivity	Slope	1.3755	0.1769	1.3755	0.1769
Selectivity	s_m	1.2430	0.1699	1.2430	0.16994
Specificity	s_b	0.5207	0.1038	0.5207	0.1038
Error of Slope	y-intercept	0.1560	0.0218	0.1560	0.0218
t_{crit} at 95 % confidence interval		4.30			
t-value		-1.48	1.26	0.24	1.42
Decision		Accept	Accept	Accept	Accept

Table 7.43: Validation of Ti in weak basic Dowex Marathon WBA and Dowex 66 free 3.0 M and 5.0 M H_3PO_4 column by elusion with 5.0 M HCl

Validation Criteria	Parameter	Dowex Marathon WBA		Dowex 66 free base	
		3.0 M	5.0 M	3.0 M	5.0 M
Recovery	Mean % (*s*)	101(2)	102(4)	103(5)	101(1)
Precision	RSD	1.98	3.72	4.80	1.16
Linearity	R^2	0.9997	0.9997	0.9997	0.9997
Sensitivity	Slope	1.9803	1.4867	1.9803	1.4867
Selectivity	s_m	1.7989	1.3463	1.7989	1.3463
Specificity	s_b	0.7536	0.5640	0.7536	0.5640
Error of Slope	y-intercept	0.2560	0.2119	0.2560	0.2119
t_{crit} at 95 % confidence interval		4.30			
t-value		0.55	0.91	1.07	0.87
Decision		Accept	Accept	Accept	Accept

7.4 Conclusion

The results obtained in this study were validated with regards to the set of objectives stated in **Chapter 1** and were found to be relatively satisfactory using the null hypothesis and can still be further improved. The results which were found not be satisfactory were rejected. Those with low Ti and Fe recoveries were mostly rejected due to the incomplete dissolution and the non-separation of Ti and Fe under investigated methods. The accepted results are those which provided complete dissolution and good separation of Ti and Fe. All calibration curves gave good linearity with R^2 values greater than 0.997.

8 Evaluation of the Study and Future research

8.1 Introduction

The main objective in this study was the development of cost and energy efficient separation and analytical techniques for the beneficiation of Ti and Fe in ilmenite (see **Chapter 1)**. In this chapter we evaluate the set objectives and identify the possible future research projects.

8.2 Evaluation of the study

The objectives outlined in **Chapter 1**, **Section 1.3** are as follows:

- Performing an in-depth literature study on analytical techniques for analysis of titanium in ilmenite.
- Development of analytical procedure to accurately quantity Fe and Ti in commercial samples with simpler matrix and in ilmenite mineral.
- Development of low energy demanding dissolution method for ilmenite using techniques such as flux fusion and microwave digestion.
- Investigation in the use of different inorganic/organic ligands for selective precipitation of Fe and/or Ti.
- Investigating the separation of Fe and Ti using ion exchange with different resins
- Investigating the separation of Fe and Ti with solvent extraction using different chelating agents and different solvent systems.
- Performing statistical evaluation of the analytical data and report the results as a thesis.

The results reported in **Chapters 5** and **Chapter 6** clearly indicate the all of the experimental set objectives were successfully met and excellent results were obtained**.** Different Ti and Fe containing samples (inorganic salts, pure metals and ilmenite mineral) were quantified in different mineral acids using ICP-OES. Complete dissolution of Ti and Fe metals were achieved in H_2SO_4 and H_3PO_4 at elevated temperatures (150 and 200 ºC). Ilmenite was partially insoluble in most of the acids investigated but H_2SO_4 and H_3PO_4 proofed to be the best acids at high temperatures. Complete dissolution of the mineral was accomplished using the basic fluxes such as borates ($LiBO_2$ and $Na_2B_4O_7$) and NaH_2PO_4:Na_2HPO_4. Comparison of the products obtained from the flux fusion dissolution and the semi-quantitative SEM-EDS analysis indicate relatively good agreement for the elements most of the elements in the mineral.

Selective crystallization using sodium mecartpopyridine salt (NaTP) indicated a preferential precipitation of Fe from the aqueous mineral solution. Titanium remained in the filtrate solution under the selected condition at a pH of 9.00. Selective precipitation/separation using sodium tetraphenyl borate (NaTPB) was unsuccessful with both Ti and Fe precipitated in comparable amounts.

Addition of the NaTP ligand to the mineral solution in acidic medium prevented the formation of a Fe precipitate but solvent extraction of the subsequent mixture using MIBK and 1-octanol as extractants indicated a successful and selective extraction process of the Fe into the organic phase. The MIBK was found to be the better extractant of the two solvents. Extraction of the ilmenite mineral solution in HCl using TOPO/kerosene and acacH/MIBK (or 1-octanol) showed similar preferential extraction of Fe into the organic phase. Interestingly the use of acacH showed the extraction of Fe at high HCl concentration and prompted further investigation without the addition of acacH.

Cationic exchange separation was unsuccessful in the separation of the two elements with both Ti and Fe readily eluted with dilute acids (HCl and H_3PO_4) from the column. Successful separation was accomplished using anionic exchange resins and a combination of H_3PO_4 and HCl as mobile solvents. The Fe compound was eluted with 3.0 to 5.0 M H_3PO_4 while Ti was recovered with 5.0 M HCl elution.

The experimental results in this study were also validated and most of the results were found to be acceptable at a 95 % confidence level. Good calibration curve linearity with r^2 between 0.997 and 1 was obtained. The LODs for both Ti and Fe ranged from 0.0021 to 0.1278 while the LOQs ranged between 0.0212 and 1.2779 in different mineral acids.

8.3 Future research

Possible future studies from this thesis are as follow:

- The dissolution of Ti and Fe in ilmenite in this study was limited to open system acid digestion and flux fusion. The use of microwave- acid assisted digestion of ilmenite can also be studied for effective dissolution.
- The separation of Ti and Fe within $LiBO_2$ or $Na_2B_4O_7$ matrix
- Characterization of the isolated Ti and Fe products with analytical techniques such as CHNS-micro analysis and X-ray crystallography.
- Isolation and purification of Ti and Fe compounds
- Separation of Ti and Fe in complex matrix by membrane separation process
- Separation of Ti and Fe on anion exchange resins using solutions of salts such as NH_4Cl or $(NH_4)_3PO_4$ as mobile solvents instead of acids.
- Quantification and characterization of ilmenite using different analytical techniques such as ICP-MS and AAS with XRD and XRF.

Summary

The aim of this project was to investigate the dissolution and possible separation of Ti and Fe in ilmenite using eco-friendly and economically viable procedures. Method validation was established with commercial salts such as $FeCl_3 \cdot 6H_2O$ and $TiCl_3$ including Ti and Fe metal powders with high purity. The successful procedures were evaluated for the dissolution of ilmenite and subsequent separations of Ti and Fe in the mineral matrix. Dissolution techniques such as open-beaker acid digestion and flux fusion were evaluated. The separation techniques which were investigated include selective precipitation, solvent extraction and ion exchange. Analytical determinations were performed with inductively coupled plasma-optical emission spectroscopy (ICP-OES) while infrared spectroscopic (IR) analyses was used to characterize the Ti and Fe containing compounds.

Acid dissolution was investigated with different mineral acids which included *aqua regia*, HCl, HNO_3, H_2SO_4 and H_3PO_4. Analytical results showed good average recoveries ranging from 98(1) to 105.2(2) % Ti in $TiCl_3$ and 100(4) to 103(2) % Fe in $FeCl_3 \cdot 6H_2O$ after these salts were dissolved in water. The dissolution of the Ti and Fe metal powders was investigated with *aqua regia*, HCl, HNO_3, H_2SO_4 and H_3PO_4 and only H_2SO_4 and H_3PO_4 successfully dissolves the metal powders and excellent Ti and Fe recoveries of 103.6(5) and 105.2(6) % Ti with 103(2) and 103(2) % Fe were obtained.

The dissolution of ilmenite with acid digestion yielded 38.39 % TiO_2 and 45.25 % Fe_2O_3 with H_2SO_4 and 34.79 % TiO_2 and 19.50 % Fe_2O_3 in H_3PO_4 with clearly pointed to incomplete sample dissolution. Flux fusion using $NH_4 \cdot HF_2$, KF, $K_2S_2O_7$, Na_2CO_3, $LiBO_2$, $Na_2B_4O_7$ and phosphate mixture ($Na_2HPO_4/NaH_2PO_4 \cdot H_2O$) as fluxes was also investigated. Only the borates ($LiBO_2$ and $Na_2B_4O_7$) and the phosphate flux mixture ($Na_2HPO_4/NaH_2PO_4 \cdot H_2O$) indicated complete ilmenite dissolution.

The quantitative results obtained after the flux fusion method (borates and phosphate), were compared with the non-destructive SEM-EDS semi-quantitative results. Comparative results were obtained for Ti, Mg, Mn and Al with some difference observed in the Fe quantities that were recovered.

The separation of Ti and Fe in the ilmenite was further investigated using only the phosphate flux method. Selective precipitation using NaTPB/phenantroline was unsuccessful with both Ti and Fe precipitated in solution. However the use of only NaPT resulted in the complete precipitation of Fe (99.60(1) %) while Ti remained in solution (103(1) %). Separation using solvent extraction indicated that Fe was preferentially isolated with 100 % Fe and 0.00 % Ti and thus achieving a complete separation using NaPT in different organic solvents. Separation of Fe and Ti using the MIBK/NaPT and 1-octanol/NaPT combinations indicated a selective extraction of Fe into the MIBK and 1-octanol with 95.9(3) to 103(3) % Fe and 0.0 to 24(9) % Ti obtained in the organic phase using HCl, H_2SO_4 and H_3PO_4, depending on the acid concentrations. Separation factors were calculated to in the range of 1.7 to 8.6 x 10^7. Solvent extraction using kerosene/TOPO and MIBK/acacH systems indicated a selective extraction of Fe into the organic phase (0.8(1) to 22(6) % Ti and 2(2) to 99.0(8) % Fe in kerosene, 0.7(2) to 7(2) % Ti and 22.5(2) to 100(2) % Fe in MIBK) with separation factors of 1.4 x 10^2 to 3.3 x 10^5 in kerosene and 23 x 10^0 to 1.6 x 10^5 in MIBK in HCl matrix.

The separation of Ti and Fe with strong and weak basic ion exchange resins (Amberlite IRA-900, Amberlite IRA 402, Dowex 1x4 ion exchange resin, weak basic Dowex Marathon WBA and Dowex 66 free base) indicated the successful separations with Ti the strongly retained species during elution with H_3PO_4 solution. Fe recoveries of 96(1) to 103.46(1) % were obtained for the weak anionic resins using 3.0 and 5.0 M H_3PO_4 as eluent. The strongly retained Ti was eluted with 5.0 M HCl with recoveries of 99.1(1) to 103(4) %. Recoveries were generally poor with the use of strong anionic exchange resins for both Fe and Ti resins (62(2) to 74(5) % for Fe and 68(4) to 84(3) % for Ti). The separation factor (α) for strong and weak anionic resins were in the range of 1.4 (Fe/Ti) to 6.7 (Fe/Ti) in 3.0 to 10.0 M H_3PO_4.

Opsomming

Die doel van hierdie projek was die ondersoek van die oplos en moontlike skeiding van Ti en Fe in ilmeniet deur van omgewingsvriendelike en ekonomiese prosedures gebruik te maak. Metodevalidasie is met behulp van kommersiële anorganiese soute soos $FeCl_3 \cdot 6H_2O$ en $TiCl_3$, asook die suiwer metaalpoeiers van Ti en Fe uitgevoer. Die suksesvolle prosedure is daarna vir die suksesvolle oplos van ilmeniet geëvalueer gevolg deur die skeiding van Ti en Fe in die mineraalmatriks. Oplossingstegnieke soos oop-beker suurvertering en soutsmelting is as oplostegnieke geëvalueer. Die skeidingstegnieke wat ondersoek is, sluit onderandere selektiewe presipitering, vloeistofekstraksie en ioon-uitruiling in. Die kwantifisering van die onderskeie elemente is met behulp van induktief-gekoppelde plasma optiese-emissiespektroskopie (IGP-OES) uitgevoer terwyl infrarooispektroskopie (IR) vir die karakterisering van die onderskeie Ti- en Fe-bevattende verbindings aangewend is.

Verskillende mineraalsure *koningswater*, HCl, HNO_3, H_2SO_4 en H_3PO_4 insluit, is vir die oop-beker suurvertering van die monsters ondersoek. Analitiese resultate toon dat kwantitatiewe herwinning van die elemente verkry is en herwinnings van 98(1) tot 105.2(2) % is vir Ti in $TiCl_3$ verkry, terwyl tussen 100(4) en 103(2) % Fe in $FeCl_3 \cdot 6H_2O$ waargeneem is. Die oplos van die Ti- en Fe-metaalpoeiers is ook met behulp van *koningswater*, HCl, HNO_3, H_2SO_4 en H_3PO_4 ondersoek en slegs H_2SO_4 en H_3PO_4 was suksesvol in die oplos van die metaalpoeiers. Uitstekende Ti- en Fe-herwinning is met 103.6(5) en 105.2(6) % Ti en 103(2) en 103(2) % Fe in die onderskeie metaalpoeiers verkry.

Die oplos van ilmeniet deur suurvertering was onvolledig en het metaalherwinnings van 38.39 % TiO_2 en 45.25 % Fe_2O_3 met H_2SO_4 gelewer, terwyl H_3PO_4 slegs 34.79 % TiO_2 en 19.50 % Fe_2O_3 opgelos het. Soutsmelting is met behulp van $NH_4 \cdot HF_2$, KF, $K_2S_2O_7$, Na_2CO_3, $LiBO_2$, $Na_2B_4O_7$, en fosfaatmengsel ($Na_2HPO_4/NaH_2PO_4 \cdot H_2O$) ondersoek.

Slegs die boraatsoute ($LiBO_2$ en $Na_2B_4O_7$), asook die alkalimetaal-fosfaatsoute ($Na_2HPO_4/NaH_2PO_4{\cdot}H_2O$) was in staat om die ilmeniet volledig op te los.

Die verskillende kwantitatiewe resultate wat met die onderskeie soutsmeltingsprosedures verkry is, is verder met nie-destruktiewe skandeer-elektronmikroskopie asook energieverspreidende spektroskopie (SEM-EVS) vergelyk. Die resultate wat op hierdie twee metodes verkry is (oplos *vs* nie-oplos) toon vergelelykbare Ti, Mg, Mn en Al hoeveelhede terwyl die Fe waardes tussen die metodes effens verskil het.

Die skeiding van Ti en Fe in die ilmeniet is verder slegs met behulp van die fosfaatvloedmetode, ondersoek. Selektiewe presipitering is aanvanklik met met behulp van NaTPB/fenantrolien ondersoek, maar hierdie metode was onsuksesvol aangesien betekenisvolle hoeveelhede Ti en Fe in die presispitaat teenwoordig was. Die gebruik van slegs NaPT as cheleermiddel was uiters susksevol en die Fe (99.60(1) %) het volledig gepresipiteer terwyl die Ti (103(1) %) in die ilmeniet in oplossing gebly het. Skeidingsresultate wat met behulp van vloeistofekstraksie verkry is, dui daarop dat die Fe by voorkeur geïsoleer word met 100 % Fe en 0.00 % Ti en dus is die volledige skeiding van die twee elemente met NaPT opgelos in verskillende organiese oplosmiddels, bewerkstellig. Skeiding van die Fe en Ti deur middel van die MIBK/NaPT en 1-oktanol/NaPT kombinasies dui ook die op selektiewe ekstraksie van Fe in die MIBK en 1-oktanol met 95.9(3) tot 103(3) % Fe terwyl 0.0 tot 24(9) % Ti verkry in die organiese fase in die teenwoordigheid van HCl, H_2SO_4 en H_3PO_4, teenwoordig was. Die suurkonsentrasie-variasie het duidelik ’n invloed op die % metaal in die organiesse fase uitgeoefen en skeidingsfaktore het tussen 1.7 en tot 8.6×10^7 gevarieër. Oplossingsekstraksie met keroseen/TOPO- en MIBK/asasH-stelsels was ook slektied in die ten opsigte van element-ekstraksie en die Ti in die organiese fase het tussen 0.8(1) en 22(6) % gewissel terwyl 2(2) tot 99.0(8) % Fe in keroseen teenwoordig was. In die MIBK sistee het die Ti tussen 0.7(2) tot 7(2) % Ti gewissel terwyl die Fe tussen 22.5(2) tot 100(2) % Fe in gewissel het. Skeidingsfaktore van 1.4×10^2 tot 3.3×10^5 in keroseen en 23×10^0 tot 1.6×10^5 in MIBK in ’n HCl matriks is bereken.

Die skeiding van Ti en Fe met sterk en swak alkaliese ioonuitruilingsharse (Amberlite IRA-900, Amberlite IRA 402, Dowex 1x4 ioonuitruilingshars, swak basiese Dowex Marathon WBA, en Dowex 66 vry-basis) was ook suksesvol in die skeiding van die twee elemente. Resultate het getoon dat Ti die sterkste op die ioonuitruilers geadsorbeer het tydens die eluering met H_3PO_4. Fe herwinnings wat tussen 96(1) en 103.46(1) % gewissel het, is vir swak alkaliese anioniese harse verkry indien hulle met 3.0 en 5.0 M H_3PO_4 ge-elueer is. Die sterk ge-adsorbeerde Ti is daarna met 5.0 M HCl geëlueer en herwinnings van 99.1(1) tot 103(4) % is verkry. Die sterk anioniese uitruilingsharse het oor die algemeen swak resultate gelewer en slegs 62(2) tot 74(5) % Fe en 68(4) tot 84(3) % Ti is herwin. Die skeidingsfaktor (α) vir sterk en swak anioniese harse is as 1.4 (Fe /Ti) en 6.7 (Fe / Ti) in 3.0 tot 10.0 M H_3PO_4 bereken.